Applications of Liquid Biopsies in Metastatic Castration Resistant Prostate Cancer

September 2019

Dr. Semini Sumanasuriya, M.B.B.S

Division of Cancer Therapeutics
The Institute of Cancer Research

Thesis submitted to The University of London for the Degree of
Doctor of Philosophy

Declaration

I confirm that the work presented in this thesis has been performed by me unless otherwise acknowledged in the relevant sections.

Semini Sumanasuriya

Acknowledgements

It has been an absolute pleasure and a complete privilege to spend the last few years as part of a group who have changed, and continue to shape the field of prostate cancer care. This team, led by Professor Johann de Bono, have so much to be proud of and I in turn am full of pride of to have played even a small part in their work.

Johann, you have been a true mentor and advisor, continuing to support me both professionally and personally throughout. I am truly grateful for your time, your endless knowledge and your ongoing encouragement.

Within the Cancer Biomarkers team, several key individuals have helped me immensely and whilst I cannot name everybody a few individuals deserve a particular mention. Maryou Lambros, Suzanne Carreira, Susana Miranda, Adam Sharp, Ruth Riisnaes, Ines Figuiredo, Antje Neeb, Jane Goodall, Claudia Bertran, Ana Ferreira, Wei Yuan and Penny Flohr – I am truly lucky to have learnt from people so technically skilled and so infinitely patient. George Seed, thank you for being a programming wizard. I am also thankful to all the members of the Prostate Cancer Targeted Therapy Group, the wonderful doctors I have worked alongside and all the other staff; Lucy, Sheena and Jo to name a few – I leave with the fondest memories of our time together.

I would also like to thank Prostate Cancer UK and their donors for funding my studentship and supporting my research. My family; my mum and dad and my brother who have always been my biggest fans and my best friends, thank you for your never-ending love and support. None of this would have been possible without the love and unwavering support of my husband Ed; thank you for always believing in me.

Last, but by no means least, I would like to extend my heartfelt thanks to all the patients who agree to participate in research. Without this effort and dedication of so many patients and their families, our work would be impossible. *“Alone we can do so little, but together we can do so much.”*

Abstract

Despite many recent advances, treating advanced prostate cancer (PC) remains clinically challenging. The need for validated circulating biomarkers is well recognised in almost all cancers, including in PC. Whilst circulating biomarkers such as plasma cell-free DNA (cfDNA) and circulating tumour cells (CTCs) are being investigated for their clinical utility, there has been a lack of consensus with regards to analyses, reporting and clinical effectiveness of these biomarkers. I begin by presenting the findings of experts in the field addressing these issues at an international consensus meeting.

Following this, I present analysis of cfDNA concentrations of patients treated with taxanes on two large Phase III trials. Here I show that baseline cfDNA concentrations correlate with radiographic progression free survival and overall survival, but not with response to taxanes, confirming their use as independent prognostic marker but not a predictive biomarker in this setting.

Low pass whole genome sequencing of plasma cfDNA performed in this same cohort of patients had superior clinical utility, with changes in tumour purity associating with response to taxane therapy, suggesting that it may be acting as a response biomarker evaluating changes in overall tumour burden. Genomic changes identified require further validation but may provide key insights into understanding drivers of taxane resistance.

I also explored the role of apheresis in increasing CTC numbers, finding it to be a well-tolerated and safe procedure which allowed significant enrichment of CTCs and facilitated the interrogation of tumour genomics and dissection of inter- and intra-patient heterogeneity.

Together, this work has highlighted the possible utility of less invasive liquid biopsies, with both cfDNA and CTCs (acquired by apheresis) showing promise. Currently, interrogating tumour genomics by tissue biopsy remains the gold standard but liquid biopsies have huge potential as multi-purpose biomarkers to serially and safely evaluate changes imposed by therapeutic selective pressures.

Publications arising from this thesis

ORIGINAL PUBLICATIONS ARISING FROM THIS THESIS

Sumanasuriya S*, de Bono JS. *Treatment of Advanced Prostate Cancer—A Review of Current Therapies and Future Promise*. Cold Spring Harb Perspect Med. 2017:a030635. doi:10.1101/cshperspect.a030635

Sumanasuriya S*, Lambros M, de Bono JS. *Application of Liquid Biopsies in Cancer Targeted Therapy*. Clin Pharmacol Ther. July 2017. doi:10.1002/cpt.764

Sumanasuriya S*, Omlin A*, Armstrong A, Attard G, Chi KN, Bevan CL, Shibakawa A, IJzerman MJ, De Laere B, Lolkema M, Lorente D, Luo J, Mehra N, Olmos D, Scher H, Soule H, Stoecklein NH, Terstappen LWMM, Waugh D, de Bono JS. *Consensus Statement on Circulating Biomarkers for Advanced Prostate Cancer*. 2018. doi:10.1016/j.euo.2018.02.009

Mehra N*, Dolling D, **Sumanasuriya S**, Christova R, Pope L, Carreira S, Seed G, Yuan W, Goodall J, Hall E, Flohr P, Boysen G, Bianchini D, Sartor O, Eisenberger MA, Fizazi K, Oudard S, Chadjaa M, de Bono JS. *Plasma Cell-free DNA Concentration and Outcomes from Taxane Therapy in Metastatic Castration-resistant Prostate Cancer from Two Phase III Trials (FIRSTANA and PROSELICA).* Eur Urol. 2018;74(3):283-291. doi:10.1016/j.eururo.2018.02.013

Lambros MB*, Seed G*, **Sumanasuriya S***, Gil V, Crespo M, Fontes M, Chandler R, Mehra N, Fowler G, Ebbs B, Flohr P, Miranda S, Yuan W, Mackay A, Ferreira A, Pereira R, Bertan C, Figueiredo I, Riisnaes R, Rodrigues DN, Sharp A, Goodall J, Boysen G, Carreira S, Bianchini D, Rescigno P, Zafeiriou Z, Hunt J, Moloney D, Hamilton L, Neves RP, Swennenhuis J, Andree K, Stoecklein NH, Terstappen LWMM, de Bono JS. *Single-Cell Analyses of Prostate Cancer Liquid Biopsies Acquired by Apheresis.* Clin Cancer Res. 2018;24(22):5635-5644. doi:10.1158/1078-0432.CCR-18-0862

OTHER RELEVANT ORIGINAL PUBLICATIONS

Rodrigues DN*, Boysen G, **Sumanasuriya S**, Seed G, Marzo AMD, de Bono J. *The molecular underpinnings of prostate cancer: impacts on management and pathology practice*. J Pathol. 2017;241(2):173-182. doi:10.1002/path.4826

Pucci P*, Rescigno P, **Sumanasuriya S**, de Bono J, Crea F. *Hypoxia and Noncoding RNAs in Taxane Resistance*. Trends Pharmacol Sci. 2018;39(8):695-709. doi:10.1016/J.TIPS.2018.05.002

Goodall J*, Mateo J*, Yuan W, Mossop H, Miranda S, Perez-Lopz R, Dolling D, Robinson DR, Sandhu S, Fowler G, Ebbs B, Flohr P, Seed G, Rodrigues DN, Boysen G, Bertan C, Atkin M, Clarke M, Crespo M, Figueiredo I, Riisnaes R, **Sumanasuriya S**, Rescigno P, Zafeiriou Z, Sharp A, Tunariu N, Bianchini D, Gillmman A, Lord CJ, Hall E, Chinnaiyan AM, Carreira S, de Bono JS, TOPARP-A investigators. *Circulating Free DNA to Guide Prostate Cancer Treatment with PARP Inhibition*. Cancer Discov. 2017. doi:10.1158/2159-8290.CD-17-0261

Rescigno P*, Lorente D, Bianchini D, Ferraldeschi R, Kolinsky MP, Sideris S, Zafeiriou Z, **Sumanasuriya S**, Smith AD, Mehra N, Jayaram A, Perez-Lopez R, Mateo J, Parker C, Dearnaley DP, Tunariu N, Reid A, Attard G, de Bono JS. *Prostate-specific Antigen Decline After 4 Weeks of Treatment with Abiraterone Acetate and Overall Survival in Patients with Metastatic Castration-resistant Prostate Cancer.* Eur Urol. 2016. doi:10.1016/j.eururo.2016.02.055

Calcinotto A*, Spataro C, Zagato E, Di Mitri D, Gil V, Crespo M, De Bernardis G, Losa M, Mirenda M, Pasquini E, Rinaldi A, **Sumanasuriya S,** Lambros MB, Neeb A, Lucianò R, Bravi CA, Nava-Rodrigues D, Dolling D, Prayer-Galetti T, Ferreira A, Briganti A, Esposito A, Barry S, Yuan W, Sharp A, de Bono J, Alimonti A. *IL-23 secreted by myeloid cells drives castration-resistant prostate cancer.* Nature. 2018;559(7714):363-369. doi:10.1038/s41586-018-0266-0

Welti J*, Sharp A*, Yuan W, Dolling D, Nava Rodrigues D, Figueiredo I, Gil V, Neeb A, Clarke M, Seed G, Crespo M, **Sumanasuriya S**, Ning J, Knight E, Francis JC, Hughes A, Halsey WS, Paschalis A, Mani RS, Raj GV, Plymate SR, Carreira S, Boysen G, Chinnaiyan AM, Swain A, de Bono JS; International SU2C/PCF Prostate Cancer Dream Team. *Targeting Bromodomain and Extra-Terminal (BET) Family Proteins in Castration-*

Resistant Prostate Cancer (CRPC). Clin Cancer Res. 2018;24(13):3149-3162. doi:10.1158/1078-0432.CCR-17-3571

Li X*, Baek G, Ramanand SG, Sharp A, Gao Y, Yuan W, Welti J, Rodrigues DN, Dolling D, Figueiredo I, **Sumanasuriya S**, Crespo M, Aslam A, Li R, Yin Y, Mukherjee B, Kanchwala M, Hughes AM, Halsey WS, Chiang CM, Xing C, Raj GV, Burma S, de Bono J, Mani RS. *BRD4 Promotes DNA Repair and Mediates the Formation of TMPRSS2-ERG Gene Rearrangements in Prostate Cancer*. Cell Rep. 2018;22(3):796-808. doi:10.1016/j.celrep.2017.12.078

Rodrigues DN*, Rescigno P*, Liu D, Yuan W, Carreira S, Lambros MB, Seed G, Mateo J, Riisnaes R, Mullane S, Margolis C, Miao D, Miranda S, Dolling D, Clarke M, Bertan C, Crespo M, Boysen G, Ferreira A, Sharp A, Figueiredo I, Keliher D, Aldubayan S, Burke KP, **Sumanasuriya S**, Fontes MS, Bianchini D, Zafeiriou Z, Mendes LST, Mouw K, Schweizer MT, Pritchard CC, Salipante S, Taplin ME, Beltran H, Rubin MA, Cieslik M, Robinson D, Heath E, Schultz N, Armenia J, Abida W, Scher H, Lord C, D'Andrea A, Sawyers CL, Chinnaiyan AM, Alimonti A, Nelson PS, Drake CG, Van Allen EM, de Bono JS. *Mismatch repair defects in lethal prostate cancer.* Cancer Res. 2017;77(13). doi:10.1158/1538-7445.AM2017-4679

Paschalis A*, Sheehan B*, Riisnaes R, Rodrigues DN, Gurel B, Bertan C, Ferreira A, Lambros MBK, Seed G, Yuan W, Dolling D, Welti JC, Neeb A, **Sumanasuriya S**, Rescigno P, Bianchini D, Tunariu N, Carreira S, Sharp A, Oyen W, de Bono JS. 1. *Prostate-specific Membrane Antigen Heterogeneity and DNA Repair Defects in Prostate Cancer*. Eur Urol. July 2019. doi:10.1016/j.eururo.2019.06.030

Boysen G*, Rodrigues DN, Rescigno P, Seed G, Dolling D, Riisnaes R, Crespo M, Zafeiriou Z, **Sumanasuriya S**, Bianchini D, Hunt J, Moloney D, Perez-Lopez R, Tunariu N, Miranda S, Figueiredo I, Ferreira A, Christova R, Gil V, Aziz S, Bertan C, de Oliveira FM, Atkin M, Clarke M, Goodall J, Sharp A, MacDonald T, Rubin MA, Yuan W, Barbieri CE, Carreira S, Mateo J, de Bono JS. *SPOP-Mutated/CHD1-Deleted Lethal Prostate Cancer and Abiraterone Sensitivity.* Clin Cancer Res. 2018;24(22):5585-5593. doi:10.1158/1078-0432.CCR-18-0937

Zafeiriou Z*, Bianchini D, Chandler R, Rescigno P, Yuan W, Carreira S, Barrero M, Petremolo A, Miranda S, Riisnaes R, Rodrigues DN, Gurel B, **Sumanasuriya S**, Paschalis A, Sharp A, Mateo J, Tunariu N, Chinnaiyan AM, Pritchard CC, Kelly K, de

Bono JS. *Genomic Analysis of Three Metastatic Prostate Cancer Patients with Exceptional Responses to Carboplatin Indicating Different Types of DNA Repair Deficiency.* Eur Urol. 2019;75(1):184-192. doi:10.1016/j.eururo.2018.09.048

Rescigno P*, Lorente D, Dolling D, Ferraldeschi R, Rodrigues DN, Riisnaes R, Miranda S, Bianchini D, Zafeiriou Z, Sideris S, Ferreira A, Figueiredo I, **Sumanasuriya S,** Mateo J, Perez-Lopez R, Sharp A, Tunariu N, de Bono JS. *Docetaxel Treatment in PTEN- and ERG-aberrant Metastatic Prostate Cancers*. Eur Urol Oncol. 2018;1(1):71-77. doi:10.1016/j.euo.2018.02.006

Ferrarini A, Forcato C, Buson G, Tononi P, Del Monaco V, Terracciano M, Bolognesi C, Fontana F, Medoro G, Neves R, Möhlendick B, Rihawi K, Ardizzoni A, **Sumanasuriya S,** Flohr P, Lambros M, de Bono J, Stoecklein NH, Manaresi N. *A streamlined workflow for single-cells genome-wide copy-number profiling by low-pass sequencing of LM-PCR whole-genome amplification products.* PLoS One. 2018;13(3):e0193689. doi:10.1371/journal.pone.0193689

Bianchini D*, Lorente D, Rescigno P, Zafeiriou Z, Psychopaida E, O'Sullivan H, Alaras M, Kolinsky MP, **Sumanasuriya S**, Sousa Fontes M, Mateo J, Perez-Lopez R, Tunariu N, Fotiadis N, Kumar P, Tree A, Van As N, Khoo V, Parker C, Eeles R, Thompson A, Dearnaley D, de Bono JS. *Effect on Overall Survival of Locoregional Treatment in a Cohort of De Novo Metastatic Prostate Cancer Patients: A Single Institution Retrospective Analysis From the Royal Marsden Hospital*. Clin Genitourin Cancer. 2017;15(5):e801-e807. doi:10.1016/j.clgc.2017.04.013

Mehra N*, Sharp A, Lorente D, Dolling D, **Sumanasuriya S**, Johnson B, Dearnaley D, Parker C, de Bono JS. *Neutrophil to Lymphocyte Ratio in Castration-Resistant Prostate Cancer Patients Treated With Daily Oral Corticosteroids*. Clin Genitourin Cancer. 2017; 15(6):678-684.e1.doi:10.1016/j.clgc.2017.05.012

Nava Rodrigues D*, Casiraghi N, Romanel A, Crespo M, Miranda S, Rescigno P, Figueiredo I, Riisnaes R, Carreira S, **Sumanasuriya S,** Gasperini P, Sharp A, Mateo J, Makay A, McNair C, Schiewer M, Knudsen K, Boysen G, Demichelis F, de Bono JS. *RB1 Heterogeneity in Advanced Metastatic Castration-Resistant Prostate Cancer.* Clin Cancer Res. 2019;25(2):687-697. doi:10.1158/1078-0432.CCR-18-2068

Sharp A, Welti JC, Lambros MBK, Dolling D, Rodrigues DN, Pope L, Aversa C, Figueiredo I, Fraser J, Ahmad Z, Lu C, Rescigno P, Kolinsky M, Bertan C, Seed G,

Riisnaes R, Miranda S, Crespo M, Pereira R, Ferreira A, Fowler G, Ebbs B, Flohr P, Neeb A, Bianchini D, Petremolo A, **Sumanasuriya S**, Paschalis A, Mateo 7, Tunariu N, Yuan W, Carreira S, Plymate SR, Luo J, de Bono JS. *Clinical Utility of Circulating Tumour Cell Androgen Receptor Splice Variant-7 Status in Metastatic Castration-resistant Prostate Cancer*. Eur Urol. April 2019. doi:10.1016/j.eururo.2019.04.006

Table of Contents

Table of figures

Table of tables

1. Introduction

1.1 Background

In 2018, there were an estimated 164,690 new cases of prostate cancer (PC) and 29,430 deaths from prostate cancer in the United States alone (1). The rising incidence of prostate cancer is thought to be multifactorial, with the ageing population and implementation of early diagnosis strategies meaning that at least 1 in 8 men will be diagnosed with prostate cancer in their lifetime (2). Lifestyle, diet and environmental risk factors have also been implicated, with a notably higher incidence in both natives of, and migrants to, the western world (3).

Localised prostate cancer is a potentially curable disease with treatment options including active surveillance, hormonal therapy, surgery and radiotherapy (4). However it is estimated that at least 15% of newly diagnosed prostate cancer patients present with either locally advanced or metastatic disease (5). Sadly, metastatic prostate cancer, which is either diagnosed *de novo* or can be the result of relapsed local disease, is usually fatal; despite many recent advances in their treatment these diseases remain incurable.

1.1.1 Clinical picture

Both localised prostate cancer and locally advanced prostate cancer can be asymptomatic, although may be suspected on the basis of a clinical history. For example, a patient might complain of local urinary tract symptoms (such as increased urinary frequency) and/or have a strong family history. Often metastases may cause the first symptoms of prostate cancer; a patient may present with bone pain or a fracture secondary to bony metastases. The diagnosis of prostate cancer can be made on the basis of a digital rectal examination, an elevated PSA and by direct imaging +/- biopsy of the prostate. Prostate cancer can also be picked up incidentally through PSA screening.

1.1.2 Prostate cancer, a hormone sensitive disease

The mainstay of advanced prostate cancer treatment remains suppressing androgen receptor (AR) signalling, as initially described in the seminal work by Huggins and

Hodges almost 80 years ago (6). The two main androgens in men, testosterone and its potent metabolite dihydrotestosterone (DHT) are mostly present in the peripheral circulation and prostatic tissue respectively (7). DHT works by activating the androgen receptor directly, causing translocation of the AR to the nucleus and binding to AR-response elements. AR activation triggers pathways involved in several cell functions including the cell cycle, cell growth, cell death and protein synthesis.

Prostate cancer, a hormone sensitive disease is “addicted” to this androgen signalling; manipulation of this by blocking the AR with androgen deprivation therapy (ADT) can consequently drastically reduce the rates of testicular androgen production and of circulating androgen levels (8). ADT continues to be effective in both improving prognosis and symptoms (9), and can be achieved both medically and surgically. Both treatments aim to reduce serum testosterone to castrate levels, either by using luteinizing hormone-releasing hormone agonists for medical manipulation or with a surgical bilateral orchiectomy. Whilst the cancer remains controlled by ADT, the disease is referred to as hormone-sensitive prostate cancer (HSPC).

1.1.3 Castration resistant prostate cancer

Suppressing testosterone using ADT offers disease control for only an average of 18 - 36 months before the disease enters the castration-resistant phase (10). Altered AR signalling, due to AR gene copy number changes, mutations and rearrangements resulting in AR splice variants, is implicated in castration-resistant prostate cancer (CRPC). Once the disease is no longer hormone sensitive, further treatment can be offered, with the aim of increasing overall survival (OS) and, perhaps more importantly, improving symptoms and promoting quality of life. Over the last decade there have been several advances in this field but sadly, the disease remains incurable.

1.2 Therapeutic options for metastatic disease

Current approved treatment options available for metastatic CRPC (mCRPC) include taxane-based chemotherapy, novel hormone therapies such as abiraterone and enzalutamide, or with the radioisotope Radium-223 (11). Huge advances have been made over the last decade in establishing these treatments as standard of care for prostate cancer patients, although at the time of writing, no preferred sequence of treatment has been established (12). A summary of practice-changing trials that has led

to the registration of these agents is provided in a recent New England Journal of Medicine review (13) and is depicted in ***Table 1-1*****.**

Response to these limited treatment options is variable, and despite numerous recent advances the prognosis for mCRPC remains poor. Many phase III trials still fail to meet their primary endpoint (14) (15), highlighting the rising need for molecularly-stratified therapeutic strategies. Therapeutic decisions should be guided by the patient's treating clinician, with the input of a multidisciplinary team and always taken in conjunction with the patient and their families wishes. Whilst no preferential sequence of available treatment options exists, decisions also depend substantially on patient preference, their current burden of disease and symptoms experienced, as well as local availability. A typical progression of a prostate cancer patient and the available treatment options is summarised in ***Figure 1-1*** (although it should be noted that Sipuleucel-T is not available in the UK).

With all available therapies, patients should be monitored closely for evidence of clinical, biochemical, and radiological progression (biochemical monitoring alone is inadequate) in order to facilitate treatment switch decisions. Unless the timing of these is mandated by a clinical trial schedule, monitoring can be performed at the physician's discretion. However, baseline scans and repeat imaging every 3–6 months are highly recommended (16), as a major challenge remains determining the optimal timing of switching therapeutic strategies.

It is worthwhile noting that the treatment paradigm is rapidly evolving, and published results of trials such as STAMPEDE and ENZAMET (17,18) mean that docetaxel, and more recently abiraterone (18) and enzalutamide (19) are effective in the hormone-sensitive setting. As physicians are faced with increasing choices regarding available treatment options and timings, the need for ongoing trials and guidance to facilitate therapeutic decision making is greater than ever.

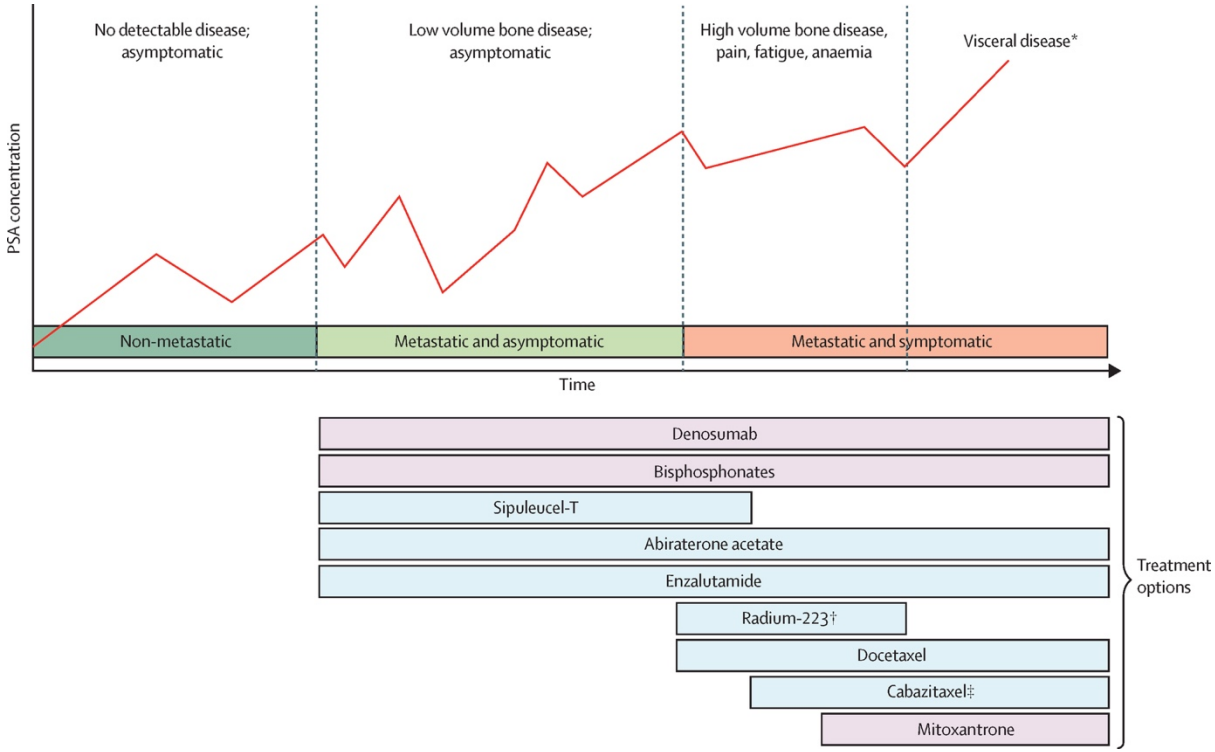

Figure 1-1: Typical progression of metastatic castration-resistant prostate cancer and treatment options (12)

Trial and Registration No.	Treatment		Median Overall Survival		Hazard Ratio for Death (95% CI)	Year of Initial Report†
	Study Treatment	Control	Study Treatment	Control		
			months			
No previous ADT						
CHAARTED, NCT00309985	Docetaxel plus ADT	ADT	57.6	44.0	0.61 (0.47–0.80)	2015[4]
STAMPEDE, NCT00268476	Docetaxel plus ADT	ADT	60	45	0.76 (0.62–0.92)	2015[5]
LATITUDE, NCT01715285	Abiraterone and prednisone, plus ADT	ADT	Not reached	34.7	0.62 (0.51–0.76)	2017[6]
STAMPEDE, NCT00268476	Abiraterone and prednisolone, plus ADT	ADT	Not reached	48	0.61 (0.49–0.75)	2017[7]
Recurrent disease after ADT without chemotherapy						
TAX 327‡	Docetaxel and prednisone	Mitoxantrone and prednisone	18.9	16.5	0.76 (0.62–0.94)	2004[8]
SWOG 9916, NCT00004001	Docetaxel and estramustine	Mitoxantrone and prednisone	17.5	15.6	0.80 (0.67–0.97)	2004[9]
COU-302, NCT00887198 (minimal or no symptoms)	Abiraterone and prednisone	Prednisone	Not reached	27.2	0.75 (0.61–0.93)	2013[10]
PREVAIL, NCT01212991 (minimal or no symptoms)	Enzalutamide	Placebo	32.4	30.2	0.71 (0.60–0.84)	2014[11]
Recurrent disease after ADT and docetaxel						
TROPIC, NCT00417079	Cabazitaxel and prednisone	Mitoxantrone and prednisone	15.1	12.7	0.70 (0.59–0.83)	2010[12]
COU-301, NCT00638690	Abiraterone and prednisone	Prednisone	14.8	10.9	0.65 (0.54–0.77)	2011[13]
AFFIRM, NCT00974311	Enzalutamide	Placebo	18.4	13.6	0.63 (0.53–0.75)	2012[14]
Recurrent disease after ADT, docetaxel status unspecified						
IMPACT, NCT00065442 (minimal symptoms)	Sipuleucel-T	Placebo	25.8	21.7	0.77 (0.61–0.98)	2010[15]
ALSYMPCA, NCT00699751 (symptomatic)	Standard of care plus radium-223	Standard of care	14.9	11.3	0.70 (0.58–0.83)	2013[16]

* ADT denotes androgen-deprivation therapy, and CI confidence interval.
† The date of the initial report may not be the same as the date of the cited publication.
‡ There is no trial registration number for TAX 327.

Table 1-1: Practice-Changing Trials of Treatments for Metastatic Prostate Cancer That Improve Survival (13)

1.2.1 Chemotherapy

1.2.1.1 Docetaxel

In two landmark Phase III clinical trials (20,21), docetaxel chemotherapy was the first treatment to demonstrate an improvement in overall survival in mCRPC. Improvements were also seen in prostate-specific antigen (PSA) and quality of life (QoL) in patients treated with docetaxel and prednisolone versus mitoxantrone and prednisolone. This survival benefit was seen across all age groups, and these studies lead to the currently established regimen of three weekly intravenous docetaxel for 10 cycles being given as first-line chemotherapy in mCRPC. Despite the results of the TAX327 trial (21) the benefits of prednisolone in this regimen remain controversial, with increasing concerns about iatrogenic steroids being able to drive resistance (22).

Currently, docetaxel is administered intravenously every 3-weeks for 10 cycles (23) although the optimal treatment duration is not well defined and merits further evaluation. The recommended treatment dose is 75 mg/m^2, although dose reductions can be introduced depending on tolerability. Side effects experienced are similar to those seen with many other types of chemotherapy, including nausea, vomiting, and cytopenia's, with some patients experiencing subsequent neutropenic sepsis. Docetaxel use is also associated with both motor and sensory peripheral neuropathy, which can develop with cumulative doses (24).

Patients are occasionally re-challenged with docetaxel, particularly if their tumours have never been determined to be refractory, and/or they have experienced more than 6 months of remission following prior docetaxel exposure. This re-challenge is currently only performed at the individual physician's discretion, for example when no other treatment options are available, with good results being reported in small numbers of patients (25). This retreatment needs further evaluation, particularly with docetaxel also now being used in the hormone-sensitive setting, retreatment for progressing mCRPC may still lead to patient benefit (26,27).

Docetaxel works principally by disrupting microtubule function, exerting its anticancer activity by targeting microtubules during mitosis and interphase. By causing stabilisation of the mitotic spindle, docetaxel triggers arrest of mitosis and cell proliferation causing resultant cell death (28). The complete mechanisms by which taxanes exert their

antitumour activity are not yet wholly understood; they are also thought to have some antiandrogenic properties by blocking nuclear translocation of the microtubule dependent androgen receptor (29–32).

1.2.1.2 Cabazitaxel

Cabazitaxel, a semi-synthetic taxane, is the only other approved chemotherapy for mCRPC. It exerts a similar mechanism of action to docetaxel, again disrupting of microtubule function and causing cell death (33). Structurally, both docetaxel and cabazitaxel are very similar and only differ by two methyl groups (***see Figure 1-2)***. Cabazitaxel was selected to overcome the emergence of docetaxel resistance, and has been shown to have activity in both the post-docetaxel and in the chemotherapy-naïve setting, as well as exerting anti-tumour activity in docetaxel-resistant cancers (34).

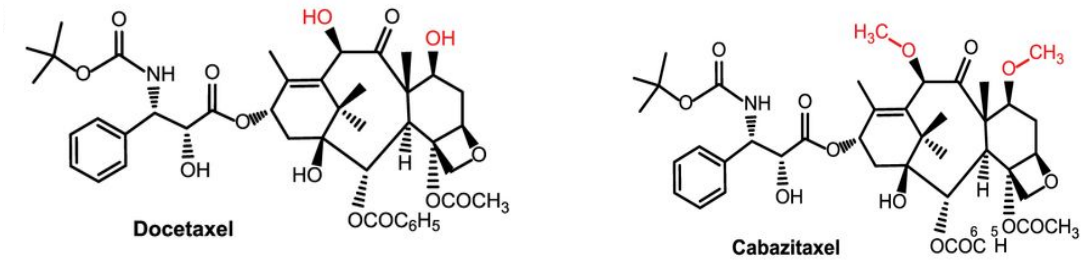

Figure 1-2: Chemical structure of docetaxel and cabazitaxel

Following the phase III TROPIC trial (35), cabazitaxel was granted approval by the Food and Drug Administration (FDA) in 2010, as a second-line treatment following docetaxel. The TROPIC trial confirmed efficacy activity of cabazitaxel with a survival advantage when combined with prednisolone compared to mitoxantrone and prednisolone.

Two further phase III studies have confirmed the antitumour activity of cabazitaxel, FIRSTANA and PROSELICA. FIRSTANA examined whether two different doses of cabazitaxel (20 mg/m² or 25 mg/m²) were superior to standard dose docetaxel (75mg/m^2) in terms of overall survival in chemotherapy-naïve patients. This FDA-mandated trial was the first head-to-head comparative study in CRPC, and did not demonstrate superiority for overall survival of either dose of cabazitaxel versus docetaxel in the 1178 patients treated. Secondary endpoints of progression-free survival and PSA response also did not differ significantly across the three treatment arms, although tumour responses were

significantly better for the higher dose of cabazitaxel (25mg/m^2) versus docetaxel. In terms of tolerability, the lower dose of cabazitaxel 20mg/m^2 was associated with the fewest side-effects of the three arms (36).

PROSELICA was a phase III non-inferiority study comparing cabazitaxel 20mg/m^2 versus cabazitaxel 25mg/m^2 in 1200 mCRPC patients who had previously received docetaxel. This FDA-mandated trial also confirmed the previously reported antitumour efficacy of cabazitaxel in post-docetaxel patients. PROSELICA met its pre-defined non-inferiority endpoint; a reduced dose of 20mg/m^2 of cabazitaxel maintained at least 50% of the overall survival benefit of the 25mg/m^2 dose (37).

Like docetaxel, cabazitaxel is administered via an intravenous infusion given once every 3-weeks. Based on the results of both FIRSTANA and PROSELICA, the standard dosing of cabazitaxel remains 25/mg^2, and this higher dose does appear to be more active. However, this can now confidently be reduced to 20mg/m^2 in selected patients, for example those with a poorer performance status or who experience treatment-associated toxicity, with limited impact on survival.

The side effects experienced with cabazitaxel are similar to those with docetaxel, although the side effect profile is thought to be slightly more favourable. Side effects experienced most commonly include fatigue, nausea, diarrhoea and neutropenia (38–40). As with docetaxel, concomitant steroids and antiemetics are given prophylactically to minimize side effects. Chemotherapy-induced peripheral neuropathy is much less common with cabazitaxel, with symptoms including peripheral numbness, cold insensitivity and pain. The current recommendation is for patients to receive up to 10 cycles of cabazitaxel, providing the patient is tolerating the treatment well and remains free from signs of clinical, biochemical or radiological disease progression (41). Again, the optimal duration of treatment with this agent remains to be defined.

1.2.1.3 Taxane resistance

Whilst both of these licensed chemotherapeutic agents result in demonstrable improvements in OS, PSA and quality of life, responses are variable and resistance inevitable. Despite extensive research into taxane resistance, the mechanisms involved remain poorly understood. It is acknowledged that resistance is likely to be multifactorial, with chromosomal instability (42), efflux transporters (43) and androgen signalling

interaction (44) being implicated. Taxane resistance will be discussed further in ***Chapter 6.***

1.2.1.4 Mitoxantrone

Mitoxantrone was initially approved by the FDA in 1996 for the palliative treatment of mCRPC after a small phase III trial showed antitumor activity and symptomatic relief, but without significant survival benefit (45). Retrospective analyses of data from phase III randomized controlled trials that include mitoxantrone in a treatment arm, have confirmed evidence of symptomatic improvement without survival benefit in unselected patients (46). Mitoxantrone is associated with significant toxicity, including pancytopenias, fatigue, and shortness of breath. Despite this, it is still prescribed by some physicians, albeit rarely, for symptom control in patients particularly when faced with limited/no remaining treatment options. However, mitoxantrone is a type II topoisomerase inhibitor that impacts DNA synthesis and DNA repair and is more likely to be active in prostate cancers with DNA repair defects. Further studies evaluating whether mitoxantrone is most active against prostate cancer with defects in DNA repair mediated by homologous recombination are warranted.

1.2.2 Novel hormonal agents

As discussed, the pivotal role of androgen signalling in both hormone-sensitive and castration-resistant prostate cancer is well established. Key aberrations in the androgen receptor have been implicated in castration resistance, including gene amplification, rearrangements, overexpression, activating mutations and the formation of splice variants. These aberrations contribute to persistent androgen receptor signalling even in an androgen deficient environment, and identifying compounds that target this pathway has been an important step of recent drug discovery. This has provided us with FDA approved drugs of important clinical significance, including abiraterone and enzalutamide. Both drugs are administered orally and generally well tolerated, making them a preferred option for many patients and clinicians.

1.2.2.1 Abiraterone

Abiraterone acetate is an irreversible, selective cytochrome p450 17A1 (CYP17) inhibitor that blocks steroid conversion, inhibiting androgen production within the prostate, testis

and adrenals (47). Several phase III studies have confirmed the antitumour efficacy of abiraterone as a pre- and post-chemotherapy treatment for mCRPC (48–50) demonstrating an improvement of overall survival by almost 5 months. Preclinical data indicates that abiraterone acetate is metabolised to generate a potent androgen receptor antagonist that is at least as potent as blocking the AR as enzalutamide is. This suggests that abiraterone not only blocks CYP17 but also the androgen receptor directly (51,52).

Abiraterone is administered orally at a dose of 1000mg once a day, and is ordinarily taken in combination with a low dose of oral steroid (usually prednisolone 5mg twice daily). Common associated side effects are linked to CYP17 blockade inducing increased mineralocorticoid levels, and include hypertension, hypokalaemia and fluid retention (49). Abiraterone is given in conjunction with prednisolone or dexamethasone to abrogate these side effects. Dexamethasone may indeed be preferable owing to its longer half-life and that it is less likely to activate the mineralocorticoid receptor. There is also a slight risk of transaminase elevation with abiraterone therapy, and liver function should therefore be monitored closely particularly in the first 12 weeks of treatment.

In approximately 1/3 of patients, performing a “steroid switch” from prednisolone to low-dose dexamethasone at the point of disease progression leads to a reversal of resistance. These patients show durable clinical, biochemical and radiological responses following this change in steroids, the rationale being that abiraterone resistance may be the result of androgen receptor point mutations activated by prednisolone but not dexamethasone. Furthermore, as previously mentioned, activation of the glucocorticoid receptor is lower with dexamethasone (53).

1.2.2.2 Enzalutamide

Enzalutamide is a next generation antiandrogen that offers a treatment advantage over older antiandrogens by antagonising full length androgen receptor and preventing its nuclear translocation (54). Large phase III trials (including AFFIRM: NCT00974311 and PREVAIL: NCT01212991) have shown significant antitumor activity of enzalutamide with improvement in overall survival (OS) in both the pre- and post-chemotherapy settings (55,56).

Like abiraterone, enzalutamide is taken orally once daily, at a dose of 160mg. Common side effects experienced include fatigue, gastrointestinal disturbance and hot flushes.

There are more serious, but much rarer side effects reported including seizures in <1% in patients treated with enzalutamide (57). Importantly, enzalutamide appears to potently penetrate the blood-brain barrier and has been reported to cause significant fatigue and neurocognitive deficits, which are thought to be reversible on cessation of the drug (58).

1.2.2.3 Abiraterone versus enzalutamide

Superiority of either abiraterone or enzalutamide over the other has not yet been demonstrated, and patient preference and comorbidities play a large role in treatment choice, particularly considering the different toxicity profiles. Abiraterone, with the mineralocorticoid side effects listed above may be best avoided in patients with cardiovascular disease or where steroids are contraindicated, for example in diabetic patients. Similarly, for patients with pre-existing structural brain damage or known seizures, enzalutamide would not be advised. Moreover, for patients still working or requiring substantial intellectual engagement, abiraterone may be preferable. Recent work suggests an increased prevalence of side effects in patients on enzalutamide (59), but overall both drugs are generally well tolerated.

Some studies have shown evidence that a small number of patents respond to abiraterone post- enzalutamide (60) and indeed to enzalutamide following abiraterone (61) but these figures have been much lower than predicted with response rates in the region of 10-15%. This is likely due to cross-resistance between these agents and the formation of AR splice variants (62). These lower response rates mean that currently across many healthcare settings, treatment with either abiraterone or enzalutamide is not currently approved if a patient has already received the other novel endocrine agent.

1.2.2.4 Newer AR-targeting agents

Newer agents, such as apalutamide and darolutamide, other non-steroidal antiandrogens which work by binding directly to the ligand-binding domain of the AR, preventing AR translocation and AR mediated transcription, are also being investigated. Phase III Trials of Apalutamide in both HSPC and CRPC (TITAN: NCT02489318 (63) and SPARTAN: NCT01946204 (64) respectively) have shown benefit in OS and rPFS. Similarly, the Phase III ARAMIS trial (NCT02200614) has shown darolutamide to improve metastases free survival (65); this drug has received recent FDA approval for treatment in the non-metastatic CRPC setting.

1.2.3 Radium-223

Radium-223, or alpharadin, is a radioisotope which emits high-energy alpha-particles over a short range (<100μm). These particles induce double-strand DNA breaks in adjacent tumour cells without a significant bystander effect, sparing normal tissue. The phase III ALSYMPCA trial (NCT00699751: alpharadin in symptomatic prostate cancer) showed a significant improvement in overall survival (of almost 3 months) compared with treatment with placebo from radium-223, with radium-223 also delaying symptomatic skeletal events and improving quality of life (66).

Radium is given intravenously for a total of 6 four-weekly cycles, although the optimal dose, schedule and duration of treatment again is not yet well defined. Due to its highly localized activity, radium-223 is generally well tolerated with a favourable side-effect profile. Common side effects seen include fatigue, gastrointestinal disturbance and bone pain. Haematological toxicity, including anaemia, thrombocytopenia and leukopenia, can be seen due to effects on the adjacent bone marrow. However, this is usually mild and can be treated with supportive treatment until the bone marrow recovers (67).

Eligibility criteria for the ALSYMPCA trial only allowed patients with bony metastases and no visceral disease, which means that radium-223 should not be recommended to patients who have disease outside of their skeleton, that is, nodal (>3 cm in short-axis) or visceral metastases or large volume soft tissue disease (68). Developments in alpha-particle emitting radioimmunoconjugates are likely to further transform the treatment of advanced prostate cancer. Trials are currently underway, for example, with antibodies to prostate-specific membrane antigen (PSMA) linked to alpha particles emitting radioisotopes showing a huge potential for patient benefit. The usage of gallium-PSMA positron-emitting-tomography (PET) may be a useful predictive biomarker for these agents (69).

1.2.4 Sipuleucel-T

Although not widely used, sipuleucel-T is currently the only form of immunotherapy approved for the treatment of mCRPC, and was the first therapeutic cancer vaccine to gain FDA approval. Sipuleucel-T is an autologous dendritic cell vaccine whereby a patient's peripheral blood mononuclear cells, including antigen-presenting cells, are initially extracted by leukapheresis. These are then activated *ex vivo* with a fusion protein

(PA202), which contains prostate acid phosphatase and granulocyte macrophage colony-stimulating factor. The activated product is then infused back into the patient, and this infusion triggers the patient's own immune response into attacking their disease (70). Several positive studies have indicated that this agent has antitumor efficacy, including a small phase III trial that showed an improvement in OS of more than 4-months in patients randomized to sipuleucel-T versus placebo (71), although some concerns have been raised about the design of this trial (72). Questions regarding its efficacy and side-effect profile, as well as high cost because of the expensive cost-of-production (estimated at ~$35,000 per cycle) (73) have meant that use is currently limited.

Based on evidence from clinical trials, the FDA-recommended dosage should be for three complete doses to be given via intravenous infusion at approximately 2-week intervals. Side effects include those associated with the initial leukapheresis procedure to harvest the patient's mononuclear cells (e.g., bleeding, bruising, and light-headedness), the infusion (e.g., rigors and pyrexia), and treatment itself (commonly fatigue, nausea, and headache) (74,75).

1.2.5 Symptom control

The therapies for mCRPC discussed thus far offer a varying degree of survival benefit, but it is important to remember that symptom control is of paramount importance in the management of advanced prostate cancer. A multidisciplinary team approach, including strong palliative care team involvement is also vital in holistic management of the patient (76,77). Other supportive treatment, with medical interventions such as blood transfusions for symptomatic anaemia and radiotherapy for painful bone metastases must also be regularly considered. Furthermore, in patients with metastatic disease at diagnosis who have never received primary treatment to the prostate itself, due consideration should be given to local control as early as possible to abrogate potentially devastating local complications such as fistulae formation and urinary obstruction (78). Studies are ongoing evaluating whether local therapy in patients with metastatic disease at diagnosis has an impact on outcome and quality of life, the results of which are eagerly awaited. In the interim, the treatment of primary disease should not be overlooked in this subgroup of patients with aggressive disease.

1.2.6 Future therapies

Despite these therapeutic advances, the prognosis and outlook for mCRPC patients remains bleak, with the plethora of available treatments realistically only providing a small survival benefit. Treatments effective for CRPC are now showing survival benefit in the HSPC setting (19,79,80), improving OS but potentially further limiting the available options for men with CRPC. It is now widely recognised that the landscape of prostate cancer is evolving, and increased understanding of the heterogeneity of the disease together with the identification and validation of predictive biomarkers could improve disease management and guide patient-specific targeted therapies (12,81).

1.3 The genomic landscape of CRPC

The development of next-generation sequencing techniques has driven significant advances in our understanding of the genomic landscape of CRPC and allowed more detailed study of its evolutionary history. In 2015, a landmark multi-institutional study published by Robinson et al identified that up to 90% of mCRPC cases possess “clinically actionable” molecular aberrations (81). This study and the common pathways affected are depicted in ***Figure 1-3***.

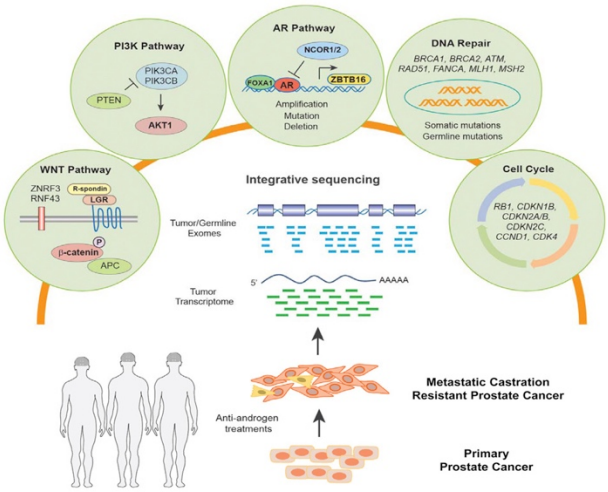

Figure 1-3: Graphical abstract from seminal 2015 Cell paper by Robinson et al (81).

Here key pathways are displayed in which clinically actionable aberrations are detected in up to 90% of CRPC cases.

1.3.1 Actionable aberrations

By performing whole-exome and transcriptome sequencing of biopsy specimens from 150 mCRPC patients, Robinson et al., were able to describe the mutational landscape of mCRPC. Many of the oncogenic mutations identified included those affecting the AR pathway (63%), PI3K pathway (49%), and DNA repair pathway (23%) ***(Figure 1-4)***. In the vast majority of patients in whom actionable aberrations were identified, the importance of performing fresh biopsies in patients was shown as many of these changes were not identified in their primary prostate cancers (82). A brief summary of the key pathways affected is provided below.

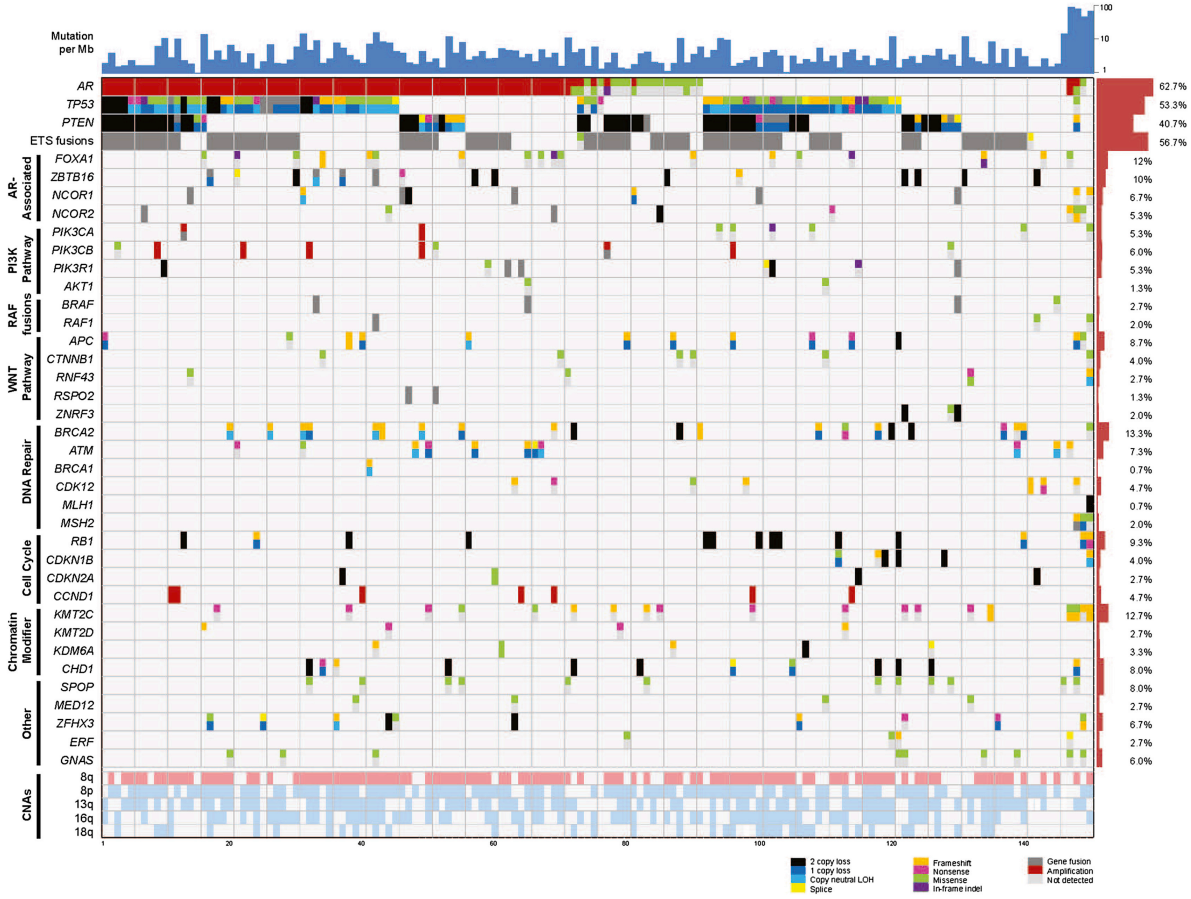

Figure 1-4: Integrative landscape analysis of somatic and germline aberrations in metastatic CRPC.

These were obtained through DNA and RNA sequencing of clinically obtained biopsies by Robinson et al (81)

1.3.1.2 AR pathway

The role of the androgen receptor and androgen receptor signalling is well recognised as the cornerstone in treating advanced prostate cancer, and as such has been discussed at the beginning of this chapter.

1.3.1.3 PI3K pathway

It is widely accepted that many mCRPC patients (~50%) have activation of the PI3K/AKT pathway, which plays a vital role in tumour growth, proliferation, survival, and also is implicated in resistance to therapies (83,84). Functional loss of the protein PTEN, which down-regulates this pathway, is found in >40% of metastatic prostate cancers, due to gene deletions, methylation, micro-RNA (miRNA) expression, mutations and post-translational modifications (85). PTEN loss is known to be associated with advanced disease and poor outcome (59,85–87).

Additionally, studies have shown crosstalk between the PI3K pathway and AR signalling, demonstrating that PTEN loss results in increased AKT activation and up-regulation of AR signalling, through p110β (88,89). This research, together with other studies, has provided a strong rationale for developing combination strategies targeting the PI3K pathway. Preclinical work and Phase I studies conducted testing single agent AKT inhibitors have had modest results thus far (90,91), which is likely multifactorial including due to the crosstalk between signalling pathways and to tumour heterogeneity. The results of further, much-needed trials exploring combination therapies, are eagerly awaited; for example, those combining p110β and AKT inhibitors with next-generation AR antagonists, such as abiraterone and enzalutamide.

1.3.1.4 DNA repair

Mutations in DNA repair have been identified in mCRPC, and these have important clinical implications. It is well established that genes involved in homologous recombination (HR) repair (e.g. *BRCA2*, *BRCA1*, *PALB2*, and *ATM*) are commonly deleteriously aberrant in this disease. Patients with deleterious germline *BRCA2* mutations have been identified as having an increased risk of prostate cancer (92,93). Furthermore, both germline *BRCA1* and *BRCA2* mutations are associated with higher grade and stage of cancer at diagnosis, and with worse overall outcomes (93,94).

Targeting these HR defective cancers has opened doors for the treatment of mCRPC. A trial reported in 2015 showed the antitumor activity of olaparib, a poly(adenosine diphosphate [ADP]-ribose) polymerase (PARP) inhibitor, in patients with both somatic and germline aberrations in *BRCA* and other genes involved in HR DNA repair (95). PARP is an enzyme key to DNA repair, and PARP enzyme inhibition has already been

well-established as a treatment for ovarian cancers (96,97). The study led by Mateo et al. has resulted in the FDA granting "breakthrough" designation in January 2016 to support the accelerated approval of olaparib for monotherapy of *BRCA1*, *BRCA2*, or *ATM*-gene-mutated mCRPC patients.

Although not currently approved for mCRPC treatment, phase II trials that include platinum-based chemotherapy in unselected mCRPC patients have shown some antitumor activity (98,99). Platinum salts work similarly to PARP inhibitors, causing double-stranded DNA damage by inducing inter- and intra-strand DNA cross-links. This DNA damage and resultant tumour cell death have been shown to induce PSA and radiological response in patients, as well as increase progression-free survival to some degree in unselected patients. However, failure to optimally identify a target group may, at least in part, explain failed registration trials. Further studies examining the safety and efficacy of platinum-based chemotherapy in selected groups of biomarker-positive patients with differing DNA repair pathway aberrations are now warranted.

1.3.1.5 Mismatch repair

Mismatch repair (MMR) defects have also been reported in a subset of prostate cancers; carriers of Lynch syndrome with deleterious aberrations of MMR genes also have an increased prostate cancer risk (100,101). The prevalence of MMR aberrations has been estimated to be in the region of 3-12%, depending on assay selection (81,100), with identification of these defects opening up a therapeutic avenue for immunotherapy strategies in CRPC (102,103). MMR protein loss of function (e.g., caused by mutations in *MLH1, MLH2* and *MSH6*) is associated with microsatellite instability and high mutational load. High-mutation frequency is thought be resultant in a higher burden of tumour-specific neo-epitopes or neoantigens, that allow for enhanced immune recognition. Targeting immune checkpoints, for example, inhibiting CTLA4 and PD-1, may therefore up-regulate the body's immune response to these neoantigens (104). Using immunotherapy to block the PD-1 axis is already established for the treatment of various tumour types, with nivolumab and pembrolizumab (both anti-PD1) having been FDA-approved for the treatment of melanoma and non-small-cell lung cancer (NSCLC) (105–108). As a higher mutational load is also associated with other DNA repair defects (109), there is now a strong rationale for evaluating immunotherapy and combination strategies for targeting this subset of mCRPC. Several clinical trials are now underway

evaluating the role of PD1 inhibitors and other drugs both alone and in combination in CRPC (e.g. NCT02787005, NCT03506997 and NCT02861573).

1.3.1.6 WNT pathway

WNT signalling has been identified as one of the key oncogenic pathways in multiple tumour types, and is particularly well documented in colon cancer (110). WNT pathway dysregulation can occur through aberrations of downstream components such as APC and β-catenin or overexpression of WNT ligands and co-stimulants.

The WNT cascade is thought to act as a master regulator, integrating signals from PI3K/mTOR, MAPK, and AR pathways (111,112), and has become an attractive pathway to target in CRPC. WNT aberrations have been identified as immunosuppressive (113); a variety of therapeutic agents have been developed against them, which range from monoclonal antibodies to small molecule inhibitors, with clinical trials ongoing (114).

1.3.1.7 Cell cycle

Both germline and somatic aberrations in cell cycle genes have been implicated in prostate cancer development and prognostication in the hormone-sensitive and castrate-resistant setting. Dysregulation of the cell cycle and resultant inappropriate cell proliferation is one of the key driving features of cancer. The key phases and proteins involved in the cell cycle are depicted in ***Figure 1-5***. Cell cycle alterations include deletions of *RB1, CDKN1A/B, CDKN2A/B* and *CDKN1A* and *CDKN1B* polymorphisms have been identified as being related to increased risk of developing advanced prostate cancer (112).

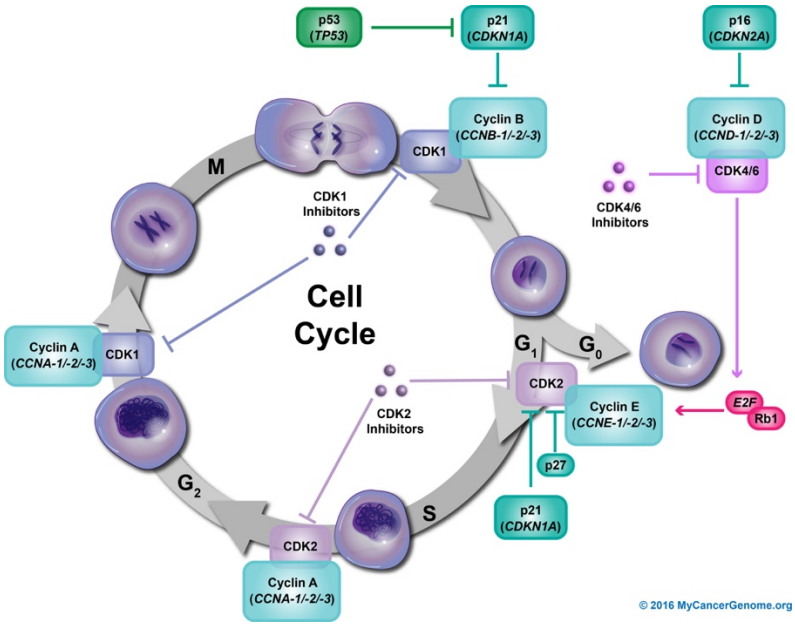

Figure 1-5: The Cell Cycle

The cell cycle, encompassing four phases including G1 (gap phase 1), S (DNA synthesis), G2 (gap phase 2) and M (mitosis). Control of the cell cycle is by the cyclin-dependent kinases (CDKs) and cyclins. (115)

RB1, a central protein in cell cycle control exerts its role in a hypophosphorylated state as a negative regulator of E2F transcription factors. *RB1* loss is one of the most frequent cell-cycle aberrations identified in CRPC, and is thought to occur in approximately 20% of cases (116). Importantly, RB1 loss has been linked with a shift from luminal to basal cells associating with a neuroendocrine phenotype (117); this may have important clinical implications (115).

Amplification of the kinases *CDK4* and *CDK6* has also been implicated, which is also of particular relevance with the role of CDK4/6 inhibitors now being established in advanced breast cancer (118). CDK4/6 phosphorylate RB1, releasing E2F transcription factors and allowing cell cycle progression (117). Inhibition of CDK4/6, for example with the drug Palbociclib, which acts upstream of RB1 requires intact RB1 protein to be effective. The role of these inhibitors in both HSPC and CRPC is also being explored.

1.3.2 Clonal evolution

As our understanding of the different genes, and their corresponding pathways that are aberrant in metastatic prostate cancer increases, this growing body of evidence also demonstrates inter- and intra-tumour heterogeneity and clonal evolution. This occurs not

only during carcinogenesis but also throughout treatment, resulting in acquired drug resistance. This “clonal diversification” is described by Gundem et al (2015) as a requirement of the cancer to bypass ADT and results in driving sub-clones towards therapeutic resistance (82).

1.3.3 Genomic analysis

Data from The Cancer Genome Atlas (TCGA) (119) and Stand Up to Cancer (SU2C) (81) have identified the single nucleotide mutation burden in the overall prostate cancer landscape to be relatively modest compared to that of other malignancies such as melanoma (120) (***see Figure 1-6);*** the overall average mutation rate in prostate cancers is estimated to be in the region of 4 mutations per megabase (81). Despite this, there is a noticeable proportion of large-scale copy number events and structural alterations that may be clinically actionable; recent advances in next-generation sequencing (NGS) technology and bioinformatics have hugely enhanced our understanding of these devastating diseases.

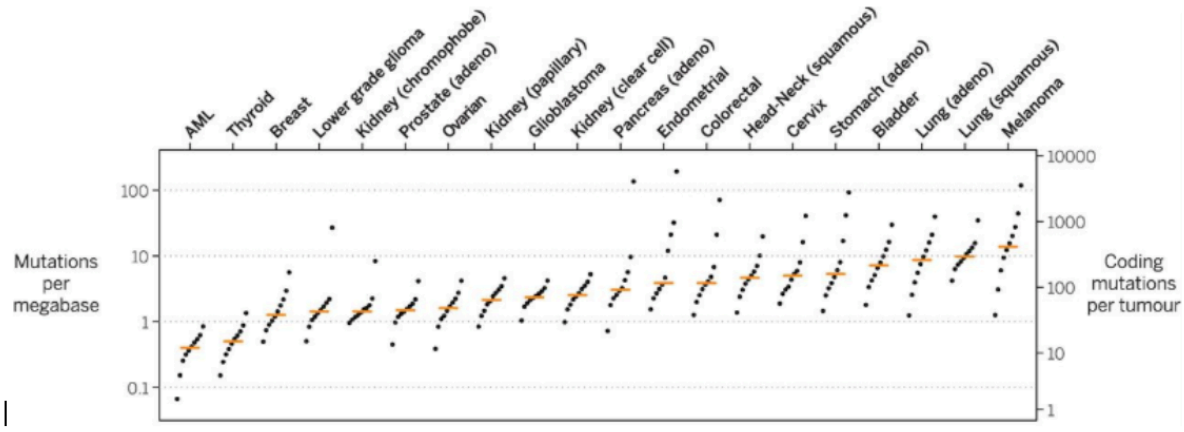

Figure 1-6: Mutation burden in 20 tumour types (120)

The median mutation burden is shown as a dot plot (substitutions and indels and orange bars denote the median burden of all samples.

1.3.4 Next Generation Sequencing

Next generation sequencing, is a term used to refer to a newer collection of sequencing techniques developed following its predecessor, Sanger sequencing. The advancement

of sequencing technology has allowed an impressive increase of data quality and throughput which is, perhaps most importantly, now performed at a reduced cost (121).

Along with technological advances, significant bioinformatic improvements such as the development of tools like the Genome Analysis Toolkit (GATK) and ichorCNA, have also played an important role in advancing this field. GATK, which allows the mapping of genome sequencing data to a reference and produces high-quality variant calls for downstream analysis (122) and ichorCNA, which was developed by the Broad Institute for estimating tumour fraction in cell-free DNA (123), are just two examples in a growing collection of publicly available computer software.

1.3.4.1 Targeted sequencing

Targeted next-generation sequencing (NGS) is a now widely-used tool, providing clinicians with the ability to implement genomics in everyday practice, and has the advantage of providing valuable information at a lower cost and within a shorter timeframe due to decreased bioinformatic requirement. Here, selected genes only are captured and sequenced; this can be with commercially available panels with key pre-selected genes or custom-made with varying panel sizes to allow investigation of specific genes of interest.

1.3.4.2 Whole-exome sequencing (WES)

Whole-exome sequencing (WES), where the entire coding region of the genome is captured and sequenced, is another cost-effective way of detecting variants implicated in disease, and has demonstrated potential in detecting clinically relevant alterations (124). Whilst it is recognised that WES provides more information than sequencing a smaller targeted gene panel, key limitations of WES include not sequencing proportions of the genome which may have important oncogenic impact, for example intronic rearrangements (125).

1.3.4.3 Whole genome sequencing

Gaining higher coverage with low-pass whole genome sequencing is an effective approach to assess genome-wide copy number events (126), with advances in technology making this more cost-efficient and allowing for high-throughput analyses of

samples. Aside from gene-level copy number events, other biomarkers from sequencing cfDNA, such as percentage of genome altered and average copy-number fragment size have also been implicated as informative (127,128).

Using these advances in sequencing techniques to monitor these evolutionary changes, and targeting treatments appropriately, remains a key clinical challenge faced by physicians. The importance and potential utility of blood-based assays or "liquid biopsies" in this setting is becoming increasingly recognized in clinical practice and trial design. "Liquid biopsies" provide a less invasive approach to interrogating tumours by tissue biopsies, which are frequently unfeasible, associated with morbidity, and cannot be performed serially.

1.4 Liquid biopsies

Over the past several years, two main forms of "liquid biopsy" have emerged:

i) Circulating (plasma) cell free (cf) nucleic acids including DNA (cfDNA) shed by tumour cells into blood.
ii) Circulating tumour cells (CTCs), intact rare cells found in blood, which can be separated and counted as well as genomically characterised.

These two main forms of investigation have been widely recognised to have the potential to change clinical practice, and their use is slowly becoming more widespread in monitoring disease, response to treatment and in identifying drug resistance. cfDNA and CTCs can provide complementary information; characterising intrapatient heterogeneity is more feasible from the analysis of CTCs, but acquiring and studying cfDNA is often easier and less costly in the majority of patients with advanced cancer.

1.4.1 Circulating nucleic acids

Although cfDNA is more widely studied, the role of other circulating nucleic acids including mRNA, microRNA (miRNA) and long non-coding RNA (lncRNA) is also being investigated. These nucleic acids are all shed in the blood of cancer patients in both primary and metastatic disease, probably through necrosis, apoptosis and potentially also through active release.

1.4.1.1 Cell free DNA

The presence of cfDNA was first described by Mandel and Metais in 1948 (129); it is now widely acknowledged that cancer patients have higher overall levels of cfDNA but that detectable levels are also found at low levels in healthy volunteers (130). The DNA released into the peripheral circulation from the tumour has been referred to as circulating tumour DNA (ctDNA), and this constitutes varying proportions of the overall cfDNA. The ctDNA fraction, although usually low, tends to be a reliable biomarker of tumour burden, but with considerable variability being observed (131). Sensitive methods of detection are therefore required to identify genomic changes, such as mutations and copy number alterations, in these low levels of ctDNA. The minimally invasive nature of ctDNA analysis has potentially transformative clinical utility, allowing monitoring over multiple timepoints in the course of disease. This is summarised in ***Figure 1-7***. Here we see the promise of cfDNA as a biomarker, in detecting cancer early, detecting minimal residual disease following definitive treatment, in molecular profiling and stratifying treatment appropriately, in identifying resistance to treatment and to monitor clonal dynamics.

Large studies in multiple tumour types have shown reasonably high levels of concordance rates (>80%) between contemporaneous plasma and tissue samples obtained for key cancer specific alterations (123,132), confirming that cfDNA testing may be a useful alternative to the current gold standard of testing tumour tissue directly for diagnostic purposes. Monitoring cfDNA levels may also have major implications in disease screening and in detecting disease recurrence post-definitive treatment e.g. surgical resection. Research into both breast (133) and colorectal cancers (131) has highlighted the role of cfDNA in identifying patients with residual disease and at risk of relapse.

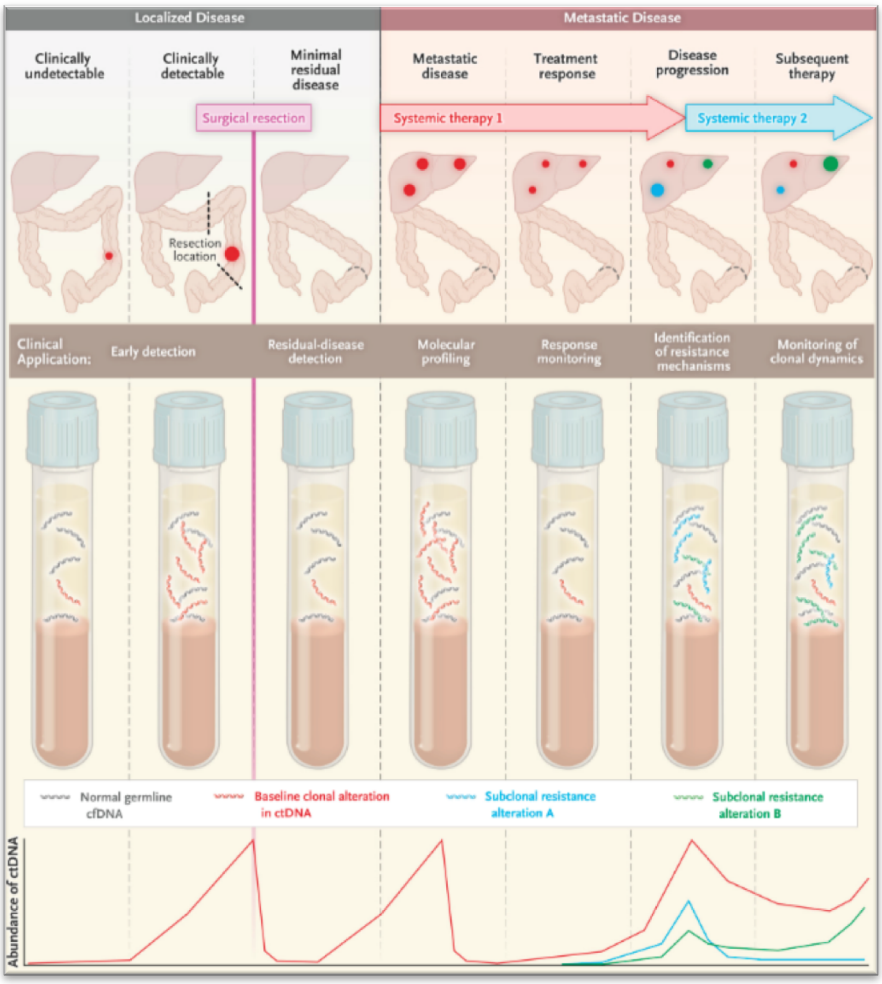

Figure 1-7: Clinical applications of cfDNA analysis at multiple timepoints throughout the natural course of cancer development (134)

We, and others have shown that responses to treatment in mCRPC can be monitored using plasma cell-free DNA (cfDNA); this can be both quantitative (135) and qualitative (136). We have recently shown that decreases in cfDNA concentration and mutation allele frequency from baseline significantly associate with response to treatment with Olaparib (a poly ADP-ribose polymerase [PARP] inhibitor). Furthermore, at disease progression, we detected the emergence of *de novo* mutations that likely result in acquired drug resistance. A patient with a germline deleterious *BRCA2* frameshift insertion that was present in both tumour and cfDNA at baseline presented at disease progression with a new frameshift deletion which restored the *BRCA2* reading frame. A second patient with a germline deleterious *BRCA2* mutation, initially responded but at progression cfDNA whole exome sequencing identified multiple clones with different, previously undetected, mutations all resulting in reversion of the *BRCA2* reading frame to normal (136).

Using these liquid biopsies to monitor disease has many advantages, and when analysed with next-generation genomics the study of cfDNA offers key insights into an individual's disease. Despite this, multiple limitations have been acknowledged specifically related to sample storage and handling and impact on cfDNA integrity (137), significant intra- and inter-patient assay result variability, as well as difficulties in dissecting intrapatient heterogeneity.

1.4.1.2 RNA

The advent of the human genome project in 2001 has increased our understanding of the human transcriptome immeasurably. Based on this work, it is now estimated that only ~2% of the genome serves as a blueprint for proteins, with a large proportion of RNA being "non-coding" (138). These non-coding RNAs (ncRNAs) are often split by their size into small ncRNAs (which include microRNAs) and into long non-coding RNAs.

1.4.1.2.1 microRNAs

Whilst RNA is generally unstable in the blood, microRNA (miRNA) which comprises short noncoding molecules made of 9-25 nucleotides, is very stable and can be easily detected. Tumour derived miRNA, which can be found in plasma, urine, saliva and semen, can be analysed by RNA sequencing. Certain miRNA signatures have been identified as significantly deregulated in cancer patients compared with healthy volunteers, signifying potential value in cancer diagnosis. Different miRNA signatures have been reported to be response biomarkers for both chemotherapy and radiotherapy, although reproducibility remains a challenge (139–141). Additional studies are warranted to further study the role of miRNA signatures for disease detection, prognostication, identification of minimal residual disease, tumour recurrence, and as a response biomarker.

1.4.1.2.1.2 Long non-coding RNAs

Long non-coding RNAs (lncRNAs) are RNA molecules longer than 200 nucleotides, and have also been implicated in prostate cancer carcinogenesis. Multiple mechanisms of actions including regulating gene expression and transcription have been described, with several key lncRNAs being identified as possible contributors to the pathophysiology of

prostate cancer (138,142). Cancer specific lncRNAs that have been identified to be exclusively associated with individual diseases may have roles in diagnosis and therapeutic monitoring (143). Anti-tumour strategies targeting lncRNAs are also being investigated, although much work remains to be done in fully understanding lncRNA biology prior to optimisation of these therapeutic strategies.

1.4.1.2.1.3Tumour educated platelet RNA

Preliminary research indicates that we may also be able to acquire data from non-cancer derived cells, including tumour educated platelets (TEPs). Tumour cells are hypothesized to interact with platelets in the circulation, “educating” them by activating surface receptors and altering cytokine expression and platelet mRNA (144,145). Investigating the mRNA profiles of these TEPs may provide additional information on cancer type, and be useful in combinatorial analysis with cfDNA, circulating tumour cells etc; work is ongoing to validate these findings.

1.4.2 Circulating tumour cells

Circulating tumour cells (CTCs) are rare cells found in the blood of cancer patients and were first described in 1869 by Thomas Ashworth (146); they are believed to be shed from tumours and circulate in the bloodstream. This process can occur at an early stage of cancer, although the number and type of CTCs have been reported to vary considerably between patients, stage of disease and tumour types. ***Figure 1-8*** demonstrates the variable numbers of CTCs identified in patients of different tumour types on Phase I clinical trials treated at the Royal Marsden Hospital over a 3 year period (147). As confirmed in other studies, higher numbers of CTCs were identified in colorectal, prostate and breast malignancies, with lower numbers detected in other tumour types like lung and sarcoma.

CTCs are thought to be detectable at 1 CTC per millilitre or less of blood in patients with advanced cancer, but precise identification remains difficult. Although multiple assays have been described for CTC evaluation, the only approved platform for their identification in metastatic breast, colorectal and prostate cancer remains the CellSearch® platform (Menarini, Silicon Biosystems, Bologna, Italy). This received FDA regulatory clearance in 2008 and has not improved since its introduction then. This analytically validated assay has been shown to have good reproducibility, displaying little

inter-laboratory and inter-patient inconsistency. The CellSearch® platform works by identifying CTCs based on epithelial cell adhesion molecule capture (EPCAM+), cytokeratin-positivity (CK+) and CD-45 negativity (CD45-). Several other CTC assays have been reported, but with different degrees of analytic validation and clinical qualification thus far. Other assays, which include techniques using manual immunomagnetic separation, centrifugation or filtration, enrich poorly for CTCs and cells are often lost in sample preparation.

CTC number is robustly associated with tumour burden and poor outcome, and declining counts have been seen with response to therapy particularly in breast (148) and prostate cancer (149). CTC cut-offs have been selected which separate patients into those with good or bad prognosis categories, and these also vary per tumour type. CTC counts >5 In breast and prostate cancers or >3 in colorectal cancers have been identified as an indicator of poor prognosis.

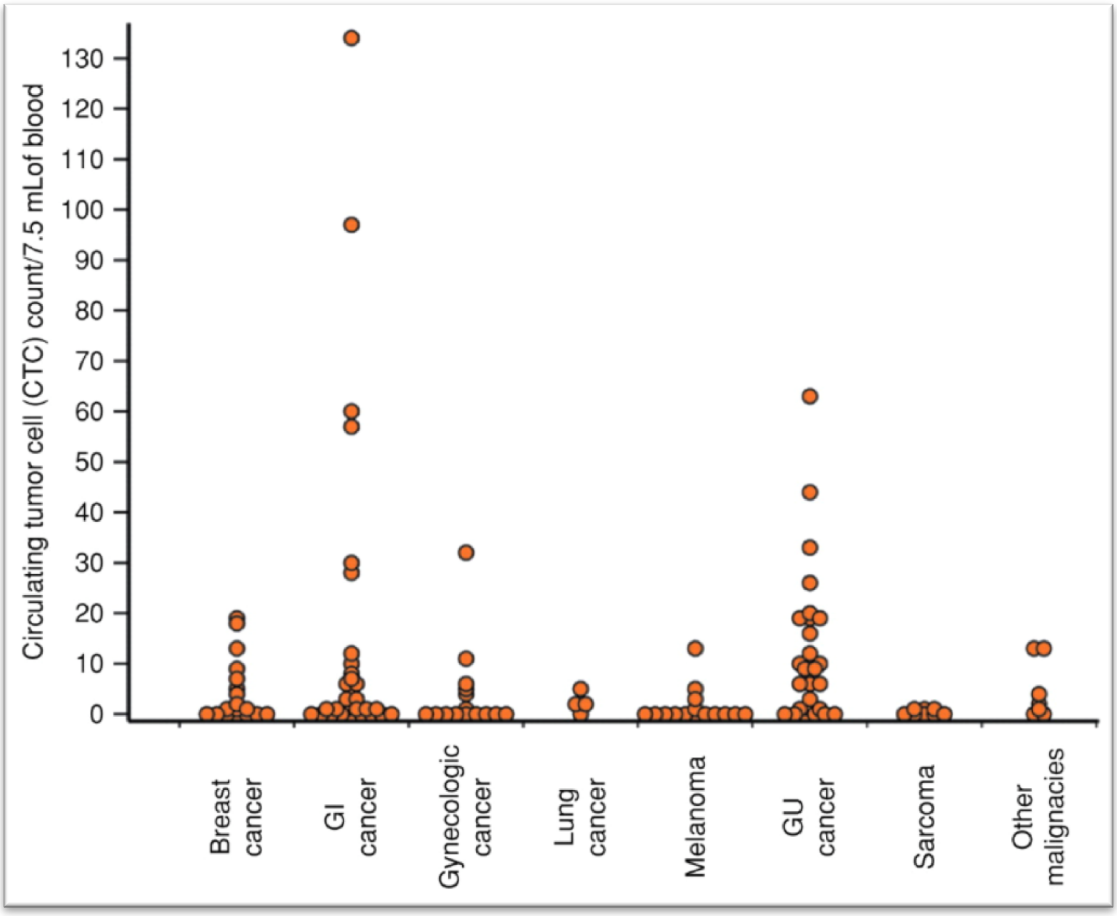

Figure 1-8: Distribution of CTC counts by tumour type

These data are from Phase I patients at a tertiary cancer centre (147)

CTC counts in themselves, as well as being highly prognostic can also serve to measure response to treatment and associate with survival, and may be true surrogate biomarkers of benefit to treatment. Performing molecular characterisation of CTCs allows investigation into tumour genomics, and allows a deeper exploration of heterogeneity than studying cfDNA alone. Single cells are amenable to most assays, including next generation sequencing (of both DNA and RNA), array comparative genomic hybridisation (aCGH) and immunohistochemical analysis such as by immunofluorescence and fluorescence *in-situ* hybridisation.

Given their diagnostic potential, CTCs may have utility in clinical trials; they may have utility for patient selection, to study pharmacodynamics and as response biomarkers. Indeed, the role of CTCs is being explored in this capacity in many ongoing clinical trials. However, even within prostate cancer, limitations in CTC detection have been acknowledged; several patients have undetectable CTCs despite relatively advanced or progressing disease, and even in those that do have large numbers there is difficulty in capturing these rare events and possible subsequent size-selection bias. Indeed, the infrequent numbers of cells that are generally captured in these studies has been a major limitation of CTC analyses thus far. We, and others, have therefore explored the role of apheresis in increasing the number of captured CTCs, and this is discussed further in ***Chapter 7.***

1.4.3 Immune cell studies

1.4.3.1 Neutrophil-to-lymphocyte ratio

The neutrophil-to-lymphocyte ratio (NLR), calculated simply from a differential white cell count which can be carried out at any routine haematology laboratory, has proven prognostic value in several disease states (150). Although a non-specific assay, this inexpensive and readily-available tool is probably a biomarker of cancer inflammation, with an elevated NLR at diagnosis associating with worse overall survival in a study of over 25,000 cancer patients (151).

Significant changes in neutrophil-to-lymphocyte ratio (NLR) during treatment correlate with treatment outcome (152) and predict the likelihood of response to treatment, associating with response to abiraterone and taxanes in advanced prostate cancer (153,154). High NLR levels may also correlate with increased myeloid-derived

suppressor cell counts, cells which have also been implicated in cancer biology and increased AR signalling.

1.4.3.2 Myeloid derived suppressor cells

Myeloid derived suppressor cells (MDSCs) originate from primitive haematopoietic precursors as a result of tumour-generated endocrine and paracrine factors, and have been found to accumulate in the blood, lymph nodes and tumour sites of cancer patients (155). They can be immunosuppressive, and support tumour growth, tumour survival and resistance to treatment (156). As well as correlating with high NLR levels, high MDSC counts have been associated with decreased response to treatment and shorter overall survival (157). Various subsets of peripheral MDSCs have been identified; these can be sorted by flow cytometry (FACS) and the proteins they release can be studied *ex vivo*; studies of these subsets and their cytokine release may also help to direct anticancer treatment. We have recently shown that interleukin-23 (IL23), a cytokine produced by MDSCs can cause activation of the androgen receptor pathway in prostate tumour cells, causing promotion of cell survival and proliferation in androgen-deplete conditions. Inactivating IL23 in mice restored sensitivity to ADT, with these results indicating that treatments blocking IL23 can be used to oppose MDSC-mediated castration resistance (158) .

There is now an urgent need to identify how these liquid biopsy components can be used as circulating biomarkers for the care of prostate cancer (and indeed all cancers) and transformative prospective trial data are eagerly awaited.

1.5 Biomarkers

The FDA definition of a biomarker is: “A defined characteristic that is measured as an indicator of normal biological processes, pathogenic processes, or responses to an exposure or intervention, including therapeutic interventions” (159). Many different types and categories of biomarker fall under this description; biomarkers can be molecular, histologic, radiographic and physiological characteristics.

FDA-established biomarker contexts are highlighted in ***Figure 1-9***. Prognostic biomarkers tend to be more easily identifiable, and are usually characteristics that have implications for patient’s overall survival or likelihood of having a disease-related

endpoint event. These different biomarker categories and their context of use is depicted in ***Figure 1-10.***

Figure 1-9: Different categories of biomarkers as per the FDA (159)

Although clinical outcomes are usually the most reliable clinical trial endpoints, biomarkers are often used as intermediate endpoints in clinical trials as a substitute for a direct measure of clinical outcome. This may occur if, for example, obtaining clinical outcome results may take many years and an alternative acceptable endpoint is more readily available. It is important to remember that although useful, biomarkers including those used intermediate endpoints do have limitations, and continual evaluation is of paramount importance.

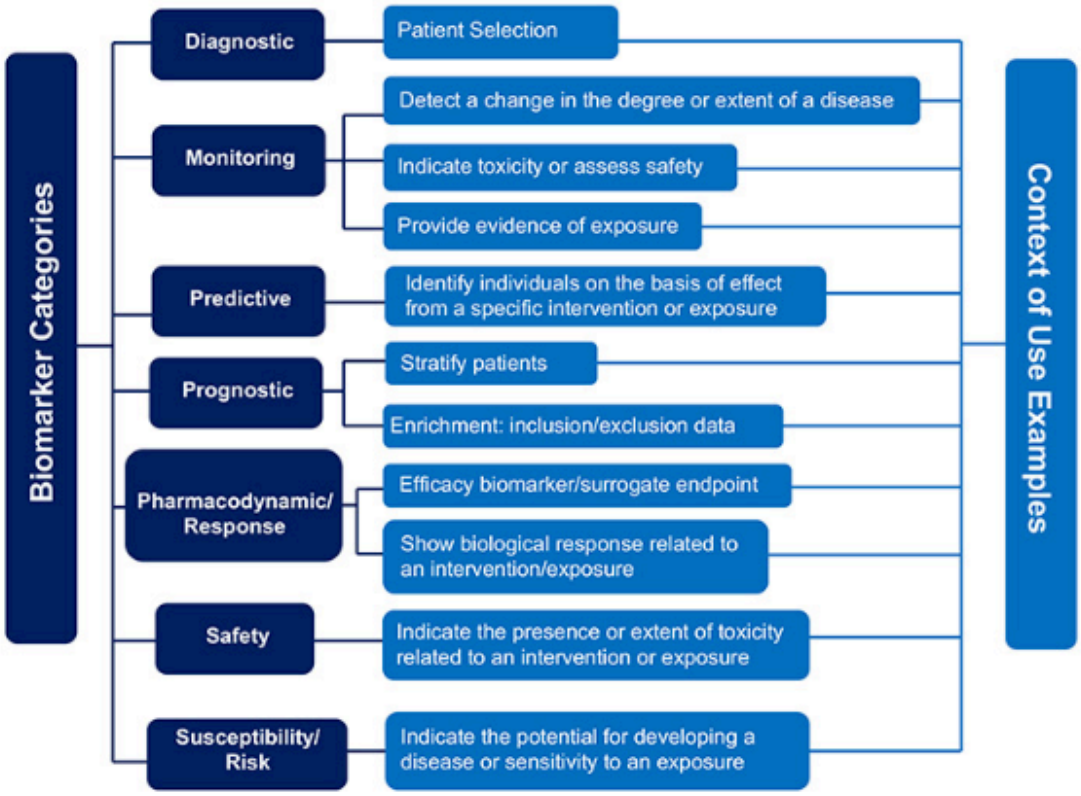

Figure 1-10: FDA Biomarker categories and examples of corresponding drug development uses (138)

1.5.1 Biomarker development

In order for biomarkers to become well-established in patient care, their development requires two important steps; analytical and clinical validation (160). Initially, analytical validation is important to ensure assay reproducibility and to calculate the risk of error and subsequent use in the clinical setting (161). Important variables to consider during analytical validation include sample handling, storage and processing, evaluating both technical and biological replicates, intra- and inter-observer reproducibility, the high and low limits of detection and the availability of suitable controls (162). Once analytical validation is established, clinical validation must occur, which is usually in the context of clinical trials. These aim to evaluate the effectiveness of a biomarker in impacting medical decisions in specific contexts of use (163), ensuring they are informative and have value by improving patient outcome. If a biomarker successfully undergoes analytical and clinical validation, it then undergoes a formal regulatory process in order to be qualified in a particular context of use.

Understandably, exploration of these biomarkers has significant cost implications, but conversely, liquid biopsies may be able to play a crucial role in limiting some of the huge financial burden that treating CRPC places on health systems (160). For example, identifying patients unlikely to respond to expensive anti-neoplastic therapies or recognising when to stop ineffective drugs could decrease treatment and toxicity related costs, with the obvious added benefit of preventing patients receiving potentially harmful and futile medication.

1.5.2 Biomarkers in prostate cancer

1.5.2.1 Prostate specific antigen

Prostate cancer differs from other malignancies in that biomarkers have been used in its management for many years. Initially, this was by monitoring prostatic acid phosphatase (PAP), which was first described in the 1930s to be present in the serum of men with metastatic prostate cancer (164). PAP was replaced by prostate specific antigen (PSA), in the 1980s, which was also detected in the serum of men and found to be more sensitive than PAP in monitoring disease (165). The PSA protein is encoded by the prostate-specific gene kallikrein 3 (*KLK3*) – part of a gene family of serine proteases located on chromosome 19q (166). Unfortunately, PSA lacks specificity; the protein can also be detected in a number of benign conditions including prostatitis and benign prostatic hyperplasia. Furthermore, variability in both sensitivity and specificity have been identified with different cut-off levels (167). Despite these major issues, PSA testing remains useful in clinical practice; PSA's relatively low-cost means it is currently used widely used in screening, diagnosis, detecting disease recurrence, in monitoring disease and response to treatment.

1.5.2.1.1 Screening and diagnosis

In the UK, the lack of reliable and reproducible tests means that there is no national screening programme, but PSA is often checked routinely and when clinical suspicion is high, in screening for and to help in diagnosing prostate cancer.

Since the introduction of PSA testing, there has been an increase in the number of localised and lower-stage prostate cancers diagnosed (168), nearly doubling the lifetime risk of men receiving a prostate cancer diagnosis. Determining the accuracy of PSA

testing is tricky, with the majority of men with normal PSA values not undergoing a tissue biopsy unless they have had an abnormal digital rectal examination or significant symptoms. This verification bias tends to overestimate sensitivity and underestimate specificity (169). National Institute of Clinical Excellence (NICE) Guidelines recommend considering a PSA test, together with a digital rectal examination to assess for prostate cancer in any men with lower urinary tract symptoms, erective dysfunction or visible haematuria (170).

The efficacy of screening using PSA has been questioned, with risks of overdiagnosis and complications associated with treatment undertaken for indolent disease being reported. A 2014 Cochrane Review (8) suggests that PSA testing should only be undertaken in men who express a definite preference for screening, and only after their clinician has thoroughly discussed the pros and cons of testing. A more recent meta-analyses suggested that suggested that screening *may* result in a small absolute benefit in disease-specific mortality over a 10 year period but, importantly, does not improve overall mortality (171). This needs to be closely weighed up with the risks associated with PSA screening, which include complications associated with biopsies and with treatment for prostate cancer.

1.5.2.1.2 Detecting disease recurrence

A rising PSA is usually the first sign of disease recurrence, and tends to be followed by clinical and radiographic progression. It is acknowledged that at low PSA levels, the likelihood of detecting metastatic disease is limited (172) and this often needs to be monitored closely, in conjunction with other markers, and sensitive imaging modalities considered.

1.5.2.1.3 Monitoring disease progression and response to treatment

The most recent consensus criteria reached by the prostate cancer working group (PCWG3) continue to report PSA response as an outcome measure, and suggest that PSA monitoring should involve careful recording of baseline values, nadir values and values at progression. PSA declines of 30% or 50% from baseline are associated with improved survival (173,174), and PSA rises with shorter survival (175).

The Prostate Cancer Working Group also acknowledges that a favourable effect on PSA may be delayed by greater than 12-weeks, and recommends ignoring any early rises (a

"PSA flare") where possible. However, we have shown that patients not achieving a 30% PSA decline after 4-weeks of abiraterone treatment have a lower likelihood of achieving a PSA response at 12 weeks and also have a significantly worse overall survival (176). In patients receiving treatment with Radium-223, mixed PSA responses have been reported, with studies suggesting PSA may be a more unreliable biomarker in treatment with bone-targeting agents (177). This is, at least in part, attributed to the mechanism of action of Radium-223, which does not target the androgen receptor and may therefore have less of an effect on PSA (178). These varied findings highlight the inconsistencies in PSA and the difficulty in using PSA values as a reliable biomarker.

1.5.3 Tissue biomarkers

Tissue based biomarkers are also used in prostate cancer, to varying degrees of success. Obtaining tissue remains the gold standard for diagnosis, and clinicopathologic variables such as Gleason grade and tumour stage remain useful in risk-stratifying patients (179). Whilst clinical trials are in progress using tissue-based assays to determine patient eligibility and stratify treatment accordingly, there are difficulties associated with this. Obtaining tissue is not always feasible; there may be contraindications to biopsy or tumour inaccessible. Monitoring disease progression with serial sampling is also problematic and can be associated with increased morbidity and mortality (180,181).

1.5.4 Unmet needs

It is widely acknowledged that there is an unmet and urgent clinical need for predictive biomarkers whose identification will allow us to better stratify patients according to the likelihood of therapeutic benefit. Some of these, discussed at a recent consensus meeting that I co-led will be discussed further in ***Chapter 4***. Circulating assays allowing detection of genes commonly aberrant in CRPC, such as those involved in DNA repair predicting PARP inhibitor sensitivity, and *PTEN* loss which may indicate sensitivity to AKT inhibition, have been considered as promising but in need of further development and validation.

1.6 Summary

Of all solid tumours, prostate cancer has some of the highest levels of cfDNA, and numbers of CTCs, which could may allow serial tumour genomic analyses during disease progression and on treatment. This potential can transform prostate cancer care, allowing a non-invasive and practical approach to stratifying treatment and allow serial disease monitoring, pursuing the study of both treatment efficacy and resistance. However, many questions remain unanswered as to the feasibility of this approach and to the lack of data and validation studies needed with regard to confirming the functionality of these circulating biomarkers. In this thesis, I aim to further explore this area of critically unmet need, focusing on cfDNA and CTCs in mCRPC.

2. Hypotheses and Aims

2.1 Hypotheses

I hypothesised that blood-based biomarkers, in particular plasma cell-free DNA (cfDNA) and circulating tumour cells (CTCs) can be used reliably and safely to identify advanced prostate cancer genomic aberrations. There is an urgent need for validation of these circulating biomarkers and international consensus regarding their use.

I further hypothesised that serial blood-based analyses could be more informative than single tumour analyses and can allow the study of disease evolution during treatment. Serial plasma cfDNA quantification and qualification may both prove informative, with these results being used to monitor and predict outcomes from taxane chemotherapy.

Lastly, I hypothesised that as CTCs are rare and difficult to capture events in the peripheral circulation, apheresis could be used to safely increase CTC numbers and allow for molecular characterisation. Taken together, using liquid biopsies to detect biomarkers for prognostic and predictive purposes could bring us closer to delivering precision medicine in a consistent manner, without subjecting patients to repeated tissue biopsies and their associated risks.

2.2 Aims

1) To gather clinicians and academics with expertise in the field of liquid biopsies to **determine a consensus regarding the use of circulating biomarkers** in clinical practice, and to present the findings of this meeting in an international consensus statement.

2) To **clinically qualify baseline and on-treatment cfDNA concentrations as biomarkers** of patient outcome in patients treated with taxane chemotherapy in two large, prospective Phase III clinical trials (FIRSTANA and PROSELICA).

3) To **optimise and validate low pass whole genome sequencing of cfDNA** from these plasma samples and to determine the prognostic and predictive power of any biomarkers identified.

4) To **evaluate the safety, tolerability and utility of apheresis** in increasing CTC yield and allowing the study of single cell genomics.

3. Materials and Methods

3.1 Sample collection and clinical data

All patient samples that were collected and analysed as part of this thesis were done with informed consent, under different institutional protocols. Peripheral blood samples and tissue samples were collected under the CCR2472 protocol approved by the Royal Marsden NHS Foundation Trust Hospital (London, UK). Details of blood samples collected are detailed in relevant chapters. Tissue samples collected were acquired from either prostatic diagnostic biopsies, transurethral resections of the prostate (TURPs), prostatectomies, or from metastatic disease biopsies. Metastatic samples included blind bone marrow trephine biopsies, or radiologically guided (ultrasound guided or computed tomography) biopsies of lymph node and visceral disease. Clinical data pertaining to these samples were collected retrospectively from the Royal Marsden electronic patient record system.

Peripheral blood samples were also collected as part of two prospective phase III trials, FIRSTANA (NCT01308567) (36) and PROSELICA (NCT01308580) (37). Again, all patients provided informed consent, and both studies were overseen by independent data monitoring committees. As these were international, multi-institutional studies, clinical data were collated by Sanofi Aventis and provided to us under a collaborative agreement.

In FIRSTANA, 1168 chemotherapy-naïve patients were randomised to receive either docetaxel 75mg/m^2 (n=391), cabazitaxel 20mg/m^2 (n=389), or cabazitaxel 25mg/m^2 (n=388). In PROSELICA, 1200 patients who had previously progressed on docetaxel were randomized to cabazitaxel 20mg/m^2 (n=598) or 25mg/m^2 (n=602). Both studies incorporated overall survival (OS) as the primary endpoint, with secondary endpoints including radiological progression-free survival (rPFS), PSA response, and RECIST response in patients with measurable disease (Version 1.1) (182). rPFS was defined as per Prostate cancer working group 2 criteria (183).

The study designs of both FIRSTANA (A) and PROSELICA (B) are depicted in ***Figure 3-1.*** Blood was collected for exploratory biomarker analyses, with samples taken during screening (SCR), at Cycle 1 (C1), C2, C4 and end of study (EOS).

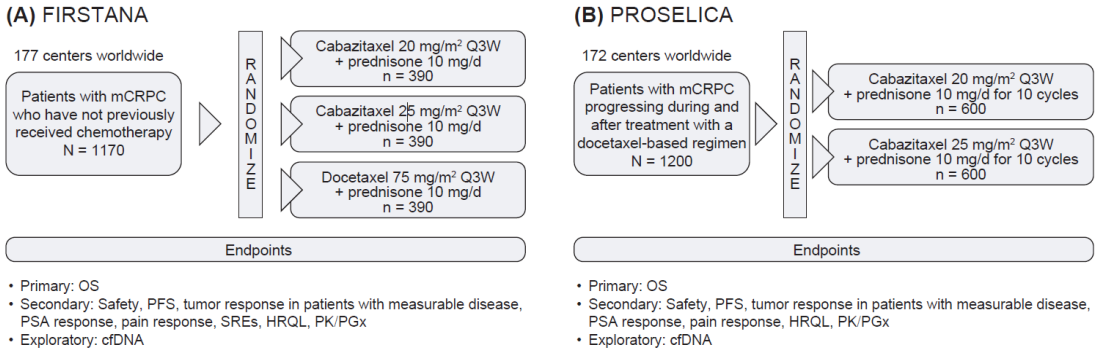

Figure 3-1: Study designs of FIRSTANA and PROSELICA

FIRSTANA (A) recruited chemotherapy naïve mCRPC patients and PROSELICA (B) recruited mCRPC patients who had progressed following 1 line of taxanes therapy

Blood and apheresis samples were collected under the CCR2996 protocol approved by the Royal Marsden NHS Foundation Trust Hospital (London, UK). Clinical data were collected prospectively for consenting patients from the Royal Marsden electronic patient record system. Apheresis was undertaken at the point of treatment discontinuation or prior to starting a new line of therapy (either within a clinical trial or as standard of care therapy).

Patients were deemed eligible to undergo apheresis if they met strict inclusion criteria, including having histologically confirmed mCRPC, detectable peripheral blood CTCs, adequate bilateral antecubital fossa access and no evidence of coagulopathy. Patients underwent thorough clinical assessments including medical history and physical examination, as well as blood tests prior to the procedure which comprised of a full blood count, biochemistry and coagulation tests as well as a peripheral blood CTC count. Patients were monitored closely during the procedure, and a full safety follow-up assessment was carried out at 30 days after the procedure.

All studies were conducted in accordance with the Declaration of Helsinki and with appropriate ethical approval of corresponding committees.

3.2 DNA extraction

3.2.1 Tissue

All tumour samples used were reviewed by a pathologist (Dr. Daniel Nava Rodrigues or Dr. Bora Gurel, within the Cancer Biomarkers Team at the Institute of Cancer Research) prior to sectioning. FFPE (formalin-fixed, paraffin embedded) tumour blocks with an estimated tumour content of >70% were used for DNA extraction. Six sections of at least 10µm thickness were cut, with additional sections being used for smaller samples. Tumour samples with a lower estimated tumour content (<30%) were microdissected to increase tumour purity.

Tissue DNA was manually extracted using the QIAamp DNA Tissue kit (Qiagen, Hilden, Germany), according to manufacturer instructions (184). In summary, the paraffin from the FFPE samples was dissolved in xylene and removed. The samples were then lysed under denaturing conditions with a short proteinase K digestion step. They were then incubated at 90°C to reverse formalin crosslinking. Samples were purified using the QIAamp MinElute spin columns (Qiagen, Hilden, Germany) and the final DNA eluted in 200µl water and stored at -20°C.

3.2.2 Plasma

Under the Royal Marsden 2472 protocol, blood was collected in CTP tubes or Streck^{TM} tubes (Streck ,Nebraska, USA) from patients at specified time points (during screening, during trial drug administration, and at the point of disease progression). Within the Sanofi-Aventis trials (FIRSTANA and PROSELICA), heparinized plasma tubes (BD Vacutainer, BD Biosciences, New Jersey, USA) were used for blood collection as per the trial protocols.

cfDNA was extracted using the QIAsymphony (Qiagen, Hilden, Germany) DSP Circulating DNA Kit as per the manufacturer's instructions (185). An outline of the workflow is detailed in ***Figure 3-2***. A minimum of 1ml of plasma, and a maximum of 4ml, was used for cfDNA extraction. When less than 4ml was available, samples were made up to 4ml using phosphate buffered saline (PBS); 24 samples were prepared for extraction per run. The QIAsymphony was set up following on-screen instructions for initialization. The elution rack, reagent cartridge and consumables were loaded as

prompted, followed by the sample rack and proteinase K. After the QIAsymphony robot had completed DNA extraction, samples were quantified as described below.

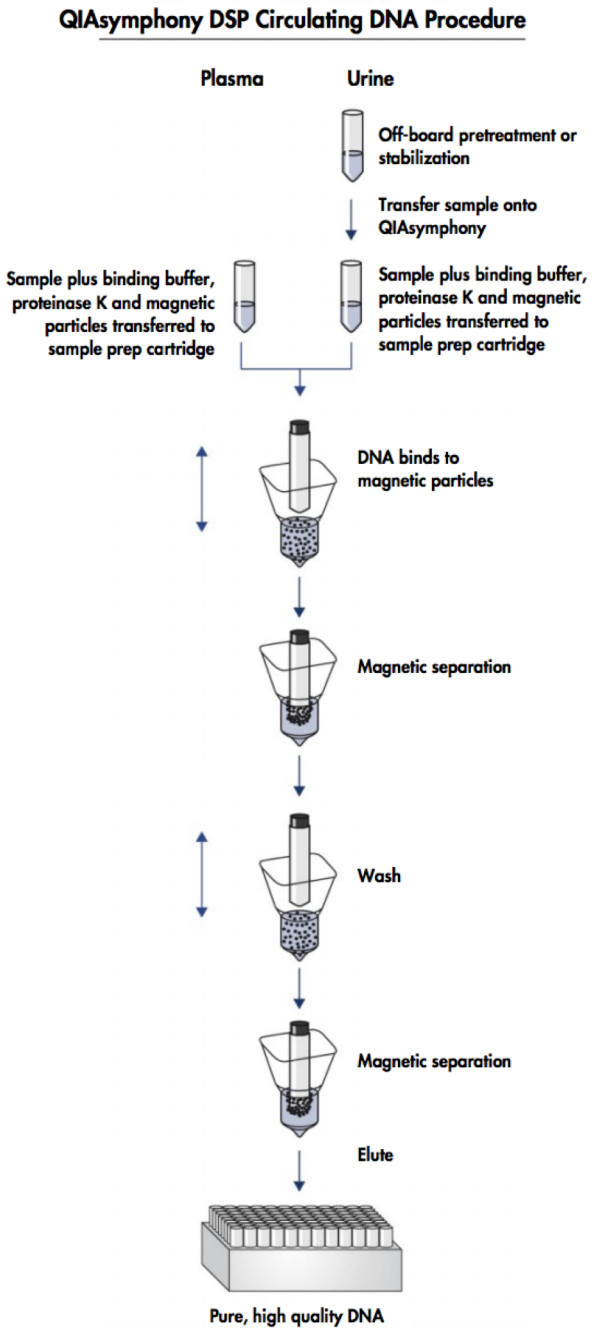

Figure 3-2: QIASYMPHONY DSP Circulating DNA Procedure (185)

For samples collected in Lithium heparin tubes, prior to the availability of Streck™ Tubes, cfDNA was extracted as above, and then an additional step to remove the heparin was carried out to remove the inhibitory PCR effect of heparin. Heparinase I from *Flavobacterium heparinum* (Sigma-Aldrich, Missouri, USA) was used as per

manufacturer protocol to remove the heparin prior to sequencing. Briefly, 10µl of 1M Tris pH 7.5, 2µl 1M $CaCl_2$ and 500µl of water were added to 50 units of Heparinase I. The heparinase solution was added to each cfDNA sample (1U [2µl] per 100ng), gently vortexed and then incubated at 37˚C for 2 hours (186).

3.3 DNA quantification and qualification

For both DNA extracted from tissue and for cfDNA, quantification was carried out using the Quant-iT high-sensitivity Picogreen double-stranded DNA Assay Kit (Invitrogen, California, USA) as recommended by the manufacturer's guidelines (187) and laboratory standard operating procedure (SOP). This is summarised here. Firstly, Quant-iT reagents were equilibrated to room temperature. A working solution was made by diluting the Quant-iT dsDNA HS reagent 1:200 in Quant-iT dsDNA HS buffer; 200µL of the working solution was then loaded into Eppendorf tubes, and 10 µL of each λ DNA standard or 1-10 µL of sample to be measured was added to separate tubes. These were then vortexed, spun, and added to consecutive wells of a microplate.

Fluorescence was read using a microplate reader (excitation/emission maxima are 510/527nm). Standard fluorescein wavelengths (excitation/emission at ~480/530nm) were used for this dye. A standard curve was calculated to determine the DNA amounts, with the background (standard 0 ng/µL) subtracted. For the λ DNA standards, I plotted amount vs. fluorescence and fitted a straight line to the data points. The background (blank) was subtracted from the samples, and results allowed me to calculate the DNA concentrations of my samples. Raw data were processed using the software 'gen5', which was also used to generate the standard curve. As a rule, a p value of 0.98 or higher was required to accept the standard curve, otherwise the process was repeated to ensure the accuracy of DNA quantification.

DNA quality was also checked using the Agilent BioAnalyzer (Agilent Technologies, California, USA), predominantly using the High Sensitivity D1000 Screentape and kit as per manufacturers guidelines (188). In brief, the HSD1000 buffer was allowed to equilibrate to room temperature, then vortexed and spun down prior to use; 2µL of HSD1000 buffer was mixed with 2µL of sample, vortexed at 2000 rpm for 1 minute, and then spun down. Samples were loaded onto the Tapestation 2200 instrument and run on a HSD1000 Screentape, using the electronic ladder for profile comparison. This SOP is represented in ***Figure 3-3***.

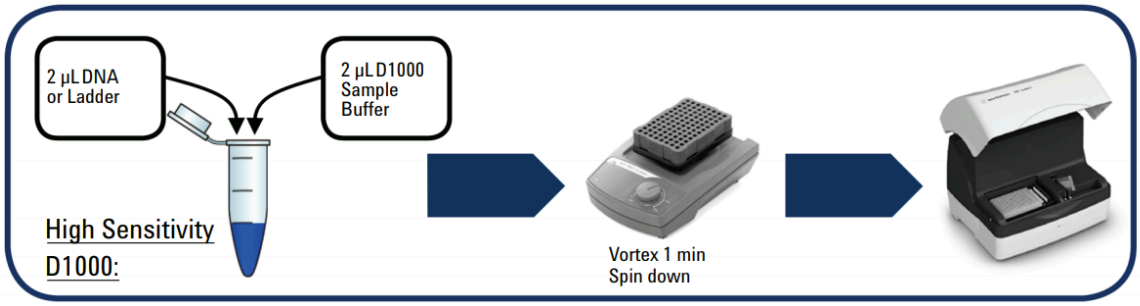

Figure 3-3: Agilent bioanalyzer workflow (188)

3.4 Library preparation

3.4.1 Targeted library preparation

Libraries were sequenced using a targeted AmpliSeq™ panel (ThermoFisher Scientific, Massachusetts, USA) of 30 genes, pre-selected for their putative roles in taxane resistance was custom-designed. These genes are listed below in ***Table 3-1***. Picogreen measurements of DNA concentration were used to determine a minimum of 10ng input DNA per sample for library preparation.

Table 3-1:Customised AmpliSeq panel of 30 genes pre-selected for their known role in prostate cancer or cell-cycle

MUL1	**E2F4**	**CDKN2A**
E2F2	**TP53**	**CTRL**
PCBP1	**SPOP**	**CCND1**
RHOH	**E2F1**	**CDK4**
CHD1	**EPHB2**	**FOXA1**
E2F3	**NLRP3**	**ZFHX3**
E2F5	**TET3**	**LASP1**
DKK3	**PRSS48**	**SEH1L**
CDKN1B	**APC**	**SDC4**
RB1	**CDK6**	**PTEN**

Library construction was performed as per the Ion AmpliSeq™ DNA and RNA library preparation user guide (189). Briefly, DNA targets were amplified using a 2X primer pool and 5X Ion AmpliSeq HiFi Mix for 19 cycles. The amplified targets were then partially digested using FuPa and then barcode adapters ligated to the amplicons. After the ligation reaction the unamplified library was purified using Agencourt AMPure XP beads (Beckman Coulter, England) and then washed with 70% ethanol. After a last amplification step the final library underwent a two-round purification process with the

Agencourt AMPure XP beads. A final quality check was carried out on the Agilent Tapestation HSD1000 Screentape as detailed above. The final Tapestation concentration and molarity was used for calculating stock dilutions for loading onto the chip.

Template preparation and chip loading was performed using the Ion Torrent Ion Chef System (ThermoFisher Scientific, Massachusetts, USA) and samples sequenced on the Ion Torrent Proton as per SOP (190). Stock libraries were freshly diluted using nuclease-free water to 50pM, and 25µL of each diluted library was pipetted to the Ion Chef Library Sample Tube. Two v3 chips were prepared for sequencing in parallel by the IonChef and then run subsequently on the Ion Torrent Proton. The Torrent Suite Browser was used to review the results and export the data for bioinformatic analysis.

3.4.2 Whole genome sequencing library preparation

cfDNA extracted as above was also sequenced using low pass whole genome sequencing (lp-WGS), using the QIAGEN QIAseq FX DNA Library Kit (96) (Qiagen, Tilden, Germany) (191). This method was optimised using varied inputs of DNA for comparison and also biological replicates, which will be discussed further in ***Chapter 6.*** Where possible, 10ng input DNA was used for library preparation, but owing to the limited availability of DNA input, this was sometimes as little as 1ng. When DNA input was low (<10ng), FX enhancer was used as per manufacturer recommendations.

For fragmentation and end-repair, the FX reaction mix was prepared on ice by adding 10X FX buffer, purified DNA, nuclease free water ± FX enhancer. After mixing, 10µl of FX enzyme was added to each reaction and again mixed well by pipetting. A pre-determined fragmentation time of 3 minutes was used based on DNA input. Adapter ligation of barcodes using 5X ligation buffer was followed by clean-up using 0.8x Agencourt AMPure XP beads. After an 80% ethanol wash, a second 1x purification was carried out, and then the washed and purified DNA was used for library amplification. Based on the DNA input and quality, 9 amplification cycles were used and the final product purified again with Agencourt AMPure XP beads (1x). As above, the quality and quantity of the libraries constructed was assessed using the Agilent BioAnalyzer to confirm suitability for further downstream analysis.

3.4.3 Whole-exome sequencing

Whole-exome sequencing (WES) was also performed on a subset of samples reported in ***Chapter 7***. Unlike the methods described above, this was performed using tissue samples collected from mCRPC patients treated at the Royal Marsden Hospital and collected under our CC2472 protocol. Library preparation was carried out using the Kapa HyperPlus library preparation kits (Roche Diagnostics, Risch-Rotkreuz, Switzerland) (192), and the Agilent SureSelect XT V6 target enrichment system (Agilent Technologies, California, USA) (193). The NextSeq 500 ™ (2x150 cycles; Illumina, California, USA) was used for paired-end sequencing.

3.5 Bioinformatic Analyses

George Seed, a bioinformatician pursuing a PhD in our laboratory assisted with bioinformatic support for the majority of this thesis, under the supervision of Dr Wei Yuan, the senior bioinformatician within our Cancer Biomarkers team.

For the targeted sequencing analyses, copy-number changes were identified by using CNVkit (v0.35) software, utilising a pooled reference of healthy volunteer plasma samples as a normal sequencing coverage reference. Copy segments were assigned to panel genes, and per-gene Log_2 ratios were used for downstream analyses. For copy number calling, a Log_2 ratio of >2 was considered as threshold for amplifications and a Log_2 ratio <-1.2 used as a threshold to consider homozygous deletions (194). Mutation calling was performed using the Torrent Suite™ variant caller, and samples were annotated using Oncotator to identify predicted deleterious mutations.

For the whole exome sequencing performed, output FASTQ files were generated from the NextSeq 500™ using bcl2fastq2 software (v.2.17.1.14, Illumina, California, USA). The default chastity filter selected sequence reads for subsequent analysis. All selected sequencing reads were aligned to the human genome reference sequence (GRCh37) using the BWA (v. 0.7.12) MEM algorithm, and indels were realigned using the Stampy (v.1.0.28) package. Picard tools (v.2.1.0) were used to remove PCR duplicates and to calculate sequencing metrics for quality control check. The Genome Analysis Toolkit (GATK, v. 3.5-0) was then applied to realign local indels, to recalibrate base scores, and to identify point mutations as well small insertions and deletions. Somatic point mutations

and indels were called using MuTect2 by comparing tumour DNA to germline control, and copy-number estimation was obtained through a modified ASCAT2 package (195).

Analysis of low pass whole genome sequencing was performed very similarly to the whole exome sequencing. Initially, output FASTQ files were generated from the NovaSeq 6000™ again using the bcl2fastq2 software (v2.17.14, Ilumina, California, USA). Again, the default chastity filter selected sequence reads for subsequent analysis, selecting high quality and non-duplicate reads. All sequencing reads were aligned to the human genome reference sequence (GRCh37) using the BWA (v. 0.7.12) MEM algorithm, and indels were realigned using the Stampy (v.1.0.28) package. Picard tools (v.2.1.0) were used to remove PCR duplicates and to calculate sequencing metrics for quality control check. The Genome Analysis Toolkit (GATK, v. 3.5-0) was then applied to realign local indels and to recalibrate base scores. Copy number analysis was performed using the ichorCNA software (v0.1.0) (123)which also estimated tumour fraction of cfDNA and tumour ploidy.

Additional analysis provided in this thesis utilises publicly available data accessed through cBioPortal for Cancer Genomics (https://www.cbioportal.org/), using inbuilt tools available through the website (81,196,197). Raw copy number data were downloaded as $\log_2$ ratios and used for comparison; this will be explained further in the relevant Results chapters.

3.6 Circulating tumour cell enumeration

CTC counts were determined from 7.5ml of peripheral blood, collected in a CellSave preservation tube using the CellSearch™ system (Janssen Diagnostics, Belgium) for enumeration. This system, comprises the CellSearch™, Circulating Tumour Cell Kit (Janssen Diagnostics; #7900001), the CellTracks™ AutoPrep System for sample preparation, and uses the CellTracks™ Analyser II for sample analysis (198).

This semi-automated platform for CTC enrichment works by capturing CTCs using magnetic ferrofluid nanoparticles coated with anti-EpCAM antibodies. These captured cells are then fluorescently labelled with conjugated antibodies against cytokeratin (an epithelial marker), CD45 (a leucocyte marker) and DAPI (a nuclear marker). The machine then automatically selects events using the CellTracks analyser which functions as a semi-automated fluorescent microscope. These events are then reviewed by a

human operator and formally classified as CTCs if they fulfil the eligibility criteria of being at least 4µm in size, of a round or oval shape and staining positively for CK with nuclear DAPI but negative for CD45. The nuclear area should also be smaller than the cytoplasmic area for positive identification of a CTC.

CTC counts were also determined from apheresis product using the sample platform, and this is described in more detail below.

3.7 Circulating tumour cell isolation

Contents from CellSearch^{TM} cartridges were transferred into sterile Eppendorf tubes. The cartridge was then washed twice with 150µl of PBS, vortexing gently to ensure removal of the maximum number of CTCs possible. Cells were isolated using fluorescence activated cell sorting (FACS) on the FACSAria III (Beckton, Dickinson and Company, New Jersey, USA) to single CTCs or single white blood cells (WBCs). CTCs were sorted on the basis of being DAPI+, CK+ and CD45- whilst WBCs were DAPI+, CD45+ and CK-).

3.8 Array comparative genomic hybridisation

3.8.1 Using CTCs

Cells isolated by FACS sorting (CTCs or WBCs) underwent whole genome amplification using Ampli1^{TM} WGA kit for Single Cells (Menarini, Silicon Biosystems, Bologna, Italy) according to the manufacturer's instructions (199), with some minor modifications. The unamended protocol workflow is displayed in ***Figure 3-4***.

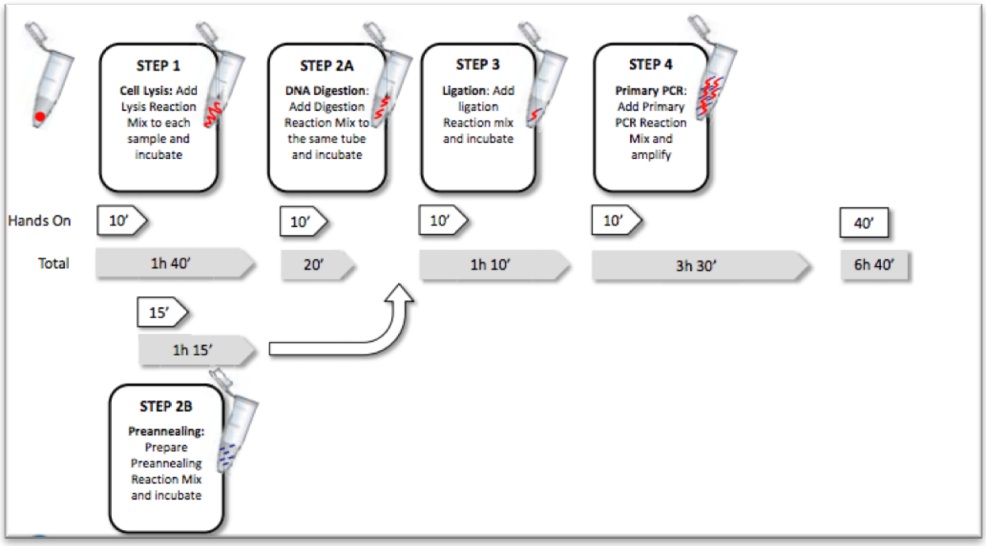

Figure 3-4: WGA procedure overview (199)

Single cell amplification was carried out in a laminar flow hood using sterile conditions and dedicated equipment to minimise contamination risk. As per Step 1, cells were lysed using a lysis reaction mix, and then digested. Our digestion step was increased to 30 minutes, and the subsequent adaptor ligation for 3 hours. Following PCR amplification (25 cycles), the amplified DNA product was then purified using the MinElute PCR Purification Kit (Qiagen, Hilden, Germany). DNA quantification was performed using the Qubit (Invitrogen, California, USA) and then stored at −20°C.

Five hundred nanograms of amplified DNA (CTC or WBC) was then used for fluorescent labelling using the SureTag Complete DNA Labelling Kit (Agilent Technologies, California, USA). A Cy5 dye was used for labelling CTCs and Cy3 for the reference (WBC DNA). Once labelled, the amplified DNA was purified using Amicon 30kDA filters (ThermoFisher Scientific, Massachusetts, USA). This purified product was used to determine the yield and specific activity or degree of labelling; I used the microarray measurement on the NanoDrop 8000 Spectrophotometer (ThermoFisher, Massachusetts, USA). Absorbance of DNA, Cy3 and Cy5 were measured and then yield, specific activity or degree of labelling was calculated using the below equations:

$$Yield\ (\mu g) = \frac{DNA\ Concentration\ (ng/\mu L) x\ Sample\ Volume(\mu L)}{1000 ng/\mu g}$$

$$Specific\ Activity = \frac{pmol\ per\ \mu L\ of\ dye}{\mu g\ per\ \mu L\ gDNA}$$

$$Degree\ of\ Labelling = \frac{340\ x\ pmol\ per\ uL\ dye}{ng\ per\ \mu L\ gDNA\ x\ 1000}\ x\ 100\%$$

Table 3-2 was used as a reference table to compare expected yield of labelled DNA and specific activity after labelling and purification.

Table 3-2: Expected Yield and Specific Activity after Labelling and Clean-up (200)

Input gDNA (µg)	Yield (µg)	Specific Activity of Cyanine 3 and Cyanine 5 Labeled Sample (pmol/µg)
0.2*	3 to 6	15 to 50
0.5	8 to 13	20 to 60
1	9 to 14	20 to 60

If matching tumour and control samples achieved adequate yield and specific activity at this point they were combined and incubated with Blocking agent and Cot-1 DNA, prior to hybridization at 67°C for 24 hours.

Following hybridization, slides were washed with Oligo aCGH Wash Buffers as per the Agilent protocol (200), placed in an ozone-barrier slide holder, and read on the SureScan microarray scanner using the AgilentGC CGH protocol. The CytoGenomics Software v4.0.3.12 (Agilent Technologies, California, USA) was used to determine copy number ratios of CTC:WBC, and $\log_2$ ratios of segments were matched with gene coordinates to assign per-gene values.

3.8.2 Using Tissue

Tissue aCGH was also performed, using DNA extracted from FFPE tumour samples as reviewed by a pathologist as described above. An input of 10ng of tumour DNA was used for whole genome amplification using the Sigma GenomePlex Whole Genome Amplification Kit (WGA2; Sigma-Aldrich, Missouri, USA) protocol. The female reference DNA provided by Agilent was used as the control DNA for later hybridisation. Sample preparation was as described above with minor modifications. Only 20 PCR cycles were

used for amplification (versus 25 for single cells), and a longer hybridisation of 40-hours was used as opposed to 24.

3.8.3 Using plasma

I also explored aCGH of plasma as a tool for validating plasma sequencing results, using a subset of cfDNA samples from the Sanofi cohort. I initially performed a preliminary assessment of the integrity of samples with the Agilent Tapestation HSD1000 kit as described above. DNA input ranging from 1ng to 10ng was used for amplification with the Sigma GenomePlex Whole Genome Amplification Kit (WGA2; Sigma-Aldrich, Missouri, USA) protocol. Pooled DNA from at least 10 different healthy volunteers was used as a control. Following this, fragmentation, library preparation and amplification was performed as described above and as per the Array-Based CGH for Genomic DNA Analysis Protocol (Agilent Technologies, California, USA).

Labelling, hybridization and scanning was again performed as above and as per the Agilent manufacturer protocol. Serial dilutions were performed using the same plasma sample in order to establish reproducibility with lower DNA inputs, and also in experiments comparing plasma aCGH of cfDNA samples to aCGH of matched tissue samples.

3.8.4 Analysis of aCGH

Consistently for the varied input (CTCs, tissue, plasma), the Agilent Feature Extraction software (version 12.0) was used to generate .txt files, and the Agilent CytoGenomics software to visualise the data. Data, extracted in the form of .vcf files was used to depict genomic regions and calculate copy number estimation. Log_2 ratio values were assigned to classify copy states of genes; values of <-0.25 were classified as losses; those >0.25 were categorized as gains, with those in between as unchanged. Smoothed log_2 ratio values of ≥1.2 were defined as an amplification and homozygous deletions as log_2 ratios of ≤-1.2.

To calculate individual copy number aberration (CNA) burden per-sample, the proportion of the human genome (3,000 megabase pairs) affected was used. With bioinformatic support, using R (v3.4) unsupervised hierarchical clustering was performed with the Ward method and the Euclidean distances of unique copy-number changes. X-

chromosome genes were excluded (aside from the *AR* gene and 10 genes on either side) due to different reference X-chromosome ploidies (as a female reference was used for tissue aCGH) when clustering samples from multiple tissue types. Functional diversity per-patient was calculated from cluster dendrograms of CTC samples (made with the R package vegan v2.4.4) using the sum of connecting branches in a dendrogram and dividing by the number of samples.

3.9 Fluorescent *in situ* Hybridisation

Fluorescence in situ hybridization (FISH) analysis was performed using the Cancer Biomarkers Laboratory SOP and as previously reported (201), with the assistance of Susana Miranda and Maryou Lambos (Cancer Biomarkers Team, Institute of Cancer Research). FISH was performed using 4μM thick FFPE sections; these were dewaxed using heated xylene and rehydrated with ethanol. After being pre-treated with heat, the slides underwent pepsin digestion and were then hybridized overnight at 37°C with the FISH probe hybridisation mix. Here, the FISH probes used were:

- *BRCA2/CEN13q* (Abnova, Taiwan)
- *RB1*(Abbott Laboratories, Illinois, USA)
- *PTEN (10q23)/SE 10* (Leica Microsystems, Wetzlar, Germany)
- *MYC (8q24)/SE 8* (Leica Microsystems, Wetzlar, Germany)
- A custom-made *AR/CEPX* probe (Menarini, Silicon Biosystems, Bologna, Italy).

Stringency washes were performed on all slides post-hybridisation. This involved 2x5 minutes in 50% formamide at 42°C, 2x5 minutes in 2xSSC at 42°C and 1x3 minutes in SSCT at room temperature with agitation. For *AR*, where the probe was indirectly labelled, a secondary incubation using anti-digoxigenin–fluorescein antibody (Roche Diagnostics, Risch-Rotkreuz, Switzerland) was also carried out. Slides were digitally imaged (BioView Ltd, Israel) and a minimum of 100 tumour cells were evaluated by a pathologist (Daniel Nava Rodrigues) who recorded the ratios between the probes of interest and the reference probes. If the ratio was >2, an amplification was reported. Heterozygous loss and homozygous deletion were reported if at least one in three cells showed loss of one copy, or loss of all copies, of the tested probe, respectively.

3.10 Organoid culture

These studies, optimised by Dr Veronica Gil in our laboratory (Cancer Biomarkers Team, The ICR), aimed to grow organoid cultures from apheresis product collected under our CCR 2996 protocol. To enrich for CTCs, EasySep Epcam-positive selection (Stem Cell Technologies, Vancouver, Canada) was used to immunomagnetically separate cells from 1mL of single-cell suspension. The selected fraction was used for organoid culture, with the negative fraction being cultured as a control. These isolated cells were then seeded in Corning Matrigel™ Matrix with depleted growth factors (Corning, New York, USA), utilising techniques as previously described (202,203). The spheroid organoids formed were passaged after 4-6 weeks and cells manually collected for molecular study using TrypLE (Sigma-Aldrich, Missouri, USA) at 37ºC for 5 minutes for dissociation.

3.11 Apheresis

Patients were eligible to participate in this apheresis study (CCR 2996) if they had histologically confirmed mCRPC, detectable peripheral blood CTCs, no coagulopathy, suitable bilateral antecubital fossa venous access and an ECOG performance status of 0-1. The study was performed in concordance with the Declaration of Helsinki (204) and with approval of the ethics boards at both the Royal Marsden NHS Foundation Trust Hospital (London, UK) and The Institute of Cancer Research (London, UK).

Apheresis was performed using the Spectra Optia™ Apheresis System (Terumo BCT, Colorado, USA) as recommended by the manufacturer's specification (205). To summarise, patients were connected to the machine via two peripheral venous catheters in each cubital vein. Whole blood was extracted via one of these catheters, and then anticoagulated before entering the rotating centrifuge. Heavier blood elements including erythrocytes migrated to the outside of the channel, plasma to the centre, and the buffy coat (which includes mononuclear cells and CTCs) to the middle. This mononuclear cell (MNC) layer was siphoned off, whilst the remaining blood cells and plasma were constantly returned to the patient via the contralateral arm. Granulocyte-colony-stimulating factor was not used. Blood was anticoagulated with citrate dextrose solution A (two to four 500-mL infusion bags were required for each procedure).

The resultant apheresis product (i.e. the siphoned off MNC layer) was transferred from the designated Royal Marsden NHS Hospital ward where the apheresis procedure was

carried, out to our laboratories at The Institute of Cancer Research. Meanwhile, a vial of the apheresis product was delivered to the Royal Marsden Hospital Haematology laboratory that provided us with an MNC count per sample. This value was used to calculate the MNC count per 1mL of the apheresis product.

The apheresis bag containing the product was opened in a microbiological safety cabinet Class II after sterilising the bag and scissors with 70% ethanol. The apheresis product was transferred from the bag to 50mL Falcon tubes and the total volume of the apheresis sample recorded. The product was used for CellSearch™ analysis to calculate CTC count; 1 sample containing $50x10^6$ MNC and another containing $200x10^6$ MNC were diluted to 8mL using the CellSearch™ Circulating Tumour Cell Kit Dilution Buffer (Menarini, Silicon Biosystems, Bologna, Italy) into a CellSave tube. These diluted samples were stored overnight as a minimum, and processed within 96-hours. For each sample, the entire volume (~8mL) was transferred from the CellSave™ tube into a labelled CellTracks™ Autoprep conical tube. The total volume was then made up to 14mL using CellSearch™ Dilution Buffer, and scanned on the CellTracks™ Analyser as described above.

After the apheresis product had been quantified using the CellSearch™ system, cells were isolated using FACS sorting as described above. Isolated cells were then used for further analyses, such as for aCGH, which is also detailed above.

Surplus apheresis product was centrifuged at 1500RPM for 10-minutes (with full acceleration and full brake). Following centrifugation, the supernatant was removed and discarded. The pellet was resuspended in freezing media and aliquoted into 2mL cryotubes. These were stored overnight at -20°C using a Mr Frosty™ container (ThermoFisher Scientific, Massachusetts, USA) and then transferred to -80°C the following day for longer-term storage.

Blood samples were also collected for analysis within this apheresis trial, both pre- & post-procedure. Prior to apheresis, a Cellsave™ tube for a peripheral blood CTC count was collected, and where possible a Streck™ tube was also taken for cell-free DNA. Routine bloods, including a full blood count were also taken prior to the procedure. Immediately after the procedure a further CellSave™ tube for a post-procedure CTC count was also taken, and a repeat full blood count taken for safety analysis.

3.12 Statistical analysis

Statistical analyses were performed using Microsoft Excel, GraphPad Prism (v8.0) and R (v3.4). Statistical support was also received from David Dolling (statistician, Cancer Biomarkers Team, ICR) and bioinformatic support from George Seed (PhD student, Cancer Biomarkers Team, ICR). Relevant methods used will be described accordingly in the relevant chapters.

4. Reaching a consensus on circulating biomarkers

4.1 Aims & Hypothesis relating to this chapter

4.1.1 Hypothesis:

The need for validated circulating biomarkers is well recognised in almost all cancers including in advanced prostate cancer. Whilst circulating biomarkers such as plasma cell-free nucleic acids and circulating tumour cells are being investigated for their clinical utility, there has been a lack of consensus with regards to analyses, reporting and clinical effectiveness of these biomarkers.

4.1.2 Aims:

To gather experts in the field of circulating biomarkers to address the issues for a consensus meeting and to present their findings in a report of a consensus statement on circulating biomarkers in advanced prostate cancer.

4.2 Research in context

In advanced prostate cancer (PC), there is increasing interest and investigation in the field of circulating biomarkers. This includes both the quantification and characterization of circulating nucleic acids including cell-free DNA (cfDNA) and of circulating tumour cells (CTCs). Whilst these blood-based biomarkers undoubtedly have clinical utility there remains a lack of consensus on how to utilize these and a need for standardization measures pertaining to their analyses, reporting, and result integration into specific clinical contexts.

Drug development in advanced prostate cancer has seen an unprecedented series of successful efforts in recent years, but despite these improvements and in the understanding of the underlying disease molecular biology, the discovery of biomarkers to effectively assess prognosis and tailor treatment for each individual patient remains

one of the most significant challenges in advanced PC care to date. Most of the molecular biomarkers identified thus far require the extraction of DNA or RNA obtained from tissue extracted from the primary tumour or a metastatic site, which can pose a number of challenges.

Firstly, relying on archival prostate tissue samples taken at a time prior to antitumour treatment may not be representative of a tumour that has progressed after several lines of therapy. Obtaining fresh tissue biopsies, on the other hand, may have risks and significant morbidity, and may not be clinically feasible outside large academic centres (181). Furthermore, a significant proportion of prostate cancer patients present with bone-only disease, which poses particular challenges to tumour processing (206). Finally, tissue obtained from a single metastatic biopsy site may not represent the molecular landscape of a patient´s tumour due to intra-patient tumour heterogeneity (207).

Novel technical advances in recent years have enabled the acquisition of tumour material from liquid biopsies either as circulating cell-free tumour nucleic acids (e.g. cfDNA), whole cells (CTCs) or cell vesicles (exosomes) (208). The assessment of a tumour's molecular landscape through liquid biopsies represents a revolution for personalised cancer medicine, by enabling a safe and feasible approach to the development and validation of clinically feasible biomarkers. Liquid biopsies may represent a more reliable picture of the dominant tumour sub-clones present at any time-point, and longitudinal sampling may provide valuable insight on the dynamic mechanisms underlying resistance to treatment and disease progression. However, in order for liquid biopsies to fulfil their potential in terms of clinical relevance, a consensus regarding their utility and context must be urgently reached.

4.3 Study design:

I oversaw the setting up, planning and conduct of a consensus meeting that was held in London with the aim of producing a statement on the future of circulating biomarkers in advanced PC. The panel members were 18 multidisciplinary cancer physicians and scientists from 9 different countries. These experts were invited based on their academic track record and involvement in clinical and/or translational research in advanced PC and biomarkers. All invited members accepted the invitation to participate and were present at the meeting. Prior to the meeting, the experts identified four areas of

controversy in the field of circulating biomarkers in the management of men with advanced PC for discussion:

1) Current utility of circulating biomarkers.
2) Unmet clinical needs for circulating biomarkers in prostate cancer care.
3) Most pressing blood-based molecular assays required.
4) Essential steps for the development of circulating biomarker assays.

A modified Delphi process was used for consensus development, following the procedures previously described by Gillessen et al 2015 (209), and as detailed in ***Figure 4-1***. The programme for the consensus meeting itself consisted of state-of-the-art lectures, presentations and debates by the panellists. Evidence relevant to the four pre-selected topics were reviewed and discussed. Following this, 50 previously agreed-upon questions were presented with options for answers in a multiple-choice format. The experts voted on the answers to these questions publicly but anonymously, with results being displayed real-time to all meeting attendees.

For all questions, unless stated otherwise, responses were based on the idealised assumptions that all diagnostic procedures (including expertise in their interpretation and application) mentioned were readily available. Importantly, in an effort to address questions from an evidence-based and clinical utility perspective, panellists were specifically instructed not to consider cost, reimbursement and access as factors in their deliberations, again unless this was stated otherwise. Clearly these would also be critical factors in decision-making for both the physician and individual patient but were removed as confounding factors here.

The results presented were intended to serve only as a guide to clinicians and industry partners for future development of circulating biomarkers for prostate cancer, as they purely reflect the opinions of a small chosen panel of experts. The option “unqualified to answer” (short form: “unqualified”) should have been chosen if a panellist lacked experience for a specific question; the “abstain” option chosen if a panellist felt unable to vote for a best choice for any reason. Detailed voting records are provided in the results section, with the denominator for each answer being based on the number of panel members who voted per particular question and excluding those who voted “unqualified to answer”.

A consensus was declared if the same option was chosen by ≥75% of the panellists excluding those who did not vote for “unqualified” or abstained (210). Throughout the results sections, the percentage (%) of voting panellists who gave a particular response is reported and the number of voters and the number of panellists for each answer are also provided.

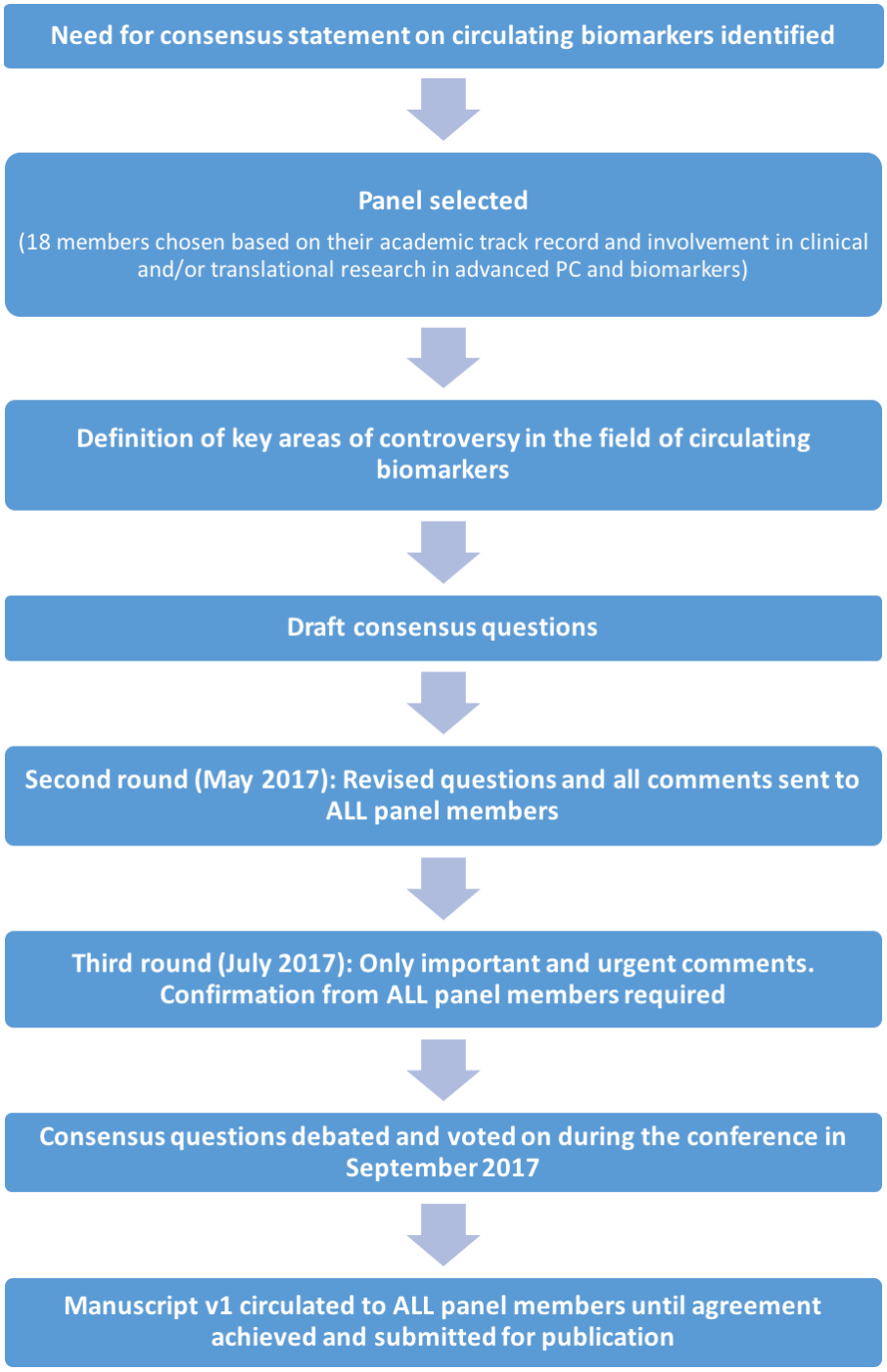

Figure 4-1: How the Consensus Process works (modified Delphi process)

4.4 Results

4.4.1 Current utility of circulating biomarkers

4.4.1.1 Circulating tumour cell assays

Although multiple assays have been described for CTC enumeration and evaluation only the CellSearch™ system has received regulatory clearance for monitoring PC. For CTC testing/enumeration with any assay, 33% (6/18) of the experts voted that testing was ready for use in daily routine clinical practice, 61% (11/18) that current data support testing in prospective trials and the remaining 6% (1/18) that clinical studies are required before prospective clinical validation trials. When asked about CellSearch™ CTC count estimation specifically, 67% (12/18) of the experts voted that testing was ready for use in daily routine clinical practice, 22% (4/18) voted that current data support testing in prospective trials and 11% (2/18) voted that clinical studies are required prior to prospective, clinical validation studies.

Overall, the majority of the experts did endorse the utility of CTC enumeration via CellSearch™ in clinical practice and trials (given the available data and the FDA regulatory clearance) but consensus was not reached regarding routine clinical use.

4.4.1.2 Alternative CTC detection

Following the success of the CellSearch™ system, many other alternative CTC detection platforms have been developed but their use remains limited. For genomic analyses of CTCs, none of the experts (0/18) voted that testing was ready for use in daily routine clinical practice, but 61% (11/18) did vote that the current data supports testing in prospective trials and 39% (7/18) that clinical studies are required prior to prospective, clinical validation trials.

Based on current knowledge, experts voted on the most appropriate clinical situation for CTC testing *if* the tests were readily available, with 28% (5/18) voting for testing before starting first-line PC treatment, 16.5% (3/18) for testing before starting second-line or greater treatment, 39% (7/18) for testing before starting treatment for advanced disease and the remaining 16.5% (3/18) that there is currently no appropriate clinical situation. These results are highlighted in ***Figure 4-2***. Overall, the experts suggested that in order

to validate and qualify CTC-based genomic biomarkers there is an urgent need for prospective clinical trials.

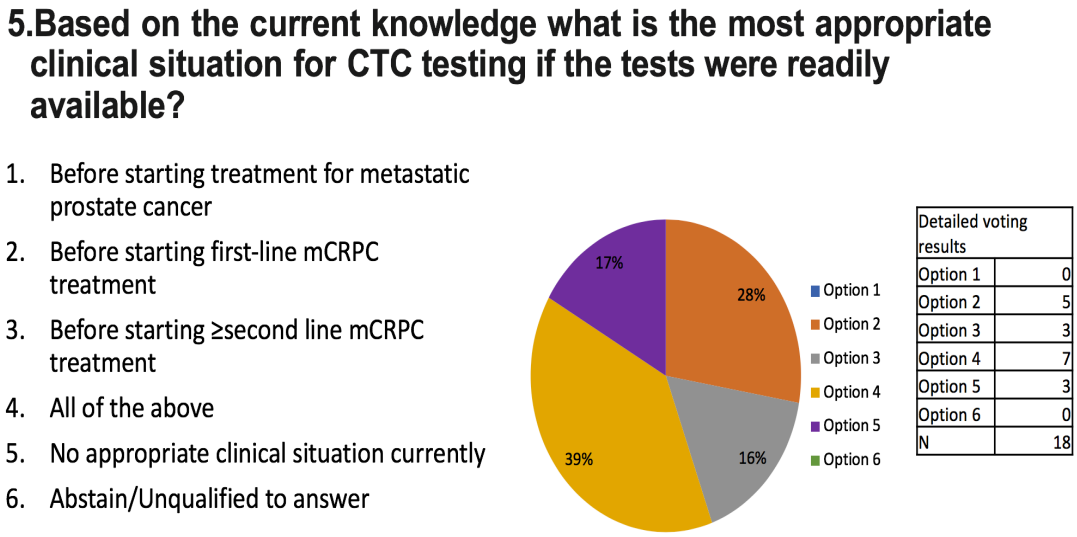

Figure 4-2: Question 5 regarding CTCs and the detailed voting results

CTC – circulating tumour cell; mCRPC = metastatic castration resistant prostate cancer.

4.4.1.3 Androgen receptor splice variant 7 expression in circulating tumour cells

mRNA transcripts for many androgen receptor (AR) variants have been defined and characterized with respect to their structural and functional features (211). Of these, the *AR* splice variant 7 (ARV7) is the most well studied due to its abundance, detectability, constitutional activity and functional relevance. Although various tests for ARV7 exist, for example the blood-based Adnagen CTC test, validation studies for these assays are still ongoing.

For ARV7 testing, 6% (1/18) voted that testing was ready for use in daily routine clinical practice, 72% (13/18) that current data support testing in prospective trials and 22% (4/18) that clinical studies are needed prior to prospective clinical validation trials. Regarding which ARV7 test should be used in daily routine clinical practice if only one of the tests were funded, 31% (4/13) voted for the EPIC ARV7 CTC protein assay, 7.67% (1/13) for custom RT-PCR based CTC assay, 7.67% (1/13) for any/either of these tests and 46% (6/14) for the option that there is currently no suitable assay. Five panellists abstained from voting in this question. Overall, the experts felt that prospective clinical

trial data is needed to validate and qualify ARV7 testing before this can be used routinely in clinical practice.

4.4.1.4 Cell-free DNA assays

The prognostic and potentially predictive value of quantification of cfDNA and of qualification in allowing the identification of tumour genomic aberrations has been described (212,213). When voting if cfDNA testing was ready for use in clinical practice, 6% (1/17) voted that testing was ready for use, 59% (10/17) that current data support testing in prospective trials and 35% (6/17) that clinical studies are required before prospective clinical validation trials. For quantitative analysis of cfDNA, none of the experts voted that testing was ready for use in daily routine clinical practice, 39% (7/18) that current data support testing in prospective trials and 61% (11/18) that clinical studies are required before prospective clinical validation trials.

Detecting genomic alterations from cfDNA, including *AR* mutations, changes in DNA repair genes etc. may assist in identifying patients likely to respond to novel treatment approaches. For genomic analysis of gene panels in cfDNA, 6% (1/18) of experts voted that testing was ready for use in daily routine practice, 72% (13/18) that current data support testing in prospective trials and 22% (4/18) that clinical studies are required before prospective clinical validation trials.

Based on current knowledge, the experts voted on the most appropriate clinical situation for cfDNA testing if this was readily available, with 6% (1/16) voting for testing before starting treatment for metastatic PC, 6% (1/16) for testing before starting first-line treatment, 38% (6/16) for testing before starting second-line PC treatment, 31% (5/16) for testing before all three options whilst 19% (3/16) voted that there is no appropriate clinical situation currently. Overall, the expert's consensus was that cfDNA genomic analysis should not yet be used in clinical practice based on currently available data, with 94% (17/18) of the panel requiring further prospective clinical trial validation and/or qualification.

4.4.1.5 Androgen Receptor genomic aberrations

Aberrations in the *AR* gene have been identified as potentially predictive biomarkers in the context of advanced PC. These include *AR* mutations, overexpression, amplification,

expression of splice variants and genomic structural rearrangements. For *AR* copy gain/mutations in cfDNA testing, none of the experts voted that testing was ready for use in daily practice but 83% (15/18) voted that current data support testing in prospective trials. The remaining 17% (3/18) voted that clinical studies are required before prospective clinical validation trials.

With regards to the most appropriate clinical situation for ARV7/*AR* copy gain/*AR* mutation testing, based on current knowledge, 18% (3/17) of the experts voted for testing before starting first-line PC treatment, 29% (5/17) for before starting second-line PC treatment, 29% (5/17) for before all three options and 24% (4/17) for there being no appropriate clinical situation currently. On whether cfDNA assays would be likely to impact patient care by 2020, 67% (12/18) voted yes, 17% (3/18) voted that this was likely, 11% (2/18) voted possibly and 5% (1/18) voted no. Overall, the expert consensus indicated that prospective clinical trials are needed for further evaluation before *AR* genomic aberration testing can be implemented into daily clinical practice, with most experts believing cfDNA biomarkers will impact patient care by 2020.

4.4.1.6 microRNAs

MicroRNAs (MiRs) which have been shown to be deregulated in tumours and released into the circulation have demonstrated promise as prognostic, predictive and therapy-monitoring biomarkers (139,214). However, 81% (13/16) of the experts voted that the clinical need for PC-focused MiR profiling was of low priority, and only 19% (3/16) that this was a relevant clinical need.

4.4.2 Unmet clinical needs for circulating biomarkers in monitoring prostate cancer care

The need for superior circulating biomarkers in advanced prostate cancer care is widely acknowledged, to guide physicians in stratifying treatment and identifying resistance. With regards to the clinical need for circulating response biomarkers, 72% (13/18) of the experts voted for there being a very high need (development urgently needed) for this, 17% (3/18) as this being a high/relevant clinical need, and 11% (2/18) as this being a low clinical need. Regarding the clinical situation for which this development of circulating response biomarkers is most needed, 100% (17/17) voted for metastatic PC (see ***Figure 4-3***). On the subject of the clinical need for circulating biomarkers as surrogate endpoints

in clinical trials, 72% (13/18) of the experts voted for this being a very high need (development urgently needed), 6% (1/18) for this being a high/relevant clinical need and 22% (4/18) that this was a low clinical need.

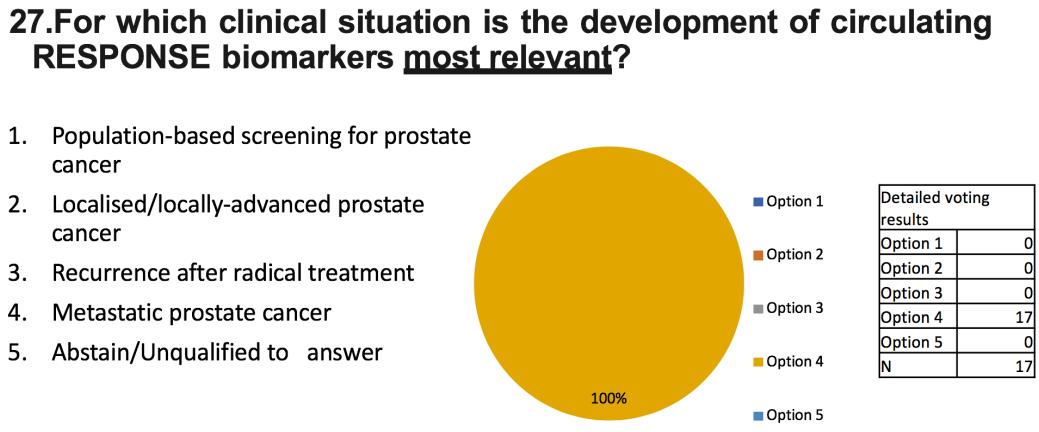

Figure 4-3: Detailed voting from Question 27 regarding response biomarkers

The responses from question 27 from the meeting showed 100% concordance amongst the experts for developing response biomarkers being most relevant in metastatic prostate cancer.

On the topic of the clinical situation for which the development of circulating biomarkers as surrogate endpoints for clinical trials is most relevant, none of the experts voted for population-based screening, 5.5% (1/18) voted for localized/locally advanced PC, 5.5% (1/18) for recurrence after radical treatment and 89% (16/18) for metastatic PC. Overall, the expert consensus was that there is a very high or high need for circulating response and surrogate endpoint biomarkers, with all experts agreeing that this need was highest and most relevant in metastatic PC.

4.4.3 Most pressing blood-based molecular assays required

The urgent, unmet clinical need for biomarkers that can predict treatment benefit and allow a stratified treatment approach as potential predictive biomarkers measurable from cfDNA and CTCs was also deliberated. Predictive biomarkers measurable in cfDNA and CTC discussed are outlined in ***Table 4-1***. These include genes commonly aberrant in PC such as those involved in DNA repair which may confer sensitivity to PARP inhibition and *PTEN* loss to predict efficacy of PI3K/AKT pathway inhibition. Whilst these were considered promising, experts agreed that these circulating assays need further development and validation.

Regarding the clinical need for predictive circulating biomarkers, 94% (17/18) of the experts voted that there was a very high need i.e. development is urgently needed and the remaining 6% (1/18) for this being a high need (see ***Figure 4-4***). Nobody voted that this was a low clinical need or not a key priority for this purpose. With regards to the clinical situation where the development of predictive circulating biomarkers is most relevant, none of the experts voted for population-based screening for PC, 11% (2/18) for localized/locally advanced PC, none for recurrence after radical treatment and 89% (16/18) for metastatic PC.

On the topic of the systemic treatment in greatest need of a predictive circulating biomarker in men with PC, 11% (2/18) of the experts voted for the novel hormonal agents abiraterone and enzalutamide. Eleven percent (2/18) of the experts voted for PARP inhibition or platinum-based chemotherapy, 28% (5/18) for immunotherapy and the remaining 50% (9/18) for all systemic therapies. Conversely, for the systemic treatment with the least need for predictive circulating biomarker in men with PC, 6% (1/17) of the experts voted for abiraterone/enzalutamide, 18% (3/17) for taxane chemotherapy, 35% (6/17) for radium-223, and 41% (7/17) for none of the systemic treatments.

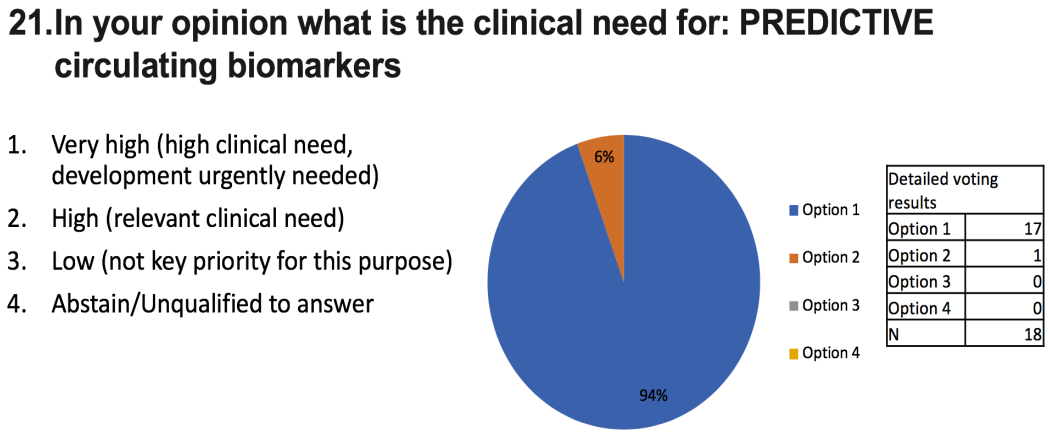

Figure 4-4: The results from Question 21 from the consensus meeting

Question 21 saw experts reach a consensus on the clinical need for predictive circulating biomarkers being very high and that development was urgently needed.

For prognostic circulating biomarkers, 17% (3/18) voted that there was a very high need for them (development urgently needed), 28% (5/18) a high/relevant clinical need and 55% (10/18) for a low clinical need. Fifty-nine percent (10/17) thought that the clinical

situation these prognostic circulating biomarkers would be most relevant was for localized/locally advanced prostate cancer, 18% (3/17) for recurrence after radical treatment and 23% (4/17) for metastatic PC. Nobody voted that prognostic circulating biomarkers were needed for population-based screening. Overall, the overwhelming expert consensus was that there is an urgent clinical need for circulating predictive biomarkers and that the greatest need is in metastatic PC.

Table 4-1: Predictive biomarkers that may be measurable in the peripheral circulation in cfDNA or CTCs

PREDICTIVE BIOMARKER	CONTEXT OF USE	MECHANISM	THERAPIES LINKED TO PREDICTIVE BIOMARKER	NOVEL STRATEGIC APPROACHES
AR variants (i.e. AR-V7) in CTCs (EPIC AR-V7 protein, Qiagen/Hopkins Adnatest RT-PCR)	Second-line mCRPC following enzalutamide or abiraterone failure	Lack of AR LBD and drug target of abiraterone or enzalutamide (ligand independent signalling)	Lack of benefit with abiraterone or enzalutamide (requires validation) Not predictive of taxane benefit clinically	N-terminal or DNA binding domain AR inhibitors, BRD4 inhibitors, novel strategies
AR copy gain (amplification)	mCRPC	High levels of receptor may lead to altered splicing decisions, activity despite low testosterone levels	Possible lack of benefit with abiraterone or enzalutamide (unclear, requires validation)	Novel AR pathway inhibitors
AR mutations (i.e. F876L, T878A, H875Y, L702H) in ctDNA, biopsies, CTCs	mCRPC	Agonistic mutations for anti-androgens, glucocorticoids, progesterone.	May be associated with resistance to bicalutamide, enzalutamide, abiraterone/prednisone	Novel AR pathway inhibitors
3βHSD1 mutations, N367T	mHSPC/CRPC	Gain of function mutation promoting DHT synthesis from DHEA	Resistance to ADT, early CRPC development	Early use of AR pathway inhibition in mHSPC
Homologous DNA Repair Defects (i.e. BRCA2, BRCA1, FANCA, PALB2, ATM)	mCRPC	Sensitivity to PARP inhibition synthetic lethality	May be associated with greater benefit to PARP inhibitors, platinum-compounds	PARP inhibitors or platinum-based chemotherapy
DNA Mismatch Repair Defects (i.e. Lynch Syndrome genes)	mCRPC	High mutational load, neo-antigen generation, immune responsiveness and infiltration, PDL-1 upregulation	PD-1 or PDL-1 inhibition possibly based on small trials in MMR deficient	Requires prospective validation of PD-1/PDL-1 inhibition
PTEN loss, PI3K/AKT pathway activation	mCRPC	Activation of PI3K/AKT/mTOR pathway	Possible benefit to PI3K or AKT inhibition, ideally in combination with AR inhibition given reciprocal feedback of pathways	PI3K/AKT inhibition with abiraterone or enzalutamide
MAPK activation (RAF1 mutations, MEK activation)	mCRPC	MAPK signalling, survival, metastasis	MEK or BRAF inhibitors potentially	Trametinib, regorafenib, others
Intact RB, gain in CDK4/6 or Cyclin-D1	mCRPC	Intact cell cycle pathway checkpoints	Susceptibility to CDK4/6 inhibitors	CDK4/6 inhibitors +/- AR directed therapies
Wnt pathway alterations	mCRPC	Beta-catenin activation and Wnt canonical or non-canonical pathway activation	Wnt pathway inhibition under study	Porcupine inhibition, immunotherapy

ADT = androgen deprivation therapy; AR = androgen receptor; cfDNA = cell free DNA; ctDNA = circulating tumour DNA; CTCs = circulating tumour DNA; DHEA = dehydroepiandrosterone; DHT = dihydrogen-testosterone; LBD = ligand binding domain; mCRPC = metastatic castration resistant prostate cancer; mHSPC = metastatic hormone sensitive prostate cancer; PC = prostate cancer.

Voting by the expert panel on a number of blood-based molecular assays and the clinical need for their development is shown below in ***Table 4-2***. The experts agreed there was a very high clinical need and that development was urgently needed for predictive circulating biomarkers particularly in DNA repair defects (94%; 16/17) and mismatch repair signatures (71%; 12/17).

Table 4-2: Expert voting on the clinical need for predictive circulating biomarkers that may be present in circulating nucleic acids or CTCs

TEST	VOTES ON CLINICAL NEED, % (n/N)		
	VERY HIGH (high clinical need, development urgently needed)	HIGH (relevant clinical need)	LOW (not key priority for this purpose)
CTC phenotyping and genotyping	61 (11/18)	28 (5/18)	11 (2/18)
AR-variant assays	33 (6/18)	56 (10/18)	11 (2/18)
Neuroendocrine biomarker analyses	24 (4/17)	41 (7/17)	35 (6/17)
PTEN loss analyses	19 (3/16)	25 (4/16)	56 (9/16)
DNA repair defect analyses	94 (16/17)	6 (1/17)	0 (0/17)
RB1 loss	12 (2/16)	50 (8/16)	38 (6/16)
MMR/MSI signatures	71 (12/17)	23 (4/17)	6 (1/17)
Immunological biomarker studies (e.g. PD-L1, PD-L2)	39 (7/18)	33 (6/18)	28 (5/18)
Prostate cancer focused, targeted next generation sequencing gene panel	67 (12/18)	33 (6/18)	0 (0/18)
Prostate cancer focused, targeted MiR profiling	0 (0/16)	19 (3/16)	81 (13/16)

AR = androgen receptor; CTC – circulating tumour cell; MiR = microRNA; MMR = mismatch repair; MSI = microsatellite instability; NGS = next generation sequencing; PC = prostate cancer

4.4.4 Essential steps for the development of circulating biomarker assays

The critical steps in biomarker development have been previously discussed in ***Chapter 1 (Introduction)***. The experts voted on what the panel felt were critically important steps in the development of circulating biomarkers for PC. On the subject of the need for healthy volunteer data in circulating biomarker validation, 65% (11/17) of the experts voted this was very high, 29% (5/17) high and 6% (1/17) that this was of low importance. For the importance of reproducibility studies in biomarker development, the experts voted unanimously that this was of very high importance; 100% (17/17). For variability studies, 94% (15/16) voted that this was of very high importance in biomarker development and the remaining 6% (1/16) that this was of high importance.

When voting on the importance of comparing different platforms in biomarker development, 44% (7/16) felt this was of very high importance, 31% (5/16) of high importance, 19% (3/16) of low importance and the remaining 6% (1/16) that this was not important. Qualification of biomarkers involving prospective clinical trials was deemed of very high importance by 82% (14/17) and high importance by the remaining 18% (3/17). The experts also voted as to whether a tumour biopsy-based assay was preferable to a blood-based assay if both were feasible, and 29% (5/17) voted yes with 71% (12/17) voting no.

For the clinical need for circulating biomarkers for diagnostic purposes, 44% (8/18) of the experts voted there was a very high need for this and development was urgently needed, 28% (5/18) voted there was a high/relevant clinical need while a further 28% (5/18) voted this was a low clinical need. In terms of the clinical situation for which the development of circulating biomarkers for diagnostic purposes was most relevant, 50% (9/18) of the experts voted for population-based screening for PC, 11% (2/18) for localized/locally advanced PC, 6% (1/18) for recurrence after radical treatment for PC and 33% (6/18) for metastatic PC.

When asked about the specific clinical setting which had the greatest utility for a circulating biomarker of DNA homologous repair deficiency, 6% (1/17) voted for localized disease, 47% (8/17) for diagnosis of metastatic disease, 23% (4/17) for diagnosis of metastatic castration-resistant disease, 6% (1/17) for PC following progression on abiraterone/enzalutamide and 18% (3/17) for PC following progression on all licensed therapies.

The experts then performed a series of votes, considering which assay, if all tests were available, would be the best performing in specific clinical situations. For men with high-risk localized/locally advanced PC, 34% (5/15) voted for cfDNA quantification and sequencing, 13% (2/15) for CTC enumeration and 53% (8/15) for none of the tests. For patients with biochemical disease recurrence (rising PSA following previous radical treatment), 12% (2/17) of the experts voted for cfDNA quantification and sequencing, 6% (1/17) for CTC enumeration and 82% (14/17) for none of the available tests. In patients who had newly diagnosed metastatic disease, 65% (11/17) of the experts voted for cfDNA quantification and sequencing, 12% (2/17) for CTC enumeration and 23% (4/17) for none of the tests. Finally, for men with metastatic PC, 67% (12/18) of the experts

voted for cfDNA quantification and sequencing, 22% (4/18) for CTC enumeration, 5.5% (1/18) for ARV7 testing and 5.5% (1/18) for none of the available tests.

When considering biomarker development, the experts also discussed the cost implications of liquid biopsies. The health economic benefits of liquid biopsies need to be ascertained in prospective clinical trials, with 65% of the experts voting that health economic analyses were of very high importance, 29% (5/17) of high importance and 6% (1/17) of low importance.

Overall, the expert consensus was that in order to analytically validate circulating biomarkers, there is a significant need for reproducibility (the same sample and time point) and variability (different samples and different time points) studies, healthy volunteer analyses as negative controls and prospective clinical trials. In terms of comparing different biomarker platforms, a consensus was not reached. Perhaps surprisingly, although a consensus was not quite reached, the majority of the panel seemed to prefer a liquid biopsy to a tumour biopsy.

4.5 Discussion

Precision medicine mandates the discovery, validation and qualification of biomarkers in the context of randomized clinical trials. Identification of biomarkers that are ultimately intended to guide patient care is a serious endeavour that needs to follow strict experimental rules and should only be attempted by very qualified investigators. This work is as complex as the drug development process, and, as highlighted by the consensus meeting, much work is still needed in the field. However, as prostate cancer has some of the highest cfDNA and CTC levels of all solid tumours, serial tumour genomic analyses has the potential to transform clinical care.

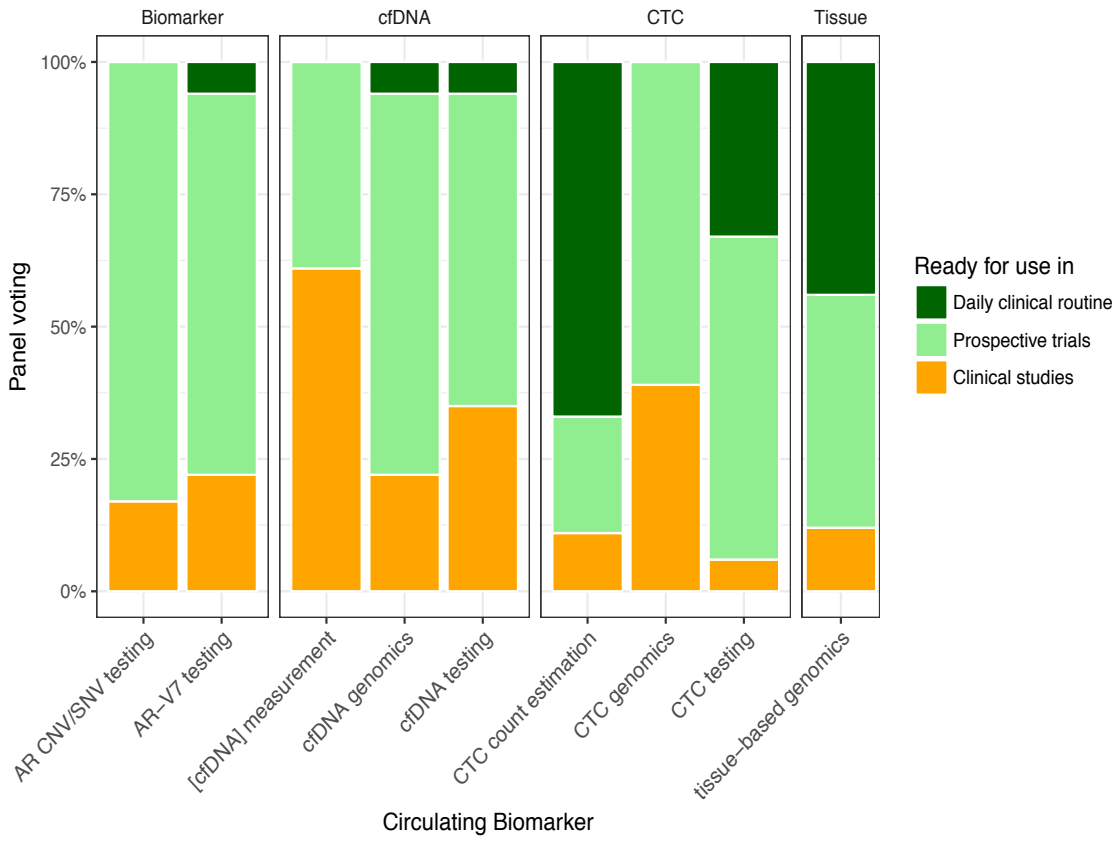

Figure 4-5: Expert voting on circulating biomarkers and their current utility in clinical practice

AR = androgen receptor; AR-V7 = AR splice variant 7; cfDNA = cell-free DNA; CNV = copy number variation; CTC = circulating tumour cell; SNV = single-nucleotide variation.

As shown in ***Figure 4-5***, the panel did not reach consensus on any of the biomarkers discussed being ready for use in daily clinical practice although CTC enumeration came close. On the whole, the meeting was able to highlight areas of disagreement and identified priorities for future clinical research, acknowledging areas where additional data acquisition is warranted. This was critically important to what I pursued in my PhD. Clearly, there is a need for bespoke, prospective trials incorporating circulating biomarker studies for the field to progress. The majority of experts did prefer liquid biopsy over tissue biopsy, again underlining the transformative potential this non-invasive and practical approach to selecting and monitoring treatment could have and endorsing the focus of my PhD studies.

Biomarker research in oncology is an expensive and challenging activity. Development of reagents, understanding the pre-analytical variation in the marker due to sample handling and processing, calibration of instruments, statistical considerations and integration into prospective clinical trials requires a team of highly trained and

experienced experts. With few exceptions, corporate sponsors are reluctant to fund biomarker development projects. Obtaining traditional grants for this critical work is not often successful as it is outside the usual hypothesis-driven proposals. One solution to this funding conundrum is for physicians and regulatory agencies to refuse to perform clinical trials lacking biomarkers for patient selection and/or treatment response. Industry must be convinced that in the era of precision medicine, “all comer” clinical trials should become extinct. Another solution is for a team of expert drug developers with expertise in medical, regulatory and analytical science to lobby traditional national funders, including regulatory agencies, to support these projects. Finally, it would be useful for major cancer centres to centralize their biomarker research and qualification efforts in credentialed clinical lab medicine departments with dedicated medical oncology and molecular pathology leadership.

While the health economic potential of liquid biopsies is clear, future work should be on the design and analysis of prospective clinical trials including health economic data collection (direct and indirect medical cost such as cost of adverse events). While current health economic analyses focus on single biomarker assays or cell enumeration, the potential of more advanced biomarkers such as CTC single-cell sequencing, cfDNA, miRNA and extracellular vesicles remain to be explored.

There are limitations to this consensus statement, and it is acknowledged that the results are the opinions of a small group of experts. Despite this, the voting results reflect the great need for circulating biomarkers, particularly for prediction of treatment response and as surrogate endpoints. The meeting also emphasized the lack of data, validation studies and regulatory approval for the majority of the biomarker tests discussed. The experts felt that these assays were likely to impact patient care in the near-term, and that this was particularly important in the setting of metastatic prostate cancer where response biomarkers and surrogate endpoints are desperately needed.

Moving forward, identification, analytical validation, and prioritisation of circulating biomarkers intended to guide patient care must follow strict experimental rules and this was a focus of my overall PhD. Biomarker integration into prospective clinical trials requires teams of highly trained and experienced experts, and I was determined to work in such a team. Coordinated efforts of experts are needed to support these endeavours. The outcomes of this expert consensus helped to guide my work in developing better circulating biomarkers for PC care, identifying key areas for prioritisation. I therefore

aimed to identify ways to improve CTC count yields by apheresis, since low yields had limited their utility and to develop better validated genomic assays for both CTC and plasma analyses. These are discussed in the proceeding chapters.

5. Plasma cell-free DNA concentrations

5.1 Aims and Hypotheses relating to this chapter

5.1.1 Hypothesis:

Blood based biomarkers have clinical utility, and plasma cell-free DNA concentrations can be used to predict and monitor outcomes from taxane therapy.

5.1.2 Aim:

To clinically qualify baseline and on-treatment cell-free DNA (cfDNA) concentrations as biomarkers of patient outcome in patients treated with taxane chemotherapy utilising plasma samples acquired from two large, prospective Phase III clinical trials (FIRSTANA and PROSELICA).

5.2 Research in context

It is acknowledged that there is an urgent need for non-invasive biomarkers to guide metastatic castration-resistant prostate cancer (mCRPC) treatment. Disease processes, including malignancy, lead to increased levels of cfDNA in the blood compared to that of healthy volunteers (130). cfDNA levels have important implications as a prognostic biomarker in mCRPC, and herein I have aimed to establish whether cfDNA concentrations from plasma can be used to predict patient outcome and response to chemotherapy in mCRPC.

5.3 Study design

5.3.1 Patient cohort

Blood for cfDNA analysis was collected prospectively from mCRPC patients treated on two phase III clinical trials, FIRSTANA (NCT01308567) and PROSELICA (NCT01308580). In FIRSTANA, chemotherapy-naïve patients were randomised to

receive docetaxel (75mg/m^2) (*n* = 391) or one of two doses of cabazitaxel (20mg/m^2 or 25mg/m^2) (*n* = 389 and *n* = 388 respectively). In PROSELICA, patients with previous docetaxel exposure were randomised to receive one of two doses of cabazitaxel (20mg/m^2 or 25mg/m^2) (*n* = 598 and *n* = 602 respectively) as second-line chemotherapy. The outcomes of both trials have previously been reported (15,215). In both of these trials, the primary endpoint measured was overall survival (OS), which was defined as time from randomisation to death from any cause. Secondary endpoints for both trials included radiographic progression free survival (rPFS), safety and tolerability, health-related quality of life, prostate specific antigen (PSA) response, pharmacokinetics and pain response. Outcome measures were reported as recommended by the Prostate Cancer Working Group Criteria 2 (PCWG2) (216). These studies were large, international and multi-institutional trials; selected sites collected plasma for cfDNA for evaluation as an exploratory biomarker. Samples were collected for pre-planned biomarker analyses, from cohorts of consenting patients within each study at pre-specified timepoints.

5.3.2 Sample collection

As described in ***Chapter 2 (Materials and Methods)***, and as required by the both trial protocols, blood samples were taken twice at baseline (at least 24 hours apart) from all treatment arms, and then at 3-time points after the start of the study; Cycle 2 day 1 (C2), Cycle 4 Day 1 (C4) and when patients reached the end of the study (end of study; EOS). Blood was collected in 8mL BD Vacutainer^{TM} CPT cell preparation tubes containing sodium heparin (this was planned before the availability of specialised tubes for cfDNA collection). Prior to blood collection, tubes were stored at room temperature. After collecting the blood, tubes were inverted 8 - 10 times and stored upright at room temperature until centrifugation. Samples were then centrifuged within 2-hours of blood collection, and were remixed immediately prior to centrifugation again by gently inverting the tube 8-10 times. Samples were centrifuged, again at room temperature, in a horizontal rotor for a maximum of 15-minutes at 1500 to 1800 relative centrifugal force (RCF). Following the centrifugation process, approximately 4mL of plasma was available for collection, and was aliquoted using a sterile Pasteur pipette into 1mL tubes for storage at -80^{o}C.

5.3.3 Cell-free DNA extraction and quantification

Again, this is described in detail in ***Chapter 2 (Materials and Methods).*** Briefly, cfDNA was extracted from 1ml of plasma using the QIAamp Circulating Nucleic Acid Kit (Qiagen, Hilden, Germany as per the manufacturers guidelines (217). Of the resultant 50µl eluate, 10µl was used for quantification with the Quant-IT Picogreen HS DNA Kit (ThermoFisher, Massachussets, USA) (187). This was done in duplicate for all samples, which were then read using a BioTek microplate spectrophotometer at 480ex/520em.

5.3.4 Statistical analysis

In order to ascertain that my selected sub-study populations did not substantially differ from the overall trial populations, the baseline characteristics of the selected patients were compared with the baseline characteristics of the study patients not selected from the two trials, using both the X^2 and *t*-test as appropriate. Baseline characteristics between the two trials (of selected patients) were also compared, again using the X^2 and *t*-test.

To establish the biological variability of cfDNA, I measured both the screening and C1 baseline plasma $\log_{10}$cfDNA concentrations, and calculated the coefficient of variation from these. For all analyses, where possible the average of the two baseline samples was used for testing correlations. The exception for this was when only a single baseline sample was available, and then this was used alone. For associations between the established baseline $\log_{10}$ cfDNA concentration and other prognostic variables, Pearson's correlation (*r*) was used.

Both median radiographic progression free survival time (rPFS) and overall survival (OS) time were estimated using the Kaplan-Meier method. The multivariable Cox proportional hazard model was used to test for associations between $\log_{10}$ cfDNA concentrations and other known prognostic variables with radiographic progression free survival and overall survival. The proportional hazards assumption was tested using Schoenfeld residuals; no violation for $\log_{10}$-transformed cfDNA concentration was found.

The multivariable analyses performed were adjusted for several factors including albumin, alkaline phosphatase (ALP), baseline Eastern Cooperative Oncology Group performance status, bone-only disease, Gleason score, haemoglobin, lactate

dehydrogenase (LDH), neutrophil-to-lymphocyte ratio (NLR), pain at baseline, prostate specific antigen (PSA), treatment arm, trial and visceral disease. One or more of these variables was missing from the data collection in 22% of patients, but these variables were considered to be missing at random. Multiple imputation by chained equations with the named coefficients was used to generate 20 imputations, with per imputation estimates combined using Rubin's rules, to ensure that there was no loss in the efficiency of the multivariable analyses performed. Uno's inverse-probability weighted C-index and receiver operating characteristic (ROC) area under the curve (AUC) values were used to assess the prognostic value of adding baseline cfDNA to models of rPFS and OS (218).

To calculate the 95% confidence interval (CI) and the change (delta; Δ) between C-indices of each of the models, bootstrapping was used (219). Time-independent incident dynamic ROC curves, using the dataset median rPFS (10 months) and median OS (19months), and time-dependent AUC curves were calculated using methods previously described by Blanche et al (220).

The difference in cfDNA concentrations at C2 and C4 from the baseline concentration was calculated (ΔcfDNA). Per study logistic regression models were used to test associations between $\log_{10}$ cfDNA concentrations, ΔcfDNA, ΔcfDNA cut-off (>20% and >30% change) and PSA response.

Utilising a landmark approach, Cox models were performed to assess the association between these cfDNA values with both rPFS and OS. Two-stage individual patient meta-analyses were used to combine results for per-study logistic regression and Cox model analyses of average baseline $\log_{10}$ cfDNA concentrations. These results are displayed in forest plots, showing both per study and the combined results.

The association of patient characteristics on $\log_{10}$ cfDNA concentrations during the first four cycles was assessed using linear mixed-effect models. Patient characteristics assessed included a PSA response (>50% at any time point), a PSA flare (defined as any increase from baseline PSA followed by a >50% decline) and white blood cell count (WBC) at week 2. Random patient intercept effects were nested with random study intercept effects to assess the association of these characteristics.

Any *p* value <0.05 was considered statistically significant. For all statistical analysis and for the creating of figures used in this chapter, Microsoft Excel v16.16.10, Stata v13, R v3.4.1, SPSS Statistics for Macintosh v22.0 (IBM Corp, New York, USA), and GraphPad Prism version 6.0 for Macintosh (GraphPad Software, California, USA) were used.

5.4 Results:

5.4.1 Patients and samples

Overall, 571 mCRPC patients were consented to the optional sub-study; 315 of the 1168 patients enrolled in FIRSTANA (27%) and 256 of the 1200 patients who participated in PROSELICA (21%). Patient samples were collected between April 2011 and December 2013. From the 315 FIRSTANA patients, 1400 plasma samples were available, and from the 256 PROSELICA patients there were 1102 plasma samples available for analysis.

The baseline characteristics of the patients used in this sub-study are shown in ***Table 5-1***. As expected, differences between the populations of the two trials were noted, as FIRSTANA comprised a docetaxel-naïve population compared to PROSELICA where patients were post-docetaxel and had more advanced disease. As such, there was noticeable difference in some baseline characteristics with patients in PROSELICA having a significantly worse ECOG performance status, higher lactate dehydrogenase (LDH), alkaline phosphatase (ALP) and PSA levels as well as a lower haemoglobin concentration.

At the time of data cut-off, 203 patients from FIRSTANA had died and 149 patients had evidence of radiographic progression. In PROSELICA, 220 of the patients had died with 142 patients having shown evidence of radiographic progression. For patients who had not died, the median follow-up period for FIRSTANA was 33 months and for PROSELICA, 27 months. For patients who did not show evidence of radiographic progression the median follow-up periods were 8 months for FIRSTANA and 5 months for PROSELICA. PSA responses, which were defined by the PCWG2 definition of a confirmed >50% fall in PSA, were seen in 68% of FIRSTANA patients and 43% of PROSELICA patients (p <0.001). A PSA response of >50% at 12 weeks was seen in 54% of FIRSTANA patients and 31% of PROSELICA patients (p <0.001).

Table 5-1: Baseline characteristics of patients included in this sub-study

CHARACTERISTIC	FIRSTANA N = 215 N (%)	PROSELICA N = 256 N (%)	*P* VALUE[a]
ECOG PS[b]			
0-1	305 (97)	235 (92)	0.008
2	10 (3)	21 (8)	
RECIST measurable[b]			
No	141 (45)	121 (47)	0.8
Yes	174 (55)	135 (53)	
Visceral disease			
No	245 (78)	183 (71)	0.08
Yes	70 (22)	73 (29)	
Pain at baseline[c]			
No	79 (28)	60 (26)	0.9
Yes	208 (72)	171 (74)	
Gleason score at diagnosis[d]			
<8	117 (39)	117 (49)	0.02
≥8	182 (61)	122 (51)	
	MEDIAN (IQR)	**MEDIAN (IQR)**	***P* VALUE[e]**
Age (yr)	69 (63 - 74)	68 (64 - 73)	0.9
LDH (U/l)	234 (188 - 350)	331 (221 - 547)	<0.001
ALP (U/l)	113 (77 - 243)	178 (96 - 387)	<0.001
Haemoglobin (g/dl)	130.0 (119.2 - 137.0)	119.0 (106.0 - 127.5)	<0.001
Albumin (g/dl)	40.0 (37.5 - 43.0)	40.7 (37.0 - 43.1)	0.7
PSA (ng/ml)	80.0 (30.0 - 189.0)	207.6 (59.7 - 598.9)	<0.001
PSA doubling time (mo)	2.1 (1.3 - 3.4)	1.9 (1.3 - 3.1)	0.3
Log_{10} cfDNA concentration (ng/ml)	1.21 (0.97 - 1.54)	1.45 (1.18 - 1.86)	<0.001
NLR	3.0 (2.1 - 4.3)	3.7 (2.4 - 5.7)	<0.001
Outcome	**N (%)**	**N (%)**	***P* VALUE[f]**
>50% PSA response at 12 weeks			
No	141 (46)	165 (69)	<0.001
Yes	163 (54)	73 (31)	
>50% PSA response at any time			
No	96 (32)	136 (57)	<0.001
Yes	208 (68)	102 (43)	

ALP = alkaline phosphatase; cfDNA = cell-free DNA; CI = confidence interval; ECOG PS = Eastern Cooperative Oncology Group performance status; HR = hazard ratio; IQR = interquartile range; LDH = lactate dehydrogenase; mo = months; NLR = neutrophil-lymphocyte ratio; OS = overall survival; PSA = prostate-specific antigen; RECIST = Response Evaluation Criteria in Solid Tumours; rPFS = radiological progression-free survival; U = unit, yr = years

a χ^2 test.

b Stratification parameters

c Fifty-three assessments missing (28 in FIRSTANA and 25 in PROSELICA)

d Thirty-three assessments missing (16 in FIRSTANA and 17 in PROSELICA)

e Wilcoxon rank-sum test

f Proportional hazards Cox model

Table 5-2 shows the baseline characteristics of patients included in this sub-study compared to the overall study population, in order to compare whether an accurate representation of each trial cohort was analysed. For the most part, the biomarker subsets studied did not display any significant differences from the non-biomarker subset. However, a significant imbalance (p <0.05) was noted in the FIRSTANA subset for baseline pain, Gleason score at diagnosis, baseline haemoglobin and baseline albumin. In the PROSELICA subset, the only significant difference from the main study cohort was in baseline PSA (p = 0.02). These statistically significant differences (p <0.05) are shown in ***Table 5-2***.

Table 5-2: Baseline characteristics in this sub-study cohort vs. all trial participants

	FIRSTANA			PROSELICA		
CHARACTERISTIC	**BIOMARKER SUBSET N=315 N (%)**	**NON-BIOMARKER SUBSET N=853 N (%)**	***P*-VALUE**	**BIOMARKER SUBSET N=256 N (%)**	**NON-BIOMARKER SUBSET N=944 N (%)**	***P*-VALUE**
ECOG PS						
0–1	305 (97)	815 (96)	0.33	235 (92)	844 (89)	0.26
2	10 (3)	38 (4)		21 (8)	100 (11)	
RECIST measurable						
No	141 (45)	365 (43)	0.48	121 (47)	492 (52)	0.14
Yes	174 (55)	488 (57)		135 (53)	452 (48)	
Visceral disease						
No	245 (78)	673 (79)	0.68	183 (71)	682 (72)	0.81
Yes	70 (22)	180 (21)		73 (29)	262 (28)	
Pain at baseline						
No	79 (28)	295 (38)	0.002	60 (26)	250 (29)	0.42
Yes	208 (72)	487 (62)		171 (74)	622 (71)	
Gleason score at diagnosis						
<8	117 (39)	374 (49)	0.005	117 (49)	420 (47)	0.62
≥8	182 (61)	395 (51)		122 (51)	471 (53)	
	MEDIAN (IQR)	**MEDIAN (IQR)**	***P*-VALUE**	**MEDIAN (IQR)**	**MEDIAN (IQR)**	***P*-VALUE**
Age (yr)	69 (63–74)	68 (63–73)	0.83	68 (64–73)	69 (63–74)	0.41
LDH (U/L)	234 (188–350)	244 (193–350)	0.05	331 (221–547)	324 (221–498)	0.74
ALP (U/L)	113 (77–243)	131 (81–279)	0.05	178 (96–387)	163 (92–387)	0.1
Haemoglobin (g/dl)	130 (119.2–137.0)	127 (116.0–136.0)	0.02	119 (106.0–127.5)	120 (109–130)	0.12
Albumin (g/dl)	40 (37.5–43.0)	41.7 (38.0–44.5)	<0.001	40.7 (37.0–43.1)	40 (36.6–43.0)	0.17
PSA (ng/ml)	80 (30.0–189.0)	75.9 (28.9–201.3)	0.77	207.6 (59.7–598.9)	150.9 (53.3–394.1)	0.02
PSA-doubling time (mo)	2.1 (1.3–3.4)	2.0 (1.3–3.3)	0.95	1.9 (1.3–3.1)	1.9 (1.2–3.1)	0.78
NLR	3.0 (2.1–4.3)	2.9 (2.0–4.1)	0.14	3.7 (2.4–5.7)	3.3 (2.2–5.4)	0.06
OUTCOME	**N (%)**	**N (%)**	***P*-VALUE**	**N (%)**	**N (%)**	***P*-VALUE**
>50% PSA response at 12 weeks						
No	148 (47)	385 (45)	0.57	178 (70)	648 (69)	0.79
Yes	167 (53)	468 (55)		78 (30)	296 (31)	
>50% PSA response at any time						
No	103 (33)	242 (28)	0.15	149 (58)	562 (60)	0.7
Yes	212 (67)	611 (72)		107 (42)	382 (400	

ALP = alkaline phosphatase; cfDNA = cell-free DNA; CI = confidence interval; ECOG PS = Eastern Cooperative Oncology Group performance status; HR = hazard ratio; IQR=interquartile range; LDH = lactate dehydrogenase; mo = months; NLR = neutrophil-lymphocyte ratio; OS = overall survival; PSA = prostate-specific antigen; RECIST=Response Evaluation Criteria in Solid Tumours; rPFS = radiological progression-free survival; U = unit, yr = years.

5.4.2 Baseline cfDNA concentrations

Where two baseline samples where available (SCR & C1) for patients, I explored the biological variability between the $\log_{10}$ cfDNA concentrations in these paired samples. Samples collected between 1 and 7 days apart were accessible for 507/571 patients (89%). There was evidence of a strong correlation (r = 0.84, p <0.001) between these baseline samples, and the mean coefficient of variation between the biological replicates was 12% (95% CI: 11-13%). ***Figure 5-1(A)*** shows the relationship between the $\log_{10}$-transformed cfDNA concentration (ng/ml) with the screening sample on the x axis and the C1 sample on the y axis. ***Figure 5-1(B)*** shows the coefficient of variation of these baseline samples in a frequency chart; the mean coefficient of variation was 0.12 (95% CI 0.11) and is shown in a solid line. The median coefficient of variation was 0.08 (95% CI 0.13).

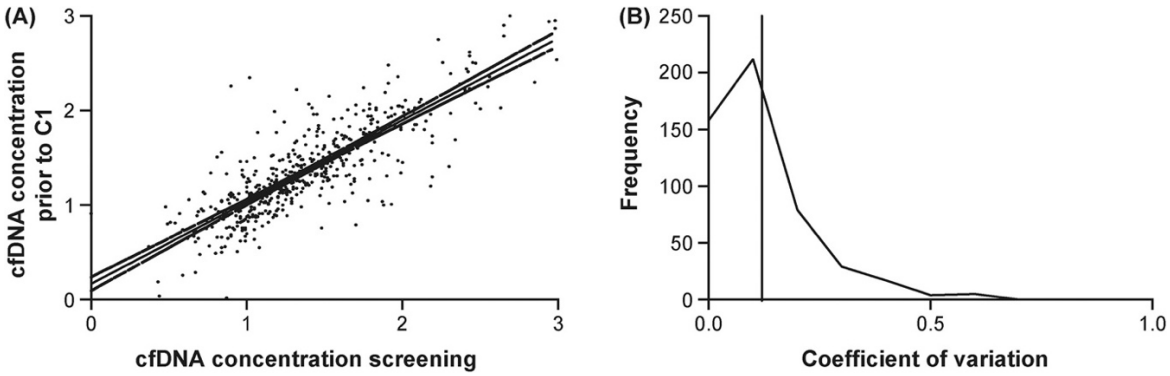

Figure 5-1: Correlation and coefficient of variation between baseline (SCR/C1) $\log_{10}$cfDNA concentrations (ng/ml).

(A) Relationship between $\log_{10}$ cfDNA concentrations at SCR and C1. Correlation coefficient = 0.84 (Pearson's rho, p <0.001). (B) Coefficient of variation between samples mean 0.12 (solid line), median 0.08. C=cycle, cfDNA = cell free DNA.

Baseline $\log_{10}$ cfDNA were compared to established prognostic variables, such as haemoglobin, alkaline phosphatase and PSA, as previously described by Halabi et al (221) and Fizazi et al (222). Some clinical variables were missing from the dataset, the number available for analysis is included in each variable reported (n =). Robust correlations were seen between $\log_{10}$ cfDNA concentrations and $\log_{10}$ lactate dehydrogenase (LDH) where the correlation coefficient was r = 0.46, p <0.001 for n = 566. This was also true for the correlation between haemoglobin (r = -0.45, p <0.001, n

= 570), $\log_{10}$ alkaline phosphatase (ALP, r = 0.40, p <0.001, n = 569) and for $\log_{10}$ PSA (r = 0.34, p <0.001, n = 568). Slightly weaker associations were also seen with white blood cells and albumin; for white blood cells r = 0.14, p = 0.001, n = 570, and for albumin; r = 0.12, p = 0.004, n = 560. ***Table 5-3*** shows these prognostic variables and their relationship with baseline $\log_{10}$ cfDNA concentrations from FIRSTANA and PROSELICA.

Table 5-3: Baseline cfDNA concentrations FIRSTANA and PROSELICA and their association with known prognostic variables

	FIRSTANA				PROSELICA			
CHARACTERISTIC	**N**	**MEAN LOG_{10} CFDNA**	**SD**	***P*-VALUE[1]**	**N**	**MEAN LOG_{10} CFDNA**	**SD**	***P*-VALUE[1]**
Age								
<65	106	1.21	0.4	0.04	76	1.58	0.52	0.3
≥65	209	1.32	0.46		180	1.51	0.47	
ECOG PS at baseline								
0	305	1.27	0.44	0.04	235	1.49	0.46	<0.001
1–2	10	1.57	0.41		21	1.96	0.51	
Prior radical treatment of the prostate								
No	191	1.33	0.46	0.01	148	1.52	0.47	0.86
Yes	124	1.2	0.4		108	1.54	0.51	
Bone-only disease								
No	240	1.29	0.45	0.3	179	1.55	0.5	0.4
Yes	75	1.23	0.43		77	1.49	0.44	
Nodal-only disease								
No	299	1.29	0.45	0.06	246	1.54	0.49	0.009
Yes	16	1.07	0.3		10	1.14	0.25	
Visceral metastases								
No	245	1.26	0.47	0.16	183	1.5	0.47	0.08
Yes	70	1.35	0.33		73	1.61	0.52	
Pain at baseline								
No	79	1.18	0.37	0.04	70	1.36	0.34	<0.001
Yes	208	1.3	0.44		171	1.61	0.52	
Gleason score at baseline								
<8	117	1.24	0.48	0.24	117	1.57	0.49	0.4
≥8	182	1.31	0.42		122	1.52	0.48	
Albumin								
<35 g/L	29	1.46	0.42	0.02	36	1.67	0.5	0.08
≥35 g/L	280	1.26	0.44		215	1.51	0.48	
ALP								
≤ULN	153	1.17	0.37	<0.001	79	1.33	0.38	<0.001
>ULN	156	1.39	0.48		172	1.63	0.5	
Haemoglobin								
<LLN	163	1.42	0.49	<0.001	206	1.57	0.49	0.005
≥LLN	151	1.13	0.33		50	1.36	0.41	
LDH								
≤ULN	85	1.13	0.3	0.001	36	1.22	0.3	<0.001
>ULN	227	1.34	0.47		218	1.58	0.49	
PSA doubling time								
<2 mo	137	1.34	0.48	0.01	124	1.62	0.49	0.002
≥2 mo	151	1.22	0.4		108	1.42	0.44	
NLR at baseline								
<3	157	1.2	0.4	<0.001	88	1.42	0.48	0.01
≥3	156	1.36	0.47		167	1.58	0.48	
Trial Arm								
Cabazitaxel 20 mg/m^2	111	1.27	0.49	0.19	120	1.53	0.49	0.96
Cabazitaxel 25mg/m^2	89	1.22	0.42		136	1.53	0.49	
Docetaxel 75mg/m^2	115	1.34	0.4		0	N/A	N/A	N/A

[1] t-test; ALP = alkaline phosphatase; cfDNA = cell-free DNA; ECOG PS = Eastern Cooperative Oncology Group performance status; LDH = lactate dehydrogenase; mo = months; NLR = neutrophil: lymphocyte ratio; PSA = prostate-specific antigen; SD = standard deviation; ULN = upper limit of normal.

5.4.3 Response to taxanes: baseline and longitudinal cfDNA concentrations

Univariable logistic regression analysis was performed to assess whether baseline $\log_{10}$ cfDNA concentrations associated with a confirmed PSA response in either trial. No association was found in FIRSTANA or PROSELICA; for FIRSTANA the odds ratio (OR) was 0.91 (p = 0.7). In PROSELICA, the OR was 0.76 (p = 0.3). The results from both studies were also combined in a two-stage meta-analysis, but again no significant association was found; OR = 0.82, p = 0.3. Results from univariable logistic regression analysis for the individual studies and the combined approach are shown at the top of ***Table 5-6.*** Multivariable logistic regression models of baseline $\log_{10}$ cfDNA concentrations with PSA and radiographic responses are shown in ***Figure 5-2***, again showing no association of baseline $\log_{10}$ cfDNA concentrations with PSA response (at 12 weeks; ***Figure 5-2A***, or at any time; ***Figure 5-2B***). Likewise, baseline $\log_{10}$ cfDNA concentrations did not associate with radiographic response at any time in either study alone or in the combined approach ***(Figure 5-2C***).

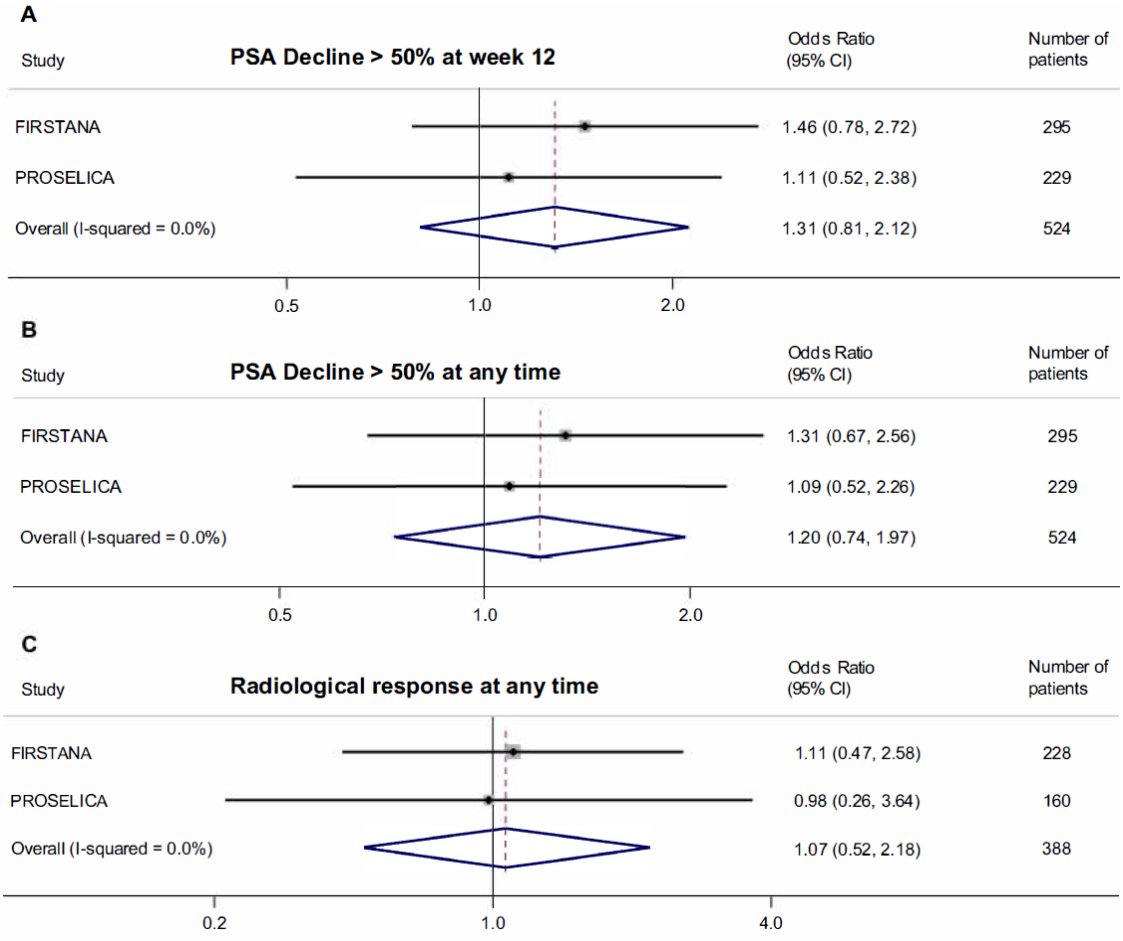

Figure 5-2 Multivariable logistic regression models of baseline log_{10} plasma cfDNA concentration correlation

(A) with PSA response at 12 weeks, (B) with PSA response at any time, and (C) with radiological response at any time. cfDNA = cell-free DNA; CI = confidence interval; PSA = prostate-specific antigen.

Longitudinal cfDNA concentrations were also measured, from Cycle 2 (C2), Cycle 4 (C4) and End of treatment (EOT) samples where available, to allow study of the effect of taxane treatment on serial log_{10} cfDNA concentrations. As expected, the mean plasma cfDNA concentration decreased with the 1st four cycles, after chemotherapy administration. Consistent with disease progression, I also observed an increased from baseline cfDNA concentration, compared to the end of treatment cfDNA concentration. These changes in concentrations and the numbers of samples available for each time-point are detailed in ***Table 5-4***.

Table 5-4: Change in plasma log10 cfDNA concentration (ng/ml) from baseline in FIRSTANA and PROSELICA

	FIRSTANA			PROSELICA		
Change in Log_{10} plasma cfDNA concentration (ng/ml)	**Mean change (ng/ml)**	**95% CI**	**n**	**Mean change (ng/ml)**	**95% CI**	**n**
Cycle 2 (week 4)	−0.04	−0.08 to 0.007	280	−0.07	−0.12 to −0.02	231
Cycle 4 (week 10)	−0.04	−0.09 to 0.00	244	−0.07	−0.13 to −0.02	189
End of treatment	0.07	0.01 to 0.13	255	0.1	0.02 to 0.17	193

The trend in changing concentrations with treatment and progression appeared to be more marked in the PROSELICA samples. ***Figure 5-3*** shows log_{10} cfDNA for both trials combined, decreasing from baseline to C2 and C4 in both PSA responders and non-responders. This is followed by an increase in cfDNA concentrations at the end of treatment, which is evident in both responders and non-responders. Unsurprisingly, the cfDNA concentration at end of treatment is considerably higher in the non-responder group than that of the responders.

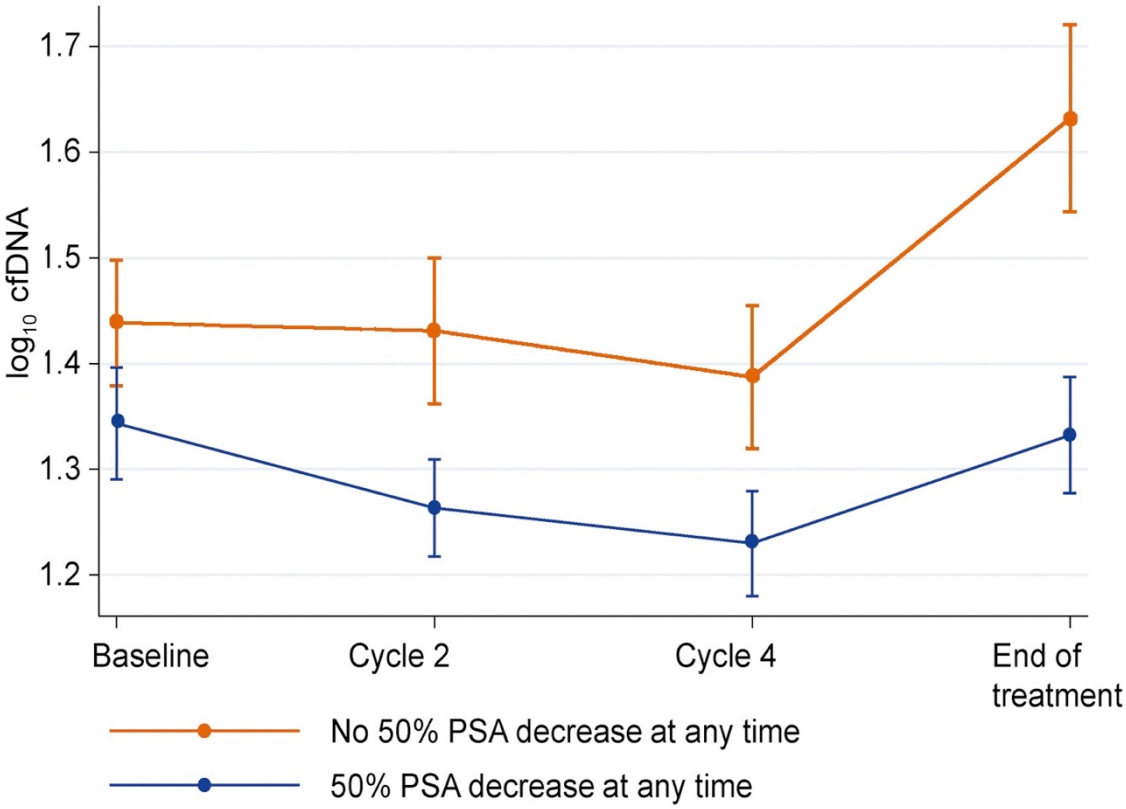

Figure 5-3: Mean log_{10} cfDNA concentrations with 95% confidence intervals over time in PSA responders and non-responders (defined as those with a ≥50% decrease at any time point).

cfDNA = cell-free DNA; PSA = prostate specific antigen.

A multivariable mixed-effect model which analysed predictors of cfDNA concentrations during the first four cycles of treatment is shown in ***Table 5-5***. No difference was seen in baseline cfDNA concentrations by PSA response (a ≤50% PSA decline at any time). After adjusting for other baseline characteristics, patients who did have a PSA response (≥50% decline at any time) had lower per-cycle $\log_{10}$ cfDNA concentrations (- 0.026; CI - 0.044 – - 0.009, p = 0.003). A PSA flare, defined as any increase from baseline PSA followed by a ≥50% decrease, was experienced by 4.9% of patients (28/571) but this did not influence $\log_{10}$ cfDNA concentrations.

Table 5-5:Multivariable mixed-effect model of cfDNA during the first four cycles of treatment

cfDNA (log_{10})	Coef.	95% CI	*p*-value
Cycle	0.001	-0.012 to 0.015	0.841
PSA decrease of 50% at any time	-0.017	-0.084 to 0.051	0.631
PSA decrease of 50% at any time#cycle[1]	-0.026	-0.044 to -0.009	0.003
ECOG PS			
0 - 1	0	-	-
2	0.215	0.083 to 0.346	0.001
Trial Arm			
Cabazitaxel 20 mg/m^2	0	-	0.974
Cabazitaxel, 25mg/m^2	-0.005	-0.069 to 0.06	-
Docetaxel, 75mg/m^2	-0.008	-0.087 to 0.071	-
Gleason score at diagnosis			
<8	0	-	-
≥8	0.057	-0.002 to 0.117	0.058
Visceral disease	0.047	-0.024 to 0.118	0.198
Bone-only disease	-0.011	-0.08 to 0.058	0.757
Baseline Pain	0.03	-0.039 to 0.098	0.393
Albumin (g/dl)	0.004	-0.043 to 0.051	0.858
ALP (log_{10} U/L)	0.077	-0.011 to 0.164	0.086
Haemoglobin (g/dl)	-0.056	-0.079 to -0.033	<0.001
LDH (log_{10} U/L)	0.485	0.336 to 0.634	<0.001
NLR (log_{10})	0.089	-0.026 to 0.204	0.128
PSA (log_{10} ng/ml)	0.08	0.035 to 0.124	0.001
PSA flare (any increase from baseline followed by 50% decrease)	0.107	-0.022 to 0.236	0.105
WBC (Week 2)	0.015	0.007 to 0.023	<0.001
Constant	0.274	-0.279 to 0.826	0.331

ALP = alkaline phosphatase; cfDNA = cell-free DNA; ECOG PS = Eastern Cooperative Oncology Group performance status; LDH = lactate dehydrogenase; NLR = neutrophil lymphocyte ratio; PSA = prostate specific antigen; WBC = white blood cell count.

[1] #Cycle denotes an interaction term

Analysis of Cycle 2 samples showed that in PROSELICA, log_{10} cfDNA concentration, absolute change in log_{10} cfDNA concentration (at C2 compared with baseline or ΔcfDNA C2) and a >20% decline in log10 cfDNA concentration at C2 compared with baseline, all associated with PSA response. Analysis of samples taken 10 weeks into treatment (i.e. Cycle 4 samples) showed changes in cfDNA concentrations to be significantly

associated with PSA response in both studies; the absolute change in log10 cfDNA concentration (at C4 compared with baseline or ΔcfDNA C2) had an odds ratio of 0.4 (95% CI: 0.2 – 0.7, p = 0.002 in FIRSTANA and an odds ratio of 0.3 (95% CI: 0.2 – 0.6, *p* <0.001) in PROSELICA. This significant association was also seen in a two-stage meta-analysis with an OR of 0.3, 95% CI 0.2 – 0.5, *p* <0.001). This, and other time points and exploratory parameters are shown in ***Table 5-6***. Here, results are shown per study and also reported using the combined method.

Table 5-6: Univariate logistic regression of >50% PSA decline (at any time) by cfDNA concentrations

	FIRSTANA			PROSELICA			OVERALL		
	OR	**95% CI**	***P*-VALUE**	**OR**	**95% CI**	***P*-VALUE**	**OR**	**95%CI**	***P*-VALUE**
Log_{10} cfDNA concentration baseline	0.91	0.53–1.56	0.73	0.76	0.44–1.31	0.32	0.82	0.56–1.20	0.3
Log_{10} cfDNA concentration C2	0.73	0.40–1.34	0.32	0.37	0.20–0.69	0.002	0.51	0.33–0.78	0.002
Log_{10} cfDNA concentration C4	0.38	0.20–0.69	0.002	0.42	0.24–0.71	0.001	0.39	0.26–0.59	<0.001
Absolute change in log_{10} cfDNA concentration									
C2	0.71	0.36–1.40	0.32	0.43	0.21–0.90	0.02	0.56	0.34–0.92	0.02
C4	0.37	0.20–0.69	0.002	0.32	0.17–0.59	<0.001	0.34	0.22–0.53	<0.001
Log_{10} cfDNA concentration decline >20%									
C2	1.72	0.87–3.39	0.12	1.8	0.95–3.40	0.07	1.76	1.10–2.79	0.02
C4	6.57	1.96–22.00	0.002	3.56	1.66–7.61	0.001	4.29	2.30–8.01	<0.001
Log_{10} cfDNA concentration decline >30%									
C2	2.31	0.92–5.80	0.07	1.64	0.73–3.69	0.23	1.92	1.05–3.47	0.03
C4	9.38	1.24–71.08	0.03	1.81	0.72–4.53	0.21	2.78	1.30–5.94	0.009
Log_{10} cfDNA concentration increase >20%									
C2	1.37	0.71–2.62	0.35	0.46	0.22–0.97	0.04	0.85	0.54–1.35	0.5
C4	0.93	0.51–1.71	0.83	0.53	0.26–1.09	0.09	0.74	0.47–1.17	0.2
Log_{10} cfDNA concentration increase >30%									
C2	1.22	0.58–2.59	0.59	0.47	0.19–1.19	0.11	0.84	0.49–1.45	0.54
C4	0.8	0.42–1.53	0.5	0.49	0.21–1.13	0.09	0.67	0.41–1.11	0.12

C = cycle; cfDNA = cell-free DNA; CI = confidence interval; OR = odds ratio;

5.4.4 Radiological progression-free survival

When grouped by quartiles for cfDNA concentrations, median radiographic progression free survival (rPFS) in FIRSTANA was 17, 11, 10 and 11 months from the lowest to the highest total cfDNA quartiles. In PROSELICA, rPFS by quartiles was 12, 10, 8 and 6 months from lowest to highest cfDNA quartiles. This correlation of baseline cfDNA concentration quartiles with rPFS is shown with Kaplan-Meier survival curves in ***Figure 5-4.***

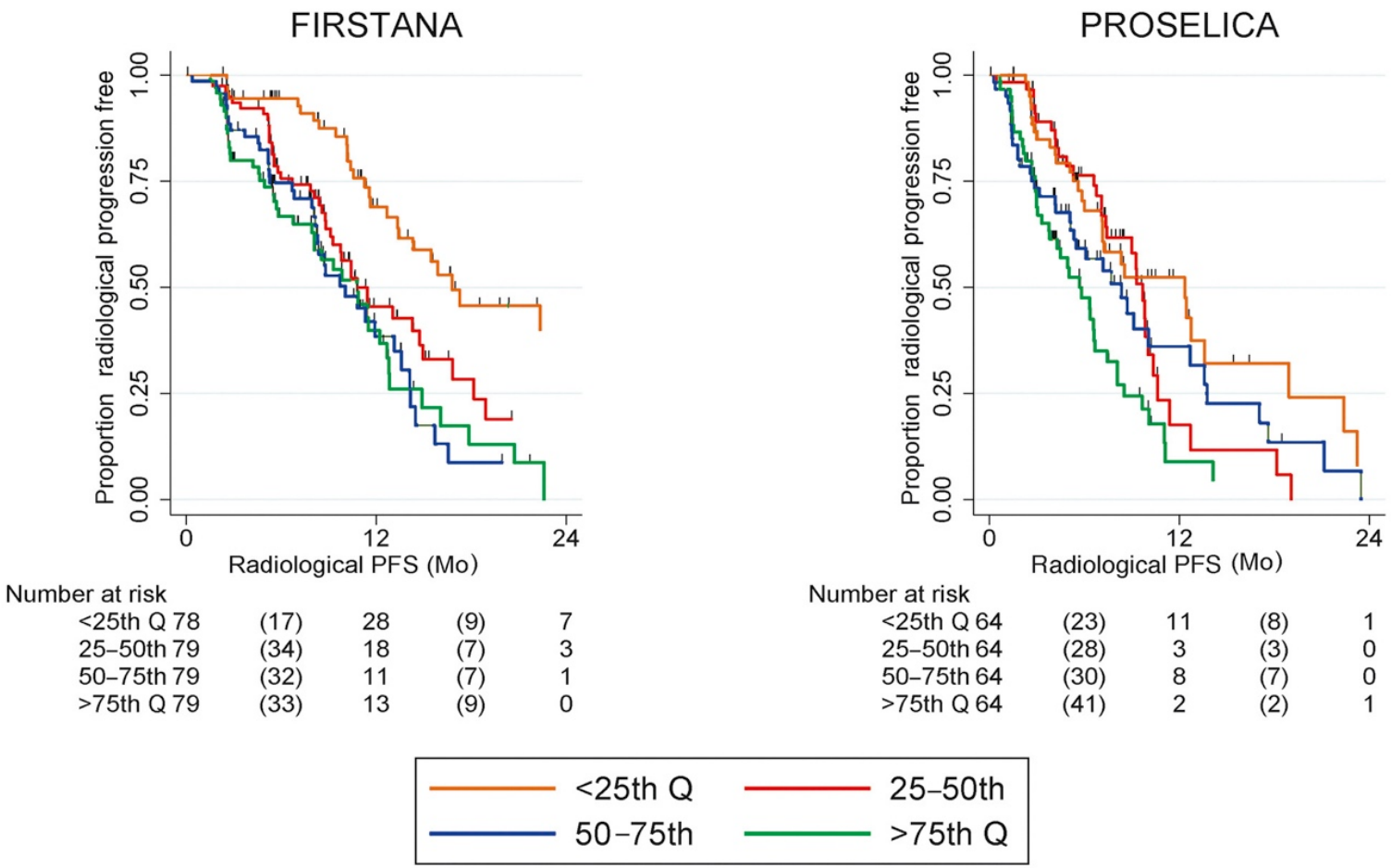

Figure 5-4: Kaplan-Meier curve of rPFS by baseline log_{10} cfDNA concentration quartiles for FIRSTANA and PROSELICA.

Mo = months; PFS = progression free survival; Q = quartile

Figure 5-5 shows a forest plot for rPFS using a multivariable analysis model for baseline log_{10} cfDNA concentrations for each study and also for an overall combined estimate, which had a HR of 1.56 (95% CI: 1.08 – 2.24, p = 0.323).

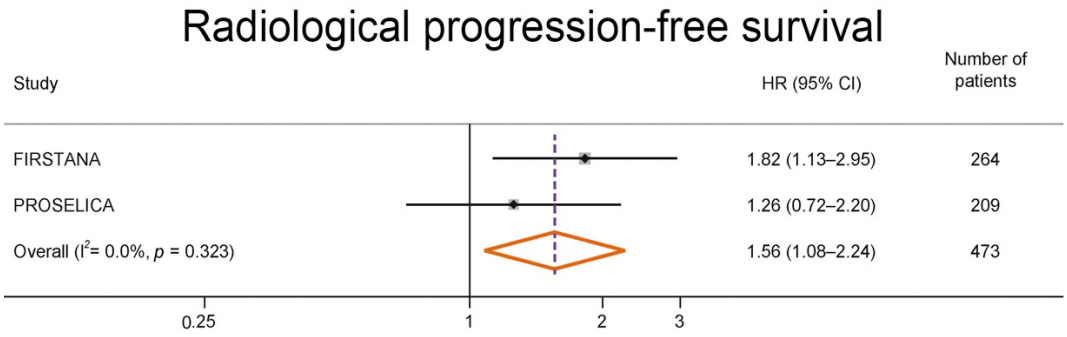

Figure 5-5: Forest plot of rPFS for baseline log_{10} cfDNA concentration

Shown for each study and combined estimate (multivariable analysis). HR = hazard ratio; CI = confidence interval

Multivariable survival analyses of baseline prognostic factors and rPFS are shown in ***Table 5-7***. Log_{10} cfDNA concentrations had an HR of 1.54 with a 95% CI of 1.15 - 2.08; p = 0.004. Uno's inverse-probably weighted C-index for this model with time truncated at 24 months was 0.70 with a 95% CI of 0.67 - 0.73. This model did not provide significantly improved model fit compared with the model not including log_{10} cfDNA (C-index: 0.69; 95% CI: 0.66–0.73; delta (Δ) = 0.006; −0.003 to 0.02; p = 0.2). The AUC of the time-dependent ROC curve for the model with cfDNA at 10 months was 0.78 (95% CI: 0.73 – 0.84) and again was not significantly different from the model not including log_{10} cfDNA (p = 0.5). This is shown in ***Figure 5-6A*** (ROC at 10 months) and ***Figure 5-6B*** (time-dependent).

In both FIRSTANA and PROSELICA, C2 and C4 (i.e. post-treatment) log_{10} cfDNA concentrations were associated similarly with rPFS. Estimates combining the studies for log_{10} cfDNA concentrations at C2 had a HR of 1.89 (95% CI: 1.36 – 2.63, p <0.001) and at C4 a HR of 1.88 (95% CI: 1.32 – 2.68, p <0.001). The absolute change in log_{10} cfDNA concentrations at C2 or C4 did not associate significantly with rPFS in the combined study estimates; HR = 1.12, 95% CI: 0.78–1.59, p = 0.5 and HR = 1.37, 95% CI: 0.92–2.02, p = 0.1 respectively.

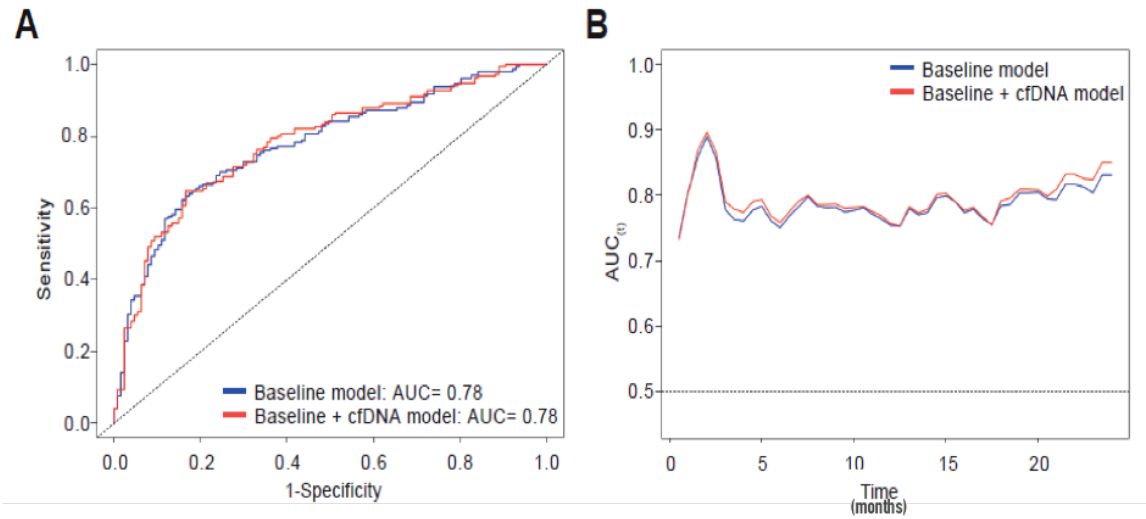

Figure 5-6: ROC at 10 months (A) and time dependent AUC for rPFS (B)

AUC = area under the curve; cfDNA = cell-free DNA; ROC = receiver operating characteristics; rPFS = radiographic progression free survival

Baseline prognostic factors including $\log_{10}$ cfDNA concentrations, baseline ECOG performance status, visceral metastases, bone-only disease, Gleason score at diagnosis, baseline pain, albumin, ALP, haemoglobin, LDH, neutrophil:lymphocyte ratio (NLR) and PSA were used for multivariate analysis as shown in ***Table 5-7***. In this multivariable analysis, $\log_{10}$ cfDNA concentrations had a hazard ratio of 1.54 (95% CI of 1.15 – 2.08, p = 0.004) for rPFS.

Table 5-7: Multivariable analysis of radiographic Progression Free Survival and Overall Survival

Baseline characteristics	rPFS			OS		
	aHR	95% CI	*p* value	aHR	95% CI	*p* value
Log_{10} cfDNA	1.54	1.15–2.08	0.004	1.53	1.18–1.97	0.001
ECOG PS						
0 - 1	1	–	–	1	–	–
≥2	1.16	0.68–1.96	0.7	1.15	0.76–1.74	0.5
Visceral disease						
No	1	–	–	1	–	–
Yes	1.77	1.33–2.36	<0.001	1.46	1.15–1.86	0.002
Bone-only disease						
No	1	–	–	1	–	–
Yes	0.54	0.39–0.75	<0.001	0.79	0.62–1.01	0.06
Gleason score						
<8	1	–	–	1	–	–
≥8	1.43	1.11–1.85	0.006	1.17	0.95–1.44	0.13
Baseline pain						
No	1	–	–	1	–	–
Yes	1.2	0.88–1.63	0.3	1.29	1.00–1.67	0.06
Study						
FIRSTANA	1	–	–	1	–	–
PROSELICA	1.49	1.11–2.00	0.008	1.65	1.29–2.13	<0.001
Trial arm						
Cabazitaxel 20 mg/m^2	1	–	0.8	1	–	0.6
Cabazitaxel 25 mg/m^2	1	0.77–1.30	–	0.91	0.73–1.13	–
Docetaxel 75 mg/m^2	1.14	0.79–1.64	–	1.04	0.77–1.41	–
LDH (Log_{10} U/l)	2.4	1.32–4.37	0.004	2.41	1.43–4.05	0.001
ALP (Log_{10} U/l)	1.12	0.78–1.61	0.5	1.53	1.14–2.04	0.004
Haemoglobin (g/dl)	0.85	0.77–0.94	<0.001	0.86	0.79–0.94	<0.001
Albumin (g/dl)	1	0.85–1.17	1	1.04	0.87–1.25	0.7
PSA (log_{10} ng/ml)	0.86	0.72–1.03	0.1	1.03	0.87–1.21	0.7
NLR (log_{10})	1.42	0.88–2.28	0.2	1.78	1.18–2.70	0.006

aHR = adjusted hazard ratio; ALP = alkaline phosphatase; cfDNA = cell-free DNA; CI = confidence interval; ECOG PS = Eastern Cooperative Oncology Group performance status; LDH = lactate dehydrogenase; NLR = neutrophil lymphocyte ratio; rPFS = radiographic progression-free survival; PSA = prostate specific antigen; WBC = white blood cell count; U = unit.

5.4.5 Overall survival

When grouped by quartiles for cfDNA concentrations, median overall survival (OS) for FIRSTANA patients was 39, 30, 22 and 15 months from the lowest to the highest cfDNA quartiles. In PROSELICA, median OS was 18, 18, 12 and 9 months from the lowest to the highest quartile. Kaplan-Meier survival curves with the numbers at risk are shown per study by quartiles in ***Figure 5-7.***

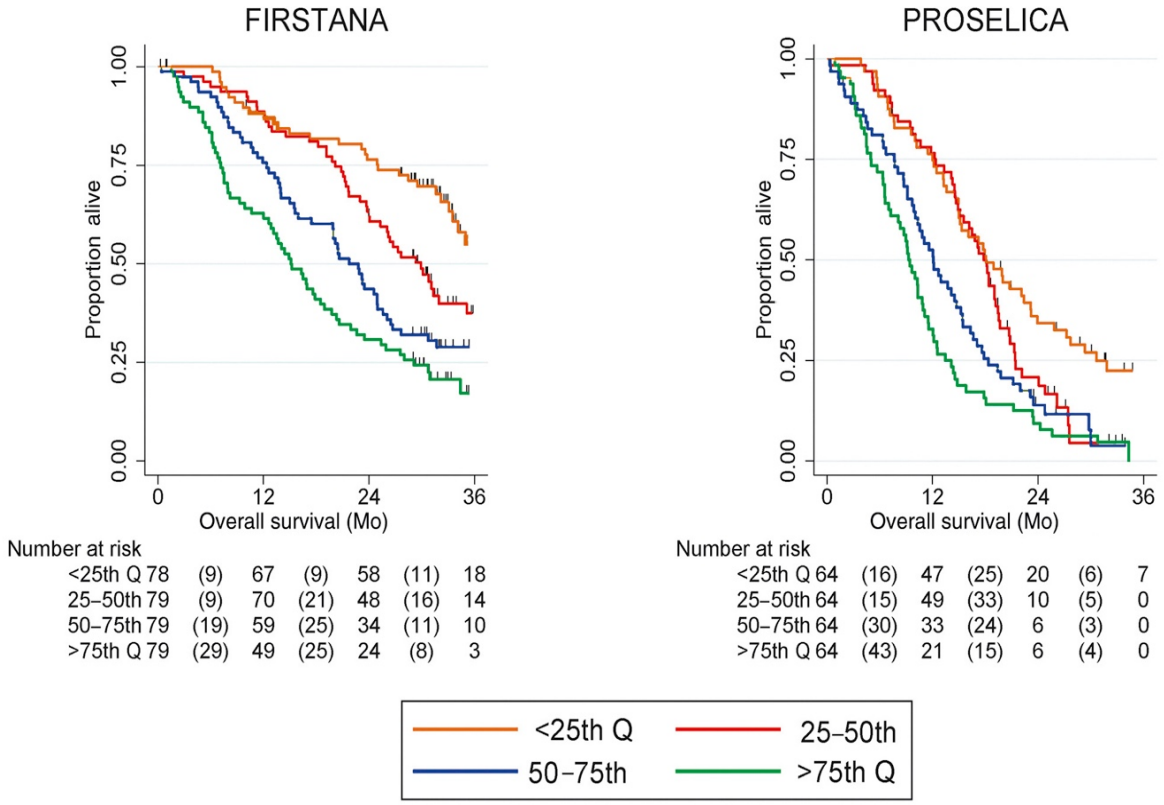

Figure 5-7: Kaplan-Meier survival curves of overall survival plotted by baseline cfDNA concentration quartiles.

Mo = months; Q = quartile

Figure 5-8 shows a forest plot for OS using a multivariable analysis model for baseline log_{10} cfDNA concentrations for each study and also for an overall combined estimate which had a HR of 1.55 (95% CI: 1.15 – 2.09, *p* = 0.360).

Multivariable survival analyses of baseline prognostic factors and OS are also shown in ***Table 5-7***. For OS, log_{10} cfDNA concentrations had a HR of 1.53 (95% CI: 1.18–1.97; *p* = 0.001). Uno's inverse-probability weighted C-index for this model with time truncated at 36 months was 0.73, with a 95% CI of 0.70 – 0.75. This model did not show a significantly improved model fit compared with the model not including log_{10} cfDNA (C-index: 0.72, 95% CI: 0.70–0.75, delta (Δ) = 0.004, −0.0009 to 0.008, *p* = 0.12).

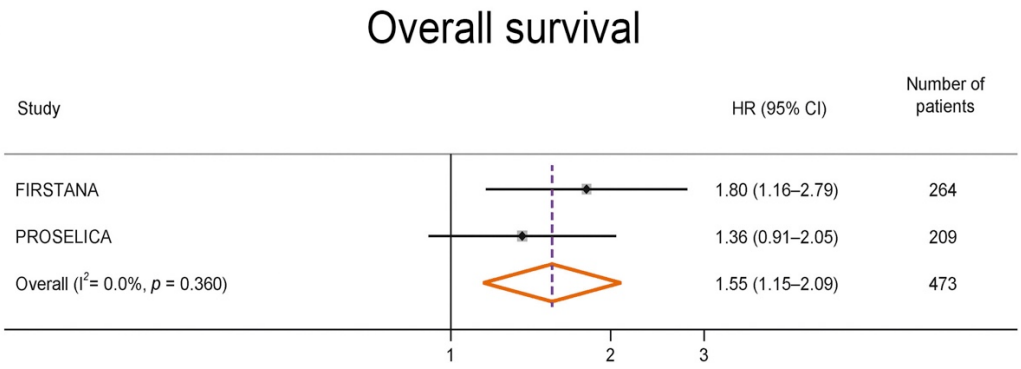

Figure 5-8: Forest plot of overall survival for baseline log_{10} cfDNA concentration

Shown for each study and the combined estimate (multivariable analysis). HR = hazard ratio; CI = confidence interval

For the model including cfDNA, the AUC under the time-dependent ROC curve at 19 months was 0.82 (95% CI: 0.78–0.86) and was not significantly higher than that for the model without cfDNA (*p* = 0.05) (see ***Figure 5-9***).

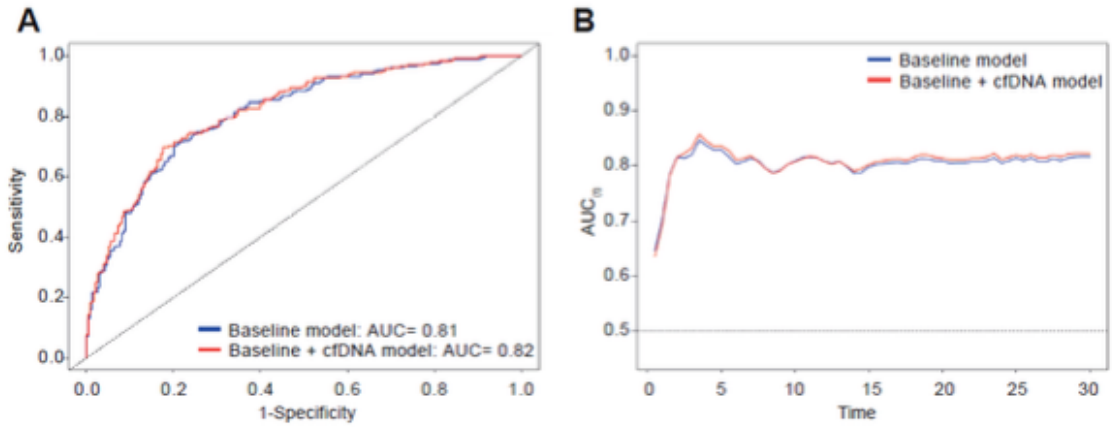

Figure 5-9: ROC at 19 months (A) and time-dependent AUC for OS (B)

AUC = area under the curve; cfDNA = cell-free DNA; ROC = receiver operating characteristics

Combined study-estimated OS of patients who had post-treatment (i.e. C2 and C4) samples available showed that at C2 the HR was 1.77 (95% CI: 1.37–2.29; p <0.001) and at C4 the HR was 1.75 (95% CI: 1.30–2.35; p <0.001). There was no significant association between the absolute change in $\log_{10}$ cfDNA concentrations from these post-treatment samples with overall survival in the combined study estimates (C2 HR = 1.26, 95% CI: 0.94-1.68, p = 0.12 and C4 HR = 1.29, 95% CI: 0.92–1.79, p = 0.14).

5.5 Discussion

This analysis of cfDNA concentrations in 751 patients treated with taxane chemotherapy on two large Phase III trials, shows that baseline cfDNA concentrations correlate with both rPFS and OS. When split by quartiles of cfDNA concentrations, those with low concentrations both live longer and have longer before there is radiographic evidence of disease progression. This utility of cfDNA as a prognostic marker was maintained in multivariable analyses with models including other known prognostic variables. However, baseline cfDNA concentrations did not show a significant relationship with a biochemical, radiological or clinical response to taxanes, confirming that cfDNA has use as an independent prognostic marker, but not as a predictive biomarker in this setting.

It is important to note that the sample collection for biomarker analyses was optional in both of these trials, which means only a proportion of patients had this extra plasma collected. This subset was selected randomly and not matched for baseline characteristics, and thus may not be an accurate representation of the full study population. Corrections for any imbalances between the sub-study population and full population must be made before extrapolating from any results of this sub-study alone to the overall population.

Issues with plasma storage, processing, transportation and handling must also be mentioned, as these may have compromised cfDNA integrity and consequent results. Studies have shown that plasma cfDNA degrades by approximately 30% per year of storage (137), and even the length of time taken to process a blood sample to aliquots of plasma may affect the volume of plasma obtained and thus the amount of cfDNA isolated (223). Despite the fact that the samples used here were all processed as per protocol, a degree of inter-sample and inter-site variability is to be expected. However,

the high concordance seen between the biological replicates (r = 0.84, p <0.001) is reassuring here. Additionally, as per protocol, these samples were collected in heparinised tubes, which are known to have an inhibitory effect on polymerase-chain reactions. Other storage tubes, such as EDTA and citric acid may be superior in terms of maintain cfDNA stability, and certainly now, the ready availability of cell-stabilising blood collection tubes like Streck™ BCT and PAXgene™ tubes has transformed this field (224).

Other factors, including high interpatient variability in cfDNA concentrations must also be considered. Whilst higher levels are found in cancer patients, cfDNA can also be identified in the blood of healthy volunteers, and there may be a significant degree of overlap, with cfDNA concentrations being linked to inflammation and infection (225). Furthermore, whereas cfDNA levels appear to correlate with disease burden and closely resemble changes in LDH, PSA, and radiographic differences, it is acknowledged that different proportions of the overall total cfDNA can be made up by circulating tumour DNA (ctDNA) and this proportion can vary significantly.

The fraction of ctDNA within the overall cfDNA level is typically small, but can constitute anywhere in the range of 0.01% to 95% of the cfDNA, and also displays substantial high interpatient variability (226). Highly sensitive methods are required to identify genomic alterations such as mutations and copy number changes that may be present at very low allele frequencies in these patients. These low levels make detection of these alterations very challenging, but using bioinformatic algorithms to try and estimate tumour content from single nucleotide polymorphisms and clonal mutations may increase the utility of cfDNA as a biomarker.

Despite these limitations, cfDNA shows potential as an independent prognostic biomarker, although external validation is still warranted to confirm this clinical utility. Whilst undeniably useful, quantification of cfDNA does not satisfy the urgent need for biomarkers predicting response to taxane therapy; qualification of cfDNA by genomic analysis may therefore be much more informative. This is explored further in ***Chapter 6***.

6. Sequencing plasma cell-free DNA

6.1 Aims and Hypotheses relating to this chapter

6.1.1 Hypothesis:

Blood-based biomarkers have clinical utility, and genomic analyses of plasma cell-free DNA may have both prognostic and predictive value in monitoring outcomes from taxanes therapy.

6.1.2 Aim:

To clinically qualify baseline, and on-treatment, cell-free DNA (cfDNA) genomic analyses as a biomarker of patient outcome in patients treated with taxane chemotherapy, utilising plasma samples acquired from two large, prospective Phase III clinical trials (FIRSTANA and PROSELICA).

6.2 Research in context

Taxanes, specifically the drugs docetaxel and cabazitaxel, are currently the only class of chemotherapy licensed for the treatment of metastatic castration-resistant prostate cancer (mCRPC). Whilst both of these licensed chemotherapeutic agents result in demonstrable improvements in overall survival (OS), prostate-specific antigen (PSA) and quality of life (QoL), responses are variable and resistance inevitable. We and others have shown that responses to treatment in mCRPC can be monitored using plasma cell-free DNA (cfDNA); this can be both quantitative (227) and qualitative (136).

Using these liquid biopsies to monitor disease has many advantages, and when analysed with next-generation genomics, cfDNA offers key insights into the driving elements of an individual's disease. Low-pass whole genome sequencing is an effective approach to assess genome-wide copy number events (228) with advances in technology making this more cost-efficient and allowing for a high-throughput of samples. Aside from gene-level copy number events, other biomarkers from sequencing cfDNA, such as percentage of genome altered and average copy-number fragment size have also been implicated as informative (127,128).

After exploring cell-free DNA concentrations and their role as biomarkers of patient outcome in patients treated with taxane chemotherapy, I now use this same cohort to investigate whether genomic analysis by sequencing cfDNA from plasma can be used to predict patient outcome and response to chemotherapy in mCRPC.

6.3 Study design

6.3.1 Clinical data

Blood for cfDNA analysis was collected prospectively from mCRPC patients treated on two phase III clinical trials, FIRSTANA (NCT01308567) and PROSELICA (NCT01308580). As described previously, in FIRSTANA chemotherapy-naïve patients were randomised to receive docetaxel (75mg/m^2) (*n* = 391) or one of two doses of cabazitaxel (20mg/m^2 or 25mg/m^2) (*n* = 389 and *n* = 388 respectively). In PROSELICA, patients with previous docetaxel exposure were randomised to receive one of two doses of cabazitaxel (20mg/m^2 or 25mg/m^2) (*n* = 598 and *n* = 602 respectively) as second-line chemotherapy. The outcomes of both trials have previously been reported (15,215) and here I present the sequencing data on plasma cfDNA collected for biomarker subgroup analyses.

In both of these trials, the primary endpoint measured was overall survival (OS), which was defined as time from randomisation to death from any cause. Secondary endpoints for both trials included radiographic progression free survival (rPFS), safety and tolerability, health-related quality of life, PSA response, pharmacokinetics and pain response. Outcome measures were reported as recommended by the Prostate Cancer Working Group Criteria 2 (PCWG2) (216). A database was collated from these Sanofi-Aventis sponsored trials of all the relevant clinical variables. These studies were large, international and multi-institutional trials; selected sites collected plasma for cfDNA for evaluation as an exploratory biomarker. Samples were collected for pre-planned biomarker analyses, from cohorts of consenting patients within each study at pre-specified timepoints.

6.3.2 Sample Collection

This is also described in ***Chapter 2*** (Materials and Methods) and in ***Chapter 5*** (Plasma cfDNA concentrations). Biomarker collection was optional, with patients who consented to the substudy having blood samples taken twice at baseline (at least 24 hours apart) from all treatment arms, and then at 3-time points after the start of the study; Cycle 2 day 1 (C2), Cycle 4 Day 1 (C4) and when patients came off the study (end of study; EOS). Blood was collected in 8mL BD Vacutainer^{TM} CPT cell preparation tubes containing sodium heparin (this was planned before the availability of specialised tubes for cfDNA collection and before our work validating Streck^{TM} tubes for cfDNA studies). Prior to blood collection, tubes were stored at room temperature. After collecting the blood, tubes were inverted 8-10 times and stored upright at room temperature until centrifugation. Samples were then centrifuged within 2-hours of blood collection, and were remixed immediately prior to centrifugation again by gently inverting the tube 8-10 times. Samples were centrifuged, again at room temperature, in a horizontal rotor for a maximum of 15-minutes at 1500 to 1800 relative centrifugal force (RCF). Following the centrifugation process, approximately 4mL of plasma was available for collection, and was aliquoted using a sterile Pasteur pipette into 1mL tubes for storage at -80^{o}C. Plasma from healthy volunteers was also collected under an ethically approved institutional protocol in Streck^{TM} Tubes.

6.3.3 Cell-free DNA extraction and quantification

This was performed utilising methods described previously, using the QIAamp Circulating Nucleic Acid Kit (Qiagen, Hilden, Germany) to extract cfDNA from 1ml of plasma (217). Quantification was carried out using the Quant-IT Picogreen HS DNA Kit (ThermoFisher, Massachusetts, USA) (187), with final values recorded and used to calculate the input volume needed for library preparation. As these samples were collated in Lithium heparin tubes, heparinase I (Sigma-Aldrich, Missouri, USA) was used as per manufacturer's protocol to remove the heparin prior to sequencing (229).

6.3.4 Low pass whole genome sequencing

This is described in detail in ***Chapter 2*** (Materials and Methods). Where possible, 10ng of the extracted cfDNA was sequenced using the QIAGEN QIAseq FX DNA Library Kit

(96) (191). Following quality control measures and subsequent clean up, samples were sequenced on the Illumina Novaseq 6000 (Illumina, California, USA).

6.3.5 Targeted sequencing

This is also described in detail in ***Chapter 2*** (Materials and Methods). Briefly, libraries were sequenced using a targeted AmpliSeq™ panel of 30 genes, pre-selected for their putative roles in taxane resistance was custom-designed. The full list of genes is given in ***Table 2-1, Chapter 2*** (Materials and Methods). A 10ng input of DNA per sample was used for library preparation, and construction performed as per the Ion AmpliSeq™ DNA and RNA library preparation user guide (189). Template preparation and chip loading was performed using the Ion Torrent Ion Chef System and samples sequenced on the Ion Torrent Proton as per SOP (ThermoFisher, Massachusetts, USA) (190).

6.3.6 Array comparative genomic hybridisation

A subset of cfDNA samples from the Sanofi-Aventis cohorts were selected for a trial of plasma array comparative genomic hybridisation (aCGH) to serve as a validation set for the sequencing data. A preliminary assessment of the integrity of samples used was performed using the Agilent Tapestation HSD1000 kit as per manufacturer protocol. DNA input ranging from 1ng to 10ng was used for amplification with the Sigma GenomePlex Whole Genome Amplification Kit (WGA2; Sigma-Aldrich) protocol. Following this, fragmentation, library preparation and amplification was performed as per the Array-Based CGH for Genomic DNA Analysis Protocol (Agilent). PCR products were cleaned using the Qiaquick PCR Purification Kit (Qiagen.) Labelling, hybridization and scanning was performed as per the Agilent manufacturer protocol. Agilent Feature Extraction software (Version 12.0) and Agilent CytoGenomics software were used for analysis.

6.3.7 Bioinformatic and statistical analysis

In order to ascertain that my selected sub-study populations did not substantially differ from the overall trial populations, the baseline characteristics of the selected patients were compared with the baseline characteristics of the study patients not selected from the two trials, using both the X^2 and *t*-test as appropriate. Baseline characteristics between the two trials (of selected patients) were also compared, again using the X^2 and *t*-test as indicated.

Bioinformatic and statistic support was provided mainly by George Seed, a bioinformatician pursuing a PhD in our laboratory, under the supervision of Dr Wei Yuan, senior bioinformatician within our Cancer Biomarkers team. Detailed approaches are provided in ***Chapter 2*** (Materials and Methods). Output FASTQ files were generated from the NovaSeq 6000^{TM} using the bcl2fastq2 software (v2.17.14, Ilumina, California, USA). The default chastity filter selected sequence reads for subsequent analysis, selecting high quality and non-duplicate reads. All sequencing reads were aligned to the human genome reference sequence (GRCh37) using the BWA (v. 0.7.12) MEM algorithm, and indels were realigned using the Stampy (v.1.0.28) package. Picard tools (v.2.1.0) were used to remove PCR duplicates and to calculate sequencing metrics for quality control check, alongside FASTQC (v.0.11.8). Samples were excluded from analysis if the sequencing depth was less than 0.05X or if they failed the FASTQC read quality filter.

Aligned reads (.bam) were converted into interval-formatted counts of reads (.wig) using HMMcopy readCounter (v. ABC), with the quality filter set to 20 and interval width set to 500kb. Copy number analysis was performed using the ichorCNA software (v0.1.0) which also estimated tumour fraction of cfDNA and tumour ploidy. Transition strength parameters (--txnE and --txnStrength) was set at 0.99999 and 100000 respectively, and the maximum copy number was set to 20 to account for high-level amplifications. We modelled normal contamination (initial values 40% to 90%), ploidy (initial values 2 and 3), and subclonal events. In lieu of a normal panel, the previously generated 500kb reference coverage dataset supplied with ichorCNA was used. To access bin-level copy number ratios, we intersected each sample's ichorCNA segment data with the initial 500kb intervals used for collation of coverage data (n=5226). This enabled comparison of copy-number profiles to be made by calculating Pearson's correlation coefficient of the smoothed $\log_2$ ratio values across the bins. For copy number calling, a $\log_2$ ratio of >2 was considered as threshold for amplifications and a $\log_2$ ratio <-1.2 used as a threshold to consider homozygous deletions.

Effects on median rPFS and OS were estimated using the Kaplan-Meier method. The multivariable Cox proportional hazard model was used to test for associations between tumour purity (based on estimated tumour fraction) and other known prognostic variables with radiographic progression free survival and overall survival. The multivariable analyses performed were adjusted for several factors which include albumin, alkaline

phosphatase (ALP), baseline Eastern Cooperative Oncology Group performance status. Logistic regression was used for multivariable analysis of response.

Any *p* value <0.05 was considered statistically significant. For all statistical analysis and for the creating of figures used in this chapter, Microsoft Excel v16.16.10, Stata v13, R v3.4.1, SPSS Statistics for Macintosh v22.0 (IBM Corp, New York, USA), and GraphPad Prism version 6.0 for Macintosh (GraphPad Software, California, USA) were used.

6.4 Results from low pass whole genome sequencing

6.4.1 Patients and samples

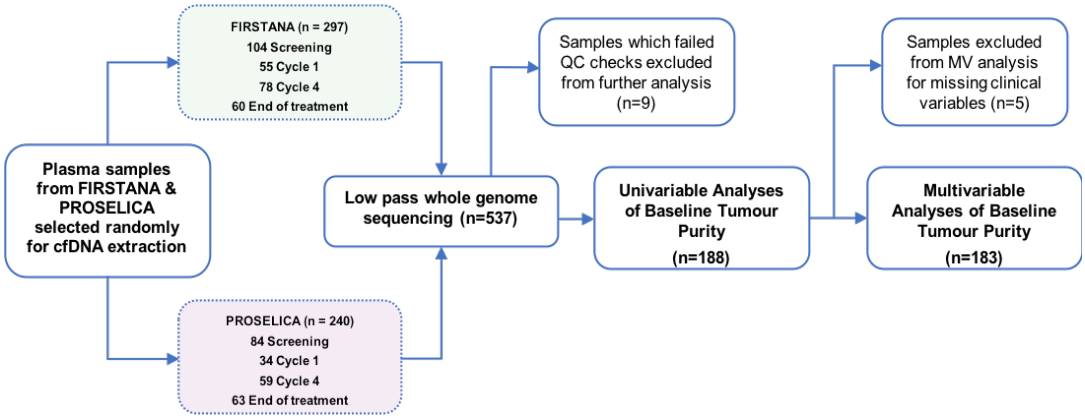

Figure 6-1: Study design.

cfDNA = cell-free DNA; MV = multivariable

Study design is shown in ***Figure 6-1***. One-hundred and ninety mCRPC patients were included in this sub-study; 105 of the 1168 patients enrolled in FIRSTANA (9%) and 85 of the 1200 patients who participated in PROSELICA (7%). Patient samples were collected between April 2011 and December 2013. From the 105 FIRSTANA patients, 297 plasma samples were available, and from the 85 PROSELICA patients there were 240 plasma samples available for analysis. Of these 190 unique patients, 135 had a paired baseline and EOS sample (77 pairs from FIRSTANA and 58 from PROSELICA).

Low pass WGS data were generated from these 537 available samples acquired at three different timepoints (baseline [SCR and C1], C4 and EOS). After QC checks, 9 samples were excluded from further analysis, which eliminated 2 patients from FIRSTANA only. Of the 528 remaining samples, these were split between the two studies as described: in FIRSTANA, n= 290 was split 101 (SCR), 55 (C1), 77 (C4) 57 (EOS) and in

PROSELICA, n=238 was split 84 (SCR), 33 (C1), 58 (C4) 63 (EOS). For analysis of the baseline data, predominantly screening samples were used and C1 used only when a screening sample was not available.

Clinical characteristics of this cohort are described in ***Table 6-1*** which compares the two patient cohorts. Of note, cohorts were similarly matched in terms of age, baseline pain, RECIST measurable disease, presence of visceral disease and for baseline albumin levels. Some differences were seen between the two cohorts with PROSELICA patients having a more advanced ECOG performance status, higher LDH and ALP levels as well as a higher baseline PSA. These changes were expected as the PROSELICA cohort comprised a more advanced group of patients. A higher response rate (a >50% reduction of PSA at both 12-weeks and at any time) was seen in FIRSTANA than in PROSELICA, which is consistent with first line taxane therapy response rates versus those of second-line taxanes.

The average cfDNA input was 10ng and following sequencing the sequencing depth achieved was ~1.7X (n=528, median = 1.72, SD = 1.23).

Table 6-1: Clinical characteristics of biomarker sub-study cohort

CHARACTERISTIC	FIRSTANA N =105 N (%)	PROSELICA N = 85 N (%)	*P* VALUE[a]
ECOG PS[b]			
0-1	102 (97)	75 (88)	0.02
2	3 (3)	10 (12)	
RECIST measurable[b]			
No	51 (40)	40 (47)	0.84
Yes	54 (51)	45 (53)	
Visceral disease			
No	85 (81)	60 (71)	0.10
Yes	20 (19)	25 (29)	
Pain at baseline[c]			
No	19 (18)	21 (25)	0.43
Yes	71 (68)	59(69)	
	Median (IQR)	**Median (IQR)**	***p* value[d]**
Age (yr)	68 (62 - 72)	67 (64-71)	0.26
LDH (U/l)	263 (207 - 368)	350 (222 - 588)	0.004
ALP (U/l)	128.5 (80.5 - 240.8)	209 (118 - 415)	0.002
Haemoglobin (g/dl)	123 (114 - 132.1)	116.8 (107.8 - 124)	<0.001
Albumin (g/dl)	40.1 (37.3 - 43)	40 (36 - 43)	0.20
PSA (ng/ml)	77.9 (22.4 - 236.5)	247.1 (93.7 - 740.8)	<0.001
PSA doubling time (mo)	2 (1.2 - 3.2)	1.7 (1.2 - 2.8)	0.34
Outcome	**N (%)**	**N (%)**	***p* value[a]**
>50% PSA response at 12 weeks			
No	49 (47)	62 (73)	0.0003
Yes	56 (53)	23 (27)	
>50% PSA response at any time			
No	36 (34)	52 (61)	0.0002
Yes	69 (66)	33 (39)	

ALP = alkaline phosphatase; ECOG PS = Eastern Cooperative Oncology Group performance status; IQR = interquartile range; LDH = lactate dehydrogenase; mo = months; PSA = prostate-specific antigen; RECIST = Response Evaluation Criteria in Solid Tumours; U = unit, yr = years
a χ^2 test.
b Stratification parameters
c Twenty assessments missing (15 in FIRSTANA and 5 in PROSELICA)
d Wilcoxon rank-sum test

Importantly, I compared this biomarker sub-study cohort with the wider trial population to ensure a fair representation of the overall study, which is shown in ***Table 6-2***. On the whole, the characteristics of the sub-study cohorts did not differ significantly from the main trial populations for both baseline characteristics and response data. In FIRSTANA, differences were noted for baseline pain, albumin and haemoglobin. For PROSELICA, differences were noted for age, baseline haemoglobin, ALP and PSA. Critically, for both trials, no significant differences were seen in the sub-study cohort PSA response data compared to the main trial populations.

Table 6-2: Baseline characteristics in this sub-study cohort vs. all trial participants

	FIRSTANA			PROSELICA		
Characteristic	**Biomarker subset n = 105 N (%)**	**Non-biomarker subset n = 1063 N (%)**	***p*-value[a]**	**Biomarker subset n = 85 N (%)**	**Non-biomarker subset n = 1115 N (%)**	***p*-value[a]**
ECOG PS[b]						
0–1	102 (7)	1018 (96)	0.5	75 (88)	1005 (90)	0.6
2	3 (3)	45 (4)		10 (1)	1110 (10)	
RECIST measurable[b]						
No	51 (49)	502 (47)	0.79	40 (47)	571 (51)	0.46
Yes	54 (51)	561 (53)		45 (53)	544 (49)	
Visceral disease						
No	85 (81)	833 (78)	0.54	60 (71)	805 (72)	0.75
Yes	20 (19)	230 (22)		25 (29)	310 (28)	
Pain at baseline[c]						
No	19 (18)	355 (33)	0.04	21 (25)	289 (26)	0.7
Yes	71 (68)	624 (59)		59 (69)	734 (66)	
	Median (IQR)	**Median (IQR)**	***p*-value[d]**	**Median (IQR)**	**Median (IQR)**	***p*-value[d]**
Age (yr)	68 (62 - 72)	68 (63 - 74)	0.14	67 (64-71)	69 (63 - 74)	0.01
LDH (U/L)	263 (207 - 368)	239 (190 - 374)	0.12	350 (222 - 588)	325 (220 - 498)	0.32
ALP (U/L)	128.5 (80.5 - 240.8)	125 (79 - 264)	0.35	209 (118 - 415)	163 (92 - 346)	0.02
Haemoglobin (g/dl)	123 (114 - 132.1)	128 (117 - 137)	0.01	116.8 (107.8 - 124)	120 (108 - 130)	0.02
Albumin (g/dl)	40.1 (37.3 - 43)	41 (38 - 44)	0.05	40 (36 - 43)	40 (36.7 - 43)	0.4
PSA (ng/ml)	77.9 (22.4 - 236.5)	76 (29.9 - 196.4)	0.43	247.1 (93.7 - 740.8)	158.3 (53.2 - 412.85)	0.001
PSA-doubling time (mo)	2 (1.2 - 3.2)	2 (1.3 - 3.4)	0.14	1.7 (1.2 - 2.8)	1.9 (1.2 - 3.1)	0.32
Outcome	**N (%)**	**N (%)**	***p*-value**	**N (%)**	**N (%)**	***p*-value**
>50% PSA response at 12 weeks						
No	49 (47)	484 (46)	0.82	62 (73)	765 (69)	0.40
Yes	56 (53)	579 (54)		23 (27)	351 (31)	
>50% PSA response at any time						
No	36 (34)	309 (30)	0.26	52 (61)	660 (59)	0.71
Yes	69 (66)	754 (70)		33 (39)	456 (41)	

ALP = alkaline phosphatase; cfDNA = cell-free DNA; ECOG PS = Eastern Cooperative Oncology Group performance status; IQR = interquartile range; LDH = lactate dehydrogenase; mo = months; PSA = prostate-specific antigen; RECIST = Response Evaluation Criteria in Solid Tumours; U = unit, yr = years.
a = χ^2 test.
b = Stratification parameters
c = For FIRSTANA 99 assessments were missing (15 in the sub-study and 84 in the main study), For PROSELICA 97 assessments were missing (5 in the sub-study and 92 in the main study).
d = Wilcoxon rank sum test

6.4.2 Cell-free DNA has clinical utility in monitoring disease

As shown in ***Figure 6-2***, clean copy number traces were generated and changes common to prostate cancer were seen. The classic 8p loss and 8q gain is seen neatly by observing *NKX3-1* (8p) and *MYC* (8q). The bottom centre panel shows an unaltered region on chromosome 11 where *ATM* lies, and the far-right panel shows a clean breakpoint with *RB1* loss in the context of an unaltered *BRCA2*.

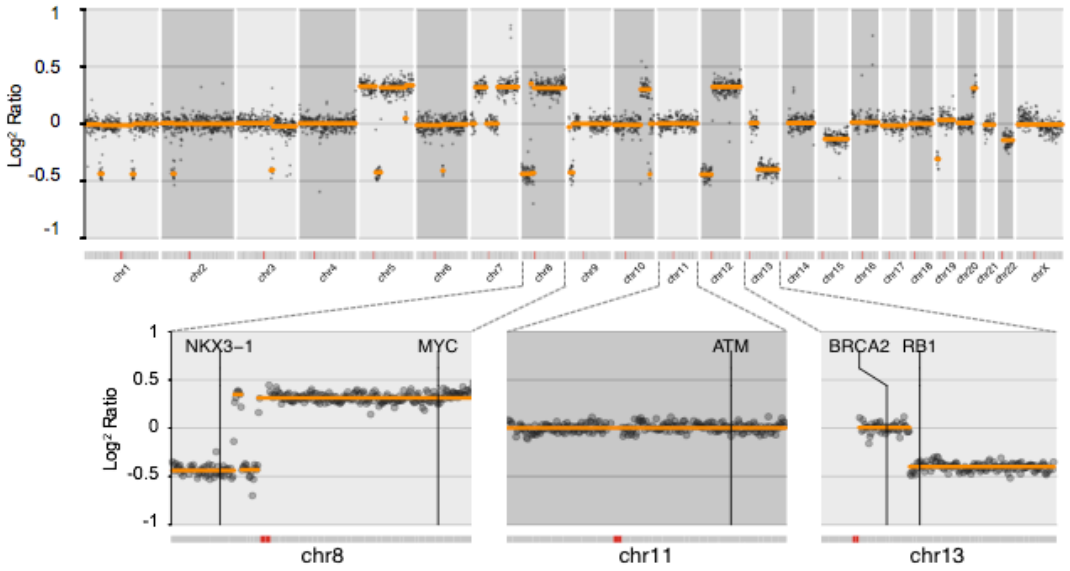

Figure 6-2: A copy number trace from a baseline sample from one patient treated within the PROSELICA trial.

The log_2 ratios are shown on the y axis and the chromosome bar from left to right on the x axis. Chr = chromosome.

We observed putative copy number profiles consistent with emerging CRPC subtypes as shown in ***Figure 6-3***: (A) sparse alterations with highly focal amplifications including AR, (B) frequent large-scale copy number changes associated with HRD and (C) a sawtooth pattern linked to CDK12 deficient tumours.

Whilst the majority of samples had similar copy number traces, some were completely flat which may be consistent with low tumour purity and/or response to treatment. Forty-five of these flat traces were baseline samples (24%; 45/190). ***Figure 6-4***, shows a series of samples from one patient with a screening sample (A), an on-treatment sample at Cycle 4 Day 1 (B) and at end of treatment (C). The profile visible at the start of treatment flattens with response to treatment, with the patient having a corresponding radiographic and biochemical response. By the end of treatment, the patient showed clinical signs of

disease progression, consistent with the trace seen in ***Figure 6-4C***, which shows the return of the cancer associated changes seen at the start of treatment.

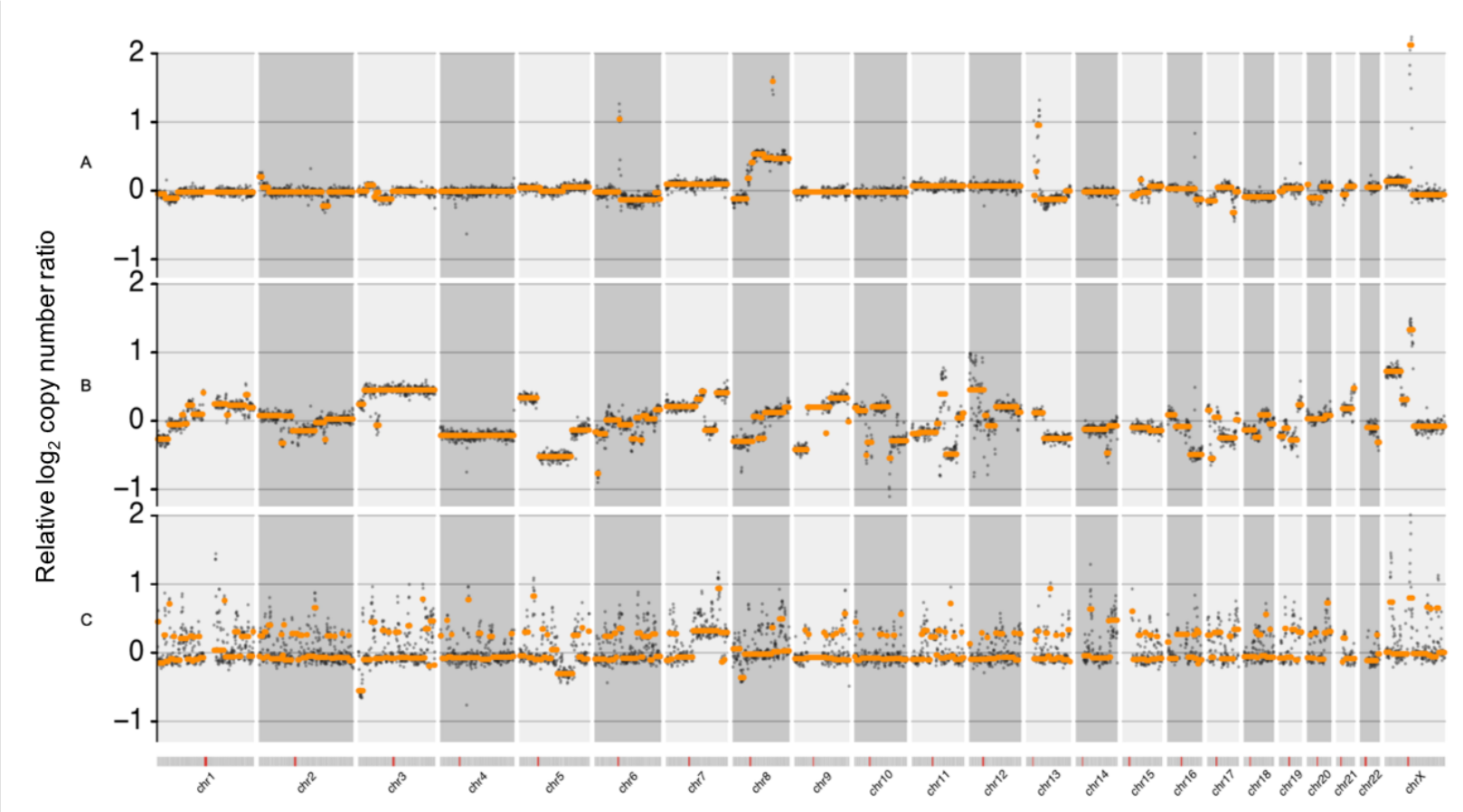

Figure 6-3:Putative copy number profiles consistent with emerging CRPC subtypes

(A) sparse alterations with focal amplifications including in AR;(B) frequent large-scale copy number changes associated with impaired DNA damage repair and (C) sawtooth pattern linked to CDK12 deficient tumours. Chr = chromosome; CRPC = castration resistant prostate cancer

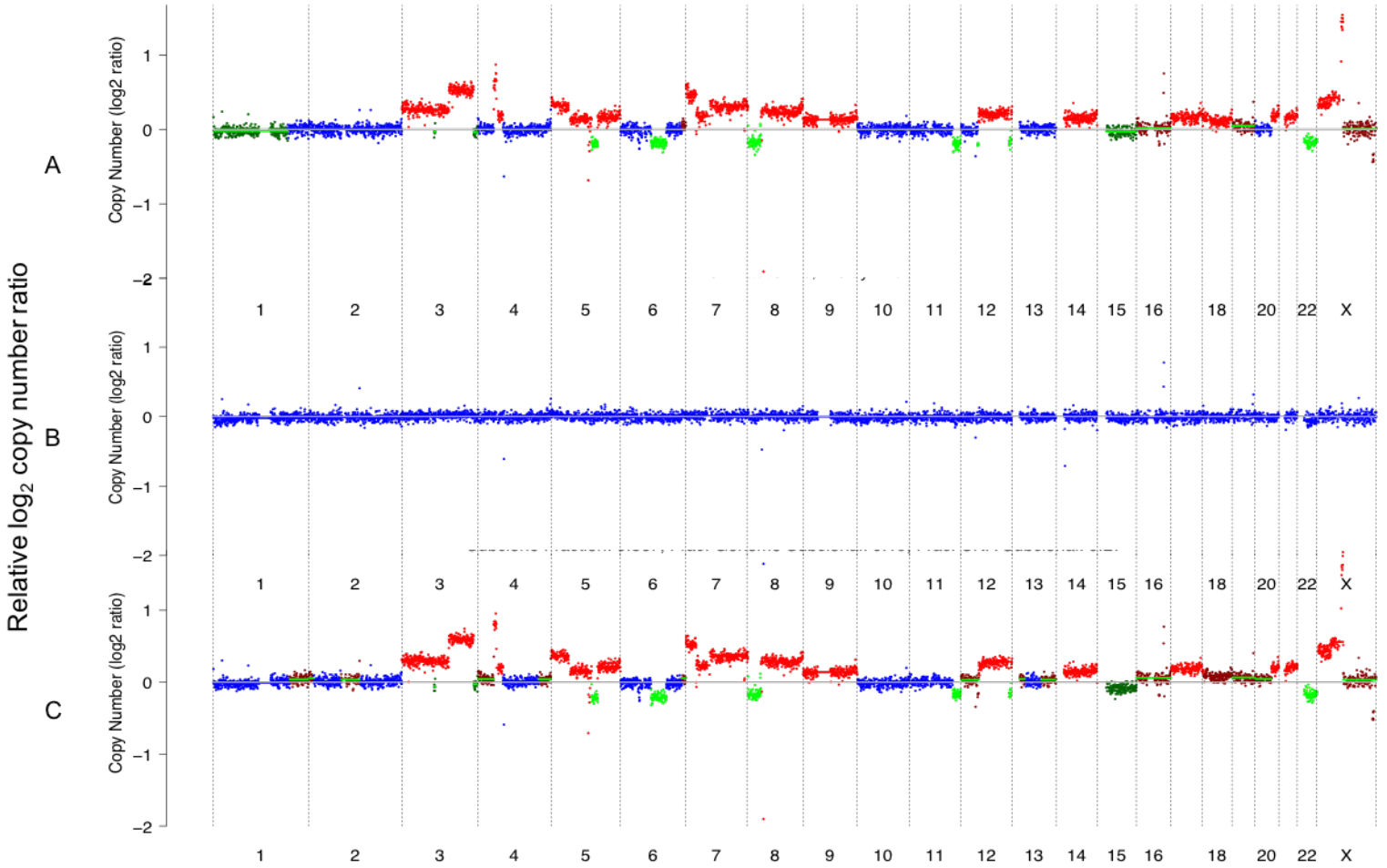

Figure 6-4: lp-WGS copy number profile from one patient at three timepoints

(A) pre-treatment (SCR), (B) during treatment (C4) and (C) post (EOS)-treatment. C4, Cycle 4; EOS, end of study; lp-WGS, low-pass whole genome sequencing; SCR, screening.

6.4.3 Validation of sequencing methods

For the patient whose baseline sample is shown in ***Figure 6-2,*** the ichorCNA tumour purity from this sample was estimated to be 0.5 (i.e. 50%). This estimated purity was used to calculate dilutions for this sample, in order to also sequence diluted samples with an estimated purity of 40%, 20%, 10% and 5% by diluting accordingly with a pool of healthy volunteer cfDNA. This same sample purity dilution showed that the dilated tumour purity was very closely correlated very closely with the ichorCNA generated estimated purity from the low pass whole genome sequencing (Pearson's r = 0.994) (see ***Figure 6-5***).

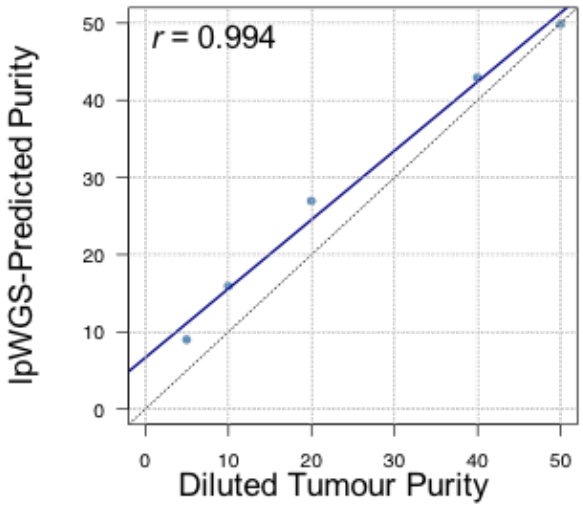

Figure 6-5:Same sample purity dilution showing diluted tumour purity correlated closely with ichorCNA generated estimated purity

(r = 0.994). lpWGS = low pass whole genome sequencing.

The traces for the diluted purities are shown in ***Figure 6-6***, and although the amplitude of the changes detected decreases as the tumour purity falls, the changes such as those shown in ***Figure 6-2***, are still detectable. For example, even in the 5% purity sample, 8p loss and 8q gain can be identified and the loss of *RB1* and *BRCA2*.

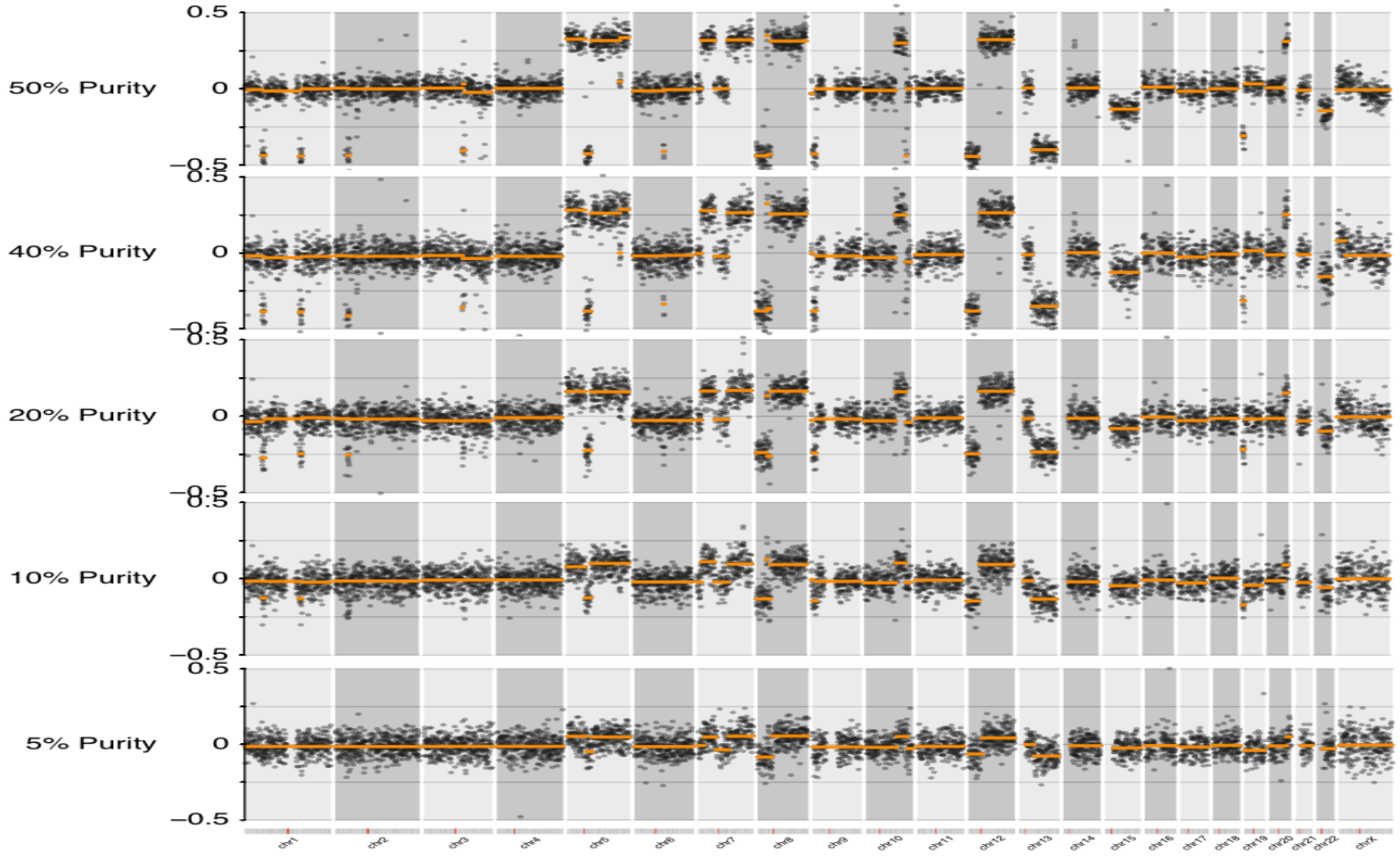

Figure 6-6: Copy number traces of diluted samples of the same case.

This shows traces from the original 50% purity down to 40%, 20%, 10% and 5%. Chr = chromosome.

The $\log_2$ ratios of copy number profiles for each of these dilutions were plotted versus the original (50%) sample to assess how well they correlated. This is shown in ***Figure 6-7***. Here, the correlation with the original sample decreased tumour purity decreased. The Pearson's r values were 0.941 for the 40% dilution, 0.885 for the 20% dilution, 0.713 for the 10% dilution and only 0.518 for the 5% dilution.

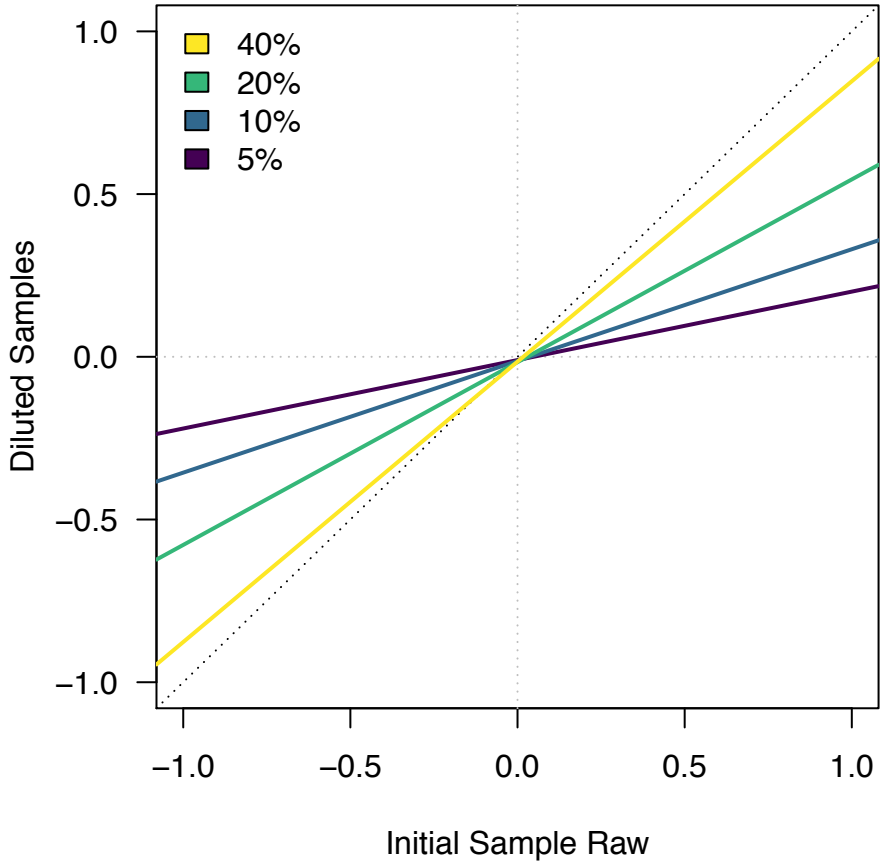

Figure 6-7: Copy number profiles of same sample dilutions correlated with the initial sample (50%) showed decreasing correlation as tumour purity decreased.

Biological replicates were also compared for assay validation, with two baseline samples (SCR and C1) taken at 2 separate blood draws but within 7 days of each other and without any interim treatment. The log_2 ratios of copy number profiles of same patient baseline samples were compared for 85 pairs. Their copy number aberration profiles of these paired samples were closely correlated (Pearson's r = 0.867) as seen in ***Figure 6-8***.

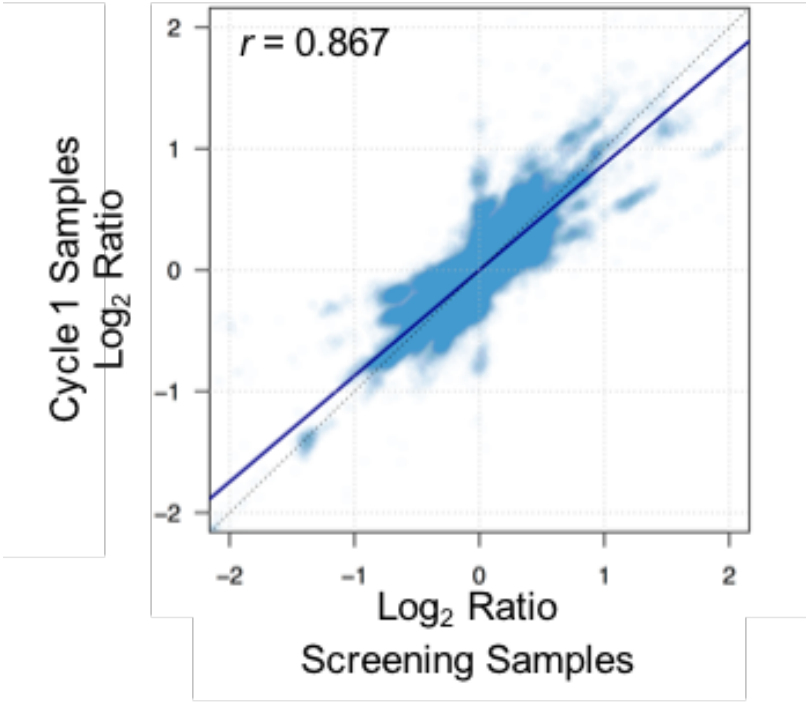

Figure 6-8: Correlation of the copy number log_2 ratios of biological replicates (same patient SCR and C1 samples). C1 = Cycle 1 Day 1; SCR = screening.

The estimated tumour purities (or tumour fraction) between these biological replicates for the same 85 pairs also showed broadly correlated values (Pearson's r = 0.656) (***Figure 6-9***). This is in keeping with cfDNA extracted from separate plasma samples at different time points.

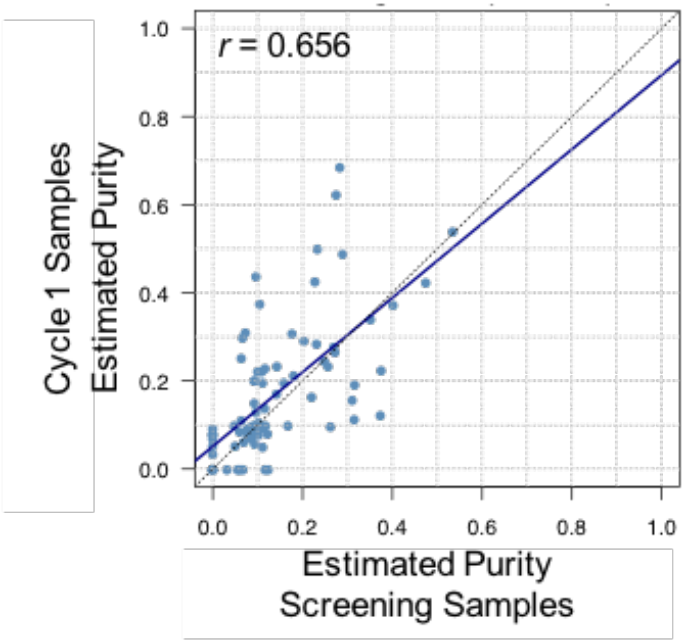

Figure 6-9: Correlation of estimated tumour purities generated by ichorCNA of biological replicates (same patient SCR and C1 samples). C1 = Cycle 1 Day 1; SCR = screening

Copy number frequencies were generated from the baseline low-pass whole-genome sequencing data (n=188). These were compared with the frequencies for the publicly available International Stand Up To Cancer/Prostate Cancer Foundation (SU2C/PCF) Prostate Cancer Dream Team dataset of whole exome sequencing performed from 150 mCRPC biopsies (81). This confirms that our low pass whole genome sequencing plasma data matched the CRPC landscape generated from genomic analysis of tissue biopsies as shown in ***Figure 6-10***, with frequent amplifications of *AR* (~30%) and *MYC* (~13%), copy-gains of *PI3KCA* (~45%) and copy-loss of *NKX3-1* (~75%), *RB1* (~70%) and *PTEN* (~50%).

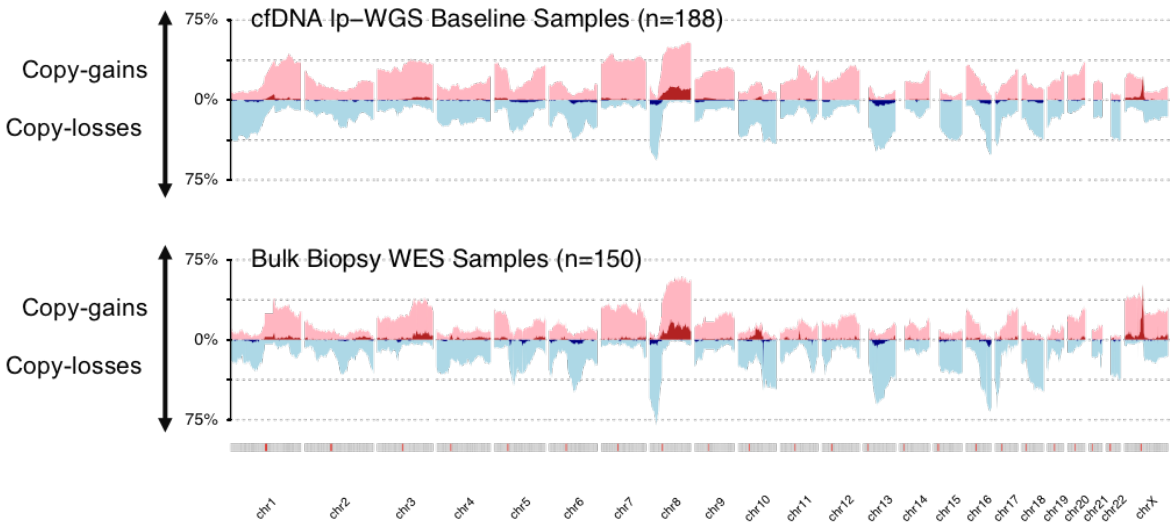

Figure 6-10: Copy number frequencies generated from lp-WGS data, compared with the frequencies for the SU2C dataset of WES performed on mCRPC tissue biopsies.

cfDNA = cell-free DNA; CNAs = copy number aberrations; lp-WGS = low pass whole genome sequencing; mCRPC = metastatic castration-resistant prostate cancer; SU2C = stand up to cancer; WES = whole exome sequencing.

6.4.4 Differences between the two studies

Clinical differences between the patient cohorts of the two studies have been shown in ***Table 6-1***. Importantly, FIRSTANA patients are a taxane-naïve population and PROSELICA patients are a post-taxane cohort receiving second line chemotherapy.

Low pass WGS-derived tumour purity was compared between the two studies for both SCR and EOS samples (***see Figure 6-11***). As shown in these violin plots, interestingly no differences in baseline (SCR) purity was seen between the two studies (Wilcoxon *p* = 0.26). However, tumour purity was higher in PROSELICA patients when comparing end of study samples in keeping with the higher burden of disease in these patients (Wilcoxon *p* = 0.0081).

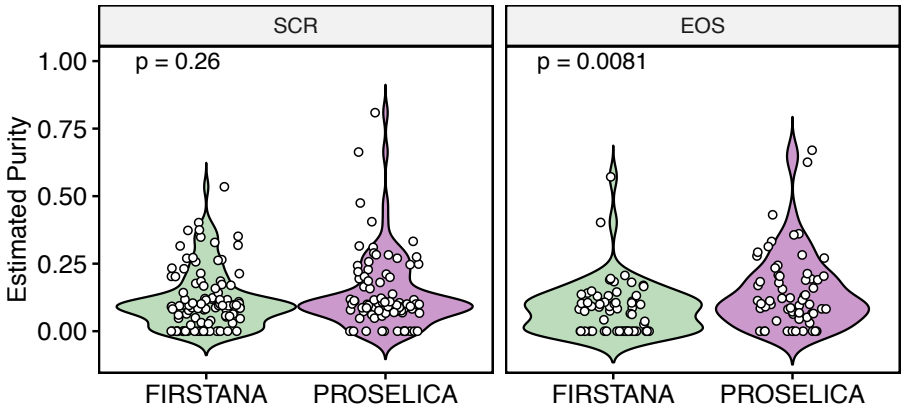

Figure 6-11: lp-WGS estimated tumour purity between studies at SCR and EOS.

EOS = end of study; lp-WGS = low pass whole genome sequencing; SCR = screening.

For estimated tumour ploidy, no differences were seen between studies in either baseline (SCR; Wilcoxon *p* = 0.98) or end of study suggesting minimal overall change in tumour ploidy with taxane failure (EOS; Wilcoxon *p* = 0.57) (See ***Figure 6-12***).

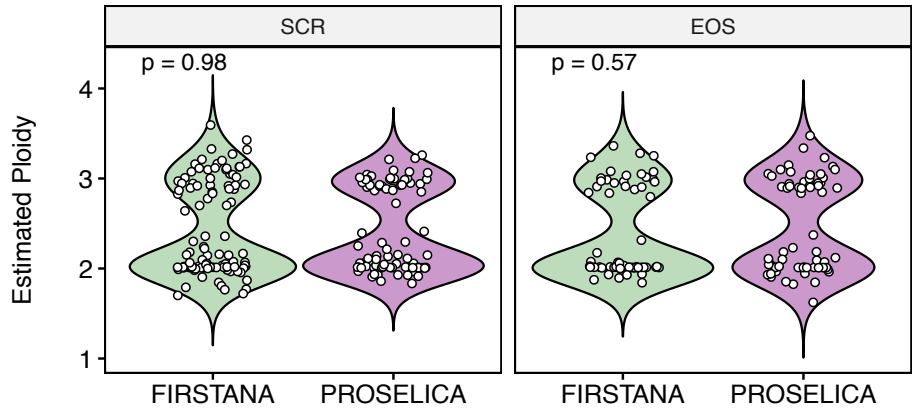

Figure 6-12: lp-WGS estimated tumour ploidy between studies at SCR and EOS.

EOS = end of study; lp-WGS = low pass whole genome sequencing; SCR = screening.

However, as depicted in ***Figure 6-13,*** PROSELICA samples featured a significantly higher number of copy-altered regions than FIRSTANA at both baseline (SCR; Wilcoxon p = 0.031) and end of study (EOS; Wilcoxon p = 0.0012), suggesting the acquisition of new genomic aberrations with taxane treatment that may be associated with treatment resistance.

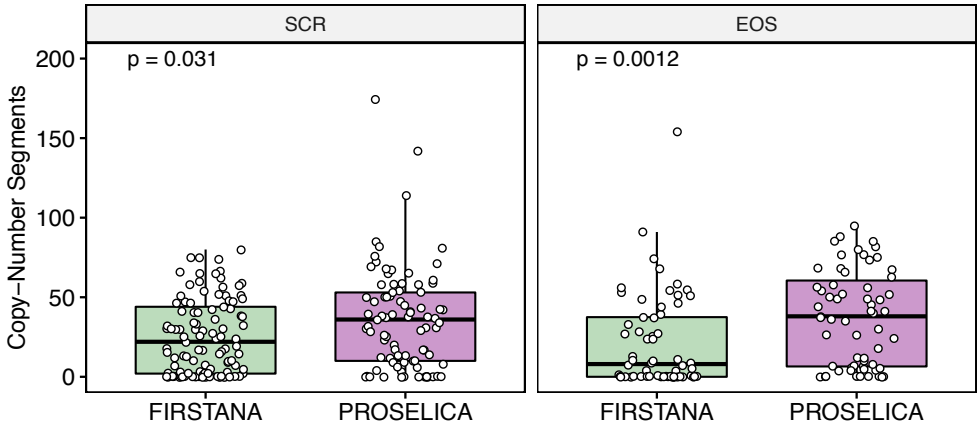

Figure 6-13: Number of copy number segments in both studies at SCR and EOS.

EOS = end of study; SCR = screening.

When comparing mean segment width, no difference was seen between FIRSTANA and PROSELICA samples at baseline (SCR; Wilcoxon p = 0.53) or at the end of study (EOS; Wilcoxon p = 0.57), as shown in ***Figure 6-14***.

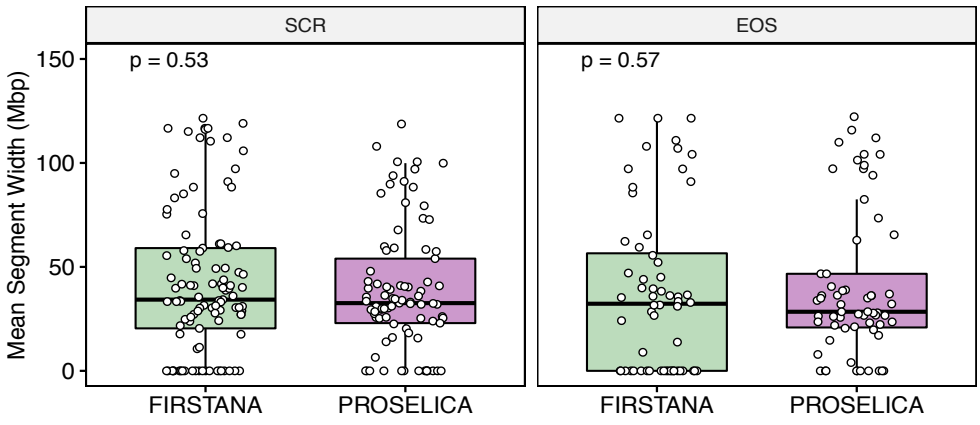

Figure 6-14: Mean segment width in both studies at SCR and EOS.

EOS = end of study; SCR = screening.

Furthermore, overall, the percentage genome altered (%GA) did not differ between the two studies for baseline (SCR; Wilcoxon p = 0.34) or end of study (EOS; Wilcoxon p = 0.27) samples (***Figure 6-15***).

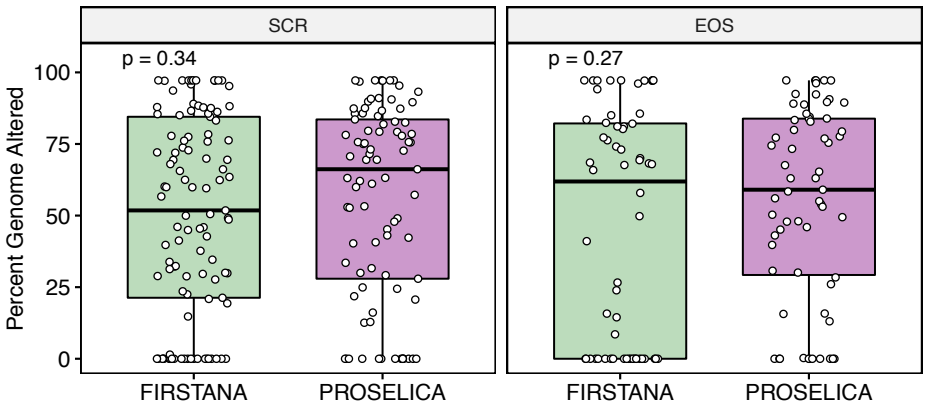

Figure 6-15: The overall percentage of the genome altered in samples from both studies at SCR and EOS. EOS = end of study; SCR = screening.

6.4.5 Baseline tumour purity as a prognostic and predictive marker

For univariable analyses of baseline tumour purity, all 188 baseline samples were used, with purity values being used to test for association with overall survival and response to treatment. The correlation of baseline purity (split by those above the median and below the median to be high or low respectively) with overall survival is shown using Kaplan-Meier survival curves in ***Figures 6-16 and 6-17.*** The high purity group is shown in green for both studies, and low purity in blue. Tumour purity was highly prognostic of overall survival (OS) in both FIRSTANA (log-rank test p-value 0.0071) and PROSELICA (log-rank test p-value = 0.00011), with the high purity group (i.e. greater than the median 9.56%) having a ~10 months shorter median overall survival than the low-purity group.

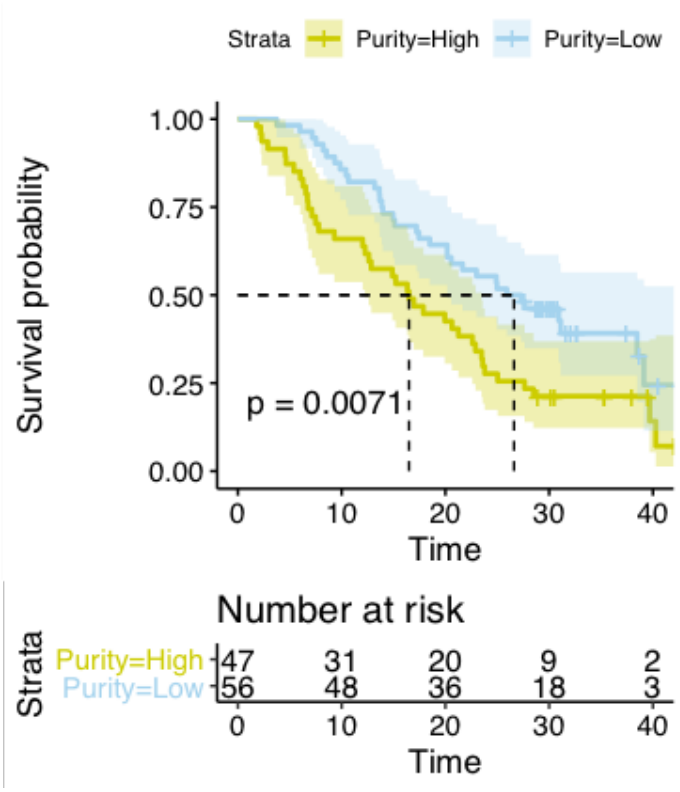

Figure 6-16: Kaplan-Meier survival curve of OS plotted by baseline tumour purity of FIRSTANA patients (time is shown in months.) OS = overall survival

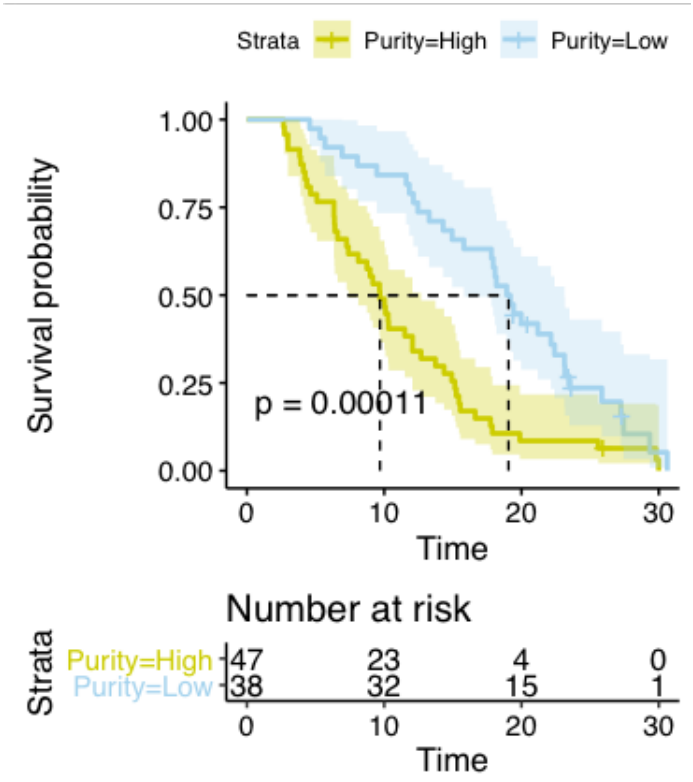

Figure 6-17: Kaplan-Meier survival curve of OS plotted by baseline tumour purity of PROSELICA patients (time is shown in months. OS = overall survival

From the 188 patients who had baseline tumour purity levels assessed for univariable analyses, 5 had to be excluded for further multivariable analysis due to missing clinical variables. A multivariable Cox proportional hazard model was applied to the remaining 183 patients to assess the impact of tumour purity on overall survival including other established prognostic factors as variables (221) such as baseline LDH, albumin and haemoglobin. This is shown in ***Figure 6-18***, with baseline tumour purity from low pass WGS being prognostic of overall survival HR = 4.42, CI: 1.09 – 17.82, p = 0.037). Other variables that had a strong effect on overall survival were being on PROSELICA over FIRSTANA (HR 1.87, CI: 1.30 – 2.69, p <0.001) which fits with this more advanced cohort having a shorter overall survival. Baseline LDH and haemoglobin levels, presence of visceral metastases, and baseline ECOG performance status also impacted overall survival as shown by their hazard ratios in ***Figure 6-18***.

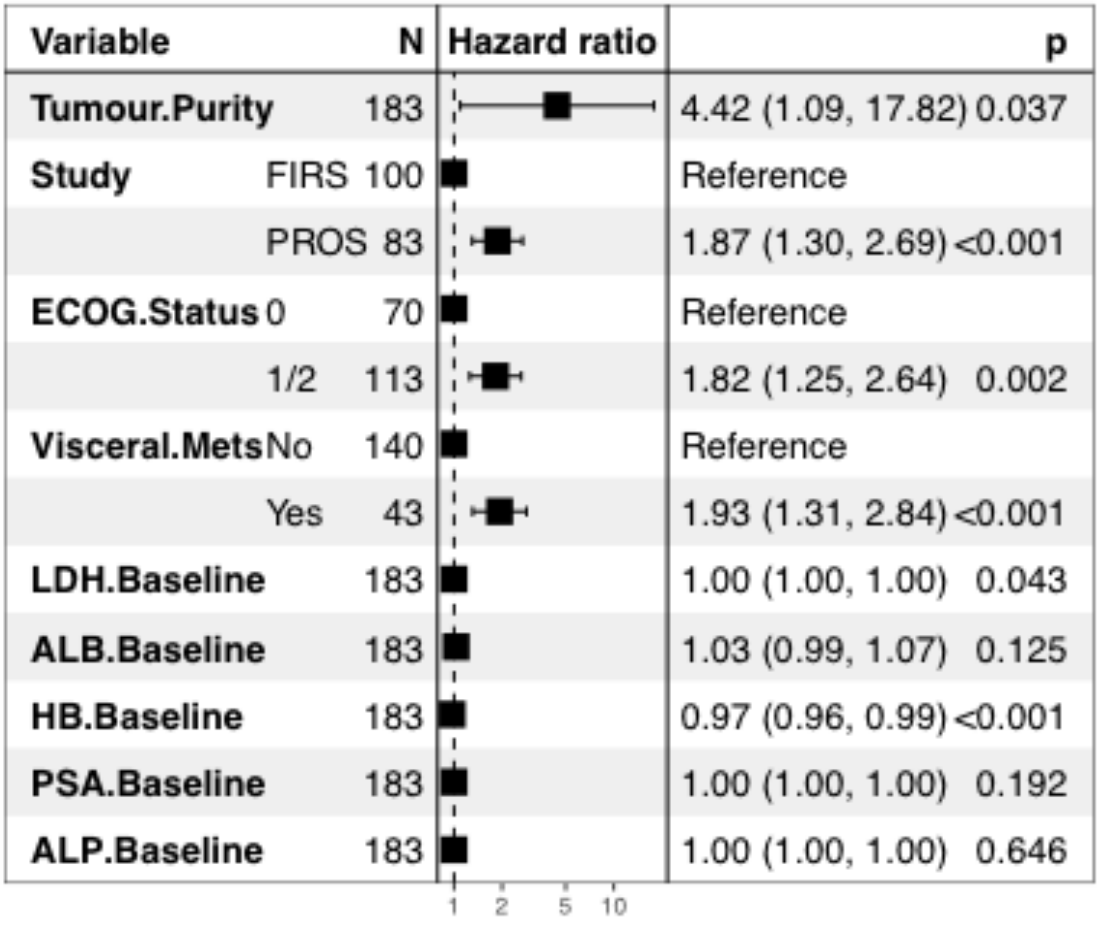

Figure 6-18: Multivariable Cox proportional hazard model for overall survival, including tumour purity as a variable along with other known prognostic factors.

Shorter OS is seen at higher tumour purity levels, higher ECOG performance status and the presence of visceral mets. Hazard ratio, confidence intervals and p values are given in the right-hand column. ALB = albumin; ALP = alkaline phosphatase; ECOG status = Eastern cooperative oncology group performance status; FIRS = FIRSTANA; Hb = haemoglobin; LDH = lactate dehydrogenase; mets = metastases; N = number; OS = overall survival; PROS = PROSELICA; PSA = prostate specific antigen.

Due to this association of baseline tumour purity with overall survival, a multivariable logistic regression model was also applied to examine the likelihood of response to treatment. Tumour purity was not predictive of response (OR = 3.75, CI: 0.22 – 83.01, *p* = 0.377) (***Figure 6-19***). The only true predictive variable associated with worse response was the study, with patients in PROSELICA doing worse than those in FIRSTANA (OR 2.86, CI: 1.50 – 5.57, *p* = 0.002), which is in-keeping with the known lower response rates seen in 2nd line taxanes.

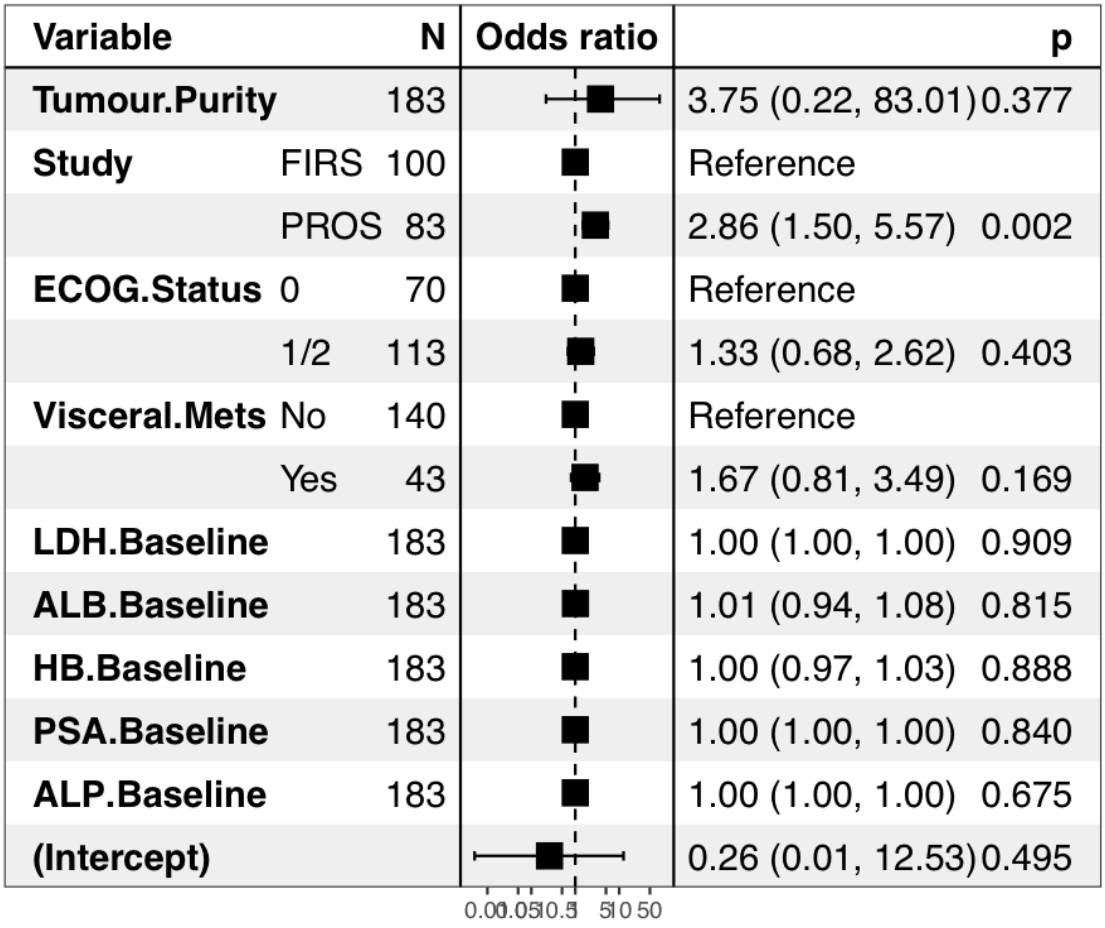

Figure 6-19: Multivariable logistic regression for response, including tumour purity as a variable along with other known prognostic factors.

*Baseline tumour purity is not predictive of response, with only study (PROSELICA) being significantly associated with a decreased response to taxanes Odds ratio shown indicates odds of **not** responding to therapy. Odds ratio, confidence intervals and p values are given in the right-hand column. ALB = albumin; ALP = alkaline phosphatase; ECOG status = Eastern cooperative oncology group performance status; FIRS = FIRSTANA; Hb = haemoglobin; LDH = lactate dehydrogenase; mets = metastases; N = number; PROS = PROSELICA; PSA = prostate specific antigen.*

6.4.6 Changes in tumour purity and response

Although baseline purity did not associate with response to treatment, observed changes in low pass whole genome sequencing tumour purity over time in responding and non-

responding patients was illustrative of response to treatment. This trend was exhibited in both FIRSTANA and PROSELICA, with samples from responding patients exhibiting significantly lower tumour purity values than samples from non-responding patients at both on-treatment (C4) and end of study (EOS) time points (see ***Figure 6-20).***

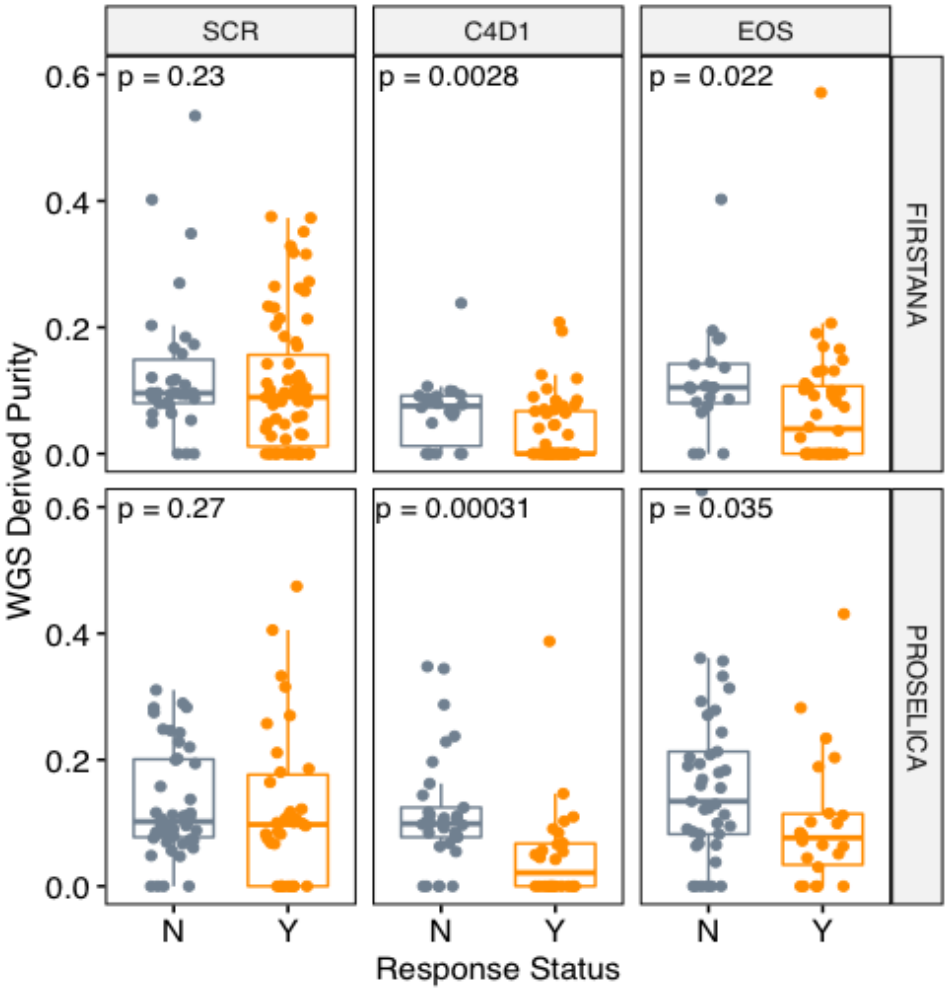

Figure 6-20: Changes in lp-WGS tumour purity over time in responding and non-responding patients is illustrative of response to treatment.

C4D1 = Cycle 4 Day 1; EOS = end of study; lp-WGS = low pass whole genome sequencing; N = no (non-responder); SCR = screening; Y = Yes (responder).

For 134 patients (across both trials), a matched baseline and C4 treatment was used to divide patients in to 4 specific clinical groups:

1) *Baseline high tumour purity which remained high tumour purity at C4 (n = 19).*
2) *Baseline High tumour purity to C4 low tumour purity (n = 47).*
3) *Baseline low tumour purity which remained low tumour purity at C4 (n = 55).*
4) *Baseline low tumour purity who progressed to C4 high tumour purity (n = 11).*

Multivariable logistic regression for these four categories and other prognostic variables and their association with response is shown in ***Figure 21***. Both baseline high to C4 low and baseline low which remained low at C4 were significantly associated with a higher likelihood of response to taxanes (p = 0.03 and 0.004 respectively), and only study (PROSELICA) was associated with a worse response as before, in keeping with expected response of second line taxanes.

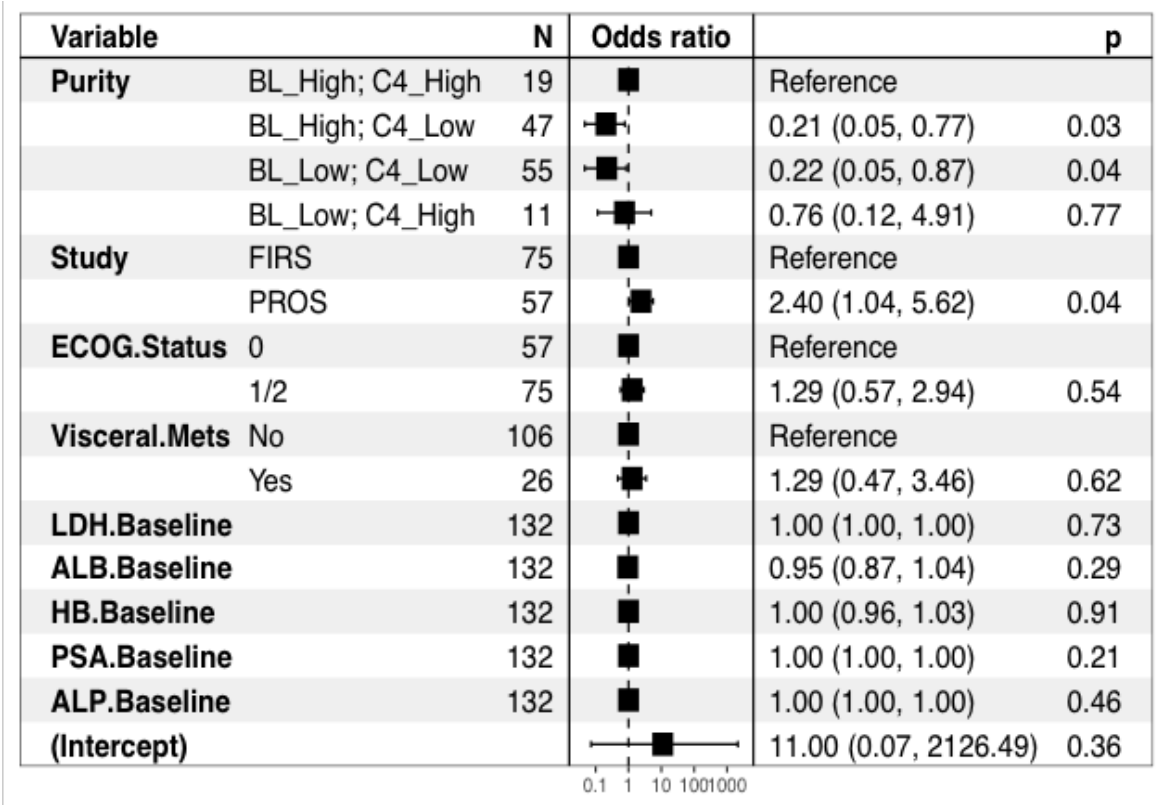

Figure 6-21 Multivariable logistic regression of patients classified by longitudinal changes in tumour purity

(4 groups; baseline high – C4 high, baseline high – C4 low, baseline low - C4 low, baseline low – C4 high) and other known prognostic variables. Odds ratio shown indicates odds of ***not*** *responding to therapy. ALB = albumin; ALP = alkaline phosphatase; BL = baseline; C4 = Cycle 4; ECOG Status = Eastern cooperative Oncology Group performance status; FIRS = FIRSTANA; HB = haemoglobin; LDH = lactate dehydrogenase; mets = metastases; N = number; PSA = prostate specific antigen.*

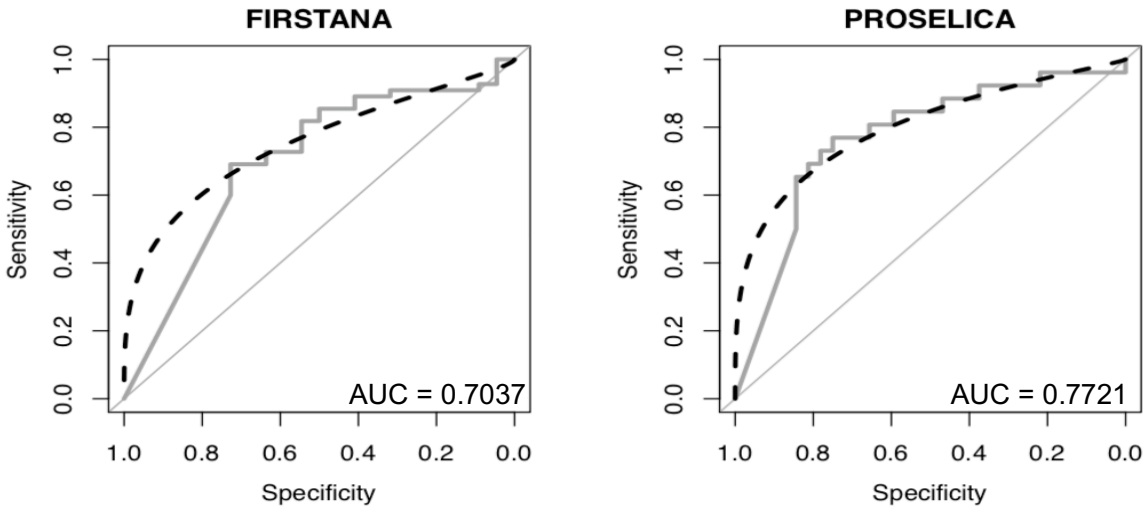

Figure 6-22: ROC curves per trial predicting response to therapy using C4 lp-WGS derived tumour purities

ROC = receiver operating characteristics

Cycle 4 tumour purities alone were informative, with ROC curves predicting response to therapy shown per trial in ***Figure 22.*** The AUC for these C4 curves was 0.7 and 0.77 for FIRSTANA and PROSELICA respectively.

6.4.7 Copy number frequencies in docetaxel-naïve and docetaxel-treated patients

The FIRSTANA cohort (docetaxel naïve) and the PROSELICA cohort (docetaxel exposed) had broadly similar copy number profiles. When observing key prostate cancer genes (*AR, MYC, PIK3CA, PTEN, RB1, CHD1, TP53* and *CDKN2A*), some regions exhibited focal variations in copy number frequency which are shown in ***Table 6-3***. Copy number differences in these key genes at baseline for the two trials and baseline to end of study in FIRSTANA were compared using Fishers test and the *p* values are given below. The only significant change seen was in *CDKN2A*; this decreased significantly from FIRSTANA baseline to FIRSTANA end of study ($p = 0.04$), which may suggest that this was taxane induced. However, this change was interestingly not observed as significantly different from FIRSTANA baseline (taxane naïve) to PROSELICA baseline or from PROSELICA baseline to end of study.

Kaplan Meier survival curves were generated for 4 of the gene loci of interest (*PTEN*, *RB1*, *CDKN2A and AR*) as shown in ***Figure 6-23,*** with FIRSTANA curves on the left and PROSELICA curves on the right. Patients with baseline *CDKN2A* loss appear to have a shorter OS in both trials (p = 0.11 in FIRSTANA and 0.034 in PROSELICA).

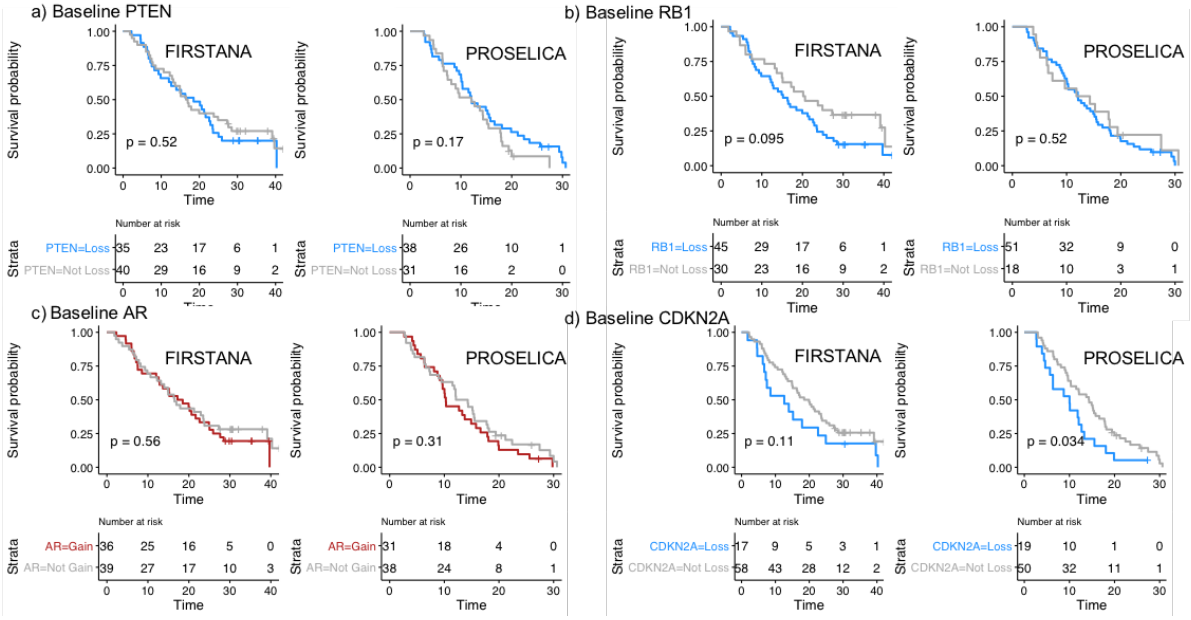

Figure 6-23: Kaplan-Meier OS curves for 4 key gene loci.

OS = overall survival

Kaplan Meier curves were also generated for these same 4 gene loci of interest (*PTEN*, *RB1*, *CDKN2A and AR*) for rPFS which are shown in ***Figure 6-24***. Again, FIRSTANA curves are on the left and PROSELICA curves on the right. Here, the only reportable difference is in PROSELICA with those with AR gain doing worse, which again could be in keeping with a more advanced patient cohort.

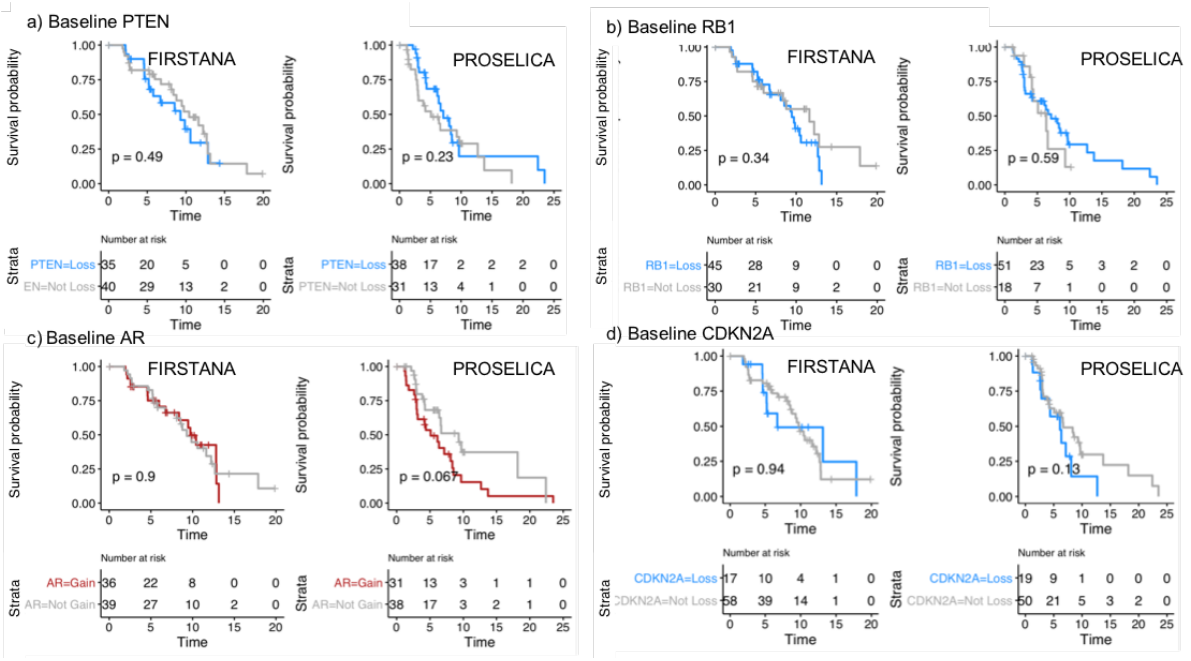

Figure 6-24: Kaplan-Meier rPFS curves for 4 key gene loci.

rPFS = radiographic progression free survival.

These genes were also tested using a multivariable Cox proportional hazards model for survival (***Figure 6-25***; they mostly did not significantly associate with overall survival, with study (PROSELICA), and tumour purity, being most associated with worse survival. *CDKN2A* loss, however, appeared to have prognostic importance (HR 1.59, CI: 1.00 – 2.54, p = 0.049). These same genes were also tested in a multivariable logistic regression model for response, as shown in ***Figure 6-26***. No genes associated with response, with only study (PROSELICA) associating with worse response again.

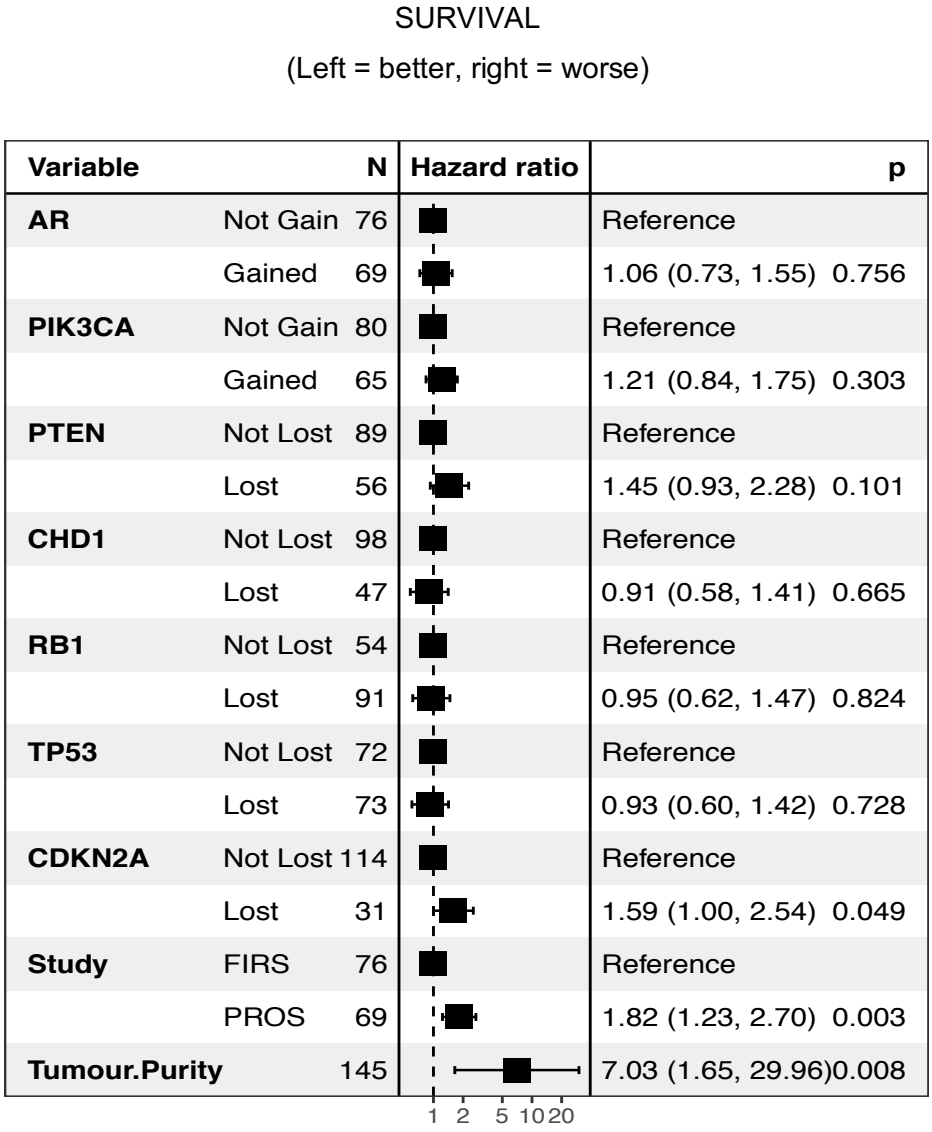

Figure 6-25: Baseline tumour purity and study (PROSELICA) are predictive of shorter overall survival.

N = number.

Figure 6-26: Study (PROSELICA) is predictive of a worse response to taxanes.

*Odds ratio shown indicates odds of **not** responding to therapy. N = number.*

A heat map of these key prostate cancer genes, ranked by overall survival per study is shown in ***Figure 6-27***. Gene loci implicated in prostate cancer studied included *AR, MYC, PIK3CA*, *PTEN, RB1, CHD1, TP53* and *CDKN2A*. For both FIRSTANA patients (to the left of the figure) and PROSELICA patients (to the right of the figure), no clear associations with known prognostic variables or genes of interest are seen. Analysis of these data is ongoing, with significant bioinformatic and statistical support.

Table 6-3:Copy number frequencies for key prostate cancer genes in both trials.

chr = chromosome; CNA = copy number aberration; EOS = end of study.

		CNA FREQUENCY DATA								Fishers test *p* values					
		FIRSTANA				PROSELICA				Baseline FIRSTANA vs Baseline PROSELICA		Baseline vs. EOS FIRSTANA		Baseline vs EOS PROSELICA	
		Baseline		End of Study		Baseline		End of Study							
gene	chr	Any Loss	Any Gain	Any Loss	Any Gain	Any Loss	Any Gain	Any Loss	Any Gain	Loss	Gain	Loss	Gain	Loss	Gain
PIK3CA	3	0.07	0.40	0.06	0.36	0.12	0.51	0.06	0.47	0.39	0.24	1.00	0.83	0.36	0.71
CHD1	5	0.36	0.19	0.36	0.15	0.43	0.10	0.41	0.14	0.40	0.16	1.00	0.79	0.85	0.57
CDKN1A	6	0.12	0.21	0.24	0.27	0.16	0.20	0.18	0.20	0.63	1.00	0.15	0.62	0.81	1.00
NKX3-1	8	0.75	0.03	0.64	0.06	0.80	0.03	0.73	0.06	0.55	1.00	0.26	0.58	0.51	0.65
MYC	8	0.00	0.77	0.00	0.79	0.00	0.83	0.00	0.76	1.00	0.53	1.00	1.00	1.00	0.36
CDKN2A	9	0.23	0.27	0.33	0.09	0.26	0.26	0.31	0.29	0.70	1.00	0.34	0.04	0.68	0.84
PTEN	10	0.42	0.07	0.33	0.10	0.52	0.07	0.51	0.07	0.29	1.00	0.50	0.70	1.00	1.00
BRCA2	13	0.40	0.15	0.48	0.06	0.43	0.16	0.35	0.22	0.74	1.00	0.53	0.34	0.35	0.47
RB1	13	0.60	0.05	0.55	0.03	0.75	0.01	0.69	0.02	0.05	0.37	0.67	1.00	0.53	1.00
TP53	17	0.65	0.03	0.64	0.06	0.49	0.10	0.59	0.06	0.06	0.09	1.00	0.58	0.35	0.52
BRCA1	17	0.25	0.15	0.33	0.21	0.13	0.26	0.20	0.22	0.09	0.10	0.49	0.41	0.32	0.67
AR	X	0.15	0.44	0.21	0.42	0.13	0.46	0.08	0.59	0.81	0.87	0.41	1.00	0.55	0.19

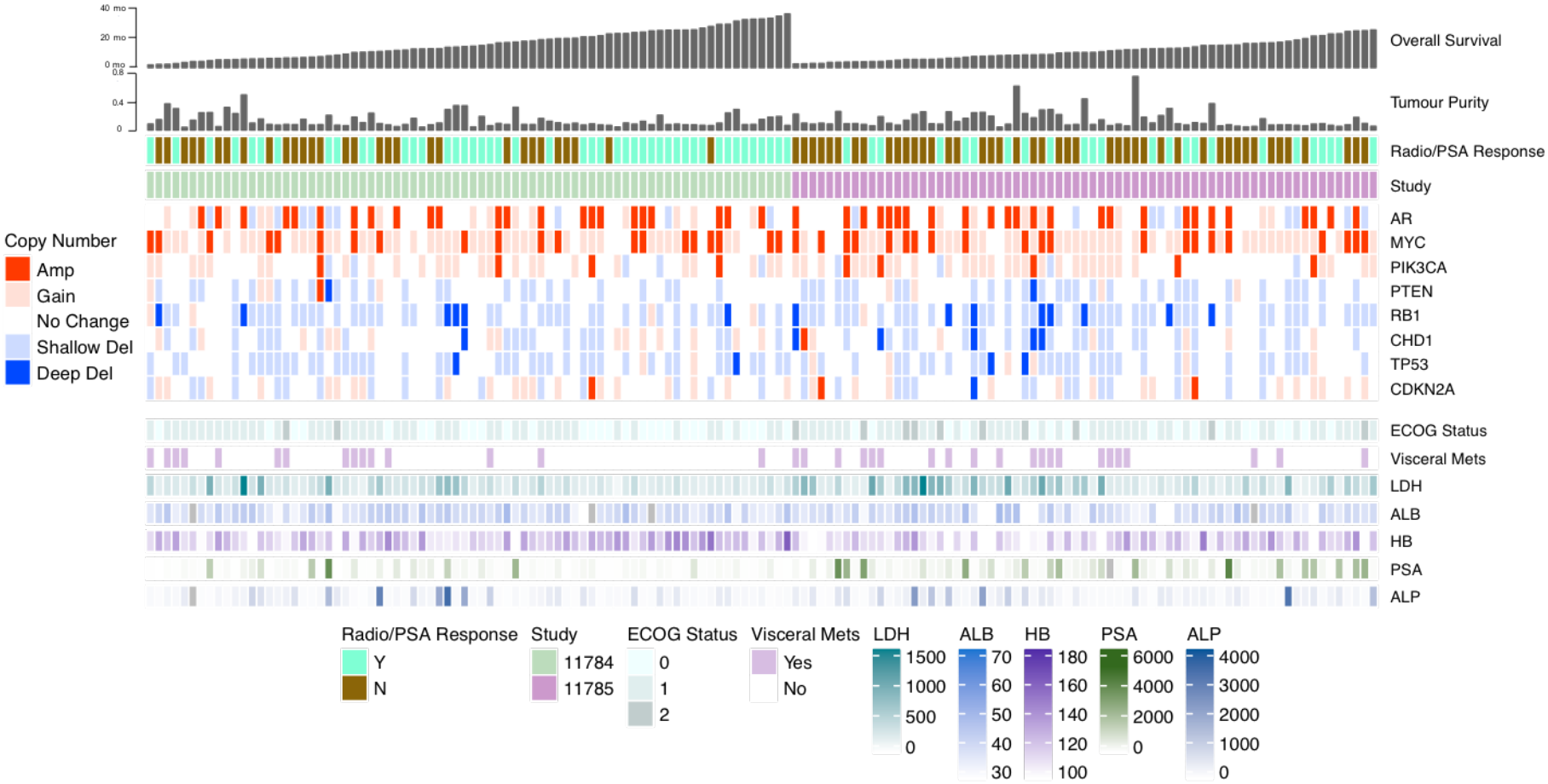

Figure 6-27: Heat map of all patients baseline samples split by study with key genes and prognostic variables shown.

11784 = FIRSTANA; 11795 = PROSELICA; ALB = albumin; ALP = alkaline phosphatase; ECOG status = Eastern Cooperative Oncology Group performance status; Hb = haemoglobin; LDH = lactate dehydrogenase; mo = months; N = no; PSA = prostate specific antigen; Y = yes

6.5 Orthogonal validation

6.5.1 Targeted sequencing

Targeted sequencing was also performed, with results available from 294 patients (153 from FIRSTANA, 141 from PROSELICA) that passed stringent quality control filters. In order to be deemed eligible for analysis, each sample had to have >100,000 mapped reads with >90% of the reads being on target. Mutation calling was performed using the Torrent Suite™ variant caller, and samples were annotated using Oncotator to identify predicted deleterious mutations. The frequencies of these are reported per trial in ***Table 6-4*** and were globally found at expected frequencies as compared to the Stand Up To Cancer/Prostate Cancer Foundation (SU2C/PCF) Prostate Cancer Dream Team dataset (81).

Table 6-4: Deleterious mutations identified as compared to expected CRPC mutation frequency as reported in SU2C

A subset of 15 genes of interest is shown. CRPC = castration resistant prostate cancer; SU2C = stand up to cancer.

Gene	% Mutations (FIRSTANA)	% Mutations (PROSELICA)	Fisher's *p*-value	Expected frequencies (SU2C)
CDK4	0	0	1	0-1 %
CDK6	0	0	1	0-1 %
CDKN1B	0	0	1	0-1 %
CDKN2A	0	0	1	0-1 %
CHD1	0	0	1	0-5 %
E2F1	0	0	1	0-1 %
E2F2	0	0	1	0-1 %
E2F3	0	0	1	0-1 %
E2F4	0	0	1	0-1 %
E2F5	0	0	1	0-1 %
PTEN	5.92	5.04	1	5-10 %
RB1	2.63	1	1	0-5 %
SPOP	4.60	7.91	1	5-10 %
TP53	15.79	17.27	1	15-25 %

For assay validation, replicate copy number profiles from technical (resequencing of same sample, n = 99) and biological (SCR compared to C1, n=106) replicates were compared and overall well correlated as shown in ***Figure 6-28***.

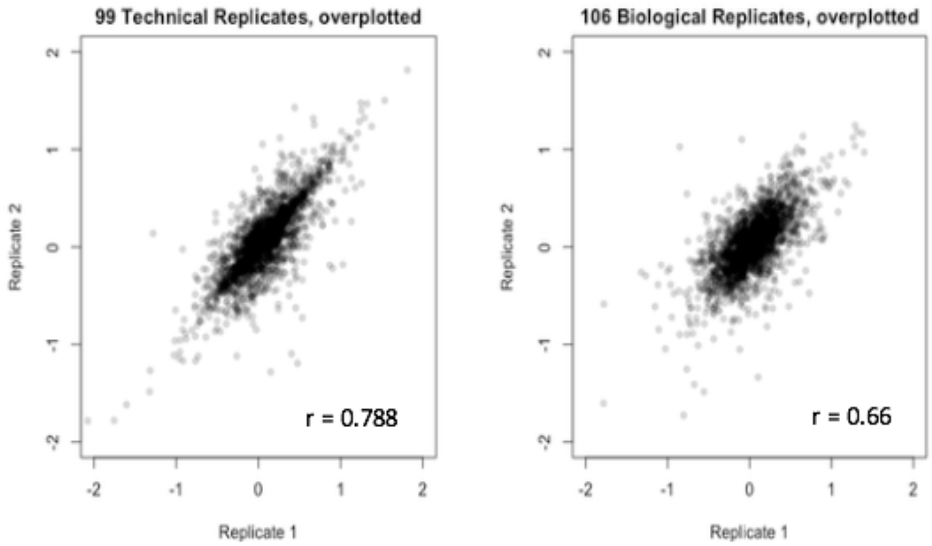

Figure 6-28: Correlations of technical and biological replicates

Technical replicates (same sample resequenced) and Biological replicates (two baseline samples - SCR and C1) correlated well (Pearson's r = 0.788 and 0.66 respectively.

As seen in the low pass WGS results, changes in tumour purity again associated with treatment response (p = 0.04). Unfortunately, some genes which were potentially of interest such as *FOXA1* and *CCND1* had to be excluded from copy number analyses due to poor sequencing performance. As well as these limitations, other limitations in copy number calling from amplicon-based targeted sequencing, particularly in detecting small losses and the inability to detect rearrangements and fusions are acknowledged. Inadequacies of a sequencing-based approach using data from a small panel, particularly when a few important genes did not perform well, were felt to be restrictive. It has also been acknowledged that there remains a risk of false-negative copy number calls, particularly in the setting of low tumour fraction and borderline alterations. Therefore, despite the aims of these experiments, and whilst the targeted tumour purity data were useful, the copy number data were not felt to be robust enough to be used as a validation tool.

6.5.2 Plasma array comparative genomic hybridisation

aCGH of cfDNA extracted from these same Sanofi samples was also explored as a validation tool. Results by other groups, although promising, have acknowledged many challenges associated with this technique (230). Unfortunately, no matched tissue was available for this cohort of patients, so patients with same time-point plasma cfDNA and tissue available were selected from samples collected within an institutional ethically approved protocol (CCR 2472). For both tissue DNA and plasma cfDNA, sample integrity was assessed for consideration of aCGH prior to amplification. These matched aCGH tissue and plasma traces are shown for two patients, V5356 and RB189, in ***Figure 6-29***, demonstrating good reproducibility between the tissue and plasma.

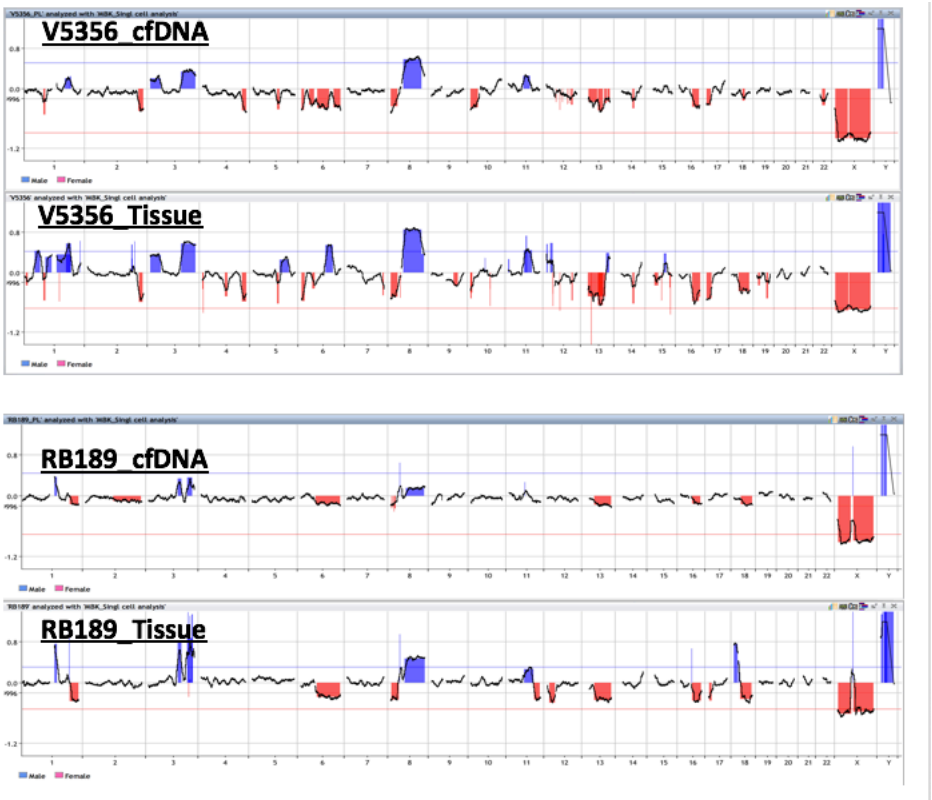

Figure 6-29: Matched cfDNA and tissue aCGH for two patients.

aCGH = array comparative genomic hybridization; cfDNA = cell free DNA.

Next, I performed serial dilutions of the same sample cfDNA sample, diluting tumour DNA with "normal" DNA extracted from healthy volunteer plasma. A cfDNA sample was diluted to 7.5ng, 5ng, 2.5ng and 1ng, and the aCGH traces from this sample are shown in ***Figure 6-30***.

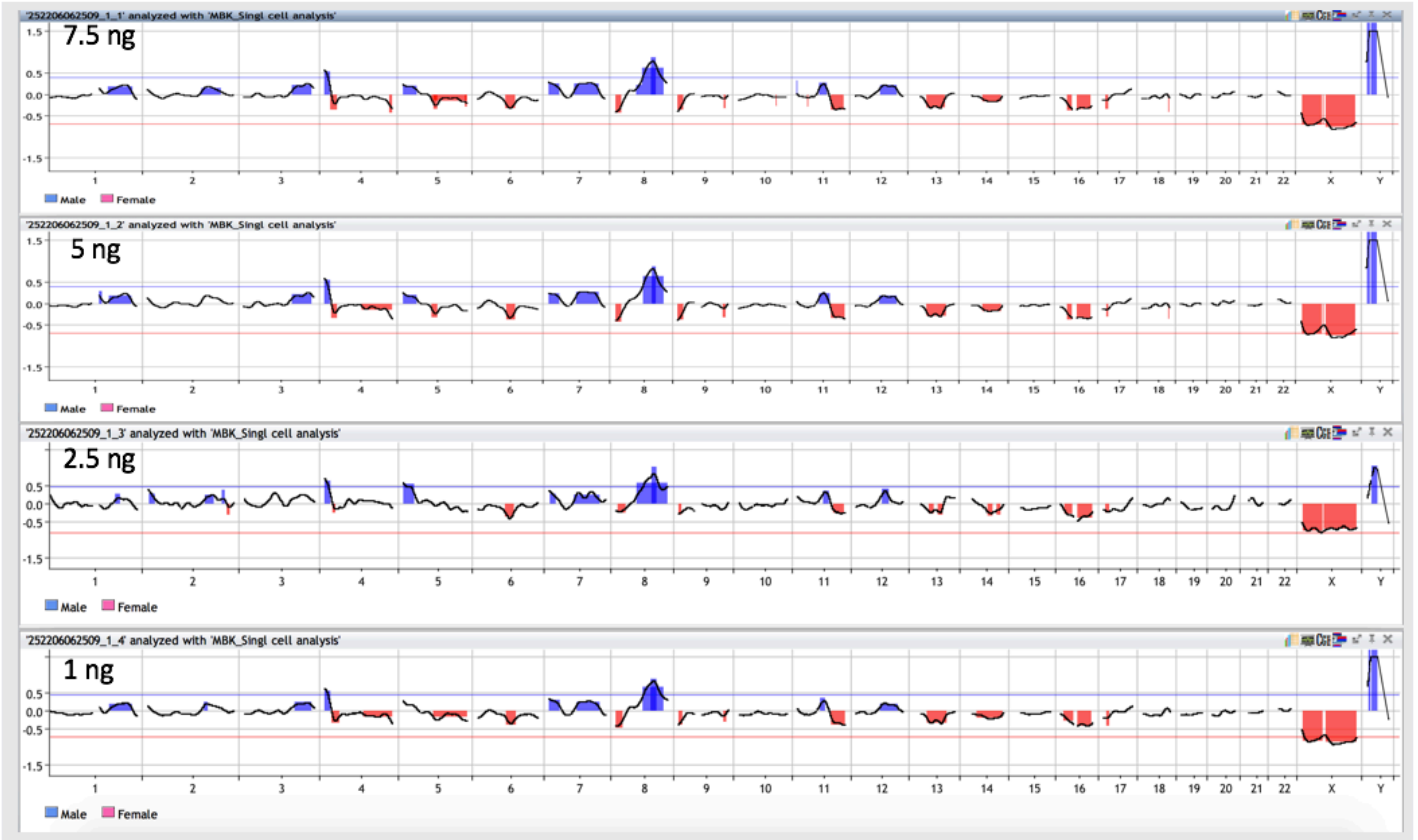

Figure 6-30: aCGH with serial dilutions of same plasma cfDNA sample.

aCGH = array comparative genomic hybridization; cfDNA = cell free DNA; ng = nanogram.

Whilst these traces showed good reproducibility even down to a 1ng input, when increasing the number of plasma samples run the aCGH trace was heavily dependent on the circulating tumour DNA (ctDNA) content. Samples with low starting cfDNA concentrations, and also with less clean profiles when assessed on the TapeStation did not perform well and were associated with flatter traces. Pre-selecting samples with high cfDNA concentrations and based on the TapeStation profile did increase success rates, but meant that several samples did not pass this initial quality control step and were deemed not evaluable.

When ctDNA concentration is adequate, as shown by the serial dilutions (***Figure 6-30***) lower DNA inputs can 1ng can be used with success, but this is only feasible if the ctDNA component of total cfDNA is high. Whilst aCGH was initially explored as a method of validation for my sequencing results and despite achieving technically reproducible traces, the failure rate was such that this was not a cost- or time-effective experiment.

6.6 Discussion:

Here I confirm that cfDNA has clinical utility in the management of lethal prostate cancer, with changes in cfDNA tumour purity from low pass WGS associating with response to taxane therapy, suggesting that it may be acting as a surrogate marker for overall tumour burden. Tumour purity measured solely at baseline does not predict response to treatment, despite a strong association with OS. However, the changes in lp-WGS derived tumour purity over time **are** associated with response, and may represent a non-invasive and reliable way of monitoring disease burden and response to treatment. Whilst these findings need further validation, corroboration of these results may provide physicians with a reliable guide to early treatment switch decisions. This may prove transformative as current markers, including biochemical markers (PSA) and radiographic markers have several recognised limitations as discussed previously.

Of the two taxane-based chemotherapies used, docetaxel was the first treatment to show an improvement in overall survival (OS), symptoms, prostate-specific antigen (PSA) and quality of life in metastatic castration-resistant prostate cancer (mCRPC) in these two landmark phase III trials (FIRSTANA and PROSELICA). Taxanes act by binding to microtubules and preventing their disassembly, leading to cell-cycle arrest and resultant apoptosis (231). Taxanes are also thought to have some anti-androgenic properties; having been shown to potentially block nuclear translocation of the microtubule-

dependent androgen receptor (AR) (232). Differences in copy number frequencies at baseline between FIRSTANA (docetaxel naive) and PROSELICA (docetaxel exposed) may represent treatment-induced changes, as well as changes seen within the studies from baseline to the end of treatment. It is worth noting that end of treatment samples were taken when patients came off trial and not necessarily at point of disease progression due to patients discontinuing due to toxicity or having completed 10 cycles of chemotherapy and having an ongoing response. Validation of these changes will be crucial in identifying regions associated with docetaxel resistance. Functional studies are now warranted to explore the role of potential biomarker genes identified such as *CDKN2A.* Unsupervised analysis of this data is also needed and is ongoing to identify response associated regions. Initially flagged regions will be merged with highly correlated and adjacent regions, and elastic net regression and stepwise model optimisation performed. These results will need to be interpreted with caution as the large number of genes being tested against a relatively small sample size will decrease the probability of detecting an effect of practical importance. Furthermore, the confidence of copy number calling decreases significantly at lower tumour purities, as shown by the worsening correlations of increasing dilutions of the same sample, and this must also be factored in to further analysis.

Despite these limitations, *CDKN2A* shows promise as a biomarker of taxane sensitivity in CRPC. The gene, which is situated on chromosome 9p21, codes for the cell cycle inhibitor p16, which binds to and inhibits CDK4/6. Loss of heterozygosity, mutations and inactivation of *CDKN2A* have been identified in many human cancers (233). CDKN2A alterations are reported in most melanoma cell lines, in non-small cell lung cancers and pancreatic cancer to name a few (234–236). Loss of p16 in breast and other cancers has been shown to reduce paclitaxel-induced cell death (237,238) and further studies assessing the role of taxanes in CDKN2A lost cancers, including prostate cancer are warranted.

Although orthogonal validation methods explored thus far have been unsuccessful, this remains a crucial step in driving this research forward. Cell line work should be pursued by knocking-in and knocking-out these genes of interest and establishing their role in taxane sensitivity and resistance. This work should be carried out in both taxane sensitive and resistant cell lines in order to better understand the complex area of taxane resistance. This is likely to be multifactorial with many contributing elements, and whilst it is theoretically possible that changes in a single gene may be predictive of response,

work in other cancers implies a cassette of genes is more likely to be responsible (239,240).

Low-pass whole genome sequencing did not allow analysis of mutations, and whilst this was possible from the targeted sequencing data, unfortunately enough genes of interest were not covered. Despite this, mutations in microtubules have been implicated in taxane resistance in both ovarian and breast cancer (43,241,242). The role of efflux transporters such as the ATP-binding cassette (ABC) superfamily, which include ABCB1 (also known as the multidrug resistance protein 1; MDR1) has also been associated with breast cancer and other malignancies (243,244). The role of the tumour microenvironment and myeloid-derived suppressor cells (MDSCs) also warrants further exploration (245). Hypoxia and non-coding RNAs are also emerging as key drivers of taxane resistance, with these transcripts interacting with epigenetic effectors to modulate the phenotype of cancer cells (246). Given all the current available evidence, it is likely that taxane resistance is a complex phenotype that requires the coordination of numerous molecular pathways, and much work is still needed in order to fully understand this.

Whilst lp-WGS has shown potential in exploring taxane resistance, there are of course several limitations to its use. Sophisticated bioinformatic systems are required, and establishing reliable and comprehensive pipelines is a time-consuming and challenging process. Studies such as this remain significantly underpowered due to the large volumes of data generated from a relatively small sample size. Despite lp-WGS allowing confident copy number calling, mutation calling would require significantly deeper levels of coverage which would exponentially increase the costs.

These limitations notwithstanding, my data prove that low-pass whole genome sequencing from cell-free DNA is both feasible and informative. Although further optimisation and validation is needed, analysis of cell-free DNA by low pass whole genome sequencing has potential to help guide treatment decision-making in the care of advanced prostate cancer patients.

7. Liquid biopsies by apheresis

7.1 Aims & Hypothesis relating to this chapter

7.1.1 Hypothesis:

Circulating tumour cells (CTCs) are rare events in the peripheral circulation, and their study has been limited due to the difficulty in their isolation. I hypothesized that apheresis, followed by methods for enriching CTCs may allow the safe acquisition of large numbers of valuable intact CTCs, permitting molecular characterisation.

7.1.2 Aims:

1) To evaluate the safety and tolerability of apheresis in metastatic castration resistant prostate cancer (mCRPC) patients.
2) To increase the yield of CTCs captured from mCRPC patients.
3) To establish whether we can elucidate single cell genomics from captured CTCs, allowing precise gene copy-number calls and study of inter- and intra-patient heterogeneity.

7.2 Research in context

Since circulating tumour cells (CTCs) were first described by Thomas Ashworth, in 1869 (146), their role in monitoring tumour burden and outcome in malignancy has become well established (147,247). Unfortunately, efforts to use CTCs for genomic characterisation have been hampered by difficulties in their identification and the relatively low frequencies in which they are detected (248,249). Discovery of a significant number of CTCs could allow genomic, transcriptomic and protein analysis. Apheresis has been suggested as a way of screening large blood volumes for CTCs and reliably increasing the numbers detected (250).

In some autoimmune, dermatological and haematological disorders, apheresis has been shown to have an effective therapeutic role, leading to clinical improvement whilst having few safety concerns (251). Patients are attached, via two peripheral venous catheters to

an apheresis machine, which allows the processing of the whole blood volume by centrifugation. Blood components (e.g. red blood cells, platelets, leucocytes and CTCs) are separated in the centrifugation process by their density, allowing certain components to be siphoned off whilst the remainder can be returned to the peripheral circulation. CTCs have a similar density to mononuclear cells, and therefore by removing the mononuclear component of the apheresis product a large number can theoretically be made available for subsequent isolation and enrichment. Downstream genomic analysis can enable minimally invasive tumour molecular characterisation, permitting a true liquid biopsy.

7.3 Study design

7.3.1 Trial design

The individual steps are described fully in ***Chapter 2 (Materials and Methods***) but relevant methods are briefly summarised here. An overview of the study methodology is shown in ***Figure 7-1***. This work was done in collaboration with Maryou Lambros and George Seed (Cancer Biomarkers team, Institute of Cancer Research).

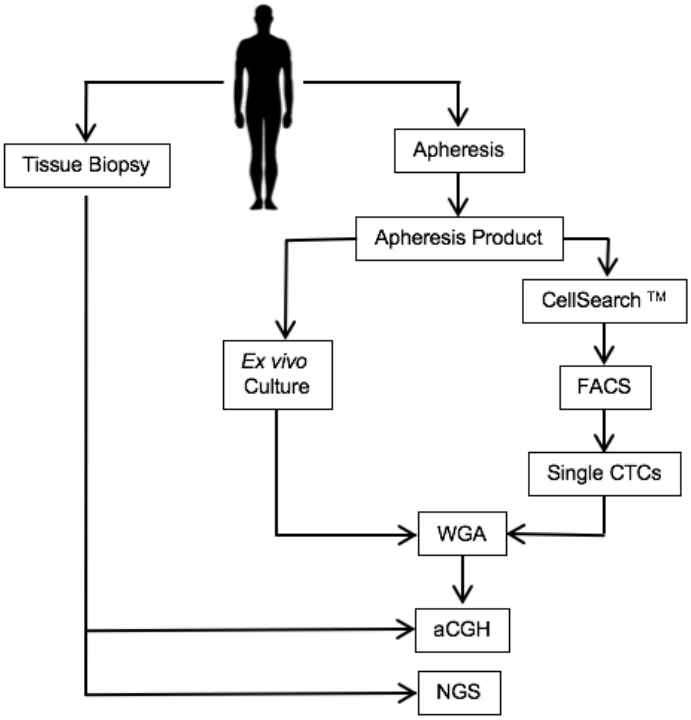

Figure 7-1: Study design workflow.

aCGH = array comparative genomic hybridisation; CTC = circulating tumour cell; FACS = fluorescent activated cell sorting; NGS = next generation sequencing; WGA = whole genome amplification.

7.3.2 Sample collection

Samples were collected from patients enrolled in an ethically approved protocol (CCR 2996) after informed consent was obtained. To be eligible, patients needed to have histologically confirmed prostate adenocarcinoma, detectable peripheral blood CTCs, no evidence of any coagulopathy, an Eastern Cooperative Oncology Group performance status (ECOG PS) of ≤1 and good bilateral antecubital fossa access. Initially, patients needed a peripheral blood CTC count of ≥50, but during the course of the study I amended the protocol to include patients with CTC counts of ≥20.

7.3.3 Clinical data

The study mandated that full clinical assessments were carried out on all enrolled patients, which included a comprehensive medical history, physical examination and peripheral blood testing for full blood count, biochemistry, coagulation and CTC counts. Safety assessments were undertaken during the apheresis procedure and a 30 day follow up assessment was also carried out.

7.3.4 Apheresis method

Apheresis was performed using a Spectra Optia apheresis system (Terumo, Colorado, USA) as per the manufacturer's specification (205). Blood was extracted from a peripheral venous catheter, and anticoagulated prior to entering the rotating centrifuge of the apheresis machine. This centrifugal force was used to separate blood components by density, with the heavier elements (such as erythrocytes) migrating to the outside channel. CTCs, together with mononuclear cells were removed and the remaining plasma returned to the patient.

7.3.5 CTC detection and enumeration

Peripheral blood CTC counts were determined from 7.5mL of blood drawn both immediately before and directly after the apheresis procedure using the CellSearch® platform as described in ***Chapter 2 (Materials and Methods).*** The CTC count of the apheresis product was also determined on the same platform, by transferring a volume of apheresis product containing approximately 200 x 10^6 white blood cells (WBCs) to a CellSave preservation tube and mixing with CellSearch dilution buffer to make a final

volume of 8mL. White blood cell count of the apheresis product was estimated by the Royal Marsden Hospital Haematology laboratory.

Both peripheral blood and apheresis CTC counts were measured using the CellSearch® system; cells were subjected to immunomagnetic capture with anti-EpCAM antibodies and stained with antibodies specific to cytokeratins, CD45 and with DAPI (a nucleic acid dye). Cells positive for cytokeratin (CK), DAPI and negative for CD45 were identified as CTCs by the system, and then manually reviewed by an operator to confirm CTC positivity. These approved counts were collated in the patient database.

7.3.6 Single cell isolation and amplification

Cells were isolated by FACS sorting using the FACSAria III from CellSearch® cartridge contents. Single CTCs and WBCs were isolated on the basis of being DAPI+, CK+, CD45- (CTCs) or DAPI+, CD45+, CK- (WBCs). Whole genome amplification was undertaken on these isolated cells using Ampli1™ as per manufacturer's instructions (199) with some minor modifications. These are described in more detail in ***Chapter 2 (Materials and Methods).*** Following amplification, the amplified DNA was purified and then stored at -20°C.

7.3.7 DNA from biopsies

Where possible, contemporaneous biopsies and archival tissue from original diagnosis was obtained for patients enrolled. DNA from these formalin-fixed paraffin-embedded (FFPE) biopsies was extracted, quantified and evaluated as described in ***Chapter 2 (Materials and Methods).*** Ten nanograms of extracted tumour DNA was used for whole-genome amplification using WGA2 as per manufacturers guidelines.

7.3.8 Array comparative genomic hybridisation

Array comparative genomic hybridisation (aCGH) was performed using 500ng of amplified single cell DNA from CTCs and WBCs. CTC DNA was labelled with Cy5 dye and WBC DNA with Cy3 dye. After purification, this labelled DNA was hybridised and slides scanned using Agilent CytoGenomics Software.

7.3.9 Fluorescent in-situ hybridisation

Fluorescent *in-situ* hybridisation (FISH) was performed using probes for *BRCA2*, *RB1*, *PTEN*, *MYC* and *AR*/*CEPX* on 3-4µm FFPE slides using methods described previously in ***Chapter 2 (Materials and Methods)***, and with support from Susana Miranda (Cancer Biomarkers team, Institute of Cancer Research). Slides were digitally imaged and then evaluated by a pathologist (Dr. Daniel Nava Rodrigues) who reviewed a minimum of 100 tumour cells. Ratios between the probes of interest and reference probes were recorded; a ratio of >2 was recorded as an amplification, heterozygous loss if at least one of three of the cells showed loss of one copy and homozygous deletion if there was loss of all copies of the tested probe.

7.3.10 Organoids

Organoid culture was carried out by Veronica Gil (Higher Scientific Officer, Cancer Biomarkers Team). CTC enrichment was performed using immunomagnetic separation from 1mL of single-cell suspension, with the positively selected fraction being used for organoid culture and seeded in 3D using Matrigel. After 4 - 6 weeks of passaging, cells were collected from these organoids for further studies.

7.3.11 Whole-exome sequencing

Whole-exome sequencing (WES) was performed using the Kapa HyperPlus library and methods previously described. Samples were run on the Illumina NextSeq500^{TM}.

7.3.12 Bioinformatic and Statistical Analyses

7.3.12.1 For array comparative genomic hybridisation

Log_2 ratios of aCGH segments were matched with gene coordinates to assign per-gene values. Assigned log_2 ratios were used to categorise copy states of genes, with log_2 ratio values <-0.25 being classified as losses and >0.25 as gains. In-between values were classified as being “normal” or unchanged. Smoothed log_2 ratio values ≥1.2 were defined as amplifications and ≤1.2 as homozygous deletions. The proportion of the human genome affected was used to calculate the per-sample copy number aberration (CNA) burden. R (v3.4) was used to perform unsupervised hierarchical clustering using the

Ward method and the Euclidean distances of unique copy-number changes. As a female reference was used, the X-chromosome genes were excluded (aside from the *AR* gene and 10 genes either side) when clustering samples from multiple tissue types. Cluster dendrograms were used to derive per-patient functional diversity by calculating the sum of connecting branches in a dendrogram, using the R package vegan (v2.4.4) and dividing by the number of samples.

7.3.12.2 For whole exome sequencing

Output files from the Illumina NextSeq500™ were transferred to FASTQ files using the Illumina bcl2fastq2 software. Sequencing reads were aligned to the human genome reference sequence using the BWA-MEM algorithm. The genome Analysis Toolkit (GATK, v.3.5-0) was used to realign local indels, recalibrate base scores and to identify point mutations as well as small insertions and deletions. The ASCAT2 package was used for copy number estimation.

7.3.12.3 Statistical analysis

Statistical analysis was performed using Excel (v16.16.10) and R (v3.4) unless otherwise specified.

7.4 Results

7.4.1 Patients and samples

Over an 18-month period, 14 patients who met the eligibility criteria were successfully enrolled in the study and underwent an apheresis procedure. Patient characteristics are detailed in ***Table 7-1***. The median age of the recruited patients was 70.4 years (mean = 69.8, range 60 – 77 years).

Table 7-1: Baseline characteristics of study patients (n=14)

Characteristic	Value
Age (yr)	
Mean	69.8
Median	70.4
Range	60 - 77
Time since initial diagnosis of PC to procedure (yr)	
Mean	6.2
Median	3.9
Range	2 – 11.6
No. of met sites at time of procedure	
Mean	2
Median	2
Range	1-3
Bone mets No. (%)	14 (100)
PSA level (ng/mL)	
Mean	1209
Median	506
Range	41 - 6089
ECOG PS – No. (%)	
0	0
1	14 (100)
Received prior regimens for CRPC – No. (%)	
1	1 (7)
2	4 (29)
3	7 (50)
≥4	2 (14)

All values given are at time of the apheresis procedure unless specified otherwise. All CRPC = castration resistant prostate cancer; ECOG PS = Eastern Cooperative Oncology Group performance status; met = metastatic; No. = number; PC = prostate cancer; PSA = prostate specific antigen; Yr = year.

The time from initial prostate cancer diagnosis to the apheresis procedure was varied, with some patients having only been diagnosed 2 years previously and others over 11 years before (mean = 6.2 years, median = 3.9 years). The prostate specific antigen (PSA) levels at the time of diagnosis ranged from 41 to 6089 (mean = 1209, median = 506). All patients (14/14, 100%) had an ECOG PS of 1. Prior to undergoing the procedure, patients had received between 1 to 5 lines of therapy for CRPC which included chemotherapy (docetaxel and cabazitaxel), novel hormonal agents (abiraterone and enzalutamide), radium-223 and also the PARP-inhibitor, olaparib. Prior exposure is shown in ***Figure 7-2***. Of note, at the time of apheresis patients were not receiving any therapy apart from routine androgen deprivation therapy (ADT).

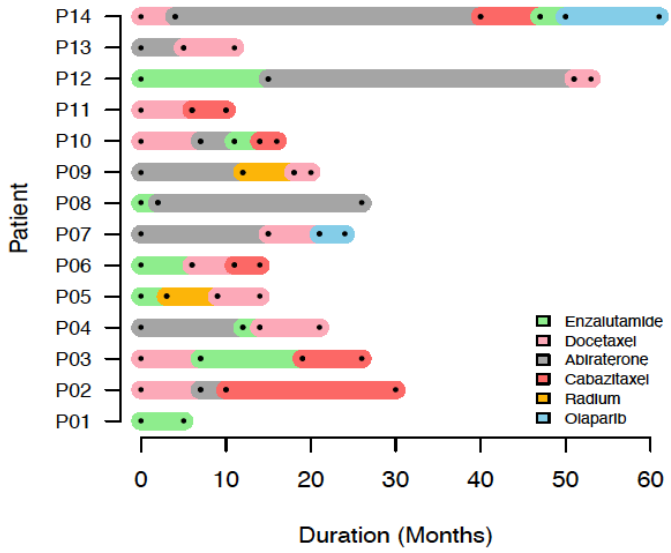

Figure 7-2: Prior therapies and duration of treatment, by patient.

All patients had received between 1 – 5 lines of therapy.

The apheresis procedure lasted between 90 – 160 minutes and the total volume of apheresis product collected ranged from 40 – 100 mL (mean = 59.5). The procedure was well tolerated with no adverse effects being observed or reported during the procedure or within the 30-day follow up period. The pre- and post- procedure white blood cell count values (neutrophils and lymphocytes) did not show any significant changes and this is shown in ***Figure 7-3.***

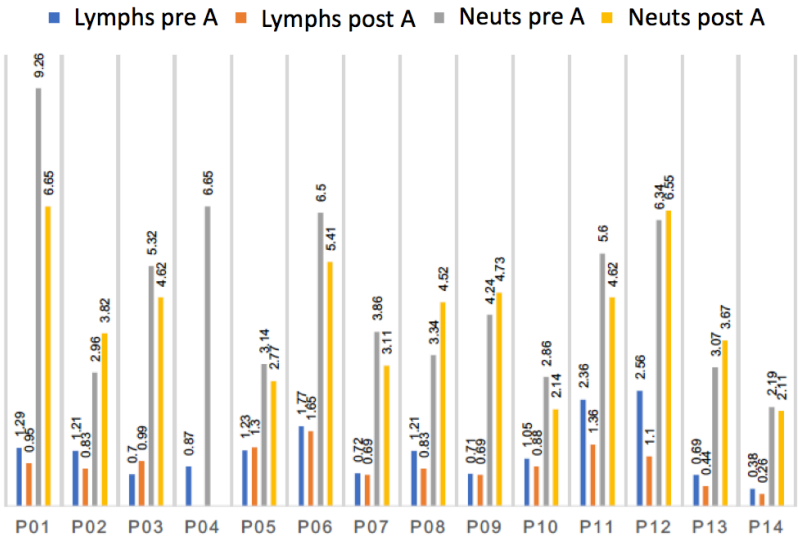

Figure 7-3: Histogram showing lymphocyte and neutrophil counts (x109/L) in peripheral blood pre- and post- apheresis procedure

Please note that P04 was missing a post-apheresis sample. A = apheresis; Lymphs = lymphocytes; Neuts = neutrophils.

7.4.2 Circulating tumour cell enumeration

The mean peripheral blood CTC count prior to apheresis was 167 and 193 from the sample taken immediately after (per 7.5mL of peripheral blood). The CTC count did not decrease significantly following apheresis (p = 0.48). To calculate the total apheresis product CTC count, a volume of the apheresis product containing 200 x 10^6 WBC was added to a CellSave tube with CellSearch dilution buffer. This CTC count was multiplied by the volume used, divided by the total apheresis product volume. The average inferred CTC harvest from these 14 patients was 12546 (range: 660 – 54364). This was an approximately 90-fold average increase compared to the peripheral blood CTC yield, shown in ***Figure 7-4***.

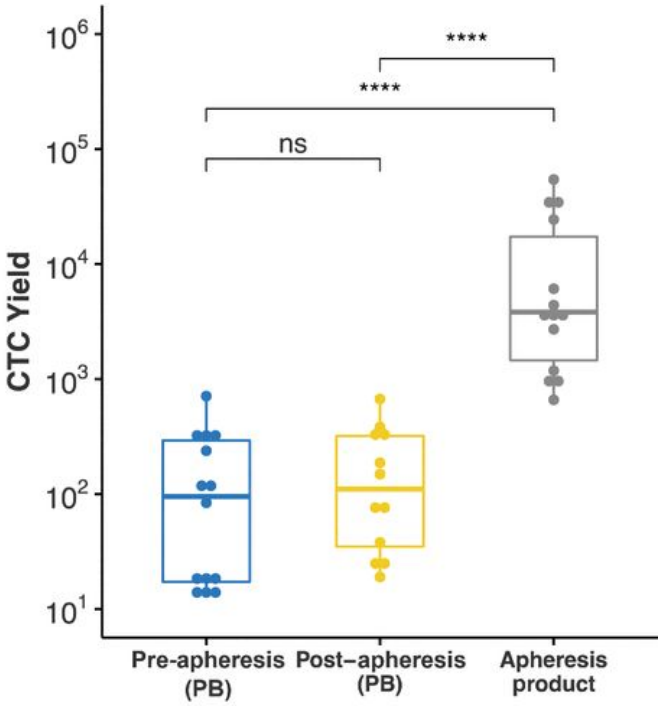

Figure 7-4: CTC counts from peripheral blood and apheresis

CTC counts from 7.5 mL of peripheral blood taken both pre-apheresis (blue) and post-apheresis (yellow) compared with inferred harvested CTC counts in the total volume of apheresis product (grey). CTC = circulating tumour cell; NS = non-significant.

The inferred total apheresis CTC count was closely correlated with both the pre-apheresis peripheral blood CTC ***(Figure 7-5A***) count and post-apheresis peripheral blood CTC count (***Figure 7-5B***). All 14 patients had peripheral blood CTC counts pre-procedure, but 2 were missing post-procedure CTC counts and are therefore not displayed in ***Figure 7-5B***.

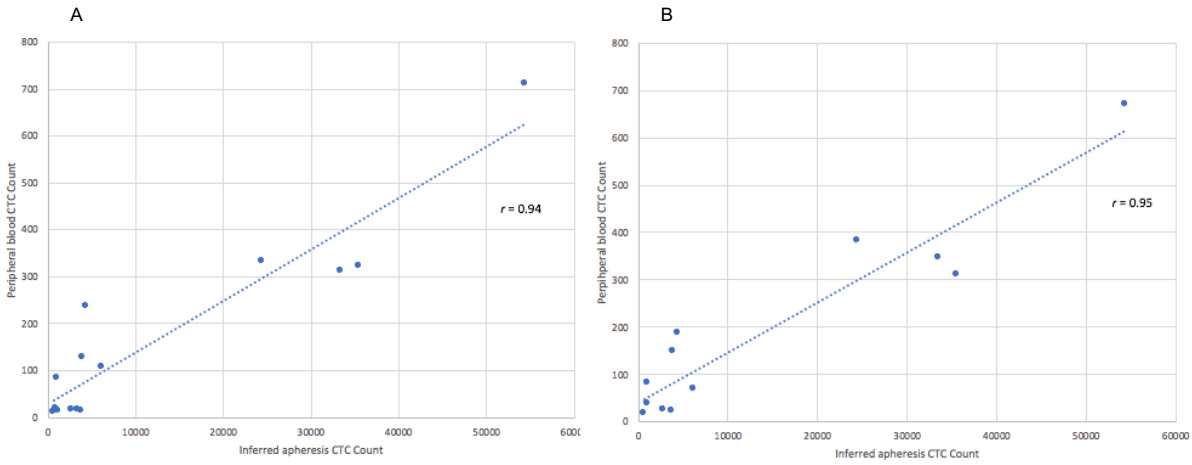

Figure 7-5: Inferred total apheresis CTC count plotted against peripheral blood CTC counts

Apheresis count plotted against pre-procedure peripheral blood CTC (A) count showed a strong correlation (Pearson's r = 0.94) and against post-procedure peripheral blood CTC count (B) (Pearson's r = 0.95). CTC = circulating tumour cell.

Baseline PSA was very weakly negatively correlated with the inferred apheresis CTC count (r= -0.3) as shown in ***Figure 56***. Interestingly, some patients with relatively low PSA values (41, 94, 147) had some of the highest CTC counts (2707, 3868, 54364) respectively. Conversely, the highest PSA value of 6089 was seen in a patient who had one of the lower apheresis CTC counts of 941.

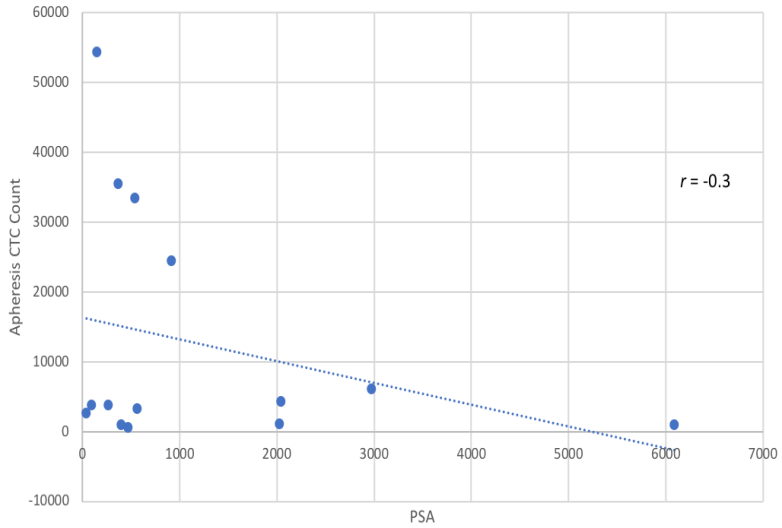

Figure 7-6: Baseline PSA was weakly negatively correlated with the inferred apheresis CTC count.

CTC = circulating tumour cell; PSA = prostate specific antigen.

7.4.3 Assay validation

To validate the whole genome amplification (WGA) methods, and the aCGH performed on single cells, I first used the Ampli1 method of WGA on normal male and female DNA (supplied by Agilent with the aCGH kit) and hybridised them together using the Agilent aCGH protocol. This is shown as a genome plot in ***Figure 7-7A***, by a flat trace with expected differences observed in the X chromosome. I then amplified white blood cell (WBCs) DNA and hybridised same patient WBCs against each other to confirm there were no bias amplifications or deletions as shown in ***Figure 7-7B***.

My final validation step was to use single cell DNA isolated from a circulating tumour cell using WGA of 1uL of serially diluted samples. My starting DNA templates were 10ng/uL, 1ng/uL, 0.1ng/uL and 0.03ng/uL. These traces, shown in ***Figure 7-7C***, with gains and amplifications depicted in blue and losses and homozygous/deep deletions shown in red, show reproducible patterns for all 4 DNA inputs.

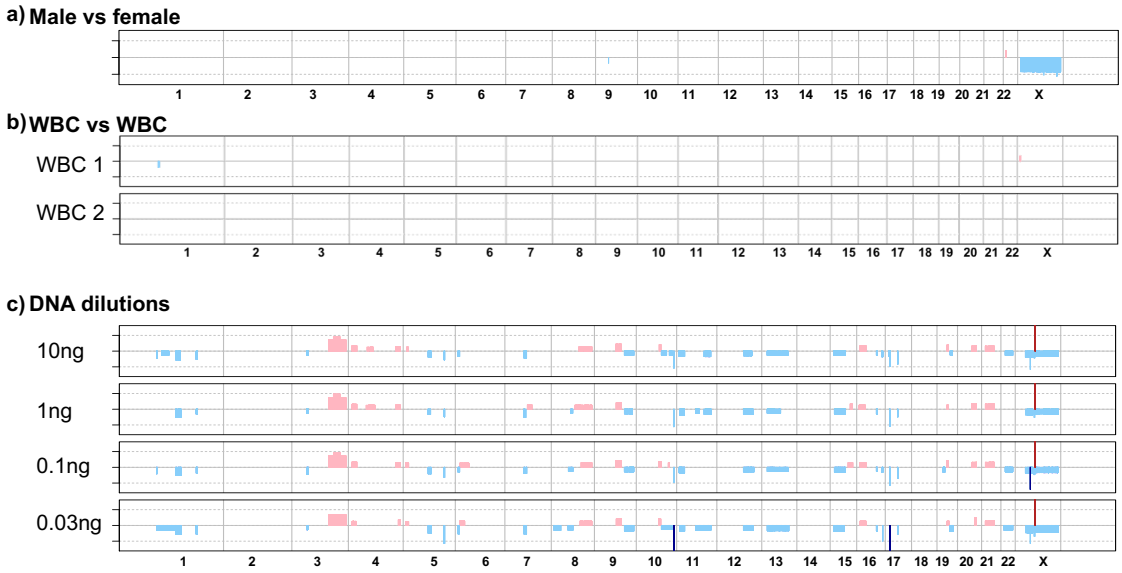

Figure 7-7: Summary of validation steps

A) Male vs. Female: A genome plot of amplified male DNA versus amplified female DNA, B) Genome profiles of amplified WBCs against other WBCs and C) same patient CTC dilutions from 10ng to 0.03ng showing similar patterns. Gains and amplifications are depicted in red/pink, and losses and heterozygous/deep deletions shown in blue.

7.4.4 Genomic profiling of single cells

I next conducted aCGH on 205 single CTCs from 14 patients. Ninety percent (90%, 185/205) of the CTCs showed complex genomic copy number profiles with the remaining 10% (20 cells) having relatively flat traces. Only 2 of the 14 evaluated patients had both flat and cancer-like aCGH profiles. This may suggest that that these cells may be induced by certain treatments or be associated with specific tumour subtypes. The individual CTCs per patient, the percentage of the genome altered and the percentage of genes altered are shown in ***Table 7-2***. An average of 13 CTCs was assessed per patient (range 7-23). The flat copy number profiles were not used in further analysis unless otherwise mentioned.

Table 7-2: Summary of individual CTCs per patient with percentage of the genome covered by a copy number segment and percentage of genes that are altered.

Patient ID	Sample Name	Genome Altered (%)	Genes Altered (%)
P01	P01_C1	30.7	27.5
P01	P01_C2	32.2	28.3
P01	P01_C3	77.7	75.2
P01	P01_C4	62	67.9
P01	P01_C5	52	43.9
P01	P01_C6	2.7	3.2
P01	P01_C7	25.4	18.6
P01	P01_C8	8.8	7.4
P01	P01_C9	25	15.5
P01	P01_C10	39.2	16
P01	P01_C11	29.3	33.6
P01	P01_C12	36.7	30.9
P02	P02_C1	39.8	22.4
P02	P02_C2	25.1	15
P02	P02_C3	68.2	72.6
P02	P02_C4	37.3	18.1
P02	P02_C5	37.5	28.8
P02	P02_C6	39.6	23.6
P02	P02_C7	51.9	53.9
P02	P02_C8	51.2	51.9
P02	P02_C9	32.5	25.2
P02	P02_C10	36.8	34.2
P02	P02_C11	29.1	33.5
P02	P02_C12	43.8	40.4
P02	P02_C13	41.1	24
P03	P03_C1	66.5	65.4
P03	P03_C2	76.8	76.5
P03	P03_C3	62.4	57.4
P03	P03_C4	52.7	52.8
P03	P03_C5	41.4	39.1
P03	P03_C6	58.9	45.2
P03	P03_C7	49.1	47.2
P03	P03_C8	47.8	47.7
P03	P03_C9	55.4	68.9
P03	P03_C10	35.8	34.6
P03	P03_C11	36.8	36.7
P03	P03_C12	21.1	15.5
P03	P03_C13	63.4	62.3
P04	P04_C1	21.6	20.5
P04	P04_C2	43.1	28.2
P04	P04_C3	33.7	34.8
P04	P04_C4	63.6	56.8
P04	P04_C5	41.6	38.7
P04	P04_C6	55.4	48.7
P04	P04_C7	40.7	33.2
P04	P04_C8	61	54
P04	P04_C9	54.5	45.6
P04	P04_C10	16.2	9.1
P05	P05_C1	60.7	58
P05	P05_C2	33.9	23.9
P05	P05_C3	13.6	12.8
P05	P05_C4	40.2	33.2
P05	P05_C5	41	38.4
P05	P05_C6	39.6	38.5
P05	P05_C7	48.6	41.8
P05	P05_C8	42.4	38.8
P05	P05_C9	56.4	58.5
P05	P05_C10	14.1	12.8
P05	P05_C11	35.4	25.9
P05	P05_C12	59.7	53.4
P06	P06_C1	85.5	74.6
P06	P06_C2	27.8	27.6
P06	P06_C3	52.5	50.2
P06	P06_C4	36.2	31.2
P06	P06_C5	38.6	29.6
P06	P06_C6	30.9	29.6
P06	P06_C7	70.6	68.1
P06	P06_C8	32.8	26.8
P06	P06_C9	55.4	47.6
P06	P06_C10	58.1	45.4
P06	P06_C11	51.5	37.5
P06	P06_C12	34	11.6
P06	P06_C13	60.5	60.8
P06	P06_C14	71.9	68.8
P06	P06_C15	53.8	50.2
P06	P06_C16	80	82.5
P06	P06_C17	31.4	25.1
P06	P06_C18	18.7	19
P07	P07_C1	56.2	43.2
P07	P07_C2	22	21.7
P07	P07_C3	22.4	22
P07	P07_C4	57.9	38.1
P07	P07_C5	40.5	36.5
P07	P07_C6	49.7	37.2
P07	P07_C7	52.4	51.6
P07	P07_C8	38.2	39
P07	P07_C9	51.6	31
P07	P07_C10	44.2	26.9
P07	P07_C11	25.2	22.1
P07	P07_C12	24	19.9
P07	P07_C13	33.5	31.8
P07	P07_C14	79.4	83.2
P07	P07_C15	34.1	20.3
P07	P07_C16	28.3	23.4
P08	P08_C1	21.6	14.1
P08	P08_C2	50.4	47.7
P08	P08_C3	37.3	20
P08	P08_C4	30.7	18.1
P08	P08_C5	16.5	13
P08	P08_C6	19.2	15.5
P08	P08_C7	23.6	15.8
P08	P08_C8	56.6	48.6
P08	P08_C9	26.9	19.8
P08	P08_C10	16.2	9.1
P08	P08_C11	15.1	15.2
P09	P09_C1	24.6	22.9
P09	P09_C2	27.9	26.1
P09	P09_C3	27.9	26.2
P09	P09_C4	28.1	26
P09	P09_C5	25.2	23.4
P09	P09_C6	28.1	26.2
P09	P09_C7	28	26.3
P09	P09_C8	27.8	25.9
P09	P09_C9	28.8	20
P10	P10_C1	53.4	44.4
P10	P10_C2	21.5	10.8
P10	P10_C3	54.2	42.8
P10	P10_C4	57.6	59
P10	P10_C5	38.9	23.6
P10	P10_C6	68.5	71.2
P10	P10_C7	63.8	66.2
P11	P11_C1	28.2	29.4
P11	P11_C2	22.3	23.5
P11	P11_C3	27	24.8
P11	P11_C4	27.4	23.6
P11	P11_C5	26.3	25.1
P11	P11_C6	24.8	25.4
P11	P11_C7	32.3	36.1
P11	P11_C8	26.5	31.1
P11	P11_C9	22.9	24.9
P11	P11_C10	23.5	24.1
P11	P11_C11	38.8	44.5
P11	P11_C12	24.7	24.4
P12	P12_C1	12.3	4
P12	P12_C2	30.3	23.4
P12	P12_C3	22.9	17.3
P12	P12_C4	2.8	0.2
P12	P12_C5	43.4	41.7
P12	P12_C6	4.6	1.7
P12	P12_C7	2.6	1.5
P12	P12_C8	70.8	73.2
P12	P12_C9	67.1	70.7
P12	P12_C10	83.8	86.2
P12	P12_C11	60.5	54.3
P12	P12_C12	17.5	17.3
P12	P12_C13	69	76.5
P12	P12_C14	56.8	54
P12	P12_C15	76.9	79.1
P12	P12_C16	53.7	53
P12	P12_C17	51.3	46.2
P13	P13_C1	27.4	22.5
P13	P13_C2	26.4	24.2
P13	P13_C3	23.3	22.1
P13	P13_C4	18.7	20.5
P13	P13_C5	25.9	24.1
P13	P13_C6	22.3	20.1
P13	P13_C7	38.2	40
P13	P13_C8	88	91.3
P13	P13_C9	91	94.3
P13	P13_C10	51.3	36
P13	P13_C11	75	73.3
P13	P13_C12	30.7	22.3
P13	P13_C13	16.5	14.4
P13	P13_C14	22	17.5
P13	P13_C15	26	21.3
P13	P13_C16	24.3	20.1
P13	P13_C17	27.6	17.8
P13	P13_C18	24.7	22.3
P13	P13_C19	22.4	12.2
P13	P13_C20	25.8	23.3
P13	P13_C21	33.4	23.6
P13	P13_C22	51.3	47.5
P13	P13_C23	24.7	23.7
P14	P14_C1	82.9	85.1
P14	P14_C2	25.8	27.8
P14	P14_C3	34.4	28.5
P14	P14_C4	10.1	9.3
P14	P14_C5	60.9	56.7
P14	P14_C6	70.3	74.4
P14	P14_C7	37.4	34.9
P14	P14_C8	63.1	60.2
P14	P14_C9	30.4	29.5
P14	P14_C10	83.7	83
P14	P14_C11	39.5	40.1
P14	P14_C12	28.8	27.2

The remaining 185 copy number profiles of individual CTCs from the 14 patients were aggregated and this trace is shown in ***Figure 7-8A***. Here, gains are depicted in light pink, losses in light blue, with amplifications in dark red and homozygous/deep deletions shown in dark blue. Publicly available data from whole exome sequencing of 150 mCRPC biopsies by the SU2C/Prostate Cancer foundation Dream Team collaboration (81) was reanalysed and is shown in ***Figure 7-8B***. For 12 of the 14 patients, tumour biopsies were also available for analysis; these were both treatment-naïve hormone-sensitive diagnostic biopsies and/or metastatic biopsies. These samples were also evaluated by aCGH and this trace is shown in the bottom panel of ***Figure 7-8C***. All 3 panels show broadly similar genomic profiles, further validating this technique and results.

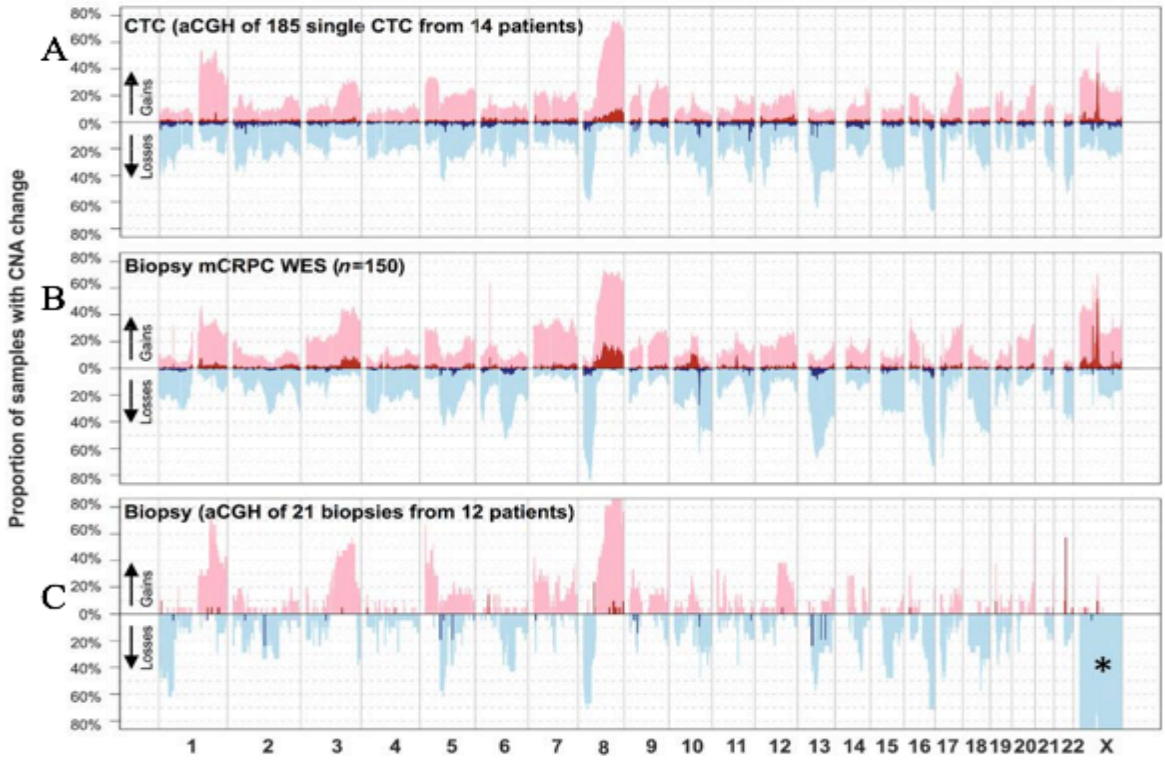

Figure 7-8: Genomic frequency plots

*A) Genomic frequency plot of aberrations found from 185 single CTCs harvested by apheresis from 14 mCRPC patients, B) the middle plot represents the frequency of genomic aberrations from 150 mCRPC exomes (SU2C/PCF cohort), and C) frequency of genomic aberrations from available tissue biopsies from 12 of 14 patients. Chromosomes are shown across the x-axis, whereas the y-axis represents the frequency of gains, losses, amplification, and homozygous deletions. Gains are depicted in light pink, losses are depicted in light blue, amplifications in dark red, and homozygous/deep deletions are in dark blue. * - aCGH of tissue biopsies were performed using female reference DNA (Agilent). aCGH = array comparative genomic hybridisation; CNA = copy number aberrations; CTC = circulating tumour cells; mCRPC = metastatic castration resistant prostate cancer; WES = whole exome sequencing.*

Differences were observed between hormone-sensitive (i.e. treatment-naïve) biopsies and castration-resistant CTCs. These included changes in Chromosome 13 (*RB1* loss), Chromosome 8q (*MYC* gain) and amplification on the X chromosome of *AR*. These changes were in keeping with tumour evolution due to selection pressures induced by treatment. Where contemporaneous biopsies were available, high concordance was noted between CTC profiles and these biopsy profiles. Discerning intrapatient genomic heterogeneity was not possible from bulk biopsy analysis but could be analysed using single CTC genomics. ***Figure 7-9*** shows an unsupervised hierarchical clustering heatmap of the copy number profiles for each individual patient, organised by patient number from left to right. Chromosome aberrations are depicted from top to bottom, and again gains are shown in pink, losses in light blue, amplifications in dark red and homozygous/deep deletions in dark blue. The tissue biopsies are highlighted in black boxes at the bottom of the heatmap whereas CTCs are shown by green in the colour bar.

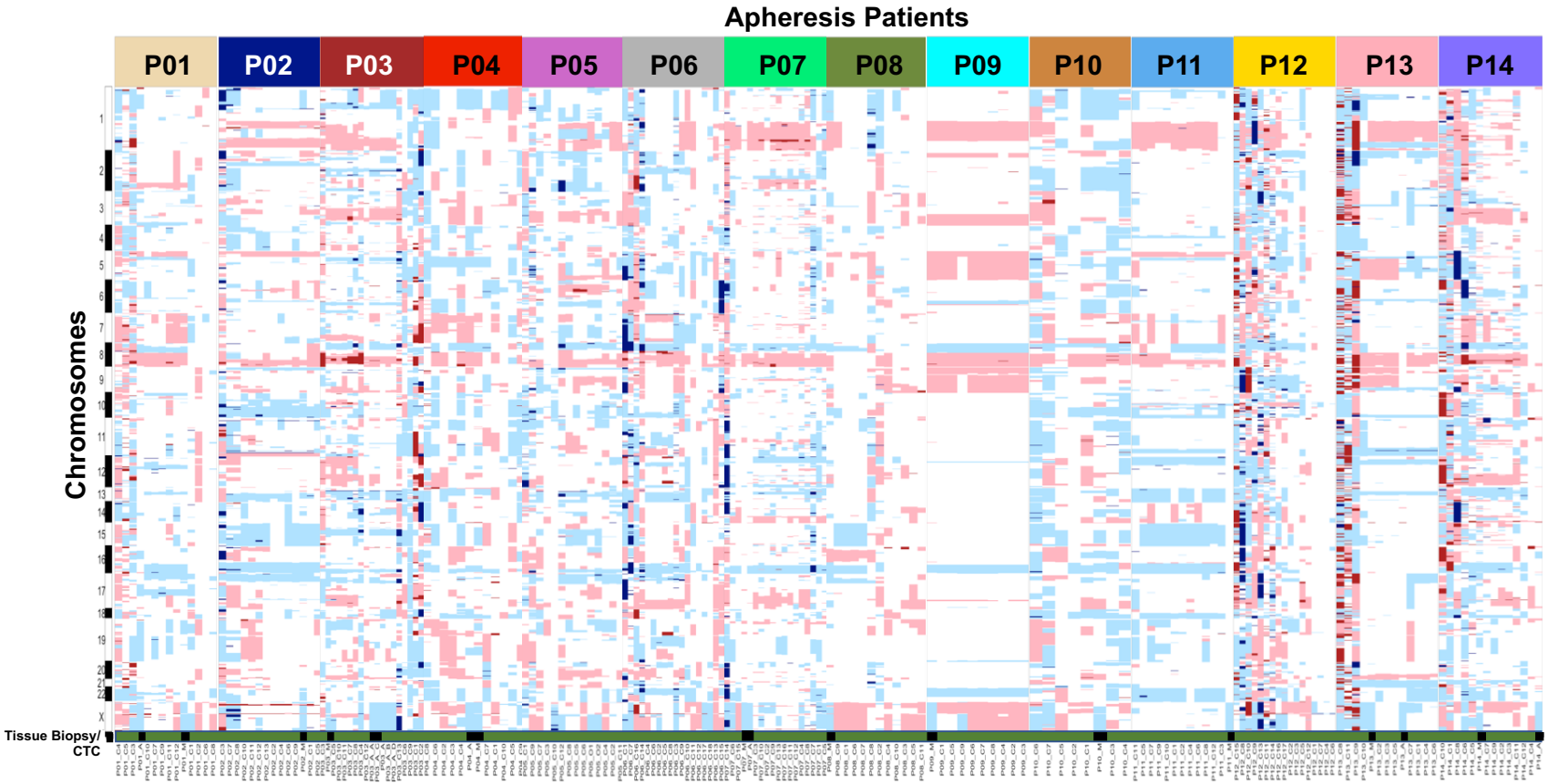

Figure 7-9: Unsupervised hierarchical clustering heatmap of the copy number aberrations of each individual apheresis patient.

The overall heatmap of all patients is organised by patient number from left to right with chromosomes aberration depicted from top to bottom. Gains are shown in pink, losses in light blue, amplifications in dark red and homozygous/deep deletions in dark blue. The tissue biopsies are highlighted in black boxes at the bottom of the heatmap whereas CTCs are shown by green in the colour bar. A = archival biopsy; CTC = circulating tumour cell; M = metastatic biopsy; P = patient number

7.4.5 Interpatient heterogeneity and the diversity of circulating tumour cells

The per-patient CTC traces, as shown in ***Figure 7-9***, were organised in an unsupervised manner, and displayed complex inter-patient and intra-patient heterogeneity. CTCs showed varying amounts of inter-patient heterogeneity, with some patients exhibiting highly homogenous CTC copy number traces (such as P09 in ***Figure 7-9***) and others showing high levels of diversity between their single CTC copy number aberration (CNA) traces.

A biopsy from a metastasis of Patient 09 (P09), whose CTCs had highly homogenous traces, also displayed a virtually identical genomic profile. The 9 CTC aCGH traces and the metastasis aCGH trace are shown in ***Figure 7-10.*** Similar changes can be seen through almost all CTCs, such as a gain in 1q, and the typical 8p loss and 8q gain often seen in CRPC.

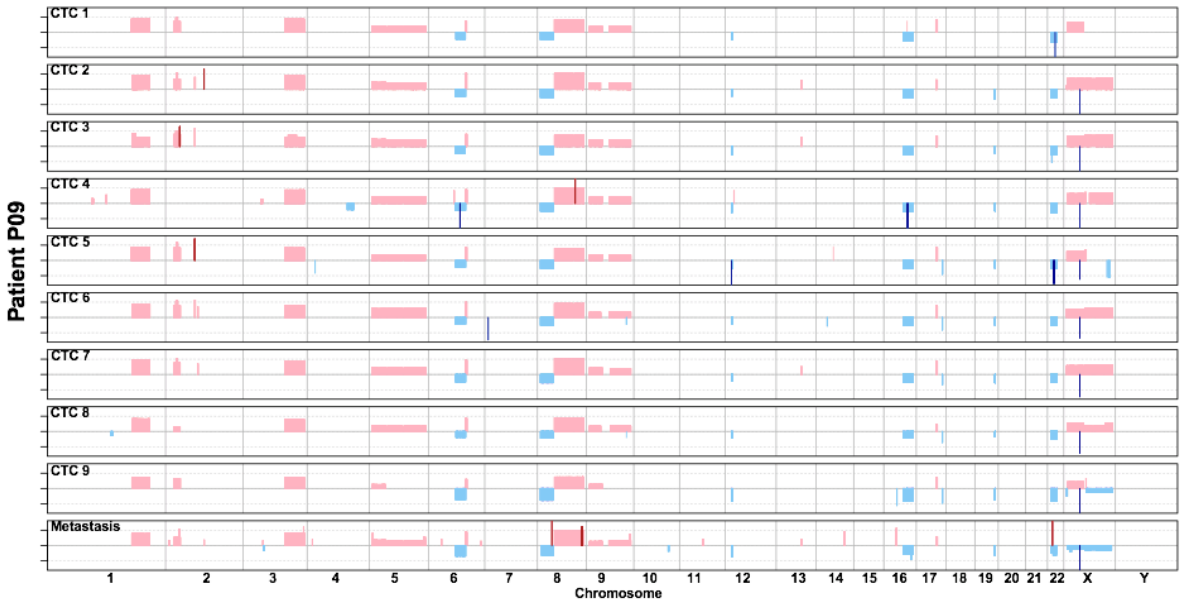

Figure 7-10: CTC genome plots of 9 CTCs from patient P09 shows highly homogeneous traces

These traces are also very similar to a metastatic bone biopsy shown in the bottom panel. Copy number gains are shown in pale pink, amplifications in dark red, copy losses in pale blue and homozygous losses/deep deletions in dark blue. CTC = circulating tumour cell.

The varying levels of inter-and intra-patient diversity are further highlighted in ***Figure 7-11***, which shows the same copy number traces previously displayed but now organised by increasing diversity (from left to right). This was calculated by using the Euclidean distance of each individual CTC analysed from each patient based on their CTC copy number aberrations. As before, each patient is shown in an individual colour, and the

heat maps are organised by these intra-patient diversity scores (lowest on the left, highest on the right). Again, chromosomal CNAs are shown from top to bottom for each individual cell, and the copy number changes using the same colour scheme as described in the legend.

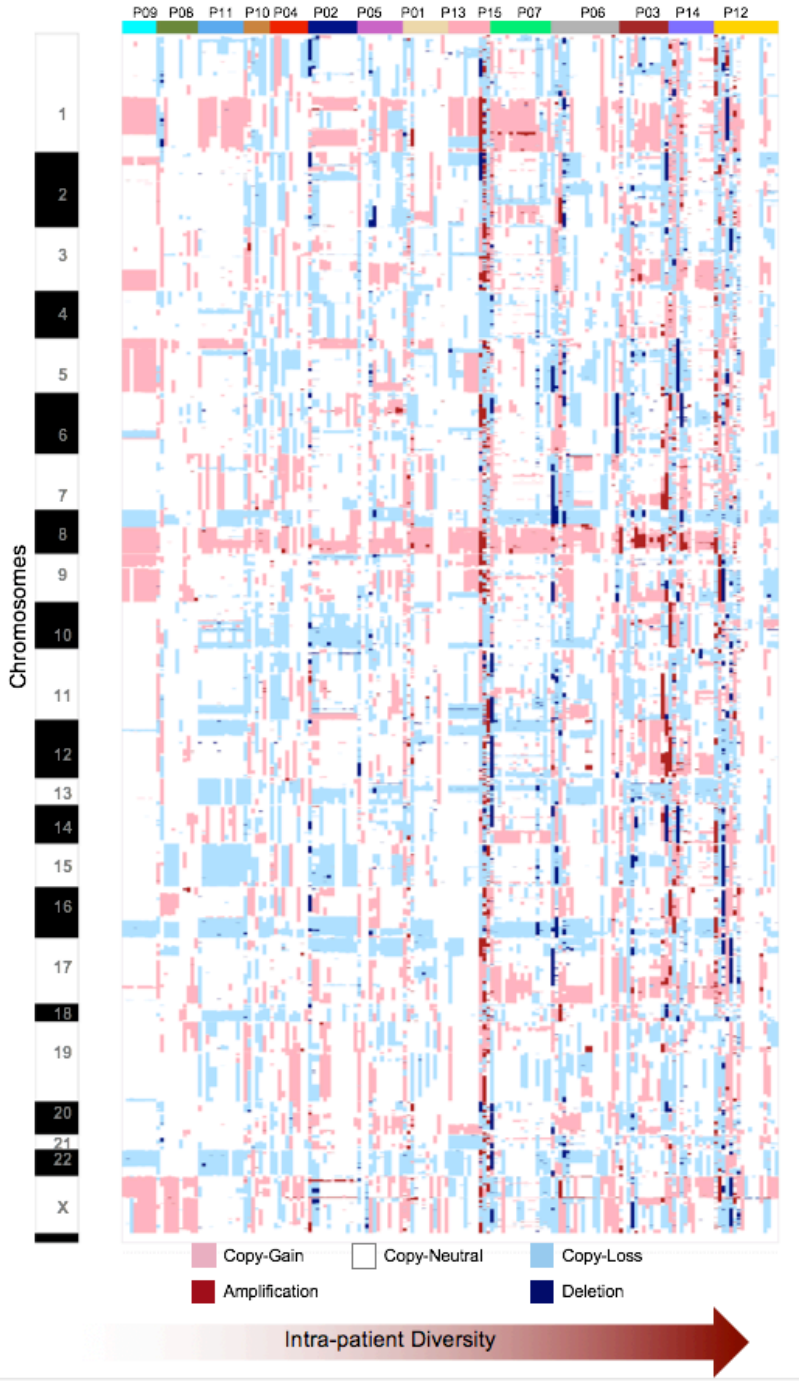

Figure 7-11: Unsupervised hierarchical clustering heat maps based on Euclidean distance of each individual CTC CNAs per patient.

Each patient is shown in an individual colour, with the per patient heatmaps organised by their intrapatient diversity score (lowest left, highest right). Chromosomal copy number aberrations are shown from top to bottom for each individual CTC. Copy number gains are shown in pale pink, amplifications in dark red, copy losses in pale blue and homozygous losses/deep deletions in dark blue. CTC = circulating tumour cell; P = patient number.

The percentage of the genome altered (%GA) per patient is shown in a box plot ***(Figure 7-12)*** organised again by increasing patient diversity from left to right, with patients coded by the same colour used in earlier figures. No significant correlation was found between median percentage genome altered and intra-patient, intra-cell diversity, which suggests genuine clonal diversity rather than just accumulation of aberrations.

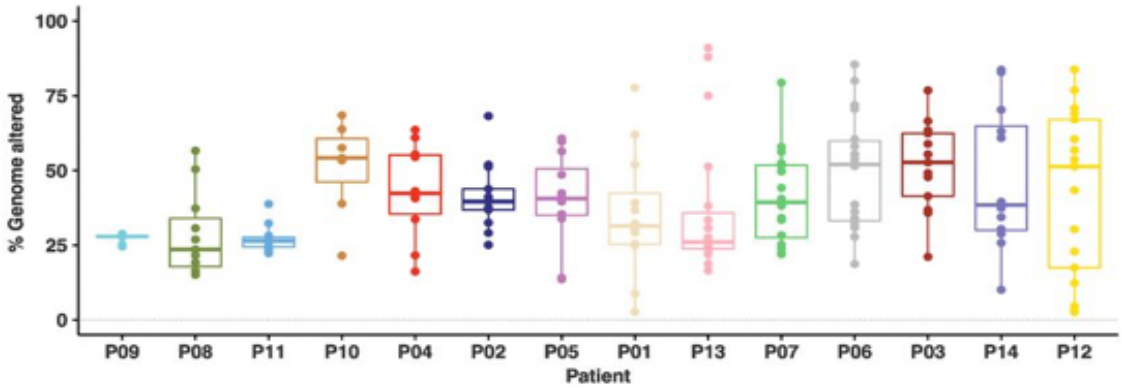

Figure 7-12:Box and whisker plot of the percentage of the genome altered by patient.

Each coloured dot represents the %GA of a single CTC. %GA = Percentage genome altered; CTC = circulating tumour cell P = Patient number.

Despite the diversity, unsupervised hierarchical clustering of the copy number aberration data from all the single CTCs and patient biopsies show that most samples from each patient do tend to cluster together when compared to a hypothetical germline sample (see ***Figure 7-13***). However, even though CTCs from the same patient tend to cluster together when ordered in this unsupervised manner, intra-patient heterogeneity means that some single cells are clustered away from the main group. Two organoids from Patient 05 (pink triangles) are highlighted with a pink arrow, and cluster with a group of the same patient CTCs and will be discussed later.

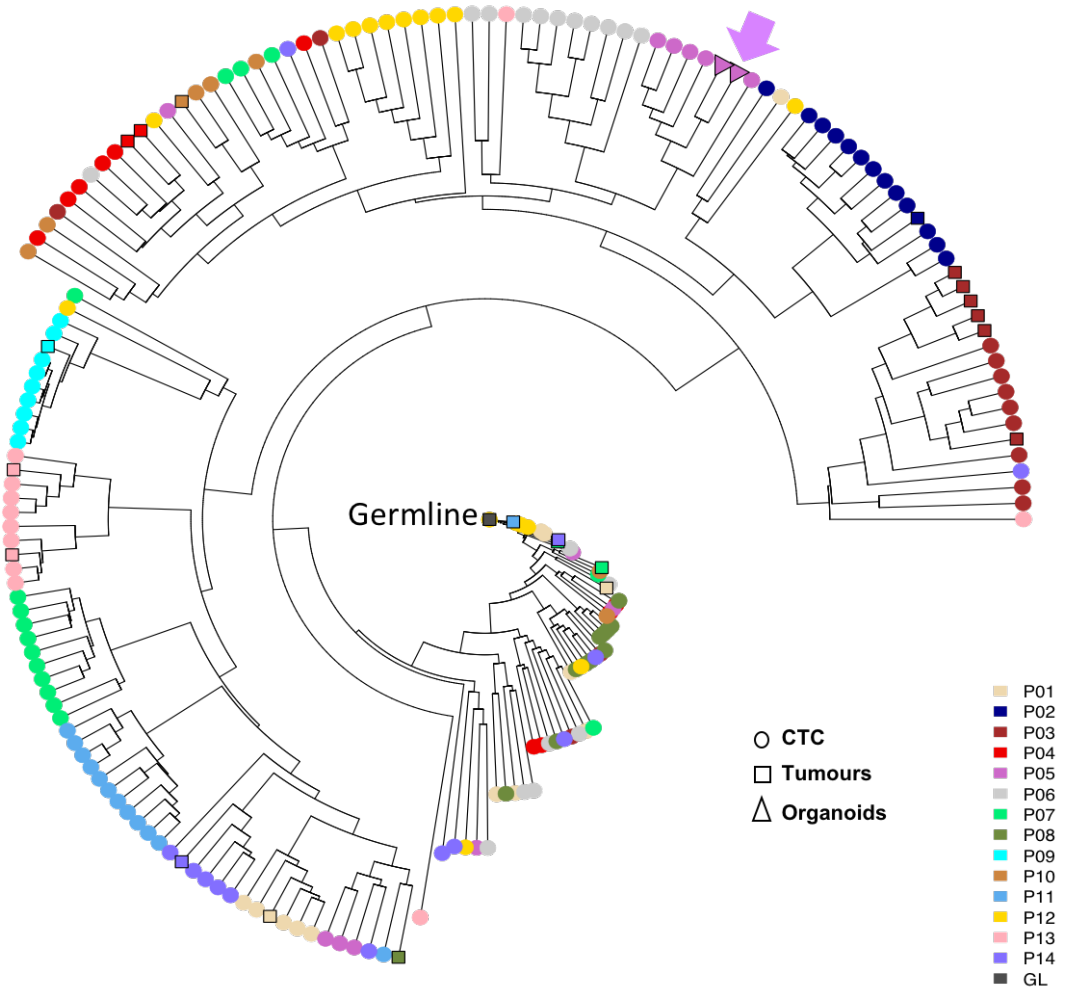

Figure 7-13: A fan presentation of unsupervised clustering of all the CTCs, biopsies and the organoids used in this study

This shows CTCs from the same patients tend to cluster with their respective tissue biopsies. Each CTC is shown by a circle, hormone-sensitive and metastatic castration-resistant biopsies are shown by a square, and organoids with triangles. The samples from each individual patient are coloured accordingly as per the phenobar. In this unsupervised manner, whilst CTCs tend to cluster together, intra-patient heterogeneity means that some single cells are clustered away from the main group. Two organoids from Patient 05 (pink triangles) are highlighted with a pink arrow, and cluster with a group of the same patient CTCs. CTC = circulating tumour cell; GL = germline; P = patient number.

7.4.6 Intrapatient heterogeneity and tumour evolution

For those patients with both tissue and CTCs available for analysis, it became evident that genomic analyses of the gross biopsy could miss some of the copy number aberrations identified in the CTCs. To investigate this discordance further, I evaluated the heterogenous CTCs isolated from Patient 13 and from whom both metastatic and hormone-sensitive tissue was available. Upon studying these copy number traces, there appeared to be 3 distinct groups of cells, some CTCs seemed to cluster with the diagnostic prostatectomy sample and others with the metastatic bone biopsy sample. This latter group had a breakpoint in the *PIK3R1* locus including most of chromosome

5q. There was also a third group of CTCs which seemed to have more complex genomic aberrations visible throughout. These are shown in ***Figure 7-14.***

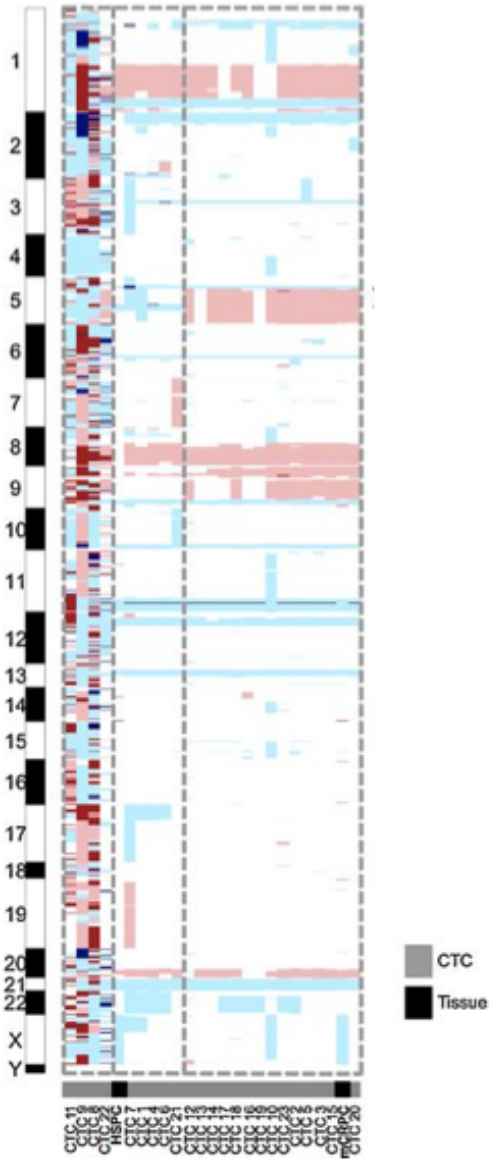

Figure 7-14: A heat map of 23 CTCs and 2 biopsies from Patient 13.

The biopsies are a metastatic bone biopsy and a hormone sensitive diagnostic prostatectomy sample. CTCs are shown in grey, and tissue in black. Each column represents a different sample. Grey dotted lines are marked around the 3 different clones seen. Two of the sub-clones are best visualised by focusing on chromosome 5q where obvious differences lie, and the third group to the left of the panel show a group of highly heterogeneous CTCs. Amplifications are shown in dark red, gains in pink, copy-losses in pale blue and deep deletions in dark blue. Copy neutral areas are white. CTC = circulating tumour cell.

FISH was performed on the hormone-sensitive sample (the prostatectomy tissue) and the bone metastasis (castration-resistant) sample to assess the 5q21.1 locus. This revealed the presence of distinct copy number aberrant cell populations. The 5q21.1 was either gained, normal or lost in this mixed cell population. In the prostatectomy sample,

these three copy states were roughly equally common. With treatment and over time (853 days from the prostatectomy sample and metastatic sample), the proportion of cells with 5q copy gain increased in the tissue. After another 105 days, this changed again in the apheresis sample. Images from the FISH analysis are shown in ***Figure 7-15***, with the treatment-naïve prostatectomy sample on the left and the metastatic bone biopsy (castration-resistant) shown on the right. Probes for 5p11 are in red and 5q21.1 in green.

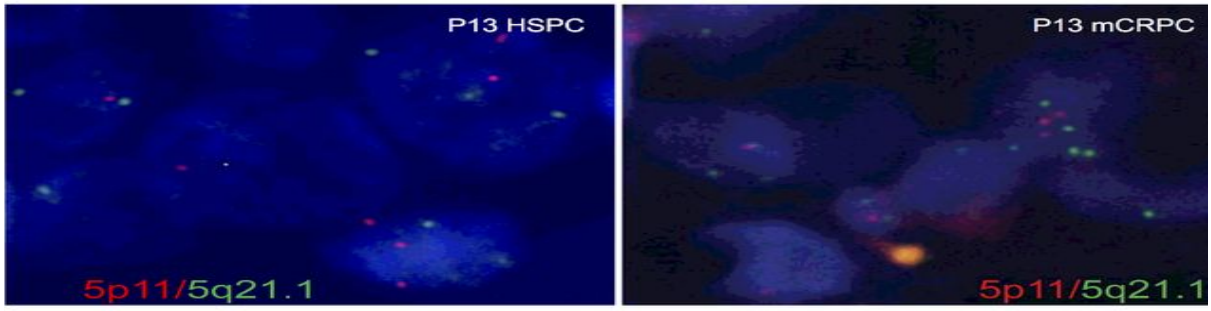

Figure 7-15: FISH analysis of two biopsies from P13

On the left is the HSPC (treatment-naïve) sample and on the right the metastatic (CRPC) biopsy. Probes for 5p11 are red and 5q21.1 green. FISH = fluorescent in-situ hybridisation; HSPC = hormone sensitive prostate cancer; mCRPC = metastatic castration resistant prostate cancer; P13 = Patient 13.

The proportion of the three copy states at these different time points is shown by a schematic in ***Figure 7-16***.

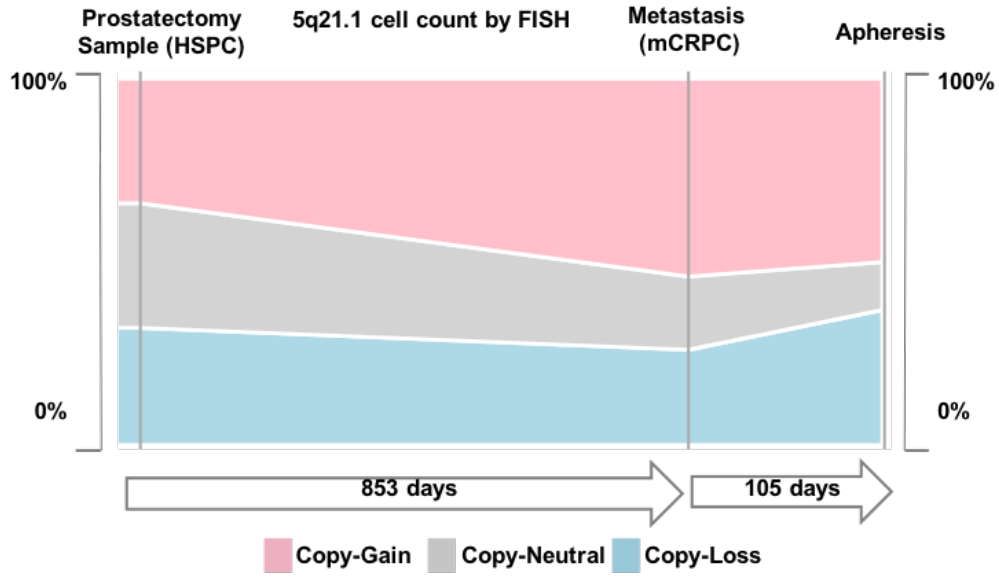

Figure 7-16: The percentage of cells with copy-number alterations on 5q21.1 with disease progression

This is shown from the time of the prostatectomy, through to the metastatic biopsy and then on until apheresis in patient P13. FISH = Fluorescent in-situ hybridisation; HSPC = hormone-sensitive prostate cancer; mCRPC = metastatic castration-resistant prostate cancer.

For patient P03, tissue from a prior transurethral resection of the prostate (TURP) was available, and was micro-dissected by our pathologist (Dr Daniel Nava Rodrigues). There was also tissue available from a previous metastatic lymph node biopsy. I then performed aCGH of DNA extracted from these micro-dissected regions and from the lymph node biopsy, as shown in ***Figure 7-17***. Four distinct morphological regions (labelled A – D in ***Figure 7-17A***) are depicted in more detail to the right of the panel in ***Figure 7-17B***. As reviewed by a pathologist, Area A and Area C showed glandular differentiation with small monomorphic hyperchromatic nuclei and inconspicuous nucleoli. This is markedly different to Areas B and D which show a more solid arrangement with pleomorphic nuclei and have large, discernible nucleoli. Regions A and C had gains of 17q and 12q and losses of 3p, whereas regions B and D had losses of chromosome 18 and 2p. All areas and the lymph node biopsy had a homozygous deletion of the *BRCA2* genomic locus. The metastatic lymph node biopsy which was taken at a later date had multiple new aberrations, including a new AR amplification.

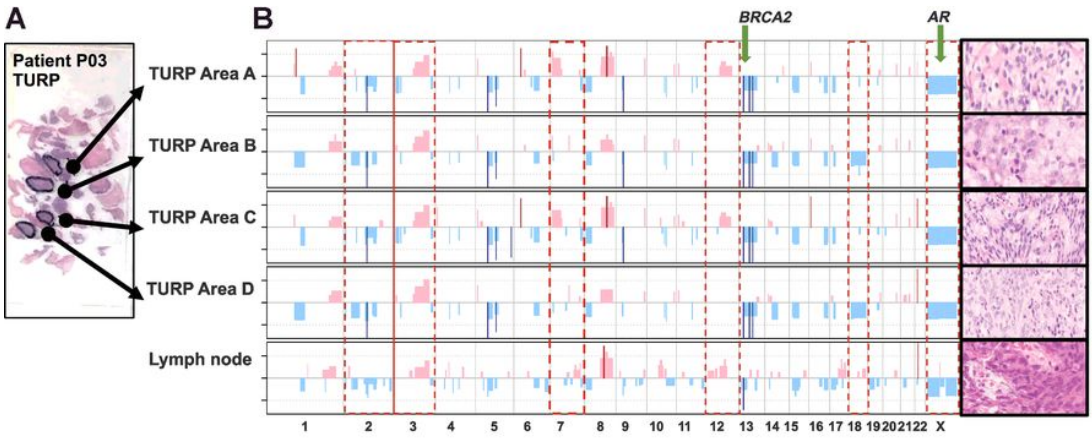

Figure 7-17: P03 TURP microdissected regions

A) Tissue from a TURP from Patient P03 where 4 distinct areas were marked and then micro-dissected. These tumour morphologies of these areas are shown on the right of the panel, where Area A and Area C show glandular differentiation with small monomorphic hyperchromatic nuclei and inconspicuous nucleoli. Area B and Area D exhibit a more solid arrangement with pleomorphic nuclei and an open chromatin pattern with large, discernible nucleoli easily seen. In B), aCGH profiles of these regions and the lymph node biopsy are shown, with areas of intrapatient heterogeneity between the areas are highlighted by a dotted red line. AR = androgen receptor; TURP = transurethral resection of the prostate.

Whole exome sequencing of these micro-dissected TURP regions identified truncal mutations of *SPOP* (p.Trp131Cys) and *FOXA1* (pHis168del), with regions A and C having similar mutation profiles to each other as did regions B and D. Whole exome sequencing of the later lymph node biopsy identified a mixture of these cell populations. There were some unifying features between the samples sequenced, for example they all had an *SPOP* mutation, but there was intra-patient heterogeneity as identified by morphology (see ***Figure 7-17)*** and copy-number analysis ***(Figure 7-18).***

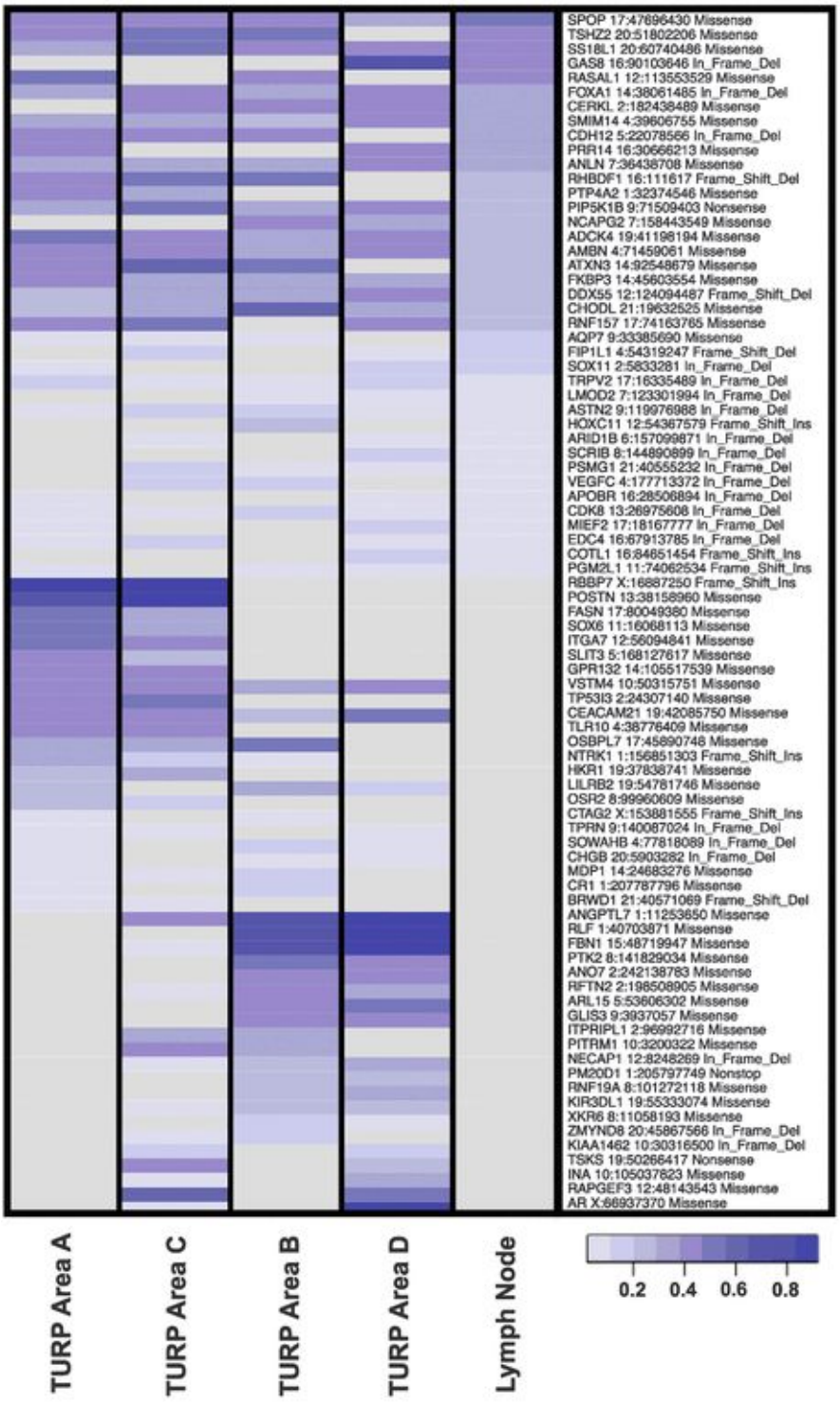

Figure 7-18: Mutations detected from exome sequencing from the 4 micro-dissected areas of a TURP and from a later metastatic lymph node biopsy from P03.

P03 = Patient 03; TURP = trans-urethral resection of the prostate.

The apheresis in Patient 03 was carried out later in the patient's disease course than the TURP and the lymph node biopsy, and analysis of single CTCs from this further delineated this cancer's evolution. This is shown in unsupervised hierarchical clustering

of 13 CTCs from the apheresis, the TURP (as a gross biopsy and also of the 4 micro-dissected areas) and of the lymph node biopsy in ***Figure 7-19.*** This heat map of 12 selected prostate cancer genes shows copy number aberration heterogeneity using hierarchical clustering of copy number data based on Euclidean distance. Here we see key genomic differences in pathways commonly altered in CRPC, with heterogeneity seen in *PTEN* and *BRCA2* loss in different sub-clones.

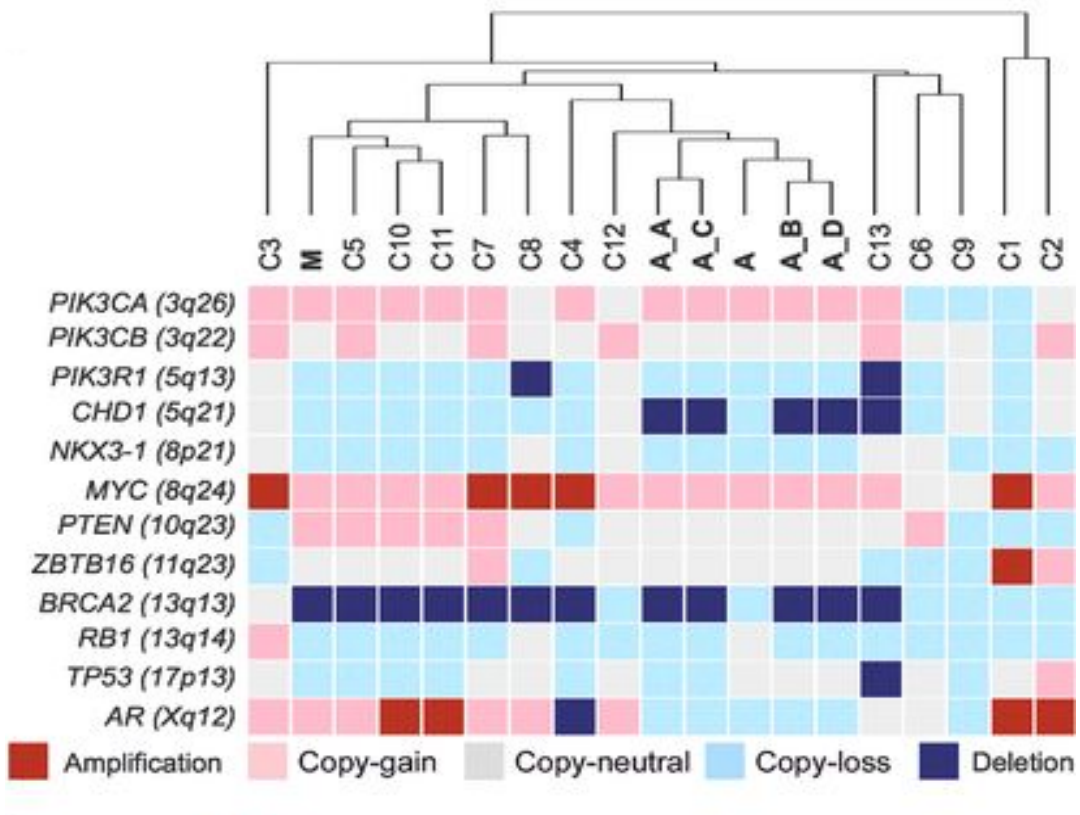

Figure 7-19: Heat map of 12 selected prostate cancer genes depicting copy number heterogeneity with a dendrogram using hierarchical clustering of copy number data, based on Euclidean distance for CTCs and tumour tissue.

A = archival TURP material with A-A, A-B, A-C and A-D representing TURP tissue from regions A, B, C and D respectively; C# = CTC with # depicting the number; CTC = circulating tumour cell; M = metastatic lymph node biopsy; TURP = transurethral resection of the prostate.

This heterogeneity is seen in more detail in ***Figure 7-20***, which is a detailed chromosome plot of chromosome 13 again from Patient 03. Here, heterogeneity of *BRCA2* loss is seen within different tissue samples and some CTCs acquired by apheresis in this patient. FISH performed on the TURP tumour tissue with a green *BRCA2* probe and a red *MYC* probe is shown in ***Figure 7-21***, where I observed *BRCA2* was homozygously deleted in most but not all cells.

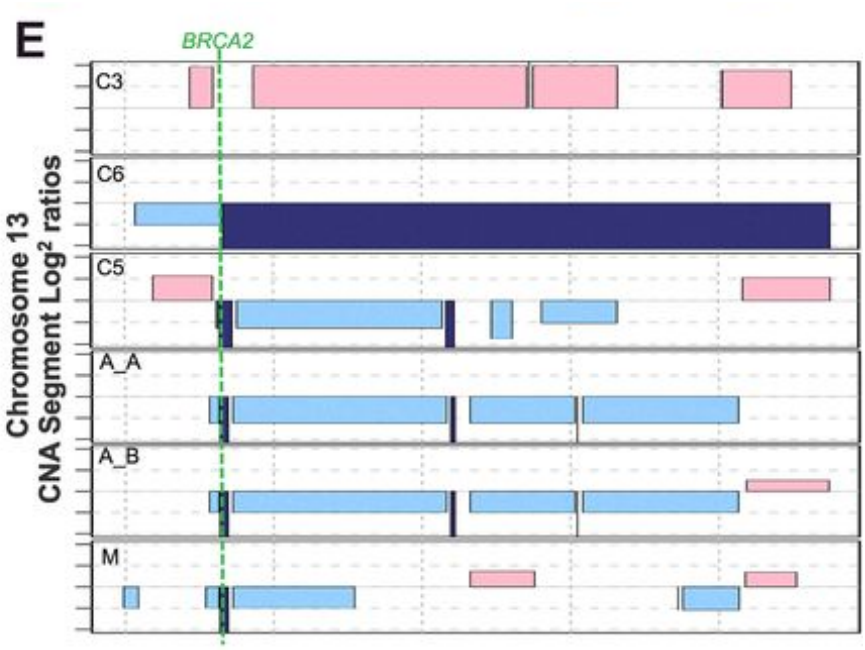

Figure 7-20: Chromosome plot of Chromosome 13 from P03 depicting heterogeneity of the BRCA2 locus.

A = archival TURP material with A-A and A-B representing TURP tissue from regions A and B respectively; C# = CTC with # depicting the number; CTC = circulating tumour cell; M = metastatic lymph node biopsy; TURP = transurethral resection of the prostate.

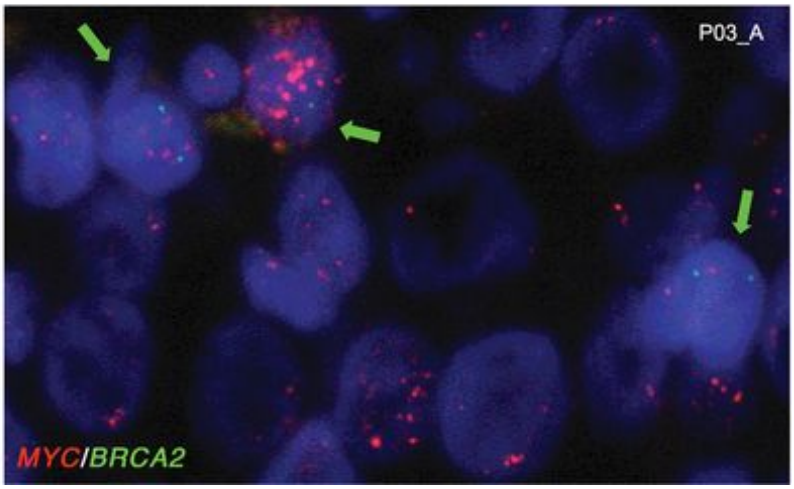

Figure 7-21:FISH performed on TURP tissue from P03

BRCA2 is shown in green and MYC in red, with the green arrows depicting tumour cells which have BRCA2 heterozygous loss or no copy loss, whilst all other cells showed BRCA homozygous loss. A = archival TURP material; P03 = Patient 03; TURP = transurethral resection of the prostate.

7.4.7 Organoid cultures

Organoid cultures were generated successfully from 1 patient (Patient 05; P05); micrographs of these are shown in ***Figure 7-22***. Array CGH was performed on these organoids, and as shown earlier in ***Figure 7-13*** the copy number profiles of these organoids cluster with the same patient CTCs.

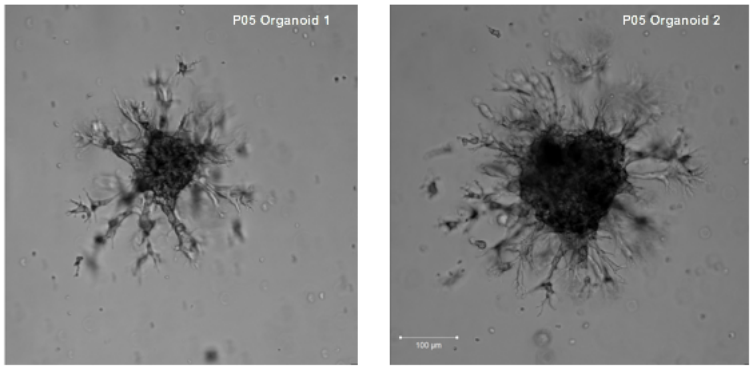

Figure 7-22: Micrographs of 2 organoids cultured from the apheresis product of Patient 05 (P05).

The copy number profiles of the organoids and the CTCs is shown in ***Figure 23***, using hierarchical clustering again based on Euclidean distance, with CTCs shown in green and the two organoids shown in red. Both organoids cluster with sub-clones detectable from the CTC analyses, which is indicative of CTC-derived organoid culture being able to recapitulate this diversity.

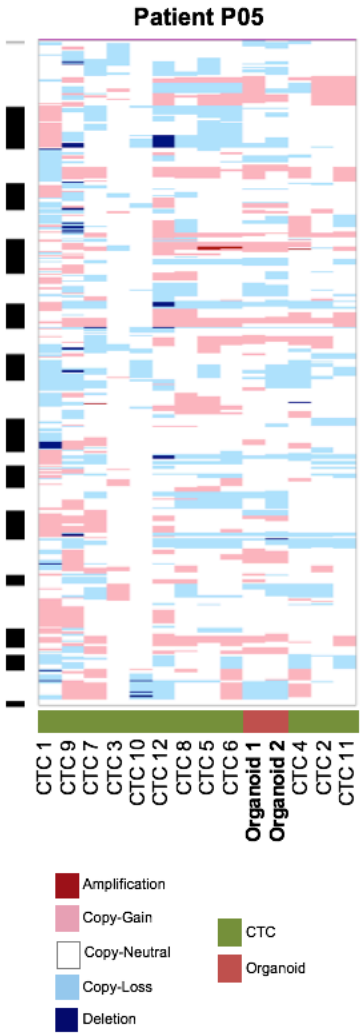

Figure 7-23: Copy number profiles of CTCs and the two organoids for Patient P05.

CTC = circulating tumour cell.

7.5 Discussion

Performing a less invasive liquid biopsy by apheresis was well-tolerated in all patients, and no adverse events were seen. Whilst other studies have reported side effects of apheresis to include vasovagal reactions and citrate toxicity (252) the safety profile in this study was reassuring. No significant difference was seen in full blood count numbers (haemoglobin, lymphocytes, platelets) before and after apheresis, again supporting the role of performing apheresis safely in patients.

The overall CTC yield of the apheresis product was considerably increased (average 100-fold) compared to the peripheral blood, and this was the case for all patients. Interestingly, peripheral blood CTC counts did not change before and after the apheresis procedure, and this remained true even when more than 54,000 CTCs were removed

from the peripheral circulation by apheresis. Whilst the consistency between pre- and post-apheresis CTC counts could suggest their inefficient capture, it could also be indicative of constant replenishment of CTCs into the circulation. It has been suggested that CTCs have significantly short half-lives, and replicating populations of tumour cells at secondary sites may keep CTC numbers relatively stable (253).

By increasing the yield of CTCs, apheresis facilitated the interrogation of tumour genomics and allowed dissection of both inter- and intra-patient heterogeneity. Clonal evolution of tumours could be explored by studying both biopsies and CTCs acquired through apheresis. These methods of capturing CTCs were validated as their genomic landscape closely mirrored that of mCRPC biopsy exomes collected by the SU2C/Prostate Cancer Foundation Dream Team collaboration (81). Moreover, copy number traces of individual CTCs closely resembled those of the same patient biopsies, with changes seen over time in the CTCs likely due to treatment pressures, such as gains in *AR* and *MYC*. Some copy number changes, missed in the bulk biopsy analyses were successfully detected by analyses of single CTCs.

Although the yield of evaluable cells was increased significantly by apheresis, it is worth noting that during the experimental procedures there was evidence of CTC numbers decreasing at each step. In order to be certain of isolating single CTCs and single WBCs, FACS settings were stringent and resulted in a 60-80% retention rate from the CellSearch cartridges. A further 20% or so were lost due to the CTC DNA failing quality control after undergoing whole genome amplification. These rates of cell loss during the experiments are irrelevant of original input source, i.e. a high percentage would be lost from processing both peripheral blood and the apheresis product. The concentrated apheresis product has the advantage of a much higher starting number of CTCs, enabling sufficient numbers in the end-product for genomic analyses, making it a much more efficient source.

Unsupervised clustering allowed observation of varying degrees of intra-patient heterogeneity; the CTCs of some patients were highly homogeneous with almost all traces looking identical, although the majority of patients did display genomic diversity between their CTCs. The genomics of these patients' CTCs often resembled the profiles of matched tissue samples, clustering with either their diagnostic biopsy or with a metastatic sample. Microdissection of a biopsy sample showed distinct morphological areas, with different CTCs clustering towards the separate areas.

All of these findings support the use of CTCs for ongoing dynamic analyses of the disease course, allowing study of clonal evolution and therapeutic selection pressures by performing serial apheresis on the same patient before, during and after treatment. Tissue biopsies are often poorly tolerated, have associated adverse events and cannot easily be performed serially. Other options, such as the isolation of cell-free DNA from the plasma is also being explored, but also has limitations, such as the inability to dissect intra-patient heterogeneity. Using CTCs from apheresis was not only well-tolerated but also highly informative, and I have now amended the apheresis protocol to perform serial apheresis on patients undergoing therapy for CRPC within our unit, the analysis of which is eagerly awaited. Ideally, apheresis will be embedded into clinical drug trials to facilitate analysis of tumour evolution during therapies whilst also monitoring response to therapy by generating estimates of CTC counts (254). This may aid key treatment decisions such as optimal identification of treatment failure, making timely therapeutic switch decisions, and reversing treatment failure by guiding the administration of drug combinations.

The implications of varying levels of heterogeneity remain to be seen and require further exploration. Different subtypes of CRPC may associate with different levels of heterogeneity. Further work is needed to identify the optimal number of single CTCs to be analysed to sufficiently explore disease heterogeneity whilst keeping the cost of doing so down. This would likely require the study of multiple CTCs from several patients in order for statistical modelling to have adequate power. The increasing ease and decreasing costs of performing low coverage whole genome sequencing may allow barcoding of DNA from each CTC to explore this in a less expensive and more efficient manner. Exploration of single-cell RNA sequencing may also permit better understanding of resistance mechanisms.

With regards to organoid cultures, whilst these initial results are promising, further optimisation of these methods to increase success rates is much needed, as effectively modelling CRPC *ex-vivo* could support drug testing and further enhance our understanding of this disease. Other limitations of this work include the varied patient cohort and small sample size. As all the patients were treated at one tertiary cancer centre, and moreover as this was not in the context of a broader drug trial, prior therapies and baseline characteristics of these patients vary significantly. This has obvious implications in drawing broader clinical conclusions, but the research here remains an important proof-of concept study.

Moving forward, in order for apheresis to have widespread utility, the procedure needs to be easily accessible and high throughput CTC isolation proved for other tumour types as well as for patients with lower burdens of disease (250). To this end, we have now amended our protocol to not only allow serial apheresis but for the inclusion criteria to now include patients who have lower peripheral blood CTC count burdens (≥5). Our centre and others are also pursuing apheresis in other tumour types. Directly comparing CTCs acquired through apheresis with peripheral blood CTCs and cell-free DNA is also warranted, as well as with single cells dissociated from tissue samples. Where possible, contemporaneous biopsies should be taken, as not only do they currently remain the gold standard but more direct comparisons between the procedures can be made.

Despite these limitations, and the future work needed, the use of apheresis has huge potential in increasing CTC yield to allow successful dissection of intrapatient tumour genomic heterogeneity which can be missed by bulk biopsy analysis and by study of cell-free DNA. It can provide previously undescribed detail on different CRPC sub-clones and may have important implications for safer, better patient care.

8. Concluding Discussion

8.1 Work thus far

Despite many recent advances in the therapy of metastatic castration-resistant prostate cancer (mCRPC), this highly prevalent but clinically heterogenous disease remains incurable. Despite the development and approval of taxane chemotherapies, novel hormonal therapies and Radium 223 having led to clinical improvements, there is still significant associated morbidity and mortality worldwide. Response to therapies remain varied, and resistance inevitable.

Selecting patients by biomarker status may significantly increase treatment efficacy and prevent unnecessary toxicity. Newer drugs, such as the PARP-inhibitor Olaparib have shown antitumour activity in patients with germline or somatic defects in multiple DNA repair genes including *BRCA2*, *BRCA1*, *PALB2* and *ATM* (95). Immunotherapy, which has shown remarkable benefits in other cancers, has thus far been disappointing in prostate cancer. This lack of success being attributed to the lower mutation burden and fewer neoantigens seen in advanced prostate cancer, as well as a potentially suppressive tumour microenvironment with a low level of baseline T cell infiltration and of PDL1 expression (255).

Identifying patients who are most likely to derive benefit from particular treatments remains a key clinical priority. Developing robust personalised medicine strategies is of particularly high importance in a disease as heterogeneous as advanced prostate cancer. In order to fully understand this heterogeneity, and to study clonal evolution and treatment selection pressures, serial biopsies are needed and ideally from multiple sites of disease. Whilst this may in theory be possible, there are many associated challenges to doing this, not least the risk of morbidity and complications. Performing liquid biopsies, in particular interrogating cell-free DNA (cfDNA) and circulating tumour cells (CTCs) allows for simpler, safer and repeated tumour interrogation, having the potential to transform patient care.

In this thesis, I have investigated the current state of play in the field of circulating biomarkers in advanced prostate cancer, focusing on these two key aspects; cfDNA and CTCs. My main findings from this work are:

- Identification of biomarkers that are ultimately intended to guide patient care is a serious endeavour that needs to follow strict experimental rules and is best attempted by highly qualified teams of investigators.
- Biomarker development is as complex as the drug development process, and, as highlighted by the consensus meeting, much work is still needed in the field.
- Amongst experts in the prostate cancer and biomarker field, there still remains considerable divergence of opinions regarding the current utility of circulating biomarkers, although agreement was reached on the importance of these unmet clinical needs.
- As prostate cancer has some of the highest cfDNA and CTC levels of all solid tumours, serial tumour genomic analyses has the potential to transform clinical care.
- The outcomes of the expert consensus, by identifying key areas for prioritisation, can help guide the development of circulating biomarkers for PC care.
- Analysis of cfDNA concentrations from 751 patients treated with taxane chemotherapy on two large Phase III trials, showed that baseline cfDNA concentrations correlate with both radiographic progression free survival (rPFS) and overall survival (OS).
- When split by quartiles of cfDNA concentrations, those with low concentrations both live longer and have longer before there is radiographic evidence of disease progression.
- This utility of cfDNA as a prognostic marker was maintained in multivariable analyses with models including other known prognostic variables.
- Baseline cfDNA concentrations did not show a significant relationship with a biochemical, radiological or clinical response to taxanes, confirming that cfDNA has use as an independent prognostic marker, but not as a predictive biomarker in this setting.
- Changes in cfDNA concentrations following taxane therapy poorly correlated with response and clinical benefit, suggesting that much of the cfDNA is not derived from tumour cells.
- Low pass whole genome sequencing (lp-WGS) of cfDNA has clinical utility in the management of lethal prostate cancer, with changes in cfDNA tumour purity associating with response to taxane therapy, suggesting that it may be acting as a response biomarker evaluating changes in overall tumour burden.
- lp-WGS derived tumour purity measured solely at baseline does not associate with response to treatment, despite a strong association with OS.

- However, the changes in lp-WGS derived tumour purity over time do associate with response, and may represent a non-invasive and reliable way of monitoring disease burden and response to treatment.
- These findings need further validation, but corroboration of these results may provide physicians with a reliable guide to early treatment switch decisions. This may prove transformative as current markers, including biochemical markers (PSA) and radiographic markers have recognised limitations, particularly in patients with bone only disease.
- Apheresis was a well-tolerated and safe procedure; no adverse events were reported in our study, nor any significant differences in full blood count numbers (haemoglobin, lymphocytes, platelets) before or after apheresis.
- In all patients, performing apheresis allowed a significant enrichment of CTCs (average 100-fold compared to the peripheral blood yield).
- Peripheral blood CTC counts were not affected by apheresis, even when >50,000 CTCs were removed from the circulation, which could be indicative of inefficient capture and/or constant replenishment of CTCs into the circulation.
- In successfully increasing the yield of CTCs, apheresis facilitated the interrogation of tumour genomics and allowed dissection of both inter- and intra-patient heterogeneity.
- Clonal evolution of tumours could be explored by studying both biopsies and CTCs acquired through apheresis.
- Validation of these methods of capturing CTCs was performed by comparing the CTC genomic landscape to that that of mCRPC biopsy exomes collected by the SU2C/Prostate Cancer Foundation Dream Team collaboration (81), and confirming they were closely correlated.
- Furthermore, copy number traces of individual CTCs closely resembled those of same patient biopsies, with changes seen over time in the CTCs likely due to treatment pressures, such as gains in AR and MYC. Some copy number changes, missed in the bulk biopsy analyses were successfully detected by analyses of single CTCs.

Taken together, this work has highlighted the possible utility of less invasive liquid biopsies, with both cfDNA and CTCs (acquired by apheresis) showing promise. Single cell analysis in particular has the ability to dissect intrapatient heterogeneity which can be missed in cfDNA and biopsy analysis. Currently, interrogating tumour genomics by tissue biopsy remains the gold standard in the management of advanced prostate cancer

(PC), but liquid biopsies have huge potential as multi-purpose biomarkers and to easily, serially and safely evaluate changes imposed by therapeutic selective pressures.

8.2 Future perspectives:

Moving forward, my recent amendments of our apheresis protocol now mean that serial procedures can be performed on patients undergoing therapy (for example during screening, on treatment and at time of disease progression.) This will allow us to interrogate disease evolution and treatment pressures on circulating tumour cell populations. Where possible, contemporaneous tissue biopsies will also be taken, and plasma samples for cfDNA at each time point. Direct comparisons need to be made of single cells dissociated from tissue as well as of cfDNA genomics.

These comparisons are necessary to prove apheresis as a comprehensive way of studying disease in the absence of other biomarkers. The optimal number of individual CTCS to be studied from one patient needs to be identified; enough CTCs are needed to sufficiently interrogate heterogeneity (probably 50-100 cells) whilst minimising effort and costs. The isolation of immune cells from plasma collected through apheresis will also be of huge importance in studying the immune biology driving CRPC. Having this biobank of tissue, CTCs, cfDNA and other cells available will allow not only a complete interrogation into each individual's disease but also a direct comparison of different blood and tissue-based biomarkers in order to determine superiority and utility in clinical practice.

There are many benefits to performing low pass whole genome sequencing, not least the high throughput and comprehensive data output. However, the lower coverage does mean a decreased confidence in copy number calls and lack of mutation data. Ongoing genomic analyses from the low-pass whole genome sequencing performed could be pivotal in identifying potential taxane biomarkers, but further functional wet lab orthogonal validation studying taxane naïve and resistant cell lines will be crucial before any considerable claims can be made. Mechanisms of treatment resistance will need to be studied further and the use of transcriptomics and metabolomics to perform dynamic studies may identify new treatment options.

Biomarker-driven clinical trials, to validate the clinical utility of tumour purity and the study of the genomic changes identified, are also still much needed. While the health economic

potential of liquid biopsies is CRPC is clear, future work should focus on the design and analysis of prospective clinical trials including health economic data collection (direct and indirect medical cost such as cost of adverse events). While current health economic analyses focus on single biomarker assays or cell enumeration, the potential of these more advanced biomarkers remain to be explored.

It is also worth mentioning that the scope of this thesis has been the setting of advanced prostate cancer, in metastatic, castration-resistant disease. However, studies are now needed to elucidate how cell-free DNA and CTCs can be used in the earlier stage, diagnostic, and hormone-sensitive settings. For example, their detection has potential as a non-invasive diagnostic tool, at initial diagnosis, for active surveillance, and in the setting of detecting minimal residual disease post attempted curative therapy (256).

8.3 Clinical relevance

Currently, many mCRPC patients are treated with taxanes despite many men going on to have little or no clinical response. The treatment itself can be both mentally and physically demanding, and correctly identifying patients with significant chance of response could decrease overtreatment and the morbidity and mortality associated with this. Furthermore, it could allow us to stratify treatment appropriately, giving taxanes to those who would derive significant clinical benefit whilst leading with alternative drugs such as abiraterone in others. Improving our understanding of resistance mechanisms to taxane chemotherapy will also be of clinical relevance in combating resistance. Finally, as treatment with taxane chemotherapy is not limited to prostate cancer, these findings could have important implications in other cancer types including breast, ovarian and oesophageal cancer. Therefore, these results could have a significant impact on healthcare economics, but also, more importantly, on patient care.

9. Glossary

aCGH: array comparative genomic hybridisation

ADT: androgen deprivation therapy

AFFIRM: A Multinational Phase 3, Randomized, Double-blind, Placebo-controlled Efficacy And Safety Study Of Oral Mdv3100 In Patients With Progressive Castration-resistant Prostate Cancer Previously Treated With Docetaxel Based Chemotherapy

aHR: adjusted hazard ratio

Alb: albumin

ALP: alkaline phosphatase

ALSYMPCA: ALpharadin in SYMPtomatic Prostate CAncer

AR: androgen receptor

ARAMIS: Efficacy and Safety Study of Darolutamide (ODM-201) in Men With High-risk Nonmetastatic Castration-resistant Prostate Cancer

ARV7: androgen receptor splice variant 7

AUC: area under the curve

C: cycle

C1: cycle 1

C2: cycle 2

C4 cycle 4

cfDNA: cell free DNA

chr: chromosome

CI: confidence interval

CNA: copy number aberration

CRPC: castration resistant prostate cancer

CTC: circulating tumour cell

ctDNA: circulating tumour DNA

DHT: dihydrotestosterone

DHEA: dehydroepiandrosterone

DNA: deoxyribonucleic acid

ECOG PS: eastern cooperative oncology group performance status

ENZAMET: Enzalutamide in First Line Androgen Deprivation Therapy for Metastatic Prostate Cancer

EOS: end of study

EOT: end of treatment

FACS: fluorescence activated cell sorting

FDA: food and drug administration

FFPE: formalin fixed paraffin embedded

FIRSTANA: Cabazitaxel Versus Docetaxel Both With Prednisone in Patients With Metastatic Castration Resistant Prostate Cancer (FIRSTANA)

FISH: fluorescent *in-situ* hybridization

GATK: genome analysis toolkit

Hb: haemoglobin

HR: hazard ratio

HSPC: hormone sensitive prostate cancer

IL23: interleukin 23

IQR: interquartile range

LBD: ligand binding domain

LDH: lactate dehydrogenase

lncRNA: long non-coding RNA

lpWGS: low pass whole genome sequencing

mCRPC: metastatic castration resistant prostate cancer

MDSC: myeloid derived suppressor cells

Mets: metastases

mHSPC: metastatic hormone sensitive prostate cancer

MiR: microRNA

MMR: mismatch repair defect

MNC: mononuclear cell

Mo: months

MSI: microsatellite instability

NGS: next generation sequencing

NICE: National Institute of Clinical Excellence

NLR: neutrophil lymphocyte ratio

OR: odds ratio

OS: overall survival

PAP: prostatic acid phosphatase

PARP: Poly (ADP-ribose) polymerase

PC: Prostate Cancer

PCR: polymerase chain reaction

PCUK: Prostate Cancer UK

PCWG: Prostate Cancer Working Group

PET: positron emission tomography

PREVAIL: A Safety and Efficacy Study of Oral MDV3100 in Chemotherapy-Naive Patients With Progressive Metastatic Prostate Cancer

PROSELICA: Cabazitaxel at 20 mg/m² Compared to 25 mg/m² With Prednisone for the Treatment of Metastatic Castration Resistant Prostate Cancer

PSA: prostate specific antigen

RECIST: Response evaluation criteria in solid tumours

Q: quartile

QoL: quality of life

RECIST:

RNA: ribonucleic acid

ROC: receiver operating characteristic

rPFS: radiographic progression free survival

SCR: screening

SOP: standard operating procedure

SPARTAN: Study of Apalutamide (ARN-509) in Men With Non-Metastatic Castration-Resistant Prostate Cancer

STAMPEDE: Systemic Therapy in Advancing or Metastatic Prostate Cancer: Evaluation of Drug Efficacy

SU2C: stand up to cancer

TAX327: Docetaxel plus Prednisone or Mitoxantrone plus Prednisone for Advanced Prostate Cancer

TCGA: The cancer genome atlas

TEP: tumour educated platelet

TITAN: A Study of Apalutamide (JNJ-56021927, ARN-509) Plus Androgen Deprivation Therapy (ADT) Versus ADT in Participants With mHSPC

TROPIC: Prednisone plus cabazitaxel or mitoxantrone for metastatic castration-resistant prostate cancer progressing after docetaxel treatment

TURP: transurethral resection of the prostate

U: unit

WBC: white blood cell

WES: whole exome sequencing

WGS: whole genome sequencing

Yr: years

10. References:

1. Siegel RL, Miller KD, Jemal A. Cancer statistics, 2018. CA Cancer J Clin. 2018 Jan 1;68(1):7–30.
2. Jemal A, Bray F, Center MM, Ferlay J, Ward E, Forman D. Global cancer statistics. CA Cancer J Clin. 2011 Mar;61(2):69–90.
3. Attard G, Parker C, Eeles RA, Schröder F, Tomlins SA, Tannock I, et al. Prostate cancer. Lancet. 2016 Jan 2;387(10013):70–82.
4. Mottet N, Bellmunt J, Bolla M, Briers E, Cumberbatch MG, De Santis M, et al. EAU-ESTRO-SIOG Guidelines on Prostate Cancer. Part 1: Screening, Diagnosis, and Local Treatment with Curative Intent. Eur Urol. 2017 Apr 1;71(4):618–29.
5. Saad F, Fizazi K. Androgen Deprivation Therapy and Secondary Hormone Therapy in the Management of Hormone-sensitive and Castration-resistant Prostate Cancer. Urology. 2015 Nov;86(5):852–61.
6. American Association for Cancer Research. C, International Cancer Research Foundation. C V., William H. Donner Foundation. Cancer research : the official organ of the American Association for Cancer Research, Inc. Vol. 1, Cancer Research. Waverly Press; 1941. 293–297 p.
7. Harris WP, Mostaghel EA, Nelson PS, Montgomery B. Androgen deprivation therapy: progress in understanding mechanisms of resistance and optimizing androgen depletion. Nat Clin Pract Urol. 2009 Feb;6(2):76–85.
8. Modi PK, Faiena I, Kim IY. Androgen Receptor. Prostate Cancer. 2016 Jan 1;21–8.
9. Ferraldeschi R, Welti J, Luo J, Attard G, de Bono JS. Targeting the androgen receptor pathway in castration-resistant prostate cancer: progresses and prospects. Oncogene. 2015 Apr 2;34(14):1745–57.
10. Lam JS, Leppert JT, Vemulapalli SN, Shvarts O, Belldegrun AS. Secondary hormonal therapy for advanced prostate cancer. J Urol. 2006 Jan;175(1):27–34.
11. Sumanasuriya S, De Bono J. Treatment of Advanced Prostate Cancer—A Review of Current Therapies and Future Promise. Cold Spring Harb Perspect Med. 2017;a030635.
12. Lorente D, Mateo J, Perez-Lopez R, de Bono JS, Attard G. Sequencing of agents in castration-resistant prostate cancer. Lancet Oncol. 2015 Jun 1;16(6):e279-92.
13. Sartor O, de Bono JS. Metastatic Prostate Cancer. Longo DL, editor. N Engl J Med. 2018 Feb 15;378(7):645–57.

14. Sternberg CN, Petrylak DP, Sartor O, Witjes JA, Demkow T, Ferrero J-M, et al. Multinational, double-blind, phase III study of prednisone and either satraplatin or placebo in patients with castrate-refractory prostate cancer progressing after prior chemotherapy: the SPARC trial. J Clin Oncol. 2009 Nov 10;27(32):5431–8.
15. Oudard S, Fizazi K, Sengeløv L, Daugaard G, Saad F, Hansen S, et al. Cabazitaxel Versus Docetaxel As First-Line Therapy for Patients With Metastatic Castration-Resistant Prostate Cancer: A Randomized Phase III Trial-FIRSTANA. J Clin Oncol. 2017 Jul 28;JCO2016721068.
16. Scher HI, Morris MJ, Stadler W, Higano C, Basch E, Fizazi K, et al. Trial Design and Objectives for Castration-Resistant Prostate Cancer : Updated Recommendations from the Prostate Cancer Clinical Trials Working Group (PCWG3). 2015;1–38.
17. Sweeney CJ, Chen Y-H, Carducci M, Liu G, Jarrard DF, Eisenberger M, et al. Chemohormonal Therapy in Metastatic Hormone-Sensitive Prostate Cancer. N Engl J Med. 2015 Aug 20;373(8):737–46.
18. James ND, de Bono JS, Spears MR, Clarke NW, Mason MD, Dearnaley DP, et al. Abiraterone for Prostate Cancer Not Previously Treated with Hormone Therapy. N Engl J Med. 2017 Jul 27;377(4):338–51.
19. Davis ID, Martin AJ, Stockler MR, Begbie S, Chi KN, Chowdhury S, et al. Enzalutamide with Standard First-Line Therapy in Metastatic Prostate Cancer. N Engl J Med. 2019 Jun 2;NEJMoa1903835.
20. Tannock IF, de Wit R, Berry WR, Horti J, Pluzanska A, Chi KN, et al. Docetaxel plus prednisone or mitoxantrone plus prednisone for advanced prostate cancer. N Engl J Med. 2004 Oct 7;351(15):1502–12.
21. Berthold DR, Pond GR, Soban F, de Wit R, Eisenberger M, Tannock IF. Docetaxel plus prednisone or mitoxantrone plus prednisone for advanced prostate cancer: updated survival in the TAX 327 study. J Clin Oncol. 2008 Jan 10;26(2):242–5.
22. Narayanan S, Srinivas S, Feldman D. Androgen–glucocorticoid interactions in the era of novel prostate cancer therapy. Nat Rev Urol. 2016 Jan 8;13(1):47–60.
23. Seruga B, Tannock IF. Chemotherapy-based treatment for castration-resistant prostate cancer. J Clin Oncol. 2011 Sep 20;29(27):3686–94.
24. Omlin A, Sartor O, Rothermundt C, Cathomas R, De Bono JS, Shen L, et al. Analysis of Side Effect Profile of Alopecia, Nail Changes, Peripheral Neuropathy, and Dysgeusia in Prostate Cancer Patients Treated With Docetaxel and Cabazitaxel. Clin Genitourin Cancer. 2015 Aug 1;13(4):e205–8.
25. Thomas C, Brandt MP, Baldauf S, Tsaur I, Frees S, Borgmann H, et al. Docetaxel-rechallenge in castration-resistant prostate cancer: defining clinical factors for

successful treatment response and improvement in overall survival. Int Urol Nephrol. 2018 Oct 17;50(10):1821–7.

26. Lavaud P, Gravis G, Foulon S, Joly F, Oudard S, Priou F, et al. Anticancer Activity and Tolerance of Treatments Received Beyond Progression in Men Treated Upfront with Androgen Deprivation Therapy With or Without Docetaxel for Metastatic Castration-naïve Prostate Cancer in the GETUG-AFU 15 Phase 3 Trial. Eur Urol. 2018 May 1;73(5):696–703.
27. Oudard S, Kramer G, Caffo O, Creppy L, Loriot Y, Hansen S, et al. Docetaxel rechallenge after an initial good response in patients with metastatic castration-resistant prostate cancer. BJU Int. 2015 May 1;115(5):744–52.
28. Azarenko O, Smiyun G, Mah J, Wilson L, Jordan MA. Antiproliferative mechanism of action of the novel taxane cabazitaxel as compared with the parent compound docetaxel in MCF7 breast cancer cells. Mol Cancer Ther. 2014 Aug 1;13(8):2092–103.
29. Darshan MS, Loftus MS, Thadani-Mulero M, Levy BP, Escuin D, Zhou XK, et al. Taxane-induced blockade to nuclear accumulation of the androgen receptor predicts clinical responses in metastatic prostate cancer. Cancer Res. 2011 Sep 15;71(18):6019–29.
30. Zhu M-L, Kyprianou N. Role of androgens and the androgen receptor in epithelial-mesenchymal transition and invasion of prostate cancer cells. FASEB J. 2010 Mar 1;24(3):769–77.
31. van Soest RJ, de Morrée ES, Shen L, Tannock IF, Eisenberger MA, de Wit R. Initial biopsy Gleason score as a predictive marker for survival benefit in patients with castration-resistant prostate cancer treated with docetaxel: data from the TAX327 study. Eur Urol. 2014 Aug 1;66(2):330–6.
32. Gan L, Chen S, Wang Y, Watahiki A, Bohrer L, Sun Z, et al. Inhibition of the androgen receptor as a novel mechanism of taxol chemotherapy in prostate cancer. Cancer Res. 2009 Nov 1;69(21):8386–94.
33. Vrignaud P, Sémiond D, Lejeune P, Bouchard H, Calvet L, Combeau C, et al. Preclinical antitumor activity of cabazitaxel, a semisynthetic taxane active in taxane-resistant tumors. Clin Cancer Res. 2013 Jun 1;19(11):2973–83.
34. Pivot X, Koralewski P, Hidalgo JL, Chan A, Gonçalves A, Schwartsmann G, et al. A multicenter phase II study of XRP6258 administered as a 1-h i.v. infusion every 3 weeks in taxane-resistant metastatic breast cancer patients. Ann Oncol. 2008 Sep 1;19(9):1547–52.
35. de Bono JS, Oudard S, Ozguroglu M, Hansen S, Machiels J-P, Kocak I, et al. Prednisone plus cabazitaxel or mitoxantrone for metastatic castration-resistant

prostate cancer progressing after docetaxel treatment: a randomised open-label trial. Lancet (London, England). 2010 Oct 2;376(9747):1147–54.

36. Oudard S, Fizazi K, Sengeløv L, Daugaard G, Saad F, Hansen S, et al. Cabazitaxel Versus Docetaxel As First-Line Therapy for Patients With Metastatic Castration-Resistant Prostate Cancer: A Randomized Phase III Trial—FIRSTANA. J Clin Oncol. 2017 Oct 1;35(28):3189–97.
37. Eisenberger M, Hardy-Bessard A-C, Kim CS, Géczi L, Ford D, Mourey L, et al. Phase III Study Comparing a Reduced Dose of Cabazitaxel (20 mg/m ^{2}) and the Currently Approved Dose (25 mg/m ^{2}) in Postdocetaxel Patients With Metastatic Castration-Resistant Prostate Cancer—PROSELICA. J Clin Oncol. 2017 Oct 1;35(28):3198–206.
38. Wissing MD, van Oort IM, Gerritsen WR, van den Eertwegh AJM, Coenen JLLM, Bergman AM, et al. Cabazitaxel in patients with metastatic castration-resistant prostate cancer: results of a compassionate use program in the Netherlands. Clin Genitourin Cancer. 2013 Sep;11(3):238-250.e1.
39. Bracarda S, Gernone A, Gasparro D, Marchetti P, Ronzoni M, Bortolus R, et al. Real-world cabazitaxel safety: the Italian early-access program in metastatic castration-resistant prostate cancer. Future Oncol. 2014 May 19;10(6):975–83.
40. Heidenreich A, Scholz H-J, Rogenhofer S, Arsov C, Retz M, Müller SC, et al. Cabazitaxel plus prednisone for metastatic castration-resistant prostate cancer progressing after docetaxel: results from the German compassionate-use programme. Eur Urol. 2013 Jun;63(6):977–82.
41. Galsky MD, Dritselis A, Kirkpatrick P, Oh WK. Cabazitaxel. Nat Rev Drug Discov. 2010 Sep;9(9):677–8.
42. Swanton C, Nicke B, Schuett M, Eklund AC, Ng C, Li Q, et al. Chromosomal instability determines taxane response. Proc Natl Acad Sci U S A. 2009 May 26;106(21):8671–6.
43. Bumbaca B, Li W. Taxane resistance in castration-resistant prostate cancer: mechanisms and therapeutic strategies. Acta Pharm Sin B. 2018 Jul;8(4):518–29.
44. Fitzpatrick JM, de Wit R. Taxane Mechanisms of Action: Potential Implications for Treatment Sequencing in Metastatic Castration-resistant Prostate Cancer. Eur Urol. 2014 Jun;65(6):1198–204.
45. Tannock I, Osoba D, Stockler M, Ernst D, Neville A, Moore M, et al. Chemotherapy with mitoxantrone plus prednisone or prednisone alone for symptomatic hormone-resistant prostate cancer: a Canadian randomized trial with palliative end points. J Clin Oncol. 1996 Jun 1;14(6):1756–64.
46. Green AK, Corty RW, Wood WA, Meeneghan M, Reeder-Hayes KE, Basch E, et

al. Comparative effectiveness of mitoxantrone plus prednisone versus prednisone alone in metastatic castrate-resistant prostate cancer after docetaxel failure. Oncologist. 2015 May 1;20(5):516–22.

47. Attard G, Belldegrun AS, de Bono JS. Selective blockade of androgenic steroid synthesis by novel lyase inhibitors as a therapeutic strategy for treating metastatic prostate cancer. BJU Int. 2005 Dec;96(9):1241–6.
48. de Bono JS, Logothetis CJ, Molina A, Fizazi K, North S, Chu L, et al. Abiraterone and increased survival in metastatic prostate cancer. N Engl J Med. 2011 May 26;364(21):1995–2005.
49. Fizazi K, Scher HI, Molina A, Logothetis CJ, Chi KN, Jones RJ, et al. Abiraterone acetate for treatment of metastatic castration-resistant prostate cancer: final overall survival analysis of the COU-AA-301 randomised, double-blind, placebo-controlled phase 3 study. Lancet Oncol. 2012 Oct;13(10):983–92.
50. Ryan CJ, Smith MR, De Bono JS, Molina A, Logothetis C, De Souza PL, et al. Interim analysis (IA) results of COU-AA-302, a randomized, phase III study of abiraterone acetate (AA) in chemotherapy-naive patients (pts) with metastatic castration-resistant prostate cancer (mCRPC). ASCO Meet Abstr. 2012 Jun 20;30(18_suppl):LBA4518.
51. Li Z, Bishop AC, Alyamani M, Garcia JA, Dreicer R, Bunch D, et al. Conversion of abiraterone to D4A drives anti-tumour activity in prostate cancer. Nature. 2015 Jun 1;523(7560):347–51.
52. Li Z, Alyamani M, Li J, Rogacki K, Abazeed M, Upadhyay SK, et al. Redirecting abiraterone metabolism to fine-tune prostate cancer anti-androgen therapy. Nature. 2016 May 25;533(7604):547–51.
53. Lorente D, Omlin A, Ferraldeschi R, Pezaro C, Perez R, Mateo J, et al. Tumour responses following a steroid switch from prednisone to dexamethasone in castration-resistant prostate cancer patients progressing on abiraterone. Br J Cancer. 2014 Dec 9;111(12):2248–53.
54. Tran C, Ouk S, Clegg NJ, Chen Y, Watson PA, Arora V, et al. Development of a Second-Generation Antiandrogen for Treatment of Advanced Prostate Cancer. Science (80-). 2009 May 8;324(5928):787–90.
55. Beer TM, Armstrong AJ, Rathkopf DE, Loriot Y, Sternberg CN, Higano CS, et al. Enzalutamide in metastatic prostate cancer before chemotherapy. N Engl J Med. 2014 Jul 31;371(5):424–33.
56. Scher HI, Fizazi K, Saad F, Taplin M-E, Sternberg CN, Miller K, et al. Increased survival with enzalutamide in prostate cancer after chemotherapy. N Engl J Med. 2012 Sep 27;367(13):1187–97.

57. Hoffman-Censits J, Kelly WK. Enzalutamide: a novel antiandrogen for patients with castrate-resistant prostate cancer. Clin Cancer Res. 2013 Mar 15;19(6):1335–9.
58. Moreira RB, Debiasi M, Francini E, Nuzzo P V, Velasco G De, Maluf FC, et al. Differential side effects profile in patients with mCRPC treated with abiraterone or enzalutamide: a meta-analysis of randomized controlled trials. Oncotarget. 2017 Oct 13;8(48):84572–8.
59. Reid AHM, Attard G, Ambroisine L, Fisher G, Kovacs G, Brewer D, et al. Molecular characterisation of ERG, ETV1 and PTEN gene loci identifies patients at low and high risk of death from prostate cancer. Br J Cancer. 2010 Feb 16;102(4):678–84.
60. Noonan KL, North S, Bitting RL, Armstrong AJ, Ellard SL, Chi KN. Clinical activity of abiraterone acetate in patients with metastatic castration-resistant prostate cancer progressing after enzalutamide. Ann Oncol. 2013 Jul 1;24(7):1802–7.
61. Schrader AJ, Boegemann M, Ohlmann C-H, Schnoeller TJ, Krabbe L-M, Hajili T, et al. Enzalutamide in Castration-resistant Prostate Cancer Patients Progressing After Docetaxel and Abiraterone. Eur Urol. 2014 Jan 1;65(1):30–6.
62. Mostaghel EA, Marck BT, Plymate SR, Vessella RL, Balk S, Matsumoto AM, et al. Resistance to CYP17A1 inhibition with abiraterone in castration-resistant prostate cancer: induction of steroidogenesis and androgen receptor splice variants. Clin Cancer Res. 2011 Sep 15;17(18):5913–25.
63. Chi KN, Agarwal N, Bjartell A, Chung BH, Pereira de Santana Gomes AJ, Given R, et al. Apalutamide for Metastatic, Castration-Sensitive Prostate Cancer. N Engl J Med. 2019 May 31;NEJMoa1903307.
64. Smith MR, Saad F, Chowdhury S, Oudard S, Hadaschik BA, Graff JN, et al. Apalutamide Treatment and Metastasis-free Survival in Prostate Cancer. N Engl J Med. 2018 Apr 12;378(15):1408–18.
65. Fizazi K, Shore N, Tammela TL, Ulys A, Vjaters E, Polyakov S, et al. Darolutamide in Nonmetastatic, Castration-Resistant Prostate Cancer. N Engl J Med. 2019 Mar 28;380(13):1235–46.
66. Parker C, Nilsson S, Heinrich D, Helle SI, O'Sullivan JM, Fosså SD, et al. Alpha emitter radium-223 and survival in metastatic prostate cancer. N Engl J Med. 2013 Jul 18;369(3):213–23.
67. Wissing MD, van Leeuwen FWB, van der Pluijm G, Gelderblom H. Radium-223 chloride: Extending life in prostate cancer patients by treating bone metastases. Clin Cancer Res. 2013 Nov 1;19(21):5822–7.
68. Sartor O, Coleman R, Nilsson S, Heinrich D, Helle SI, O'Sullivan JM, et al. Effect of radium-223 dichloride on symptomatic skeletal events in patients with

castration-resistant prostate cancer and bone metastases: results from a phase 3, double-blind, randomised trial. Lancet Oncol. 2014 Jun;15(7):738–46.

69. Kratochwil C, Bruchertseifer F, Giesel FL, Weis M, Verburg FA, Mottaghy F, et al. 225Ac-PSMA-617 for PSMA targeting alpha-radiation therapy of patients with metastatic castration-resistant prostate cancer. J Nucl Med. 2016 Jul 7;
70. Di Lorenzo G, Ferro M, Buonerba C. Sipuleucel-T (Provenge®) for castration-resistant prostate cancer. BJU Int. 2012 Jul;110(2 Pt 2):E99-104.
71. Kantoff PW, Higano CS, Shore ND, Berger ER, Small EJ, Penson DF, et al. Sipuleucel-T Immunotherapy for Castration-Resistant Prostate Cancer. N Engl J Med. 2010 Jul 29;363(5):411–22.
72. Huber ML, Haynes L, Parker C, Iversen P. Interdisciplinary critique of sipuleucel-T as immunotherapy in castration-resistant prostate cancer. J Natl Cancer Inst. 2012 Feb 22;104(4):273–9.
73. Simpson EL, Davis S, Thokala P, Breeze PR, Bryden P, Wong R. Sipuleucel-T for the Treatment of Metastatic Hormone-Relapsed Prostate Cancer: A NICE Single Technology Appraisal; An Evidence Review Group Perspective. Pharmacoeconomics. 2015 Nov;33(11):1187–94.
74. Kantoff PW, Higano CS, Shore ND, Berger ER, Small EJ, Penson DF, et al. Sipuleucel-T immunotherapy for castration-resistant prostate cancer. N Engl J Med. 2010 Jul 29;363(5):411–22.
75. Small EJ, Lance RS, Redfern CH, Millard FE, Gardner TA, Karsh LI, et al. A randomized phase II trial of sipuleucel-T with concurrent or sequential abiraterone acetate (AA) plus prednisone (P) in metastatic castrate-resistant prostate cancer (mCRPC). ASCO Meet Abstr. 2013 May 20;31(15_suppl):5047.
76. Bader P, Echtle D, Fonteyne V, Livadas K, De Meerleer G, Paez Borda A, et al. Prostate cancer pain management: EAU guidelines on pain management. World J Urol. 2012 Oct;30(5):677–86.
77. Scotté F. The importance of supportive care in optimizing treatment outcomes of patients with advanced prostate cancer. Oncologist. 2012 Jan 1;17 Suppl 1(suppl 1):23–30.
78. Donovan JL, Hamdy FC, Lane JA, Mason M, Metcalfe C, Walsh E, et al. Patient-Reported Outcomes after Monitoring, Surgery, or Radiotherapy for Prostate Cancer. N Engl J Med. 2016 Oct 13;375(15):1425–37.
79. James ND, Sydes MR, Clarke NW, Mason MD, Dearnaley DP, Spears MR, et al. Addition of docetaxel, zoledronic acid, or both to first-line long-term hormone therapy in prostate cancer (STAMPEDE): Survival results from an adaptive, multiarm, multistage, platform randomised controlled trial. Lancet.

2016;387(10024).

80. Kakizoe T, Lindauer M, Hochhaus A, Fulchiero E, Jimeno A, Blomgren D, et al. Re: Abiraterone and increased survival in metastatic prostate cancer. J Clin Oncol Conf. 2013;31(1):1.
81. Robinson D, Van Allen EM, Wu YM, Schultz N, Lonigro RJ, Mosquera JM, et al. Integrative clinical genomics of advanced prostate cancer. Cell. 2015;161(5):1215–28.
82. Gundem G, Van Loo P, Kremeyer B, Alexandrov LB, Tubio JMC, Papaemmanuil E, et al. The evolutionary history of lethal metastatic prostate cancer. Nature. 2015 Apr 1;520(7547):353–7.
83. Bellacosa A, Kumar CC, Di Cristofano A, Testa JR. Activation of AKT kinases in cancer: implications for therapeutic targeting. Adv Cancer Res. 2005 Jan;94:29–86.
84. Manning BD, Cantley LC. AKT/PKB signaling: navigating downstream. Cell. 2007 Jun 29;129(7):1261–74.
85. Yoshimoto M, Ludkovski O, DeGrace D, Williams JL, Evans A, Sircar K, et al. PTEN genomic deletions that characterize aggressive prostate cancer originate close to segmental duplications. Genes Chromosomes Cancer. 2012 Feb;51(2):149–60.
86. Ayala G, Thompson T, Yang G, Frolov A, Li R, Scardino P, et al. High levels of phosphorylated form of Akt-1 in prostate cancer and non-neoplastic prostate tissues are strong predictors of biochemical recurrence. Clin Cancer Res. 2004 Oct 1;10(19):6572–8.
87. Ferraldeschi R, Nava Rodrigues D, Riisnaes R, Miranda S, Figueiredo I, Rescigno P, et al. PTEN Protein Loss and Clinical Outcome from Castration-resistant Prostate Cancer Treated with Abiraterone Acetate. Eur Urol. 2015 Apr;67(4):795–802.
88. Carver BS, Chapinski C, Wongvipat J, Hieronymus H, Chen Y, Chandarlapaty S, et al. Reciprocal feedback regulation of PI3K and androgen receptor signaling in PTEN-deficient prostate cancer. Cancer Cell. 2011 May 17;19(5):575–86.
89. Schwartz S, Wongvipat J, Trigwell CB, Hancox U, Carver BS, Rodrik-Outmezguine V, et al. Feedback suppression of PI3Kα signaling in PTEN-mutated tumors is relieved by selective inhibition of PI3Kβ. Cancer Cell. 2015 Jan 12;27(1):109–22.
90. Chen M-L, Xu P-Z, Peng X, Chen WS, Guzman G, Yang X, et al. The deficiency of Akt1 is sufficient to suppress tumor development in Pten+/- mice. Genes Dev. 2006 Jun 15;20(12):1569–74.

91. Dienstmann R, Rodon J, Markman B, Tabernero J. Recent Developments in Anti-Cancer Agents Targeting PI3K, Akt and mTORC1/2. Recent Pat Anticancer Drug Discov. 2011 May 1;6(2):210–36.
92. Struewing JP, Hartge P, Wacholder S, Baker SM, Berlin M, McAdams M, et al. The risk of cancer associated with specific mutations of BRCA1 and BRCA2 among Ashkenazi Jews. N Engl J Med. 1997 May 15;336(20):1401–8.
93. Gallagher DJ, Gaudet MM, Pal P, Kirchhoff T, Balistreri L, Vora K, et al. Germline BRCA mutations denote a clinicopathologic subset of prostate cancer. Clin Cancer Res. 2010 Apr 1;16(7):2115–21.
94. Castro E, Goh C, Leongamornlert D, Saunders E, Tymrakiewicz M, Dadaev T, et al. Effect of BRCA Mutations on Metastatic Relapse and Cause-specific Survival After Radical Treatment for Localised Prostate Cancer. Eur Urol. 2015 Aug;68(2):186–93.
95. Mateo J, Carreira S, Sandhu S, Miranda S, Mossop H, Perez-Lopez R, et al. DNA-Repair Defects and Olaparib in Metastatic Prostate Cancer. N Engl J Med. 2015 Oct 29;373(18):1697–708.
96. Ledermann J, Harter P, Gourley C, Friedlander M, Vergote I, Rustin G, et al. Olaparib Maintenance Therapy in Platinum-Sensitive Relapsed Ovarian Cancer. N Engl J Med. 2012 Apr 12;366(15):1382–92.
97. Gelmon KA, Tischkowitz M, Mackay H, Swenerton K, Robidoux A, Tonkin K, et al. Olaparib in patients with recurrent high-grade serous or poorly differentiated ovarian carcinoma or triple-negative breast cancer: A phase 2, multicentre, open-label, non-randomised study. Lancet Oncol. 2011 Sep 1;12(9):852–61.
98. Sella A, Yarom N, Zisman A, Kovel S. Paclitaxel, estramustine and carboplatin combination chemotherapy after initial docetaxel-based chemotherapy in castration-resistant prostate cancer. Oncology. 2009 Jan 5;76(6):442–6.
99. Hager S, Ackermann CJ, Joerger M, Gillessen S, Omlin A. Anti-tumour activity of platinum compounds in advanced prostate cancer-a systematic literature review. Ann Oncol. 2016 Apr 6;27(6):975–84.
100. Pritchard CC, Morrissey C, Kumar A, Zhang X, Smith C, Coleman I, et al. Complex MSH2 and MSH6 mutations in hypermutated microsatellite unstable advanced prostate cancer. Nat Commun. 2014;5:4988.
101. Ryan S, Jenkins MA, Win AK. Risk of prostate cancer in Lynch syndrome: a systematic review and meta-analysis. Cancer Epidemiol Biomarkers Prev. 2014 Mar;23(3):437–49.
102. Graff JN, Alumkal JJ, Drake CG, Thomas G V., Redmond WL, Farhad M, et al. Early evidence of anti-PD-1 activity in enzalutamide-resistant prostate cancer.

Oncotarget. 2016;5(0).
103. Rescigno P, Rodrigues DN, Yuan W, Carreira S, Lambros M, Seed G, et al. Mismatch repair defects in lethal prostate cancer. Cancer Res. 2017;77(13).
104. Snyder A, Makarov V, Merghoub T, Yuan J, Zaretsky JM, Desrichard A, et al. Genetic Basis for Clinical Response to CTLA-4 Blockade in Melanoma. N Engl J Med. 2014 Nov 19;141119140020009.
105. Herbst RS, Soria J-C, Kowanetz M, Fine GD, Hamid O, Gordon MS, et al. Predictive correlates of response to the anti-PD-L1 antibody MPDL3280A in cancer patients. Nature. 2014 Nov 26;515(7528):563–7.
106. Tumeh PC, Harview CL, Yearley JH, Shintaku IP, Taylor EJM, Robert L, et al. PD-1 blockade induces responses by inhibiting adaptive immune resistance. Nature. 2014 Nov 26;515(7528):568–71.
107. Robert C, Schachter J, Long G V., Arance A, Grob JJ, Mortier L, et al. Pembrolizumab versus Ipilimumab in Advanced Melanoma. 2015 Jun 24;
108. Van Allen EM, Miao D, Schilling B, Shukla SA, Blank C, Zimmer L, et al. Genomic correlates of response to CTLA4 blockade in metastatic melanoma. Science (80-). 2015 Sep 10;350(6257):207–11.
109. Le DT, Uram JN, Wang H, Bartlett BR, Kemberling H, Eyring AD, et al. PD-1 Blockade in Tumors with Mismatch-Repair Deficiency. N Engl J Med. 2015 May 30;
110. Polakis P. Wnt Signaling in Cancer. Cold Spring Harb Perspect Biol. 2012 May 1;4(5):a008052–a008052.
111. Liu J, Pan S, Hsieh MH, Ng N, Sun F, Wang T, et al. Targeting Wnt-driven cancer through the inhibition of Porcupine by LGK974.
112. Ahmad I, Sansom OJ. Role of Wnt signalling in advanced prostate cancer. J Pathol. 2018 May 1;245(1):3–5.
113. Wellenstein MD, De Visser KE. Review Cancer-Cell-Intrinsic Mechanisms Shaping the Tumor Immune Landscape. 2018;
114. Kahn M. Can we safely target the WNT pathway? Nat Rev Drug Discov. 2014 Jul 1;13(7):513–32.
115. Massachusetts Medical Society. The New England journal of medicine. Massachusetts Medical Society;
116. Kumar A, Coleman I, Morrissey C, Zhang X, True LD, Gulati R, et al. Substantial interindividual and limited intraindividual genomic diversity among tumors from men with metastatic prostate cancer. Nat Med. 2016;(November 2015):1–13.
117. Rodrigues DN, Boysen G, Sumanasuriya S, Seed G, Marzo AMD, de Bono J. The molecular underpinnings of prostate cancer: impacts on management and

pathology practice. Vol. 241, Journal of Pathology. 2017. p. 173–82.

118. Turner NC, Slamon DJ, Ro J, Bondarenko I, Im S-A, Masuda N, et al. Overall Survival with Palbociclib and Fulvestrant in Advanced Breast Cancer. N Engl J Med. 2018 Nov 15;379(20):1926–36.
119. Ciriello G, Miller ML, Aksoy BA, Senbabaoglu Y, Schultz N, Sander C. Emerging landscape of oncogenic signatures across human cancers. Nat Genet. 2013 Sep;45(10):1127–33.
120. Martincorena I, Campbell PJ. Somatic mutation in cancer and normal cells. Science. 2015 Sep 25;349(6255):1483–9.
121. Muzzey D, Evans EA, Lieber C. Understanding the Basics of NGS: From Mechanism to Variant Calling. Curr Genet Med Rep. 2015 Dec 4;3(4):158–65.
122. do Valle ÍF, Giampieri E, Simonetti G, Padella A, Manfrini M, Ferrari A, et al. Optimized pipeline of MuTect and GATK tools to improve the detection of somatic single nucleotide polymorphisms in whole-exome sequencing data. BMC Bioinformatics. 2016 Oct 8;17(S12):341.
123. Adalsteinsson VA, Ha G, Freeman SS, Choudhury AD, Stover DG, Parsons HA, et al. Scalable whole-exome sequencing of cell-free DNA reveals high concordance with metastatic tumors. Nat Commun. 2017 Dec 6;8(1):1324.
124. Butler TM, Johnson-Camacho K, Peto M, Wang NJ, Macey TA, Korkola JE, et al. Exome Sequencing of Cell-Free DNA from Metastatic Cancer Patients Identifies Clinically Actionable Mutations Distinct from Primary Disease. Richards KL, editor. PLoS One. 2015 Aug 28;10(8):e0136407.
125. Biesecker LG, Shianna K V, Mullikin JC. Exome sequencing: the expert view. Genome Biol. 2011 Sep 14;12(9):128.
126. Ulz P, Belic J, Graf R, Auer M, Lafer I, Fischereder K, et al. Whole-genome plasma sequencing reveals focal amplifications as a driving force in metastatic prostate cancer. Nat Commun. 2016;7.
127. Hieronymus H, Schultz N, Gopalan A, Carver BS, Chang MT, Xiao Y, et al. Copy number alteration burden predicts prostate cancer relapse. Proc Natl Acad Sci U S A. 2014 Jul 29;111(30):11139–44.
128. Wu Y-M, Cieślik M, Lonigro RJ, Vats P, Reimers MA, Cao X, et al. Inactivation of CDK12 Delineates a Distinct Immunogenic Class of Advanced Prostate Cancer. Cell. 2018 Jun 14;173(7):1770-1782.e14.
129. MANDEL P, METAIS P. [Not Available]. C R Seances Soc Biol Fil. 1948 Feb;142(3–4):241–3.
130. Leon SA, Shapiro B, Sklaroff DM, Yaros MJ. Free DNA in the serum of cancer patients and the effect of therapy. Cancer Res. 1977 Mar 1;37(3):646–50.

131. Diehl F, Schmidt K, Choti MA, Romans K, Goodman S, Li M, et al. Circulating mutant DNA to assess tumor dynamics. Nat Med. 2008 Sep;14(9):985–90.
132. Lanman RB, Mortimer SA, Zill OA, Sebisanovic D, Lopez R, Blau S, et al. Analytical and Clinical Validation of a Digital Sequencing Panel for Quantitative, Highly Accurate Evaluation of Cell-Free Circulating Tumor DNA. Hoheisel JD, editor. PLoS One. 2015 Oct 16;10(10):e0140712.
133. Garcia-murillas I, Schiavon G, Weigelt B, Ng C, Hrebien S, Cutts RJ, et al. Mutation tracking in circulating tumor DNA predicts relapse in early breast cancer. Sci Transl Med. 2015;7(302):1–12.
134. Corcoran RB, Chabner BA. Application of Cell-free DNA Analysis to Cancer Treatment. N Engl J Med. 2018 Nov;379(18):1754–65.
135. Gundem G, Van Loo P, Kremeyer B, Alexandrov LB, Tubio JMC, Papaemmanuil E, et al. The evolutionary history of lethal metastatic prostate cancer. Nature. 2015 Apr 1;520(7547):353–7.
136. Goodall J, Mateo J, Yuan W, Mossop H, Porta N, Miranda S, et al. Circulating Free DNA to Guide Prostate Cancer Treatment with PARP Inhibition. Cancer Discov. 2017;
137. Sozzi G, Roz L, Conte D, Mariani L, Andriani F, Verderio P, et al. Effects of Prolonged Storage of Whole Plasma or Isolated Plasma DNA on the Results of Circulating DNA Quantification Assays. JNCI J Natl Cancer Inst. 2005 Dec 21;97(24):1848–50.
138. Gutschner T, Diederichs S. The hallmarks of cancer. RNA Biol. 2012 Jun 27;9(6):703–19.
139. Huang X, Yuan T, Liang M, Du M, Xia S, Dittmar R, et al. Exosomal miR-1290 and miR-375 as prognostic markers in castration-resistant prostate cancer. Eur Urol. 2015 Jan;67(1):33–41.
140. Sita-Lumsden A, Dart DA, Waxman J, Bevan CL. Circulating microRNAs as potential new biomarkers for prostate cancer. Br J Cancer. 2013 May 28;108(10):1925–30.
141. Zhang H-L, Yang L-F, Zhu Y, Yao X-D, Zhang S-L, Dai B, et al. Serum miRNA-21: Elevated levels in patients with metastatic hormone-refractory prostate cancer and potential predictive factor for the efficacy of docetaxel-based chemotherapy. Prostate. 2011 Feb 15;71(3):326–31.
142. Mitobe Y, Takayama K, Horie-Inoue K, Inoue S. Prostate cancer-associated lncRNAs. Cancer Lett. 2018 Apr 1;418:159–66.
143. Ifere G, Ananaba G. Prostate Cancer Gene Expression Marker 1 (PCGEM1): A Patented Prostate- Specific Non-Coding Gene and Regulator of Prostate Cancer

Progression. Recent Pat DNA Gene Seq. 2009 Nov 1;3(3):151–63.

144. Joosse SA, Pantel K, Kooi I, Tannous J, Westerman BA, Rustenburg F, et al. Tumor-Educated Platelets as Liquid Biopsy in Cancer Patients. Cancer Cell. 2015 Nov 9;28(5):552–4.
145. Veld SGJG In 't, Wurdinger T. Tumor-educated platelets. Blood. 2019 Mar 4;blood-2018-12-852830.
146. ASHWORTH, TR. A case of cancer in which cells similar to those in the tumours were seen in the blood after death. Aust Med J. 1869;14:146.
147. Olmos D, Baird RD, Yap TA, Massard C, Pope L, Sandhu SK, et al. Baseline Circulating Tumor Cell Counts Significantly Enhance a Prognostic Score for Patients Participating in Phase I Oncology Trials. Clin Cancer Res. 2011 Aug 1;17(15):5188–96.
148. Cristofanilli M, Budd GT, Ellis MJ, Stopeck A, Matera J, Miller MC, et al. Circulating Tumor Cells, Disease Progression, and Survival in Metastatic Breast Cancer. N Engl J Med. 2004 Aug 19;351(8):781–91.
149. Lorente D, Olmos D, Mateo J, Bianchini D, Seed G, Fleisher M, et al. Decline in Circulating Tumor Cell Count and Treatment Outcome in Advanced Prostate Cancer. Eur Urol. 2016 Dec;70(6):985–92.
150. Forget P, Khalifa C, Defour J-P, Latinne D, Pel M-C Van, Kock M De. What is the normal value of the neutrophil-to-lymphocyte ratio? BMC Res Notes. 2017 Jan 3;10(1):12.
151. Zhang Y, Brodin P, Kalnicki S, Garg M, Guha C, Kabarriti R. NLR as a prognostic factor in solid tumors. J Clin Oncol. 2018 May 20;36(15_suppl):e24057–e24057.
152. Yap TA, Smith AD, Ferraldeschi R, Al-Lazikani B, Workman P, de Bono JS. Drug discovery in advanced prostate cancer: translating biology into therapy. Nat Rev Drug Discov. 2016 Jul 22;15(10):699–718.
153. Mehra N, Sharp A, Lorente D, Dolling D, Sumanasuriya S, Johnson B, et al. Neutrophil to Lymphocyte Ratio in Castration-Resistant Prostate Cancer Patients Treated With Daily Oral Corticosteroids. Clin Genitourin Cancer. 2017;15(6).
154. Leibowitz-Amit R, Templeton AJ, Omlin A, Pezaro C, Atenafu EG, Keizman D, et al. Clinical variables associated with PSA response to abiraterone acetate in patients with metastatic castration-resistant prostate cancer. Ann Oncol. 2014;25(3):657–62.
155. Ostrand-Rosenberg S, Sinha P. Myeloid-Derived Suppressor Cells: Linking Inflammation and Cancer. J Immunol. 2009 Apr 15;182(8):4499–506.
156. Chi N, Tan Z, Ma K, Bao L, Yun Z. Increased circulating myeloid-derived suppressor cells correlate with cancer stages, interleukin-8 and -6 in prostate

cancer. Int J Clin Exp Med. 2014;7(10):3181–92.

157. Mehra N, Morilla R, Sharp A, Crespo M, Lambros M, Morilla A, et al. High neutrophil-lymphocyte ratio, myeloid-derived suppressor cells and resistance to corticosteroid therapy in castration-resistant prostate cancer. J Clin Oncol 34, 2016 (suppl; abstr 5076). 2016;
158. Calcinotto A, Spataro C, Zagato E, Di Mitri D, Gil V, Crespo M, et al. IL-23 secreted by myeloid cells drives castration-resistant prostate cancer. Nature. 2018 Jul 27;559(7714):363–9.
159. Amur S. BIOMARKER QUALIFICATION PROGRAM EDUCATIONAL MODULE SERIES-MODULE 1 BIOMARKER TERMINOLOGY: SPEAKING THE SAME LANGUAGE.
160. Dougherty ER. Biomarker development: Prudence, risk, and reproducibility. BioEssays. 2012 Apr 1;34(4):277–9.
161. Cummings J, Raynaud F, Jones L, Sugar R, Dive C. Fit-for-purpose biomarker method validation for application in clinical trials of anticancer drugs. Br J Cancer. 2010 Oct 26;103(9):1313–7.
162. McShane LM, Altman DG, Sauerbrei W, Taube SE, Gion M, Clark GM, et al. REporting recommendations for tumour MARKer prognostic studies (REMARK). Br J Cancer. 2005 Aug 22;93(4):387–91.
163. Norum J, Nieder C. Treatments for Metastatic Prostate Cancer (mPC): A Review of Costing Evidence. Pharmacoeconomics. 2017 Jul 29;
164. Lowe FC, Trauzzi SJ. Prostatic acid phosphatase in 1993. Its limited clinical utility. Urol Clin North Am. 1993 Nov;20(4):589–95.
165. Stamey TA, Yang N, Hay AR, McNeal JE, Freiha FS, Redwine E. Prostate-Specific Antigen as a Serum Marker for Adenocarcinoma of the Prostate. N Engl J Med. 1987 Oct 8;317(15):909–16.
166. Balk SP, Ko Y-J, Bubley GJ. Biology of Prostate-Specific Antigen. J Clin Oncol. 2003 Jan 15;21(2):383–91.
167. Hoffman RM. Screening for Prostate Cancer. N Engl J Med. 2011 Nov 24;365(21):2013–9.
168. Shao Y-H, Demissie K, Shih W, Mehta AR, Stein MN, Roberts CB, et al. Contemporary Risk Profile of Prostate Cancer in the United States. JNCI J Natl Cancer Inst. 2009 Sep 16;101(18):1280.
169. Punglia RS, D'Amico A V., Catalona WJ, Roehl KA, Kuntz KM. Effect of Verification Bias on Screening for Prostate Cancer by Measurement of Prostate-Specific Antigen. N Engl J Med. 2003 Jul 24;349(4):335–42.
170. 1 Recommendations organised by site of cancer | Suspected cancer: recognition

and referral | Guidance | NICE.
171. Ilic D, Djulbegovic M, Jung JH, Hwang EC, Zhou Q, Cleves A, et al. Prostate cancer screening with prostate-specific antigen (PSA) test: a systematic review and meta-analysis. BMJ. 2018 Sep 5;362:k3519.
172. Mapelli P, Picchio M. Initial prostate cancer diagnosis and disease staging—the role of choline-PET–CT. Nat Rev Urol. 2015 Sep 11;12(9):510–8.
173. Petrylak DP, Ankerst DP, Jiang CS, Tangen CM, Hussain MHA, Lara PN, et al. Evaluation of Prostate-Specific Antigen Declines for Surrogacy in Patients Treated on SWOG 99-16. JNCI J Natl Cancer Inst. 2006 Apr 19;98(8):516–21.
174. Sridhara R, Eisenberger MA, Sinibaldi VJ, Reyno LM, Egorin MJ. Evaluation of prostate-specific antigen as a surrogate marker for response of hormone-refractory prostate cancer to suramin therapy. J Clin Oncol. 1995 Dec;13(12):2944–53.
175. Armstrong AJ, Garrett-Mayer E, Ou Yang Y-C, Carducci MA, Tannock I, de Wit R, et al. Prostate-specific antigen and pain surrogacy analysis in metastatic hormone-refractory prostate cancer. J Clin Oncol. 2007 Sep 1;25(25):3965–70.
176. Rescigno P, Lorente D, Bianchini D, Ferraldeschi R, Kolinsky MP, Sideris S, et al. Prostate-specific Antigen Decline After 4 Weeks of Treatment with Abiraterone Acetate and Overall Survival in Patients with Metastatic Castration-resistant Prostate Cancer. Eur Urol. 2016;
177. Prelaj A, Rebuzzi S, Buzzacchino F, Pozzi C, Ferrara C, Frantellizzi V, et al. Radium-223 in patients with metastatic castration-resistant prostate cancer: Efficacy and safety in clinical practice. Oncol Lett. 2018 Nov 30;17(2):1467–76.
178. Parker C, Heidenreich A, Nilsson S, Shore N. Current approaches to incorporation of radium-223 in clinical practice. Prostate Cancer Prostatic Dis. 2018 Apr 3;21(1):37–47.
179. Denlinger CS, Sanft T, Baker KS, Baxi S, Broderick G, Demark-Wahnefried W, et al. Survivorship, Version 2.2017, NCCN Clinical Practice Guidelines in Oncology. J Natl Compr Canc Netw. 2017;15(9):1140–63.
180. Loeb S. Prostate Biopsy: A Risk-Benefit Analysis. J Urol. 2010 Mar;183(3):852–3.
181. Bain BJ. Bone marrow biopsy morbidity and mortality. Br J Haematol. 2003 Jun 1;121(6):949–51.
182. Eisenhauer EA, Therasse P, Bogaerts J, Schwartz LH, Sargent D, Ford R, et al. New response evaluation criteria in solid tumours: Revised RECIST guideline (version 1.1). Eur J Cancer. 2009 Jan 1;45(2):228–47.
183. Scher HI, Morris MJ, Stadler WM, Higano C, Basch E, Fizazi K, et al. Trial Design

and Objectives for Castration-Resistant Prostate Cancer: Updated Recommendations From the Prostate Cancer Clinical Trials Working Group 3. J Clin Oncol. 2016 Apr 20;34(12):1402–18.

184. QIAGEN. QIAAmp Fast DNA Tissue Kit Handbook. 2015.
185. QIAGEN. QIAsymphony DSP Circulating DNA Kit Instructions for Use (Handbook). 2017.
186. Taylor AC. Titration of heparinase for removal of the PCR-inhibitory effect of heparin in DNA samples. Mol Ecol. 1997 Apr 1;6(4):383–5.
187. Quant-iT ™ dsDNA High-Sensitivity Assay Kit | 2.
188. Technologies A. Agilent Technologies Agilent High Sensitivity D1000 ScreenTape System Quick Guide.
189. Fisher Scientific T. Ion AmpliSeq Library Kit 2.0 User Guide (Pub.No. MAN0006735 F.0).
190. Fisher Scientific T. Ion PI Hi-Q Chef Kit User Guide (Pub. No. MAN0010967 Rev. B.0).
191. QIAGEN. QIAGEN QIAseq FX DNA Library Kit (96) Handbook.
192. KAPA HyperPlus Kit.
193. Agilent Technologies SureSelect XT Target Enrichment System for Illumina Paired-End Multiplexed Sequencing Library Protocol SureSelect platform manufactured with Agilent SurePrint Technology For Research Use Only. Not for use in diagnostic procedures. 2 SureSelect XT Target Enrichment System for Illumina Multiplexed Sequencing Notices. 2018.
194. Seed G, Yuan W, Mateo J, Carreira S, Bertan C, Lambros M, et al. Gene Copy Number Estimation from Targeted Next-Generation Sequencing of Prostate Cancer Biopsies: Analytic Validation and Clinical Qualification. Clin Cancer Res. 2017 Oct 15;23(20):6070–7.
195. Van Loo P, Nordgard SH, Lingjærde OC, Russnes HG, Rye IH, Sun W, et al. Allele-specific copy number analysis of tumors. Proc Natl Acad Sci U S A. 2010 Sep 28;107(39):16910–5.
196. Gao J, Aksoy BA, Dogrusoz U, Dresdner G, Gross B, Sumer SO, et al. Integrative Analysis of Complex Cancer Genomics and Clinical Profiles Using the cBioPortal. Sci Signal. 2013 Apr 2;6(269):pl1–pl1.
197. Cerami E, Gao J, Dogrusoz U, Gross BE, Sumer SO, Aksoy BA, et al. The cBio Cancer Genomics Portal: An Open Platform for Exploring Multidimensional Cancer Genomics Data: Figure 1. Cancer Discov. 2012 May;2(5):401–4.
198. Kraan J, Sleijfer S, Strijbos MH, Ignatiadis M, Peeters D, Pierga J-Y, et al. External quality assurance of circulating tumor cell enumeration using the CellSearch®

system: A feasibility study. Cytom Part B Clin Cytom. 2011 Mar;80B(2):112–8.
199. Ampli1™ WGA Kit Whole Genome Amplification for Single Cells USER MANUAL y Version 02.
200. Agilent Oligonucleotide Array-Based CGH for Genomic DNA Analysis Enzymatic Labeling for Blood, Cells, or Tissues (with a High Throughput option) Protocol. 2016.
201. Punnoose EA, Ferraldeschi R, Szafer-Glusman E, Tucker EK, Mohan S, Flohr P, et al. PTEN loss in circulating tumour cells correlates with PTEN loss in fresh tumour tissue from castration-resistant prostate cancer patients. Br J Cancer. 2015 Oct 17;113(8):1225–33.
202. Drost J, Karthaus WR, Gao D, Driehuis E, Sawyers CL, Chen Y, et al. Organoid culture systems for prostate epithelial and cancer tissue. Nat Protoc. 2016 Feb 21;11(2):347–58.
203. Lambros MB, Seed G, Sumanasuriya S, Gil V, Crespo M, Fontes M, et al. Single-Cell Analyses of Prostate Cancer Liquid Biopsies Acquired by Apheresis. Clin Cancer Res. 2018 Nov 15;24(22):5635–44.
204. Declaration of Helsinki World Medical Association Declaration of Helsinki Ethical Principles for Medical Research Involving Human Subjects.
205. Plasma Transfer Insert Revising ther MNC insert with the Plasma Transfer option MU. SPECTRA OPTIA ® APHERESIS SYSTEM.
206. Ibrahim MFK, Hilton J, Addison C, Robertson S, Werier J, Mazzarello S, et al. Strategies for obtaining bone biopsy specimens from breast cancer patients - Past experience and future directions. J bone Oncol. 2016 Nov;5(4):180–4.
207. Bedard PL, Hansen AR, Ratain MJ, Siu LL. Tumour heterogeneity in the clinic. Nature. 2013 Sep 18;501(7467):355–64.
208. Palmirotta R, Lovero D, Cafforio P, Felici C, Mannavola F, Pellè E, et al. Liquid biopsy of cancer: a multimodal diagnostic tool in clinical oncology. Ther Adv Med Oncol. 2018;10:1758835918794630.
209. Gillessen S, Omlin A, Attard G, de Bono JS, Efstathiou E, Fizazi K, et al. Management of patients with advanced prostate cancer: recommendations of the St Gallen Advanced Prostate Cancer Consensus Conference (APCCC) 2015. Ann Oncol. 2015 Aug;26(8):1589–604.
210. Diamond IR, Grant RC, Feldman BM, Pencharz PB, Ling SC, Moore AM, et al. Defining consensus: A systematic review recommends methodologic criteria for reporting of Delphi studies. J Clin Epidemiol. 2014 Apr;67(4):401–9.
211. Lu C, Luo J. Decoding the androgen receptor splice variants. Transl Androl Urol. 2013 Sep;2(3):178–86.

212. S. EM, F. M, C. M, B. G, M. N, V. L, et al. Circulating DNA as a Strong Multimarker Prognostic Tool for Metastatic Colorectal Cancer Patient Management Care. J Clin Oncol. 2014;32(15 SUPPL. 1):1–12.
213. Madhavan D, Wallwiener M, Bents K, Zucknick M, Nees J, Schott S, et al. Plasma DNA integrity as a biomarker for primary and metastatic breast cancer and potential marker for early diagnosis. Breast Cancer Res Treat. 2014;146(1):163–74.
214. Bryant RJ, Pawlowski T, Catto JWF, Marsden G, Vessella RL, Rhees B, et al. Changes in circulating microRNA levels associated with prostate cancer. Br J Cancer. 2012 Feb 14;106(4):768–74.
215. Eisenberger M, Hardy-Bessard A-C, Kim CS, Géczi L, Ford D, Mourey L, et al. Phase III Study Comparing a Reduced Dose of Cabazitaxel (20 mg/m(2)) and the Currently Approved Dose (25 mg/m(2)) in Postdocetaxel Patients With Metastatic Castration-Resistant Prostate Cancer-PROSELICA. J Clin Oncol. 2017 Aug 15;JCO2016721076.
216. Scher HI, Halabi S, Tannock I, Morris M, Sternberg CN, Carducci MA, et al. Design and End Points of Clinical Trials for Patients With Progressive Prostate Cancer and Castrate Levels of Testosterone: Recommendations of the Prostate Cancer Clinical Trials Working Group. 2008;
217. QIAGEN. QIAamp® Circulating Nucleic Acid Handbook. 10AD.
218. Uno H, Cai T, Pencina MJ, D'Agostino RB, Wei LJ. On the C-statistics for evaluating overall adequacy of risk prediction procedures with censored survival data. Stat Med. 2011 May 10;30(10):n/a-n/a.
219. STINE R. An Introduction to Bootstrap Methods. Sociol Methods Res. 1989 Nov 30;18(2–3):243–91.
220. Blanche P, Dartigues J-F, Jacqmin-Gadda H. Estimating and comparing time-dependent areas under receiver operating characteristic curves for censored event times with competing risks. Stat Med. 2013 Dec 30;32(30):5381–97.
221. Halabi S, Lin C-Y, Kelly WK, Fizazi KS, Moul JW, Kaplan EB, et al. Updated prognostic model for predicting overall survival in first-line chemotherapy for patients with metastatic castration-resistant prostate cancer. J Clin Oncol. 2014 Mar 1;32(7):671–7.
222. Fizazi K, Massard C, Smith M, Rader M, Brown J, Milecki P, et al. Bone-related Parameters are the Main Prognostic Factors for Overall Survival in Men with Bone Metastases from Castration-resistant Prostate Cancer. Eur Urol. 2015 Jul;68(1):42–50.
223. Parpart-Li S, Bartlett B, Popoli M, Adleff V, Tucker L, Steinberg R, et al. The Effect

of Preservative and Temperature on the Analysis of Circulating Tumor DNA. 2016;
224. Sato A, Nakashima C, Abe T, Kato J, Hirai M, Nakamura T, et al. Investigation of appropriate pre-analytical procedure for circulating free DNA from liquid biopsy. Oncotarget. 2018 Aug 7;9(61):31904–14.
225. Frank MO. Circulating Cell-Free DNA Differentiates Severity of Inflammation. Biol Res Nurs. 2016 Oct 1;18(5):477–88.
226. Jahr S, Hentze H, Englisch S, Hardt D, Fackelmayer FO, Hesch R. DNA Fragments in the Blood Plasma of Cancer Patients : Quantitations and Evidence for Their Origin from Apoptotic and Necrotic Cells DNA Fragments in the Blood Plasma of Cancer Patients : Quantitations and Evidence for Their Origin from Apoptotic and Necr. Cancer Res. 2001;61:1659–65.
227. Mehra N, Dolling D, Sumanasuriya S, Christova R, Pope L, Carreira S, et al. Plasma Cell-free DNA Concentration and Outcomes from Taxane Therapy in Metastatic Castration-resistant Prostate Cancer from Two Phase III Trials (FIRSTANA and PROSELICA). Eur Urol. 2018 Sep;74(3):283–91.
228. Ulz P, Belic J, Graf R, Auer M, Lafer I, Fischereder K, et al. Whole-genome plasma sequencing reveals focal amplifications as a driving force in metastatic prostate cancer. Nat Commun. 2016 Dec 22;7(1):12008.
229. Taylor AC. Titration of heparinase for removal of the PCR-inhibitory effect of heparin in DNA samples. Mol Ecol. 1997 Apr;6(4):383–5.
230. Azad A a., Volik S V, Wyatt AW, Haegert A, Le Bihan S, Bell RH, et al. Androgen receptor gene aberrations in circulating cell-free DNA: biomarkers of therapeutic resistance in castration-resistant prostate cancer. Clin Cancer Res. 2015 Feb;2315–25.
231. Jordan MA, Wilson L. Microtubules as a target for anticancer drugs. Nat Rev Cancer. 2004 Apr;4(4):253–65.
232. Fitzpatrick JM, de Wit R. Taxane mechanisms of action: potential implications for treatment sequencing in metastatic castration-resistant prostate cancer. Eur Urol. 2014 Jun;65(6):1198–204.
233. Foulkes WD, Flanders TY, Pollock PM, Haywardt NK. THE CDKN2A (pl6) GENE AND HUMAN CANCER.
234. Castellano M, Pollock PM, Walters MK, Sparrow LE, Down LM, Gabrielli BG, et al. CDKN2A/p16 is inactivated in most melanoma cell lines. Cancer Res. 1997 Nov 1;57(21):4868–75.
235. Marchetti A, Buttitta F, Pellegrini S, Bertacca G, Chella A, Carnicelli V, et al. Alterations ofP16 (MTS1) in node-positive non-small cell lung carcinomas. J Pathol. 1997 Feb 1;181(2):178–82.

236. Salo-Mullen EE, O'Reilly EM, Kelsen DP, Ashraf AM, Lowery MA, Yu KH, et al. Identification of germline genetic mutations in patients with pancreatic cancer. Cancer. 2015 Dec 15;121(24):4382–8.
237. Arima Y, Hayashi N, Hayashi H, Sasaki M, Kai K, Sugihara E, et al. Loss of p16 expression is associated with the stem cell characteristics of surface markers and therapeutic resistance in estrogen receptor-negative breast cancer. Int J Cancer. 2012 Jun 1;130(11):2568–79.
238. Xu J-H, Hu S-L, Shen G-D, Shen G. Tumor suppressor genes and their underlying interactions in paclitaxel resistance in cancer therapy. Cancer Cell Int. 2016 Dec 20;16(1):13.
239. Wang H, Vo T, Hajar A, Li S, Chen X, Parissenti AM, et al. Multiple mechanisms underlying acquired resistance to taxanes in selected docetaxel-resistant MCF-7 breast cancer cells. BMC Cancer. 2014 Dec 22;14(1):37.
240. Ehrlichova M, Mohelnikova-Duchonova B, Hrdy J, Brynychova V, Mrhalova M, Kodet R, et al. The association of taxane resistance genes with the clinical course of ovarian carcinoma. Genomics. 2013 Aug 1;102(2):96–101.
241. Nami B, Wang Z. Genetics and Expression Profile of the Tubulin Gene Superfamily in Breast Cancer Subtypes and Its Relation to Taxane Resistance. Cancers (Basel). 2018 Aug 18;10(8).
242. Giannakakou P, Sackett DL, Kang YK, Zhan Z, Buters JTM, Fojo T, et al. Paclitaxel-resistant human ovarian cancer cells have mutant β-tubulins that exhibit impaired paclitaxel-driven polymerization. J Biol Chem. 1997 Jul 4;272(27):17118–25.
243. Choi YH, Yu A-M. ABC transporters in multidrug resistance and pharmacokinetics, and strategies for drug development. Curr Pharm Des. 2014;20(5):793–807.
244. Kathawala RJ, Wang Y-J, Shukla S, Zhang Y-K, Alqahtani S, Kaddoumi A, et al. ATP-binding cassette subfamily B member 1 (ABCB1) and subfamily C member 10 (ABCC10) are not primary resistance factors for cabazitaxel. Chin J Cancer. 2015 Dec 5;34(3):5.
245. Fleming V, Hu X, Weber R, Nagibin V, Groth C, Altevogt P, et al. Targeting Myeloid-Derived Suppressor Cells to Bypass Tumor-Induced Immunosuppression. Front Immunol. 2018;9:398.
246. Pucci P, Rescigno P, Sumanasuriya S, de Bono J, Crea F. Hypoxia and Noncoding RNAs in Taxane Resistance. Trends Pharmacol Sci. 2018 Aug 1;39(8):695–709.
247. Krebs MG, Hou J-M, Ward TH, Blackhall FH, Dive C. Circulating tumour cells: their utility in cancer management and predicting outcomes. Ther Adv Med Oncol.

2010 Nov;2(6):351–65.

248. Andree KC, van Dalum G, Terstappen LWMM. Challenges in circulating tumor cell detection by the CellSearch system. Mol Oncol. 2016 Mar;10(3):395–407.
249. Stoecklein NH, Fischer JC, Niederacher D, Terstappen LWMM. Challenges for CTC-based liquid biopsies: low CTC frequency and diagnostic leukapheresis as a potential solution. Expert Rev Mol Diagn. 2016 Feb 16;16(2):147–64.
250. Fischer JC, Niederacher D, Topp SA, Honisch E, Schumacher S, Schmitz N, et al. Diagnostic leukapheresis enables reliable detection of circulating tumor cells of nonmetastatic cancer patients. Proc Natl Acad Sci. 2013 Oct 8;110(41):16580–5.
251. Bambauer R, Latza R, Burgard D, Schiel R. Therapeutic Apheresis in Hematologic, Autoimmune and Dermatologic Diseases With Immunologic Origin. Ther Apher Dial. 2016 Oct 1;20(5):433–52.
252. Crocco I, Franchini M, Garozzo G, Gandini AR, Gandini G, Bonomo P, et al. Adverse reactions in blood and apheresis donors: experience from two Italian transfusion centres. Blood Transfus. 2009 Jan;7(1):35–8.
253. Pukazhendhi G, Glück S. Circulating tumor cells in breast cancer. J Carcinog. 2014;13:8.
254. Armstrong AJ, Eisenberger MA, Halabi S, Oudard S, Nanus DM, Petrylak DP, et al. Biomarkers in the Management and Treatment of Men with Metastatic Castration-Resistant Prostate Cancer. Eur Urol. 2012 Mar;61(3):549–59.
255. Ida Silvestri,1 Elisabetta Tortorella,1 Sabrina Giantulli,1 Susanna Scarpa 2 Alessandro Sciarra3. Immunotherapy in Prostate Cancer: Recent Advances and Future Directions - European Medical Journal. Eur Med J. 2019;
256. Pantel K, Alix-Panabières C. Liquid biopsy and minimal residual disease — latest advances and implications for cure. Nat Rev Clin Oncol. 2019 Jul 22;16(7):409–24.